

Identification of six *Cytospora* species on Chinese chestnut in China

Ning Jiang^{1*}, Qin Yang^{1,2,3*}, Xin-Lei Fan¹, Cheng-Ming Tian¹

1 The Key Laboratory for Silviculture and Conservation of the Ministry of Education, Beijing Forestry University, Beijing 100083, China **2** Forestry Biotechnology Hunan Key Laboratories, Central South University of Forestry and Technology, Changsha 410004, China **3** Hunan Key Laboratory of Forest Protection, Central South University of Forestry and Technology, Changsha 410004, China

Corresponding author: Cheng-Ming Tian (chengmt@bjfu.edu.cn)

Academic editor: R. Phookamsak | Received 19 October 2019 | Accepted 26 December 2019 | Published 13 January 2020

Citation: Jiang N, Yang Q, Fan X-L, Tian C-M (2020) Identification of six *Cytospora* species on Chinese chestnut in China. MycoKeys 62: 1–25. <https://doi.org/10.3897/mycokeys.62.47425>

Abstract

Chinese chestnut (*Castanea mollissima*) is an important crop tree species in China. In the present study, *Cytospora* specimens were collected from Chinese chestnut trees and identified using molecular data of a combined ITS, LSU, ACT and RPB2 loci, as well as morphological features. As a result, two new *Cytospora* species and four new host records were confirmed, viz. *C. kuanchengensis* sp. nov., *C. xinglongensis* sp. nov., *C. ceratostomopsis*, *C. leucostoma*, *C. myrtagina* and *C. schulzeri*.

Keywords

Castanea mollissima, Cytosporaceae, Diaporthales, systematics, taxonomy

Introduction

Chinese chestnut (*Castanea mollissima*) is a widely cultivated crop tree species in China, producing nutritious and delicious nuts for humans (Lu and Guo 2016). However, *Cryphonectria parasitica* and several fungi are causing severe chestnut diseases worldwide, which reduce the nut production, even killing the hosts. (Aghayeva et al. 2017, Shuttleworth and Guest 2017, Jiang et al. 2018a, Rigling and Prospero 2018). Recently, several diaporthalean species were described from Chinese chestnut trees for the clear taxo-

* These authors contributed equally to this work and should be considered as co-first authors.

nomic concepts of families, genera and species in Diaporthales (Rossman et al. 2007, Senanayake et al. 2017, 2018), including species of *Aurantiosacculus*, *Coryneum*, *Cryphonectria*, *Dendrostoma*, *Endothia*, *Gnomoniopsis*, *Neopseudomelanconis* and *Ophiognomonia* (Gong et al. 2017, Jiang et al. 2018b, 2018c, 2019a, 2019b, Jiang and Tian 2019).

Cytospora (Cytosporaceae, Diaporthales) is a widely distributed genus worldwide, occurring on a broad range of hosts (Sarma and Hyde 2001, Yang et al. 2015, Lawrence et al. 2017, Norphanphoun et al. 2017, 2018, Wijayawardene et al. 2018, Jayawardena et al. 2019, Phookamsak et al. 2019, Fan et al. 2020). Some species can cause severe canker diseases on woody trees, such as *Cytospora chrysosperma*, which is a common pathogen on the commercial tree genera, *Populus* and *Salix* (Fan et al. 2014b, Zhang et al. 2014, Kepley et al. 2015, Wang et al. 2015). Host affiliation was considered as the main evidence for separating species in *Cytospora* before DNA sequences were used; however, morphology combined with phylogeny has revealed many cryptic species. For example, 28 *Cytospora* species were discovered from *Eucalyptus* from South Africa (Adams et al. 2005) and six from apple trees in Iran (Mehrabi et al. 2011), three from Chinese scholar tree (Fan et al. 2014a), four from walnut tree (Fan et al. 2015a), six from anti-desertification plants in China (Fan et al. 2015b) and two from grapevine in North America (Lawrence et al. 2017). Several recent studies discovered new species of *Cytospora* using multiphasic analyses (Lawrence et al. 2018, Norphanphoun et al. 2017, 2018, Senanayake et al. 2017, 2018, Pan et al. 2018, Zhu et al. 2018, Zhang et al. 2019).

During our investigations of chestnut disease in China from 2016 to 2019, diseased branches with typical *Cytospora* fruiting bodies were discovered and collected (Fig. 1). In the present study, *Cytospora* species from *Castanea mollissima* were identified using a combined method of morphology and phylogeny.

Materials and methods

Sample collections and isolations

Chinese chestnut has a wide distribution in China. In the present study, we surveyed Hebei, Shaanxi and Shandong Provinces from 2016 to 2019. Dead and dying branches with typical *Cytospora* fruiting bodies were collected and packed in paper bags. Isolates were obtained by removing the ascospores or conidial masses from the fruiting bodies on to clean PDA plates and incubating at 25 °C until spores germinated. Single germinated spores were transferred on to the new PDA plates and incubated at 25 °C in the dark. Specimens were deposited in the Museum of the Beijing Forestry University (BJFC) and axenic cultures are maintained in the China Forestry Culture Collection Centre (CFCC).

Morphological analysis

Observation and description of *Cytospora* species from *Castanea mollissima* was based on fruiting bodies formed on tree barks. Ascomata and conidiomata from tree barks were sec-



Figure 1. Canker symptoms on *Castanea mollissima* caused by *Cytospora* spp.

tioned by hand using a double-edged blade and structures were observed under a dissecting microscope. At least 10 conidiostromata/ascostromata, 10 asci and 50 conidia/ascospores were measured to calculate the mean size and standard deviation. Measurements are reported as maximum and minimum in parentheses and the range representing the mean plus and minus the standard deviation of the number of measurements is given in parentheses (Voglmayr et al. 2017). Microscopy photographs were captured with a Nikon Eclipse 80i compound microscope equipped with a Nikon digital sight DS-Ri2 high definition colour camera, using differential interference contrast illumination. Introduction of the new species, based on molecular data, follow the recommendations of Jeewon and Hyde (2016).

DNA extraction, PCR amplification and sequencing

Genomic DNA was extracted from young mycelium growing on PDA plates following Doyle and Doyle (1990). PCR amplifications were performed in a DNA Engine Pelti-

er Thermal Cycler (PTC-200; Bio-Rad Laboratories, Hercules, CA, USA). The primer pair ITS1/ITS4 (White et al. 1990) was used to amplify the ITS region. The primer pair LR0R/LR5 (Vilgalys and Hester 1990) was used to amplify the LSU region. The primer pair ACT512F/ACT783R (Carbone and Kohn 1999) was used to amplify ACT gene. The primer pair dRPB2-5f/dRPB2-7r (Voglmayr et al. 2016) was used to amplify the RPB2 gene. The polymerase chain reaction (PCR) assay was conducted as described in Fan et al. (2020). PCR amplification products were assayed via electrophoresis in 2% agarose gels. DNA sequencing was performed using an ABI PRISM 3730XL DNA Analyzer with a BigDye Terminator Kit v.3.1 (Invitrogen, USA) at the Shanghai Invitrogen Biological Technology Company Limited (Beijing, China).

Phylogenetic analyses

The preliminary identities of the isolates sequenced were obtained by conducting a standard nucleotide BLAST search using ITS, LSU, ACT and RPB2. Then all *Cytospora* isolates were selected to conduct phylogenetic analyses, based on sequence datasets from Fan et al. (2020). *Diaporthe vaccinia* (CBS 160.32) in Diaporthaceae was selected as the outgroup taxon. All sequences were aligned using MAFFT v. 6 (Katoh and Toh 2010) and edited manually using MEGA v. 6 (Tamura et al. 2013). Phylogenetic analyses were performed using PAUP v. 4.0b10 for Maximum Parsimony (MP) analysis (Swofford 2003) and PhyML v. 3.0 for Maximum Likelihood (ML) analysis (Guindon et al. 2010).

MP analysis was run using a heuristic search option of 1000 search replicates with random-additions of sequences with a tree bisection and reconnection algorithm. Max-trees were set to 5000, branches of zero length were collapsed and all equally parsimonious trees were saved. Other calculated parsimony scores were tree length (TL), consistency index (CI), retention index (RI) and rescaled consistency (RC). ML analysis was performed using a GTR site substitution model including a gamma-distributed rate heterogeneity and a proportion of invariant sites (Guindon et al. 2010). The branch support was evaluated using a bootstrapping method of 1000 replicates (Hillis and Bull 1993). Phylograms were shown using FigTree v. 1.4.3 (Rambaut 2016). Novel sequences, generated in the current study, were deposited in GenBank (Table 1) and the aligned matrices used for phylogenetic analyses in TreeBASE (accession number: S25160).

Results

Phylogenetic analyses

The alignment based on the combined sequence dataset (ITS, LSU, ACT and RPB2) included 124 ingroup taxa and one outgroup taxon, comprising 2097 characters in the aligned matrix. Of these, 1375 characters were constant, 89 variable characters were parsimony-uninformative and 663 characters were parsimony informative.

Table 1. Strains used in the phylogenetic tree and their culture accession and GenBank numbers. Strains from this study are in bold and ex-strains are marked with *.

Species	Strain	Host	Origin	GenBank accession numbers			
				ITS	LSU	ACT	RPB2
<i>Cytospora atlanticola</i>	CFCC 89970*	<i>Ailanthus altissima</i>	China	MH933618	MH933653	MH933526	MH933592
<i>Cytospora abyssinica</i>	CMW 10181*	<i>Eucalyptus globulus</i>	Ethiopia	AY347353	NA	NA	NA
<i>Cytospora acaciae</i>	CBS 468.69	<i>Ceratonia siliqua</i>	Spain	DQ243804	NA	NA	NA
<i>Cytospora ampulliformis</i>	MFLUCC 16-0583*	<i>Sorbus intermedia</i>	Russia	KY417726	KY417760	KY417692	KY417794
	MFLUCC 16-0629	<i>Acer platanoides</i>	Russia	KY417727	KY417761	KY417693	KY417795
<i>Cytospora amygdali</i>	CBS 144233*	<i>Prunus dulcis</i>	USA	MG971853	NA	MG972002	NA
	CFCC 89615	<i>Juglans regia</i>	China	KR045618	KR045700	KF498673	KU710946
	CFCC 89616	<i>Juglans regia</i>	China	KR045619	KR045701	KF498674	KU710947
<i>Cytospora atrocinchata</i>	CFCC 89615	<i>Juglans regia</i>	China	KR045618	KR045700	KF498673	KU710946
<i>Cytospora austromontana</i>	CMW 6735*	<i>Eucalyptus pauciflora</i>	China	AY347361	NA	NA	NA
<i>Cytospora beilinenis</i>	CFCC 50493*	<i>Pinus armandii</i>	Australia	MH933619	MH933654	MH933527	NA
	CFCC 50494	<i>Pinus armandii</i>	China	MH933620	MH933655	MH933528	NA
<i>Cytospora berberidis</i>	CFCC 89927*	<i>Berberis dasystachya</i>	China	KR045620	KR045702	KU710990	KU710948
	CFCC 89933	<i>Berberis dasystachya</i>	China	KR045621	KR045703	KU710991	KU710949
<i>Cytospora berkeleyi</i>	StanfordT3*	<i>Eucalyptus globulus</i>	USA	AY347350	NA	NA	NA
	UCBTwig3	<i>Eucalyptus globulus</i>	USA	AY347349	NA	NA	NA
<i>Cytospora brevispora</i>	CBS 116811*	<i>Eucalyptus grandis</i> × <i>tereticornis</i>	Congo	AF192315	NA	NA	NA
	CBS 116829	<i>Eucalyptus grandis</i>	Venezuela	AF192321	NA	NA	NA
<i>Cytospora bungaeanae</i>	CFCC 50495*	<i>Pinus bungaeana</i>	China	MH933621	MH933656	MH933529	MH933593
	CFCC 50496	<i>Pinus bungaeana</i>	China	MH933622	MH933657	MH933530	MH933594
<i>Cytospora californica</i>	CBS 144234*	<i>Juglans regia</i>	USA	MG971935	NA	MG972083	NA
<i>Cytospora carbonacea</i>	CFCC 89947	<i>Ulmus pumila</i>	China	KR045622	KP310812	KP310842	KU710950
<i>Cytospora carpobroti</i>	CMW 48981*	<i>Carpobrotus edulis</i>	South Africa	MH382812	MH411216	NA	NA
<i>Cytospora castaneae</i>	AUCCT/DBT 183*	<i>Castanea sativa</i>	India	KC963921	NA	NA	NA
<i>Cytospora cedri</i>	CBS 196.50	NA	Italy	AF192311	NA	NA	NA
<i>Cytospora celtidicola</i>	CFCC 50497*	<i>Celtis sinensis</i>	China	MH933623	MH933658	MH933531	MH933595
	CFCC 50498	<i>Celtis sinensis</i>	China	MH933624	MH933659	MH933532	MH933596
<i>Cytospora centrivillosa</i>	MFLUCC 16-1206*	<i>Sorbus domestica</i>	Italy	MF190122	MF190068	NA	MF377601
	MFLU 17-0887	<i>Sorbus domestica</i>	Italy	MF190123	MF190069	NA	NA
	MFLUCC 17-1660	<i>Sorbus domestica</i>	Italy	MF190124	MF190070	NA	MF377600
<i>Cytospora ceratosporna</i>	CFCC 89624	<i>Juglans regia</i>	China	KR045645	KR045724	NA	KU710976
	CFCC 89625	<i>Juglans regia</i>	China	KR045646	KR045725	NA	KU710977

Species	Strain	Host	Origin	ITS	LSU	ACT	RPB2
<i>Cytospora ceratopermopsis</i>	CFCC 89626*	<i>Juglans regia</i>	China	KR045647	KR045726	KU711011	KU710978
	CFCC 89627	<i>Juglans regia</i>	China	KR045648	KR045727	KU711012	KU710979
	CFCC 52471	<i>Castanea mollissima</i>	China	MK432629	MK429899	MK442953	MK578087
<i>Cytospora chrysosperma</i>	CFCC 82472	<i>Castanea mollissima</i>	China	MK432630	MK429900	MK442954	MK578088
	CFCC 89629	<i>Salix psammophila</i>	China	KF765673	KF765689	NA	KF765705
	CFCC 89981	<i>Populus alba</i> subsp. <i>pyramidalis</i>	China	MH933625	MH933660	MH933533	MH933597
<i>Cytospora cinerosoma</i>	CFCC 89982	<i>Ulmus pumila</i>	China	KP281261	KP310805	KP310835	NA
	GMW 5700*	<i>Encalyptus globulus</i>	Chile	AY347377	NA	NA	NA
	MFLUCC 14-1050*	<i>Cotinus coggygia</i>	Russia	KX430142	KX430143	NA	KX430144
<i>Cytospora curvata</i>	MFLUCC 15-0865*	<i>Salix alba</i>	Russia	KY417728	KY417762	KY417694	KY417796
	CXY 1350*	<i>Populus davidiana</i>	China	KM034870	NA	NA	NA
	CXY 1374	<i>Populus davidiana</i>	China	KM034869	NA	NA	NA
<i>Cytospora diatrypelloidea</i>	GMW 8549*	<i>Encalyptus globulus</i>	Australia	AY347368	NA	NA	NA
	GMW 6509*	<i>Encalyptus grandis</i>	Uruguay	AY347374	NA	NA	NA
	GMW 6750	<i>Encalyptus globulus</i>	Australia	AY347359	NA	NA	NA
<i>Cytospora donetzica</i>	MFLUCC 15-0864	NA	NA	KY417729	KY417763	KY417695	KY417797
	MFLUCC 16-0574*	<i>Rosa</i> sp.	Russia	KY417731	KY417764	KY417696	KY417798
<i>Cytospora elaeagni</i>	CFCC 89632	<i>Elaeagnus angustifolia</i>	China	KR045626	KR045706	KU710995	KU710955
	CFCC 89633	<i>Elaeagnus angustifolia</i>	China	KF765677	KF765693	KU710996	KU710956
<i>Cytospora eriobotryae</i>	IMI 136523*	<i>Eriobotrya japonica</i>	India	AY347327	NA	NA	NA
<i>Cytospora erumpens</i>	CFCC 50022	<i>Prunus padus</i>	China	MH933627	MH933661	MH933534	NA
	MFLUCC 16-0580*	<i>Salix × fragilis</i>	Russia	KY417733	KY417767	KY417699	KY417801
<i>Cytospora eucalypti</i>	CBS 144241	<i>Encalyptus globulus</i>	USA	MG971907	NA	MG972056	NA
	LSEQ	<i>Sequoia sempervirens</i>	USA	AY347340	NA	NA	NA
<i>Cytospora eucalypticola</i>	ATCC 96150*	<i>Eucalyptus nitens</i>	Australia	AY347358	NA	NA	NA
	CMW 5309	<i>Eucalyptus grandis</i>	Uganda	AF260266	NA	NA	NA
<i>Cytospora eucalyptina</i>	CMW 5882	<i>Eucalyptus grandis</i>	Columbia	AY347375	NA	NA	NA
	CMW 7029	<i>Tibouchina</i> sp.	Australia	AY347364	NA	NA	NA
<i>Cytospora eugeniae</i>	CMW 8648	<i>Eugenia</i> sp.	Indonesia	AY347344	NA	NA	NA
	CFCC 50499*	<i>Euonymus kiautschovicus</i>	China	MH933628	MH933662	MH933535	MH933598
<i>Cytospora euonymicola</i>	CFCC 50500	<i>Euonymus kiautschovicus</i>	China	MH933629	MH933663	MH933536	MH933599
	CFCC 89993*	<i>Euonymus kiautschovicus</i>	China	MH933630	MH933664	MH933537	MH933600
<i>Cytospora euonymina</i>	CFCC 89999	<i>Euonymus kiautschovicus</i>	China	MH933631	MH933665	MH933538	MH933601
	MFLUCC 14-0868*	<i>Euonymus kiautschovicus</i>	China	MH933631	MH933665	MH933538	MH933601

Species	Strain	Host	Origin	ITS	GenBank accession numbers		
					LSU	ACT	RPB2
<i>Cytospora friesii</i>	CBS 194.42	<i>Abies alba</i>	Switzerland	AY347328	NA	NA	NA
<i>Cytospora fugax</i>	CXY 1381	NA	NA	KM034853	NA	NA	NA
<i>Cytospora germanica</i>	CXY 1322	<i>Elaeagnus oxycarpa</i>	China	JQ086563	JX524617	NA	NA
<i>Cytospora gigalobus</i>	CFCC 89620*	<i>Juglans regia</i>	China	KR045628	KR045708	KU710997	KU710957
	CFCC 89621	<i>Juglans regia</i>	China	KR045629	KR045709	KU710998	KU710958
<i>Cytospora gigaspora</i>	CFCC 50014	<i>Juniperus procumbens</i>	China	KR045630	KR045710	KU710999	KU710959
	CFCC 89634*	<i>Salix psammophila</i>	China	KF765671	KF765687	KU711000	KU710960
<i>Cytospora granati</i>	CBS 144237*	<i>Punica granatum</i>	USA	MG971799	NA	MG971949	NA
<i>Cytospora hippophaës</i>	CFCC 89639	<i>Hippophaë rhamnoides</i>	China	KR045632	KR045712	KU711001	KU710961
	CFCC 89640	<i>Hippophaë rhamnoides</i>	China	KF765682	KF765698	KF765730	KU710962
<i>Cytospora japonica</i>	CFCC 89956	<i>Prunus cerasifera</i>	China	KR045624	KR045704	KU710993	KU710953
	CFCC 89960	<i>Prunus cerasifera</i>	China	KR045625	KR045705	KU710994	KU710954
<i>Cytospora joaquiniensis</i>	CFCC 89960	<i>Populus deltoides</i>	USA	MG971895	NA	MG972044	NA
<i>Cytospora junipericola</i>	CBS 144235*	<i>Juniperus communis</i>	Italy	MF190125	MF190072	NA	NA
<i>Cytospora juniperina</i>	MFLU 17-0882*	<i>Juniperus communis</i>	China	MH933632	MH933666	MH933539	MH933602
	CFCC 50501*	<i>Juniperus przewalskii</i>	China	MH933634	MH933668	MH933541	MH933604
	CFCC 50503	<i>Juniperus przewalskii</i>	China	KM034867	NA	NA	NA
<i>Cytospora kantschavelii</i>	CXY 1383	<i>Populus maximowiczii</i>	China	KM034867	NA	NA	NA
<i>Cytospora kuamchengensis</i>	CFCC 52464*	<i>Castanea mollissima</i>	China	MK432616	MK429886	MK442940	MK578076
	CFCC 52465	<i>Castanea mollissima</i>	China	MK432617	MK429887	MK442941	MK578077
<i>Cytospora kunzei</i>	CBS 118556	<i>Pinus radiata</i>	South Africa	DQ243791	NA	NA	NA
<i>Cytospora leucosperma</i>	CFCC 89622	<i>Pyrus bretschneideri</i>	China	KR045616	KR045698	KU710988	KU710944
	CFCC 89894	<i>Pyrus bretschneideri</i>	China	KR045617	KR045699	KU710989	KU710945
<i>Cytospora leucostoma</i>	CFCC 50018	<i>Prunus serrulata</i>	China	MH933636	MH933670	MH933543	NA
	CFCC 50019	<i>Rosa helena</i>	China	MH933637	MH933671	MH933544	NA
	CFCC 50021	<i>Prunus salicina</i>	China	MH933639	MH933673	MH933546	NA
	CFCC 50023	<i>Cornus alba</i>	China	KR045635	KR045715	KU711003	KU710964
	CFCC 52461	<i>Castanea mollissima</i>	China	MK432624	MK429894	MK442948	NA
	CFCC 52462	<i>Castanea mollissima</i>	China	MK432625	MK429895	MK442949	NA
<i>Cytospora longostiolata</i>	MFLUCC 16-0628*	<i>Salix x fragilis</i>	Russia	KY417734	KY417768	KY417700	KY417802
<i>Cytospora longispora</i>	CBS 144236*	<i>Prunus domestica</i>	USA	MG971905	NA	MG972054	NA
<i>Cytospora lummitzericola</i>	MFLUCC 17-0508*	<i>Lummitzera racemosa</i>	Taiiland	MG975778	MH253461	MH253457	MH253453
	CFCC 50028	<i>Malus pumila</i>	China	MH933641	MH933675	MH933548	MH933606
<i>Cytospora mali</i>	CFCC 50029	<i>Malus pumila</i>	China	MH933642	MH933676	MH933549	MH933607

Species	Strain	Host	Origin	ITS	GenBank accession numbers			RPB2
					LSU	ACT	RPB2	
<i>Cytospora melnikii</i>	MFLUCC 15-0851*	<i>Malus domestica</i>	Russia	KY417735	KY417769	KY417701	KY417803	
	MFLUCC 16-0635	<i>Populus nigra</i> var. <i>italica</i>	Russia	KY417736	KY417770	KY417702	KY417804	
<i>Cytospora mougeotii</i>	ATCC 44994	<i>Picea abies</i>	Norway	AY347329	NA	NA	NA	
<i>Cytospora multicolis</i>	CBS 105-89T	<i>Quercus ilex</i> subsp. <i>rotundifolia</i>	Spain	DQ243803	NA	NA	NA	
<i>Cytospora myrtigena</i>	CBS 116843*	<i>Tibouchina urvilleana</i>	USA	AY347363	NA	NA	NA	
<i>Cytospora nitschkei</i>	CFCC 52454	<i>Castanea mollissima</i>	China	MK432614	MK429884	MK442938	MK578074	
	CFCC 52455	<i>Castanea mollissima</i>	China	MK432615	MK429885	MK442939	MK578075	
<i>Cytospora nivea</i>	CMW 10180*	<i>Encalyptus globulus</i>	Ethiopia	AY347356	NA	NA	NA	
	CMW 10184	<i>Encalyptus globulus</i>	Ethiopia	AY347355	NA	NA	NA	
<i>Cytospora olearia</i>	CFCC 89641	<i>Elaeagnus angustifolia</i>	China	KF765683	KF765699	KU711006	KU710967	
	CFCC 89643	<i>Salix psammophila</i>	China	KF765685	KF765701	NA	KU710968	
<i>Cytospora palmi</i>	CBS 144248*	<i>Olea europaea</i>	USA	MG971944	NA	MG972098	NA	
<i>Cytospora parakantschavelii</i>	CXY 1280*	<i>Cotinus coggygia</i>	China	JN411939	NA	NA	NA	
	MFLUCC 15-0857*	<i>Populus × sibirica</i>	Russia	KY417738	KY417704	KY417704	KY417806	
<i>Cytospora parapersoonii</i>	MFLUCC 16-0575	<i>Pyrus pyrauster</i>	Russia	KY417739	KY417705	KY417705	KY417807	
	T28.1*	<i>Prunus persica</i>	USA	AF191181	NA	NA	NA	
<i>Cytospora parapsittaciae</i>	CBS 144506*	<i>Pistacia vera</i>	USA	MG971804	NA	MG971954	NA	
<i>Cytospora parasittica</i>	MFLUCC 15-0507*	<i>Malus domestica</i>	Russia	KY417740	KY417774	KY417706	KY417808	
<i>Cytospora paratransluens</i>	MFLUCC 15-0506*	<i>Populus alba</i> var. <i>bolleana</i>	Russia	KY417741	KY417775	KY417707	KY417809	
	MFLUCC 16-0627	<i>Populus alba</i>	Russia	KY417742	KY417776	KY417708	KY417810	
<i>Cytospora pini</i>	CBS 197.42	<i>Pinus sylvestris</i>	Switzerland	AY347332	NA	NA	NA	
	CBS 224.52*	<i>Pinus strobus</i>	USA	AY347316	NA	NA	NA	
<i>Cytospora pistaciae</i>	CBS 144238*	<i>Pistacia vera</i>	USA	MG971802	NA	MG971952	NA	
<i>Cytospora platanicola</i>	MFLU 17-0327*	<i>Platanus hybrida</i>	Italy	MH253451	MH253452	MH253449	MH253450	
<i>Cytospora platycladi</i>	CFCC 50504*	<i>Platycladus orientalis</i>	China	MH933645	MH933679	MH933552	MH933610	
	CFCC 50505	<i>Platycladus orientalis</i>	China	MH933646	MH933680	MH933553	MH933611	
<i>Cytospora platycladicola</i>	CFCC 50506	<i>Platycladus orientalis</i>	China	MH933647	MH933681	MH933554	MH933612	
	CFCC 50038*	<i>Platycladus orientalis</i>	China	KT222840	MH933682	MH933555	MH933613	
<i>Cytospora plurinora</i>	CFCC 50039	<i>Platycladus orientalis</i>	China	KR045642	KR045721	KU711008	KU710973	
	CBS 144239*	<i>Olea europaea</i>	USA	MG971861	NA	MG972010	NA	
<i>Cytospora populicola</i>	CBS 144240*	<i>Populus deltoides</i>	USA	MG971891	NA	MG972040	NA	
<i>Cytospora populina</i>	CFCC 89644*	<i>Salix psammophila</i>	China	KF765686	KF765702	KU711007	KU710969	
<i>Cytospora populinopsis</i>	CFCC 50032*	<i>Sorbus aucuparia</i>	China	MH933648	MH933683	MH933556	MH933614	
	CFCC 50033	<i>Sorbus aucuparia</i>	China	MH933649	MH933684	MH933557	MH933615	

Species	Strain	Host	Origin	GenBank accession numbers			RPB2
				ITS	LSU	ACT	
<i>Cytospora predappioides</i>	MFLUCC 17-2458*	<i>Platanus hybrida</i>	Italy	MG873484	MG873480	NA	NA
<i>Cytospora prunicola</i>	MFLU 17-0995*	<i>Prunus</i> sp.	Italy	MG742350	MG742351	MG742353	MG742352
<i>Cytospora pruinosis</i>	CFCC 50034*	<i>Ulmus pumila</i>	China	KP281259	KP310806	KP310836	KU710970
	CFCC 50035	<i>Ulmus pumila</i>	China	KP281260	KP310807	KP310837	KU710971
	CFCC 50036	<i>Syringa oblata</i>	China	KP310800	KP310802	KP310832	NA
	CFCC 50037	<i>Syringa oblata</i>	China	MH933650	MH933685	MH933558	NA
<i>Cytospora prunicola</i>	MFLU 17-0995*	<i>Prunus</i> sp.	Italy	MG742350	MG742351	MG742353	MG742352
<i>Cytospora puniceae</i>	CBS 144244	<i>Punica granatum</i>	USA	MG971943	NA	MG972091	NA
<i>Cytospora quercicola</i>	MFLU 17-0881	<i>Quercus</i> sp.	Italy	MF190129	MF190074	NA	NA
	MFLUCC 14-0867*	<i>Quercus</i> sp.	Italy	MF190128	MF190073	NA	NA
	MUCC302	<i>Quercus</i> sp.	Italy	MF190128	MF190073	NA	NA
<i>Cytospora rhizophorae</i>		<i>Eucalyptus grandis</i>	Australia	EU301057	NA	NA	NA
<i>Cytospora ribis</i>	CFCC 50026	<i>Ulmus pumila</i>	China	KP281267	KP310813	KP310843	KU710972
	CFCC 50027	<i>Ulmus pumila</i>	China	KP281268	KP310814	KP310844	NA
<i>Cytospora rosae</i>	MFLU 17-0885	<i>Rosa canina</i>	Italy	MF190131	MF190076	NA	NA
<i>Cytospora rostrata</i>	CFCC 89909*	<i>Salix cupularis</i>	China	KR045643	KR045722	KU711009	KU710974
	CFCC 89910	<i>Salix cupularis</i>	China	KR045644	KR045723	KU711010	KU710975
<i>Cytospora rusanovii</i>	MFLUCC 15-0853	<i>Populus × sibirica</i>	Russia	KY417743	KY417778	KY417709	KY417811
	MFLUCC 15-0854*	<i>Salix babylonica</i>	Russia	KY417744	KY417778	KY417710	KY417812
<i>Cytospora salicacearum</i>	MFLUCC 16-0576	dead aerial branch	Russia	KY417747	KY417781	KY417713	KY417815
	MFLUCC 15-0509*	<i>Salix alba</i>	Russia	KY417746	KY417780	KY417712	KY417814
	MFLUCC 15-0861	<i>Salix × fragilis</i>	Russia	KY417745	KY417779	KY417711	KY417813
	MFLUCC 16-0587	NA	NA	KY417748	KY417782	KY417714	KY417816
<i>Cytospora salicicola</i>	MFLUCC 14-1052*	<i>Salix alba</i>	Russia	KU982636	KU982635	KU982637	NA
	MFLUCC 15-0866	<i>Salix alba</i>	Russia	KY417749	KY417783	KY417715	KY417817
<i>Cytospora salicina</i>	MFLUCC 15-0862*	<i>Salix alba</i>	Russia	KY417750	KY417784	KY417716	KY417818
	MFLUCC 16-0637	<i>Salix × fragilis</i>	Russia	KY417751	KY417785	KY417717	KY417819
	CFCC 50040	<i>Malus domestica</i>	China	KR045649	KR045728	KU711013	KU710980
<i>Cytospora schulzeri</i>	CFCC 50042	<i>Malus asiatica</i>	China	KR045650	KR045729	KU711014	KU710981
	CFCC 52468	<i>Castanea mollissima</i>	China	MK432626	MK429896	MK442950	MK578084
	CFCC 52469	<i>Castanea mollissima</i>	China	MK432627	MK429897	MK442951	MK578085
	CFCC 52470	<i>Castanea mollissima</i>	China	MK432628	MK429898	MK442952	MK578086
	CFCC 50045*	<i>Sibiraea angustata</i>	China	KR045651	KR045730	KU711015	KU710982
<i>Cytospora sibiricae</i>	CFCC 50046	<i>Sibiraea angustata</i>	China	KR045652	KR045731	KU711015	KU710983

Species	Strain	Host	Origin	GenBank accession numbers			RPB2
				ITS	LSU	ACT	
<i>Cytospora sophorae</i>	CFCC 50048	<i>Magnolia grandiflora</i>	China	MH820401	MH820394	MH820409	MH820397
	CFCC 89598	<i>Syphnolobium japonicum</i>	China	KR045654	KR045733	KU711018	KU710985
<i>Cytospora sophoricola</i>	CFCC 89595*	<i>Syphnolobium japonicum</i> var. <i>pendula</i>	China	KR045655	KR045734	KU711019	KU710986
	CFCC 89596	<i>Syphnolobium japonicum</i> var. <i>pendula</i>	China	KR045656	KR045735	KU711020	KU710987
<i>Cytospora sophoropsis</i>	CFCC 89600*	<i>Syphnolobium japonicum</i>	China	KR045653	KP310804	KU710992	KU710951
<i>Cytospora sorbi</i>	MFLUCC 16-0631*	<i>Sorbus aucuparia</i>	Russia	KY417752	KY417786	KY417718	KY417820
<i>Cytospora sorbicola</i>	MFLUCC 16-0584*	<i>Acer pseudoplatanus</i>	Russia	KY417755	KY417789	KY417721	KY417823
	MFLUCC 16-0633	<i>Cotoneaster melanocarpus</i>	Russia	KY417758	KY417792	KY417724	KY417826
<i>Cytospora spiratae</i>	CFCC 50049*	<i>Spiraea salicifolia</i>	China	MG707859	MG707643	MG708196	MG708199
	CFCC 50050	<i>Spiraea salicifolia</i>	China	MG707860	MG707644	MG708197	MG708200
<i>Cytospora tamaricicola</i>	CFCC 50507	<i>Rosa multiflora</i>	China	MH933651	MH933686	MH933559	MH933616
	CFCC 50508*	<i>Tamarix chinensis</i>	China	MH933652	MH933687	MH933560	MH933617
<i>Cytospora tanaitica</i>	MFLUCC 14-1057*	<i>Betula pubescens</i>	Russia	KT459411	KT459412	KT459413	NA
<i>Cytospora thailandica</i>	MFLUCC 17-0262*	<i>Xylocarpus moluccensis</i>	Thailand	MG975776	MH253463	MH253459	MH253455
	MFLUCC 17-0263	<i>Xylocarpus moluccensis</i>	Thailand	MG975777	MH253464	MH253460	MH253456
<i>Cytospora tibouchinae</i>	GPC 26333*	<i>Tibouchina semidecandra</i>	France	KX228284	KX228335	NA	NA
<i>Cytospora translucens</i>	CXY 1351	<i>Populus davidiana</i>	China	KM034874	NA	NA	NA
<i>Cytospora ulmi</i>	MFLUCC 15-0863*	<i>Ulmus minor</i>	Russia	KY417759	NA	NA	NA
<i>Cytospora ulmicola</i>	MFLUCC 18-1227*	<i>Ulmus pumila</i>	Russia	MH940220	MH940218	MH940216	NA
<i>Cytospora valsoidea</i>	CMW 4309*	<i>Eucalyptus grandis</i>	Indonesia	AF192312	NA	NA	NA
	CMW 4310	<i>Eucalyptus grandis</i>	Indonesia	AF192312	NA	NA	NA
<i>Cytospora variostromatica</i>	CBS 118086	<i>Eucalyptus grandis</i>	Indonesia	AF192312	NA	NA	NA
	CBS 141585*	<i>Eucalyptus grandis</i>	South Africa	AF260264	NA	NA	NA
	CBS 141586*	<i>Eucalyptus grandis</i>	South Africa	AF260263	NA	NA	NA
	CMW 1240	<i>Eucalyptus grandis</i>	South Africa	AF260263	NA	NA	NA
	CMW 6766*	<i>Eucalyptus globulus</i>	Australia	AY347366	NA	NA	NA
<i>Cytospora vinacea</i>	CBS 141585*	<i>Vitis</i> interspecific hybrid 'Vidal'	USA	KX256256	NA	NA	NA
<i>Cytospora viticola</i>	CBS 141586*	<i>Vitis vinifera</i> 'Cabernet Franc'	USA	KX256239	NA	NA	NA
<i>Cytospora xinglongensis</i>	CFCC 52458*	<i>Castanea mollissima</i>	China	MK432622	MK429892	MK442946	MK578082
	CFCC 52459	<i>Castanea mollissima</i>	China	MK432623	MK429893	MK442947	MK578083
<i>Cytospora xylocarpi</i>	MFLUCC 17-0251*	<i>Xylocarpus granatum</i>	Thailand	MG975775	MH253462	MH253458	MH253454
<i>Diaporthe vaccinii</i>	CBS 160.32	<i>Vaccinium macrocarpon</i>	USA	KC343228	NA	JQ807297	NA

The MP analysis resulted in 14 equally most parsimonious trees and the first tree (TL = 3270, CI = 0.344, RI = 0.815, RC = 0.281) was present as in Fig. 2. The ML analysis yielded a tree with a likelihood value of ln: -18627.915604 and the following model parameters: alpha: 0.181328; $\Pi(A)$: 0.246855, $\Pi(C)$: 0.260898, $\Pi(G)$: 0.272379 and $\Pi(T)$: 0.219868. Isolates from *Castanea mollissima* formed six clades in Fig. 2, representing two undescribed species and four known species.

Taxonomy

Cytospora ceratospermopsis C.M. Tian & X.L. Fan, *Persoonia* 45: 19. 2020

Figure 3

Description. Sexual morph: Ascostromata immersed in the bark, erumpent through the surface of bark, scattered, (350–)550–900(–1300) μm diam., with 15–40 perithecia arranged circularly or irregularly. Conceptacle absent. Ectostromatic disc black, usually surrounded by tightly ostiolar necks, circular to ovoid, (180–)240–410(–450) μm diam. Ostioles black, at the same level as the disc or slightly above, concentrated, dark brown to black, arranged circularly in a disc, (55–)60–85(–110) μm diam. Perithecia dark brown, flask-shaped to spherical, arranged circularly or irregularly, (255–)280–350(–420) μm diam. Asci clavate to elongate obovoid, 8-spored, (20.5–)27–35.5(–43) \times (4–)4.5–6.5(–8) μm (\bar{x} = 31.2 \times 5.6 μm). Ascospores biseriate, elongate-allantoid, thin-walled, hyaline, aseptate, (5.8–)7.5–9.2(–11.5) \times (3–)3.2–4.8(–5.5) μm (\bar{x} = 8.6 \times 4.1 μm). Asexual morph: Pycnidial stromata ostiolated, immersed in bark, scattered, erumpent through the surface of bark, discoid to conical, with multiple locules. Conceptacle absent. Ectostromatic disc light brown to grey, circular to ovoid, (230–)280–360(–480) μm diam., with one ostiole per disc. Ostiole in the centre of the disc, dark grey to black, conspicuous, at the same level as the disc, (60–)75–110(–135) μm diam. Locule numerous, arranged circularly or elliptically with independent walls, (300–)350–600(–950) μm diam. Peridium comprising few layers of cells of textura angularis, with innermost layer brown, outer layer brown to dark brown. Conidiophores hyaline, branched or not, thin walled, filamentous. Conidiogenous cells enteroblastic polyphialidic, (6.5–)8.5–15.5(–18) \times 1.5–2.5 μm (\bar{x} = 12.2 \times 1.9 μm). Conidia hyaline, allantoid, smooth, aseptate, thin-wall, (4.5–)5–6.5(–7) \times 1–1.5 μm (\bar{x} = 5.9 \times 1.3 μm).

Culture characters. On PDA at 25 °C in darkness. Cultures are initially white, becoming olivaceous buff in centre after 7 d and finally olivaceous at 30 d. The colony is flat, thin with a felt and tight texture in centre. Pycnidia distributed irregularly on medium surface.

Specimens examined. CHINA, Hebei Province, Chengde City, Xinglong County, chestnut plantation, 40°24'32"N, 117°27'56"E, on branches of *Castanea mollissima*, 11 October 2017, N. Jiang (BJFC-S1699, living culture CFCC 52471 from the ascospore; BJFC-S1700, living culture CFCC 52472 from the conidium).

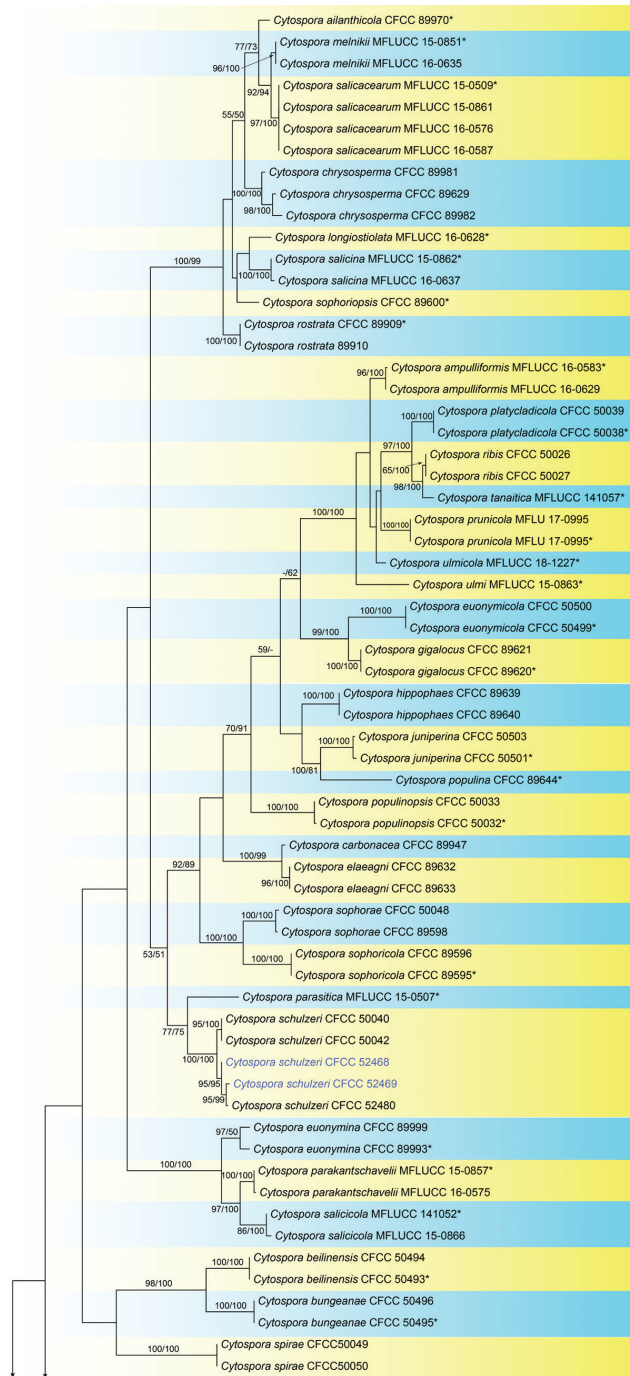


Figure 2. Maximum parsimony phylogram of *Cytospora* obtained from the combined matrix of ITS, LSU, ACT and RPB2 genes. Bootstrap value $\geq 50\%$ for MP and ML analyses are presented at the first and second position. Scale bar = 200 nucleotide substitutions. The strains in the current study are in blue and ex-strains are marked with *.

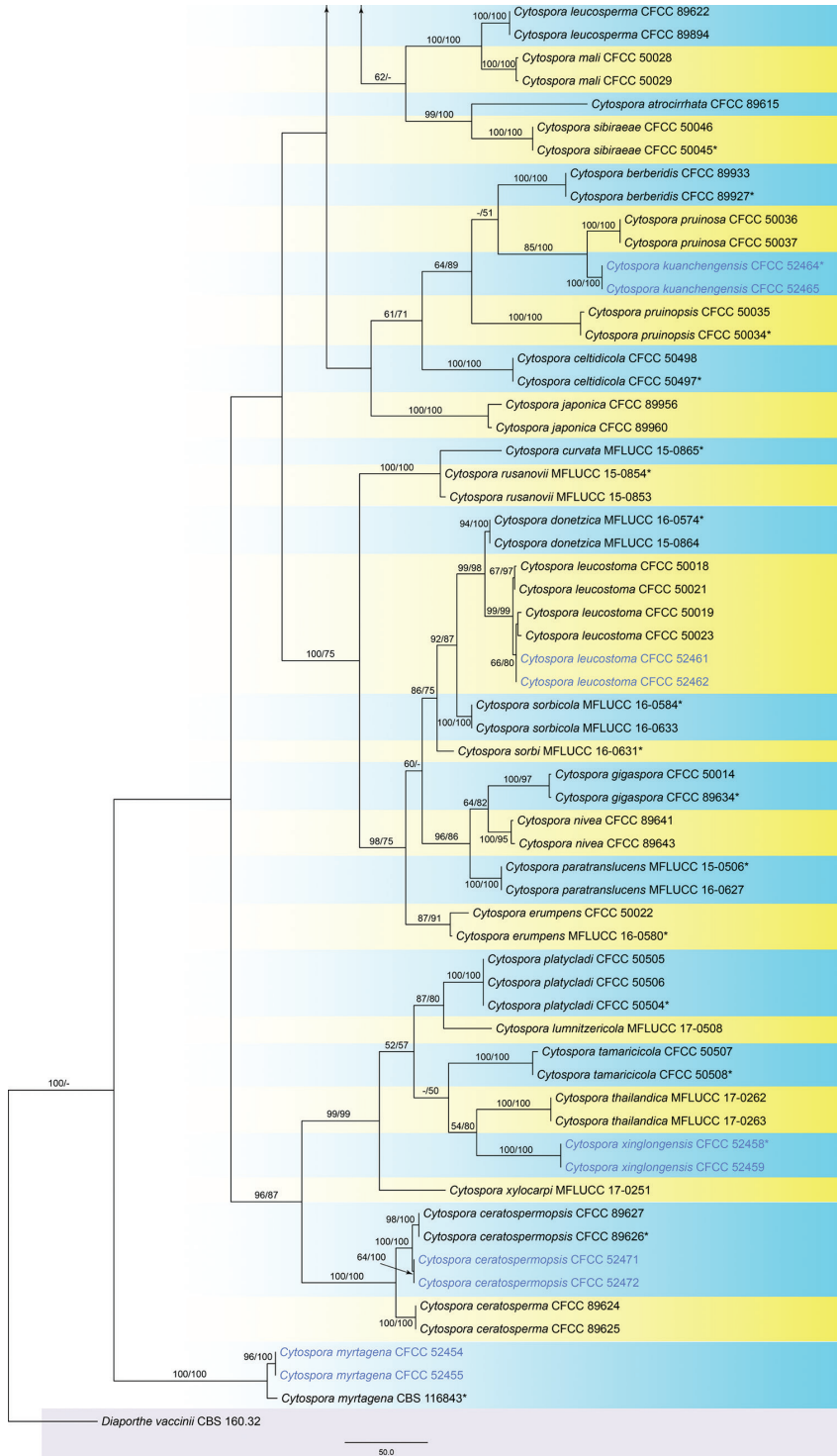


Figure 2. Continued.

Notes. Fresh specimens with both sexual and asexual morphs were collected from cankered branches of *Castanea mollissima* and two isolates were obtained from the ascospore and conidium, respectively. Phylogenically, the two isolates were close to *Cytospora ceratospermopsis* represented by CFCC 89626 and CFCC 89627 (Fig. 2). We compared their sequences and found no differences in LSU and RPB2, but 2 bp differences in ITS and 3 bp differences in ACT. Fan et al. (2020) reported the asexual morph of *Cytospora ceratospermopsis* from *Juglans regia* in China with conidial size in $4.5\text{--}6 \times 1\text{--}1.5 \mu\text{m}$, which is exactly matched with the asexual characters observed in the present study. Hence, we described the asexual morph of *Cytospora ceratospermopsis* in its sexual morph for the first time and reported a new host, *Castanea mollissima*.

***Cytospora kuanchengensis* C.M. Tian & N. Jiang, sp. nov.**

Mycobank No: 829514

Figure 4

Diagnosis. *Cytospora kuanchengensis* can be distinguished from *C. oleicola* and *C. pruinosa* by longer conidia.

Etymology. Named after the county where it was collected, Kuancheng County.

Description. Sexual morph: not observed. Asexual morph: Pycnidial stromata ostiolated, immersed in bark, scattered, erumpent through the surface of bark, discoid, with multiple locules. Conceptacle black, circular surrounded stromata. Ectostromatic disc black, circular to ovoid, $(350\text{--})455\text{--}540(\text{--}575) \mu\text{m}$ diam., with 1–7 ostiole per disc. Ostioles black, at the same level as the disc, $(40\text{--})60\text{--}85(\text{--}115) \mu\text{m}$ diam. Locule numerous, arranged circularly or elliptically with independent walls, $(285\text{--})355\text{--}520(\text{--}605) \mu\text{m}$ diam. Peridium comprising few layers of cells of *textura angularis*, with innermost layer brown, outer layer brown to dark brown. Conidiophores hyaline, unbranched, thin walled, filamentous. Conidiogenous cells enteroblastic polyphialidic, $(6.5\text{--})8.5\text{--}11(\text{--}15) \times 1\text{--}1.5 \mu\text{m}$ ($\bar{x} = 9.8 \times 1.3 \mu\text{m}$). Conidia hyaline, allantoid, smooth, aseptate, thin-walled, $(5.5\text{--})6\text{--}7.5(\text{--}8) \times 1\text{--}2 \mu\text{m}$ ($\bar{x} = 6.9 \times 1.6 \mu\text{m}$).

Culture characters. On PDA at 25 °C in darkness. Cultures are initially white, producing pale brown pigment after 10 d. The colony is flat, felt-like, with concentric circular texture. Pycnidia distributed irregularly on medium surface.

Specimens examined. CHINA, Hebei Province, Chengde City, Kuancheng County, chestnut plantation, $40^{\circ}38'37''\text{N}$, $118^{\circ}27'54''\text{E}$, on branches of *Castanea mollissima*, 13 October 2017, N. Jiang (**holotype** BJFC-S1695, ex-type living culture CFCC 52464; **paratype** BJFC-S1696, living culture CFCC 52465).

Notes. *Cytospora kuanchengensis* is associated with canker disease of *Castanea mollissima* in China. *Cytospora kuanchengensis* differs from its phylogenetically closely species, *C. pruinosa*, by ITS and ACT loci (7/470 in ITS and 21/245 in ACT). Morphologically, *C. kuanchengensis* has slightly larger conidia than *C. pruinosa* ($5.5\text{--}8 \times 1\text{--}2 \mu\text{m}$ in *Cytospora kuanchengensis* vs. $5\text{--}7.5 \times 1\text{--}1.5 \mu\text{m}$ in *C. pruinosa*) (Fan et al. 2020).

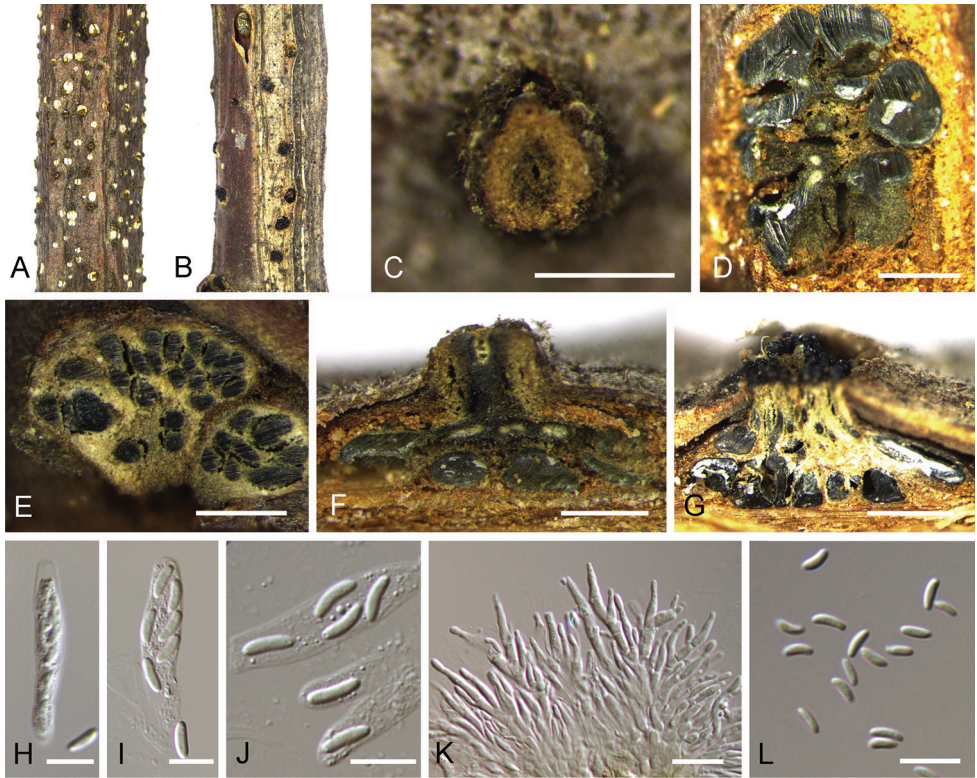


Figure 3. *Cytospora ceratospermopsis* on *Castanea mollissima* (BJFC-S1699, BJFC-S1700). **A, C** Habit of conidiomata on branches **B** habit of ascomata on branches **D** transverse section of conidiomata **E** transverse section of ascomata **F** longitudinal section through conidiomata **G** longitudinal section through ascomata **H, I** asci **J** asci spores **K** conidiogenous cells with attached conidia **L** conidia. Scale bars: 500 μm (**C-G**), 10 μm (**H-L**).

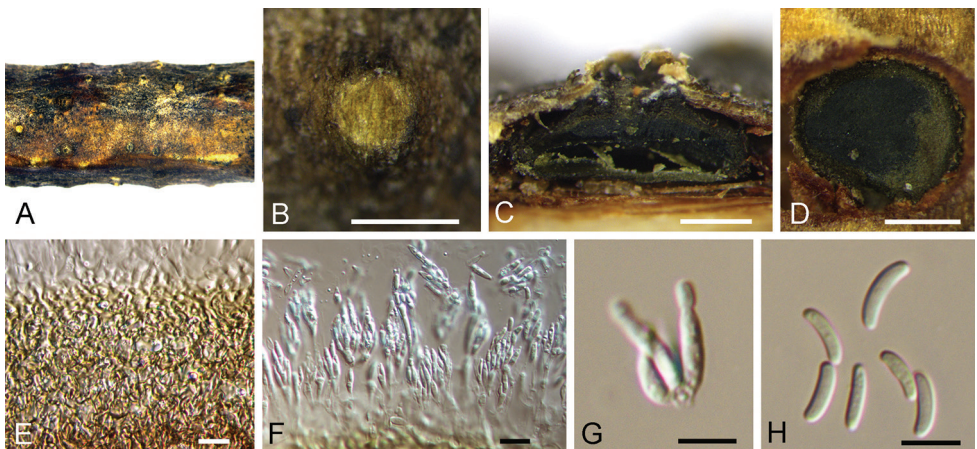


Figure 4. *Cytospora kuanchengensis* on *Castanea mollissima* (BJFC-S1695). **A, B** Habit of conidiomata on branches **C** longitudinal section through conidiomata **D** transverse section of conidiomata **E** peridium **F, G** conidiogenous cells attached with conidia **H** conidia. Scale bars: 500 μm (**B-D**), 10 μm (**E-G**), 5 μm (**H**).

***Cytospora leucostoma* (Pers.) Sacc., *Michelia* 2(7): 264. 1881.**

Figure 5

Description. Sexual morph: not observed. Asexual morph: Pycnidial stromata ostiolated, immersed in bark, scattered, erumpent through the surface of bark, with multiple locules. Conceptacle black. Ectostromatic disc black, circular to ovoid, (150–)250–300(–375) μm diam., with one ostiole per disc. Ostioles black, at the same level as the disc, (40–)50–85(–115) μm diam. Locule numerous, arranged circularly or elliptically with independent walls, (550–)700–1200(–1350) μm diam. Peridium comprising few layers of cells of *textura angularis*, with innermost layer brown, outer layer brown to dark brown. Conidiophores hyaline, unbranched, thin walled, filamentous. Conidiogenous cells enteroblastic polyphialidic, (7.5–)9.5–21(–22.5) \times 1–1.5 μm (\bar{x} = 15.2 \times 1.3 μm). Conidia hyaline, allantoid, smooth, aseptate, thin-walled, (3.5–)4.5–5.5(–7) \times 1–1.5 μm (\bar{x} = 4.9 \times 1.3 μm).

Specimens examined. CHINA, Hebei Province, Chengde City, Kuancheng County, chestnut plantation, 40°38'37"N, 118°27'5"E, on branches of *Castanea mollissima*, 13 October 2017, N. Jiang (BJFC-S1697, living culture CFCC 52461; BJFC-S1698, living culture CFCC 52462).

Notes. *Cytospora leucostoma* is a common species causing canker disease on Rosaceae in China (Teng 1963, Tai 1979, Wei 1979, Fan et al. 2020). In this study, fresh specimens were collected from diseased branches of the Chinese chestnut for the first time and identified as *Cytospora leucostoma*, based on strictly matched asexual morph (4–5.5 \times 1–2 μm from *Castanea mollissima* in this study vs. 4.5–5.5 \times 1–1.5 μm from multiple specimens in Fan et al. 2020) and phylogenetic analysis (Fig. 2).

***Cytospora myrtagena* (G.C. Adams & M.J. Wingf.) G.C. Adams & Rossman, *IMA Fungus* 6 (1): 147. 2015.**

Figure 6

Description. Sexual morph: not observed. Asexual morph: Pycnidial stromata pulvinate, immersed in bark, scattered, erumpent through the surface of bark. Conceptacle absent. Ostiole dark grey to black, conspicuous, at the same level as the disc, (50–)65–75(–82) μm diam. Locules undivided, circular to ovoid, (430–)550–720(–810) μm diam. Peridium comprising few layers of cells of *textura angularis*, with innermost layer brown, outer layer brown to dark brown. Conidiophores hyaline, unbranched, thin-walled, filamentous. Conidiogenous cells enteroblastic polyphialidic, (6.5–)8.4–12.5(–15.3) \times 0.9–1.4 μm (\bar{x} = 10.2 \times 1.2 μm). Conidia hyaline, allantoid, smooth, aseptate, thin-walled, (3.2–)3.4–5.4(–6.2) \times 1–1.5 μm (\bar{x} = 4.7 \times 1.3 μm).

Culture characters. On PDA at 25 °C in darkness. Cultures are initially white, becoming olivaceous buff in centre after 7 d and finally olivaceous at 30 d. The colony is flat, thin with a felt and tight texture in centre. Pycnidia distributed irregularly on medium surface.

Specimens examined. CHINA, Shaanxi Province, Ankang City, Xiangxidong forest park, 32°40'33"N, 109°18'57"E, on stem barks of *Castanea mollissima*, 1 July

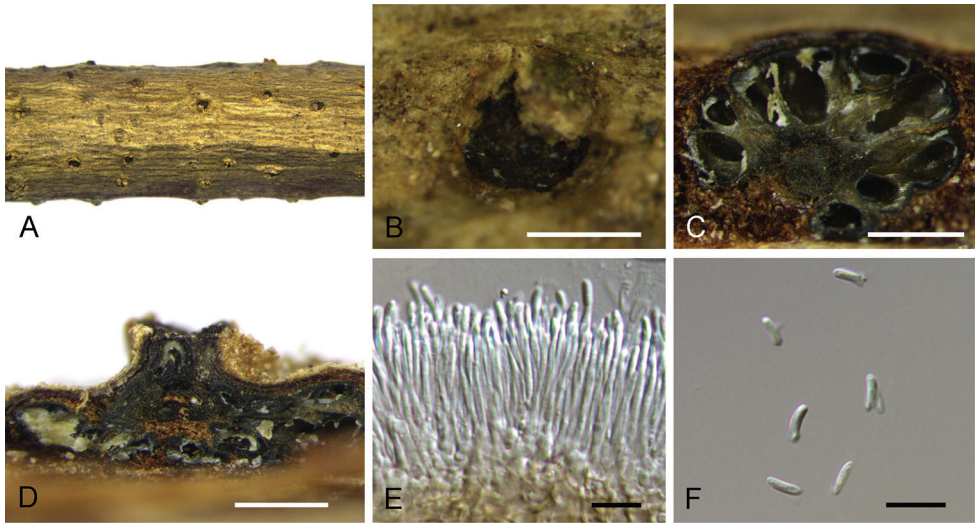


Figure 5. *Cytospora leucostoma* on *Castanea mollissima* (BJFC-S1697). **A, B** Habit of conidiomata on branches **C** transverse section of conidiomata **D** longitudinal section through conidiomata **E** conidiogenous cells attached with conidia **F** conidia. Scale bars: 500 μm (**B–D**), 10 μm (**E, F**).

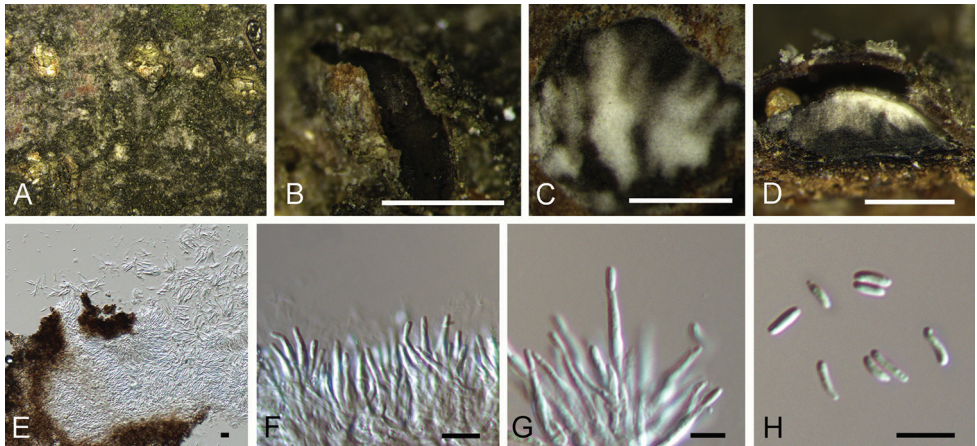


Figure 6. *Cytospora myrtagena* on *Castanea mollissima* (BJFC-S1704). **A, B** Habit of conidiomata on branches **C, E** transverse section of conidiomata **D** longitudinal section through conidiomata **F, G** conidiogenous cells attached with conidia **H** conidia. Scale bars: 500 μm (**B–D**), 5 μm (**E, G**), 10 μm (**H**).

2017, N. Jiang (BJFC-S1704, living culture CFCC 52454; BJFC-S1705, living culture CFCC 52455).

Notes. *Cytospora myrtagena* was introduced from *Eucalyptus* and *Tibouchina* in America and Indonesia (Adams et al. 2005). Two ITS sequences of *Cytospora myrtagena* were available, AY347363 from the type strain CBS 116843 and AY347380 from CBS 117013. However, there are 14 bp differences between AY347363 and AY347380. *Cytospora tibouchinae* was introduced as a phylogenetically close species to *Cytospora myrtagena*

(Suppl. material 1: Fig. S1), with 21 bp differences to CBS 116843 and 14 bp differences to CBS 117013 (Crous et al. 2016). Two isolates from *Castanea mollissima* in the present study were close to *Cytospora myrtagena* and *Cytospora tibouchinae* (Suppl. material 1: Fig. S1), with 22 bp differences to CBS 116843, 15 bp differences to CBS 117013 and 6 bp differences to *Cytospora tibouchinae*. Morphologically, they have similar conidial sizes ($3.4\text{--}5.4 \times 1\text{--}1.5 \mu\text{m}$ in BJFC-S1704 vs. $3\text{--}4 \times 1 \mu\text{m}$ in *C. myrtagena* vs. $3\text{--}4 \times 1.5\text{--}2 \mu\text{m}$ in *C. tibouchinae*) (Adams et al. 2005, Crous et al. 2016). Hence, it is hard to identify our isolates to *C. myrtagena* or *C. tibouchinae*, for the large differences between two ITS sequences in *C. myrtagena* provided by Adams et al. (2005) and absence of ACT and RPB2 loci in *C. myrtagena* and *C. tibouchinae*. We give the name *Cytospora myrtagena* to our isolates provisionally, and hope for more studies on this species.

***Cytospora schulzeri* Sacc. & P. Syd., Syll. fung. (Abellini) 14(2): 918. 1899.**

Figure 7

Description. Sexual morph: not observed. Asexual morph: Pycnidial stromata ostiolated, immersed in bark, scattered, erumpent through the surface of bark, flat, discoid, with multiple locules. Conceptacle absent. Ectostromatic disc brown, circular to ovoid, (250–)300–400(–475) μm diam., with 1–5 ostiole per disc. Ostioles black, at the same level as the disc, (40–)50–85(–115) μm diam. Locule numerous, arranged circularly with common walls, (600–)700–1500(–1750) μm diam. Peridium comprising a few layers of cells of textura angularis, with innermost layer brown, outer layer brown to dark brown. Conidiophores hyaline, unbranched, thin walled, filamentous. Conidiogenous cells enteroblastic polyphialidic, (6.5–)8.5–18.5(–21) \times 1–2 μm (\bar{x} = 13.1 \times 1.6 μm). Conidia hyaline, allantoid, smooth, aseptate, thin-walled, (3.5–)4.5–6.5(–7) \times 1–1.5 μm (\bar{x} = 5.2 \times 1.3 μm).

Specimens examined. CHINA, Hebei Province, Chengde City, Kuancheng County, chestnut plantation, 40°38'37"N, 118°27'54"E, on branches of *Castanea mollissima*, 13 October 2017, N. Jiang (living culture CFCC 52468; BJFC-S1702, living culture CFCC 52469; BJFC-S1703, living culture CFCC 52470).

Notes. *Cytospora schulzeri* is a common species causing apple canker disease in China (Teng 1963, Tai 1979, Wei 1979, Zhuang 2005, Fan et al. 2020). In this study, fresh specimens were collected from diseased branches of chestnut trees and identified as *Cytospora schulzeri*, based on the strictly matched asexual morph (4.5–6.5 \times 1–2 μm from *Castanea mollissima* in this study vs. 4–7 \times 1–1.5 μm from multiple specimens in Fan et al. (2020)) and phylogenetic analysis (Fig. 2).

***Cytospora xinglongensis* C.M. Tian & N. Jiang, sp. nov.**

Mycobank No: 829517

Figure 8

Diagnosis. *Cytospora xinglongensis* can be distinguished from *C. californica* and *C. eucalypti* by longer conidia.

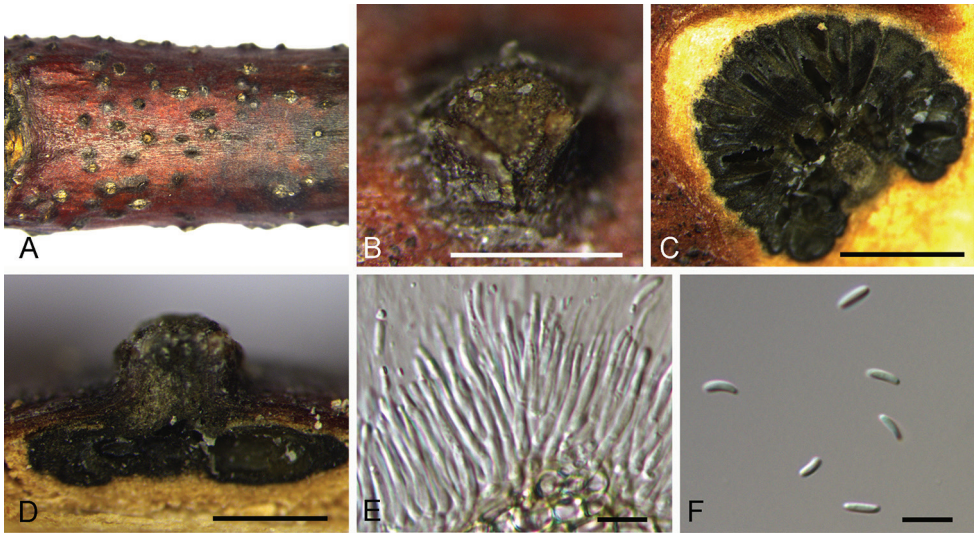


Figure 7. *Cytospora schulzeri* on *Castanea mollissima* (BJFC-S1702). **A, B** Habit of conidiomata on branches **C** transverse section of conidiomata **D** longitudinal section through conidiomata **E** conidiogenous cells attached with conidia **F** conidia. Scale bars: 500 μm (**B–D**), 10 μm (**E, F**).

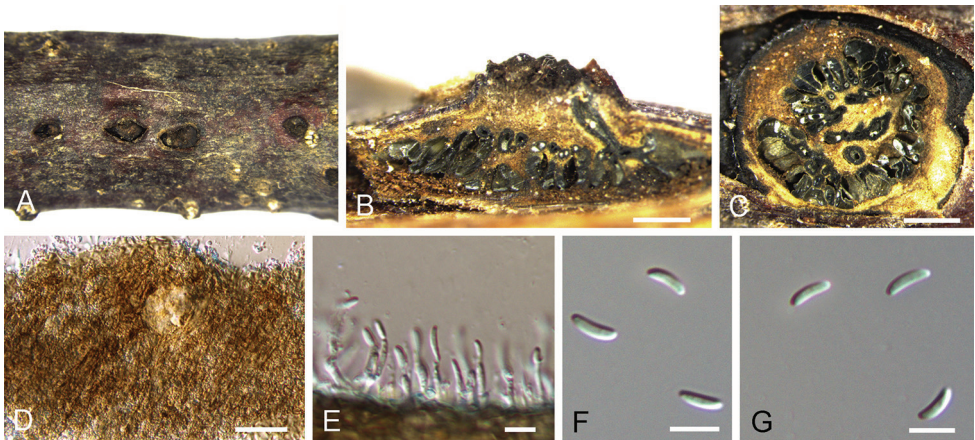


Figure 8. *Cytospora xinglongensis* on *Castanea mollissima* (BJFC-S1706). **A** Habit of conidiomata on branches **B** longitudinal section through conidiomata **C** transverse section of conidiomata **D** peridium **E** conidiogenous cells attached with conidia **F, G** conidia. Scale bars: 500 μm (**B, C**), 10 μm (**E–G**).

Etymology. Named after the county where it was collected, Xinglong County.

Description. Sexual morph: not observed. Asexual morph: Pycnidial stromata immersed in bark, erumpent through the surface of bark, discoid, with a solitary undivided locule. Conceptacle black, circular surrounded stromata. Ostiole inconspicuous. Locules undivided, circular to ovoid, (480–)540–685(–755) μm diam. Conidiophores hyaline, unbranched. Peridium comprising a few layers of cells of textura angularis,

with innermost layer brown, outer layer brown to dark brown. Conidiogenous cells enteroblastic polyphialidic, $(4.5\text{--}6.5\text{--}8.5(-12) \times 1\text{--}1.5 \mu\text{m})$ ($\bar{x} = 7.4 \times 1.3 \mu\text{m}$). Conidia hyaline, allantoid, eguttulate, smooth, aseptate, thin-walled, $(7.5\text{--}8.5\text{--}9.5(-10.5) \times 1\text{--}1.5 \mu\text{m})$ ($\bar{x} = 8.9 \times 1.3 \mu\text{m}$).

Culture characters. On PDA at 25 °C in darkness. Cultures are white. The colony is flat, thin with a uniform texture, lacking aerial mycelium. Pycnidia distributed uniformly on medium surface.

Specimens examined. CHINA, Hebei Province, Chengde City, Xinglong County, chestnut plantation, 40°24'32"N, 117°28'56"E, on branches of *Castanea mollissima*, 11 October 2017, N. Jiang (**holotype** BJFC-S1706, ex-type living culture CFCC 52458; **paratype** BJFC-S1707, living culture CFCC 52459).

Notes. *Cytospora xinglongensis* is associated with canker disease of *Castanea mollissima* in China. *Cytospora xinglongensis* can be distinguished from its phylogenetically closely species *C. thailandica* by having much longer conidia (8.5–9.5 μm in *C. xinglongensis* vs. 3.3–4 μm in *C. thailandica*) (Norphanphoun et al. 2018). In addition, *Cytospora xinglongensis* differs from *C. thailandica* by ITS, ACT and RPB2 loci (16/470 in ITS, 22/245 in ACT and 52/726 in RPB2).

Discussion

In the present study, an important fruit tree species, *Castanea mollissima* was investigated and *Cytospora* canker was found as a common disease in plantations in Hebei Province. Identification was conducted based on 13 isolates from fruiting bodies using both morphological and molecular methods. As a result, six *Cytospora* species were confirmed. *Cytospora kuanchengensis* and *C. xinglongensis* are introduced as new species, *C. ceratospermopsis*, *C. leucostoma*, *C. myrtagena* and *C. schulzeri* are firstly reported on *Castanea mollissima*.

These six chestnut *Cytospora* species can be easily distinguished using DNA sequences of single ITS sequence or combined sequences of ITS, LSU, ACT and RPB2 (Fig. 2; Suppl. material 1: Fig. S1). In addition, colonies on PDA and MEA of these six species are also different (Fig. 9). *Cytospora xinglongensis* never produce fruiting bodies on PDA or MEA, while the other five species form conidiomata in one month (Fig. 9). Morphologically, *Cytospora xinglongensis* has obviously longer conidia than others. However, the conidial dimension can hardly distinguish *C. ceratospermopsis*, *C. kuanchengensis*, *C. leucostoma*, *C. myrtagena* and *C. schulzeri*.

Dar and Rai reported *Cytospora* diseases on *Castanea sativa* in India, causing perennial cankers on stems and branches (Dar and Rai 2014). The *Cytospora* isolates were identified mainly based on ITS sequence data, which were introduced as a new species named *Cytospora castaneae* (wrongly written as *Cytospora castanae* in the original paper) (Dar and Rai 2014). However, further study is required to confirm the species position within the genus, including detailed morphological features and sequences of high quality.

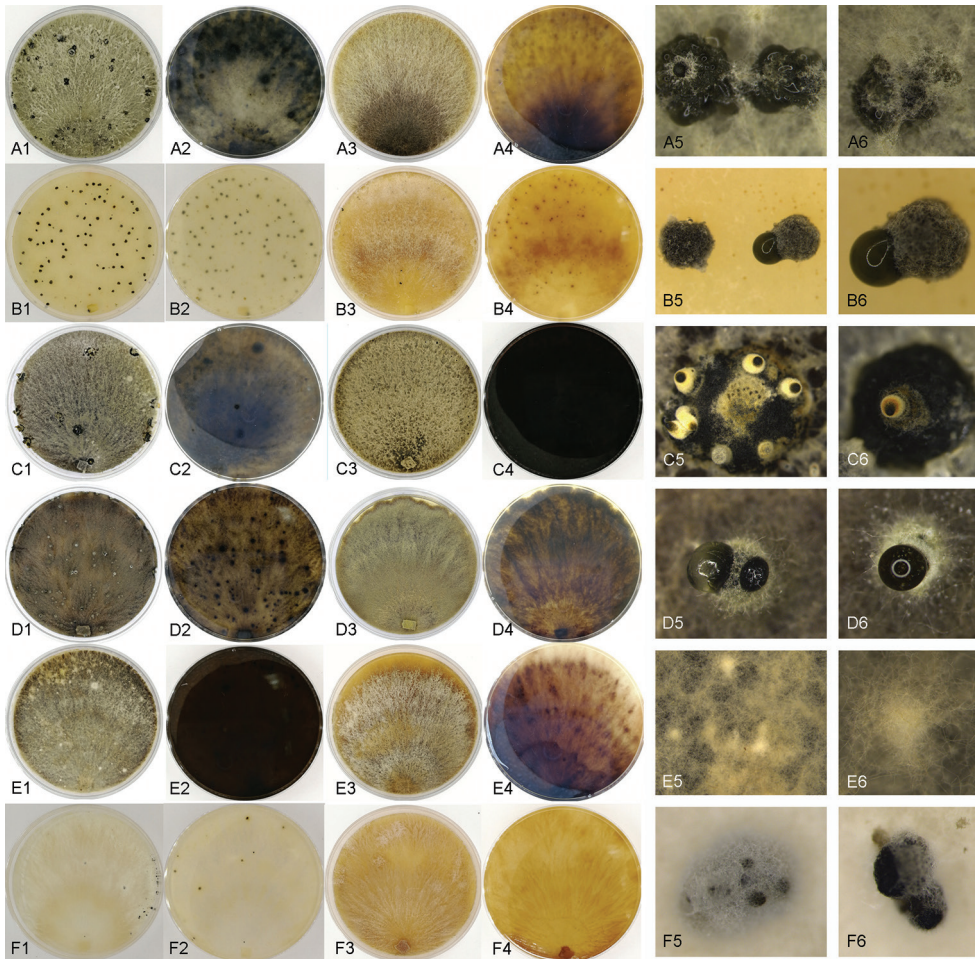


Figure 9. Cultures of *Cytospora* species from *Castanea mollissima* after 1 month at 25 °C. **A** *C. myrtagena* **B** *C. kuanchengensis* **C** *C. ceratospermopsis* **D** *C. leucostoma* **E** *C. xinglongensis* **F** *C. schulzeri* **A1–G2** cultures on PDA **A3–G4** cultures on MEA **A5–G6** fruiting bodies or hyphal masses produced on cultures

Cytospora canker is a common disease on chestnut trees, but there are few formal reports. In China, this disease is known amongst phytopathologists, but no-one conducted accurate identifications. Hence, this paper is the first formal report of *Cytospora* chestnut canker in China. From our investigations of chestnut diseases in China, *Cytospora* species are closely associated with canker diseases in chestnut plantations. In most cases, they infect twigs or small branches, causing necrotic lesions (Fig. 1A), finally forming fruiting bodies on dead tissues (Fig. 1D). However, *Cytospora myrtagena* was discovered on stems of a 15-year-old chestnut tree, causing typical *Cytospora* canker symptoms. More works should be conducted on the newly emerging pathogens from several aspects.

As the species concept of *Cytospora* has been improved a lot by using molecular data (Yang et al. 2015, Lawrence et al. 2017, Norphanphoun et al. 2017, 2018, Jaya-

wardena et al. 2019, Fan et al. 2020), many *Cytospora* canker diseases and new species have been discovered and reported in recent years. Further studies are, however, now required to confirm their pathogenicity.

Acknowledgements

This study is financed by National Natural Science Foundation of China (Project No.: 31670647). We are grateful to Chungen Piao, Minwei Guo (China Forestry Culture Collection Center (CFCC), Chinese Academy of Forestry, Beijing).

References

- Adams GC, Roux J, Wingfield MJ, Roux J (2005) Phylogenetic relationships and morphology of *Cytospora* species and related teleomorphs (Ascomycota, Diaporthales, Valsaceae) from *Eucalyptus*. *Studies in Mycology* 52: 1–144.
- Adams GC, Roux J, Wingfield MJ (2006) *Cytospora* species (Ascomycota, Diaporthales, Valsaceae), introduced and native pathogens of trees in South Africa. *Australasian Plant Pathology* 35: 521–548. <https://doi.org/10.1071/AP06058>
- Aghayeva DN, Rigling D, Meyer JB, Mustafabeyli E (2017) Diversity of fungi occurring in the bark of *Castanea sativa* in Azerbaijan. In VI International Chestnut Symposium 1220, 79–86. <https://doi.org/10.17660/ActaHortic.2018.1220.12>
- Carbone I, Kohn LM (1999) A method for designing primer sets for speciation studies in filamentous ascomycetes. *Mycologia* 3: 553–556. <https://doi.org/10.1080/00275514.1999.12061051>
- Crous PW, Wingfield MJ, Richardson DM, et al. (2016) Fungal Planet description sheets: 400–468. *Persoonia* 36: 316–458. <https://doi.org/10.3767/003158516X692185>
- Dar MA, Rai MK (2014) Occurrence of *Cytospora castanae* sp. nov., associated with perennial cankers of *Castanea sativa*. *Mycosphere* 5: 747–757. <https://doi.org/10.5943/mycosphere/5/6/5>
- Doyle JJ, Doyle JL (1990) Isolation of plant DNA from fresh tissue. *Focus* 12: 13–15. <https://doi.org/10.2307/2419362>
- Fan XL, Bezerra JDP, Tian CM, Crous PW (2020) *Cytospora* (Diaporthales) in China. *Persoonia* 45: 1–45. <https://doi.org/10.3767/persoonia.2020.45.01>
- Fan XL, Hyde KD, Liu M, Liang YM, Tian CM (2015a) *Cytospora* species associated with walnut canker disease in China, with description of a new species *C. gigalocus*. *Fungal Biology* 119: 310–319. <https://doi.org/10.1016/j.funbio.2014.12.011>
- Fan XL, Hyde KD, Yang Q, Liang YM, Ma R, Tian CM (2015b) *Cytospora* species associated with canker disease of three anti-desertification plants in northwestern China. *Phytotaxa* 197: 227–244. <https://doi.org/10.11646/phytotaxa.197.4.1>
- Fan XL, Liang YM, Ma R, Ma R, Tian CM (2014a) Morphological and phylogenetic studies of *Cytospora* (Valsaceae, Diaporthales) isolates from Chinese scholar tree, with description of a new species. *Mycoscience* 55: 252–259. <https://doi.org/10.1016/j.myc.2013.10.001>

- Fan XL, Tian CM, Yang Q, Liang YM, You CJ, Zhang YB (2014b) *Cytospora* from *Salix* in northern China. *Mycotaxon* 129: 303–315. <https://doi.org/10.5248/129.303>
- Guindon S, Dufayard JF, Lefort V, Anisimova M, Hordijk W, Gascuel O (2010) New algorithms and methods to estimate maximum-likelihood phylogenies: assessing the performance of PhyML 3.0. *Systematic Biology* 59: 307–321. <https://doi.org/10.1093/sysbio/syq010>
- Gong S, Zhang X, Jiang S, Chen C, Ma H, Nie Y (2017) A new species of *Ophiognomonia* from Northern China inhabiting the lesions of chestnut leaves infected with *Diaporthe eres*. *Mycological Progress* 16: 83–91. <https://doi.org/10.1007/s11557-016-1255-z>
- Hillis DM, Bull JJ (1993) An empirical test of bootstrapping as a method for assessing confidence in phylogenetic analysis. *Systematic Biology* 42: 182–192. <https://doi.org/10.1093/sysbio/42.2.182>
- Jayawardena RS, Hyde KD, McKenzie EHC, et al. (2019) One stop shop III: taxonomic update with molecular phylogeny for important phytopathogenic genera: 51–75. *Fungal Diversity* 98: 1–84. <https://doi.org/10.1007/s13225-019-00433-6>
- Jeewon R, Hyde KD (2016) Establishing species boundaries and new taxa among fungi: recommendations to resolve taxonomic ambiguities. *Mycosphere* 7: 1669–1677. <https://doi.org/10.5943/mycosphere/7/11/4>
- Jiang N, Fan XL, Tian CM (2019a) Identification and pathogenicity of *Cryphonectriaceae* species associated with chestnut canker in China. *Plant Pathology* 68: 1132–1145. <https://doi.org/10.1111/ppa.13033>
- Jiang N, Fan XL, Crous PW, Tian CM (2019b) Species of *Dendrostoma* (Erythroglloeaceae, Diaporthales) associated with chestnut and oak canker diseases in China. *Mycocokeys* 48: 67–96. <https://doi.org/10.3897/mycokeys.48.31715>
- Jiang N, Fan XL, Yang Q, Du Z, Tian CM (2018a) Two novel species of *Cryphonectria* from *Quercus* in China. *Phytotaxa* 347: 243–250. <https://doi.org/10.11646/phytotaxa.347.3.5>
- Jiang N, Li J, Piao CG, Guo MW, Tian CM (2018b) Identification and characterization of chestnut branch-inhabiting melanocratic fungi in China. *Mycosphere* 9: 1268–1289. <https://doi.org/10.5943/mycosphere/9/6/14>
- Jiang N, Tian CM (2019) An Emerging Pathogen from Rotted Chestnut in China: *Gnomoniopsis daii* sp. nov. *Forests* 10: 1016. <https://doi.org/10.3390/f10111016>
- Jiang N, Voglmayr H, Tian CM (2018c) New species and records of *Coryneum* from China. *Mycologia* 110: 1172–1188. <https://doi.org/10.1080/00275514.2018.1516969>
- Katoh K, Toh H (2010) Parallelization of the MAFFT multiple sequence alignment program. *Bioinformatics* 26: 1899–1900. <https://doi.org/10.1093/bioinformatics/btq224>
- Kepley JB, Reeves FB, Jacobi WR, Adams GC (2015) Species associated with *Cytospora* canker on *Populus tremuloides*. *Mycotaxon* 130: 783–805. <https://doi.org/10.5248/130.783>
- Lawrence DP, Holland LA, Nouri MT, Travadon R, Abramians A, Michailides TJ, Trouillas FP (2018) Molecular phylogeny of *Cytospora* species associated with canker diseases of fruit and nut crops in California, with the descriptions of ten new species and one new combination. *IMA Fungus* 9: 333–370. <https://doi.org/10.5598/imafungus.2018.09.02.07>
- Lawrence DP, Travadon R, Pouzoulet J, Rolshausen PE, Wilcox WF, Baumgartner K (2017) Characterization of *Cytospora* isolates from wood cankers of declining grapevine in North America, with the descriptions of two new *Cytospora* species. *Plant Pathology* 66: 713–725. <https://doi.org/10.1111/ppa.12621>

- Lu C, Guo SJ (2016) Analysis on the nutritional characters and comprehensive evaluation of 16 chestnut germplasm resources. *Science and Technology of Food Industry* 37: 357–376.
- Mehrabi ME, Mohammadi GE, Fotouhifar KB (2011) Studies on *Cytospora* canker disease of apple trees in Semirrom region of Iran. *Journal of Agricultural Technology* 7: 967–982.
- Norphanphoun C, Doilom M, Daranagama DA, Phookamsak R, Wen TC, Bulgakov TS, Hyde KD (2017) Revisiting the genus *Cytospora* and allied species. *Mycosphere* 8: 51–97. <https://doi.org/10.5943/mycosphere/8/1/7>
- Norphanphoun C, Raspé O, Jeewon R, Wen TC, Hyde KD (2018) Morphological and phylogenetic characterisation of novel *Cytospora* species associated with mangroves. *Mycokeys* 38: 93–120. <https://doi.org/10.3897/mycokeys.38.28011>
- Pan M, Zhu HY, Tian CM, Alvarez LV, Fan XL (2018) *Cytospora piceae* sp. nov. associated with canker disease of *Picea crassifolia* in China. *Phytotaxa* 383: 181–196. <https://doi.org/10.11646/phytotaxa.383.2.4>
- Phookamsak R, Hyde KD, Jeewon R, et al. (2019) Fungal diversity notes 929–1035: taxonomic and phylogenetic contributions on genera and species of fungi. *Fungal Diversity* 95: 1–273. <https://doi.org/10.1007/s13225-019-00421-w>
- Rambaut A (2016) FigTree, version 1.4.3. University of Edinburgh, Edinburgh.
- Rigling D, Prospero S (2018) *Cryphonectria parasitica*, the causal agent of chestnut blight: invasion history, population biology and disease control. *Molecular Plant Pathology* 19: 7–20. <https://doi.org/10.1111/mpp.12542>
- Rossmann AY, Farr DF, Castlebury LA (2007) A review of the phylogeny and biology of the *Diaporthales*. *Mycoscience* 48: 135–144. <https://doi.org/10.1007/S10267-007-0347-7>
- Sarma VV, Hyde KD (2001) A review on frequently occurring fungi in mangroves. *Fungal Diversity* 8: 1–34.
- Senanayake IC, Crous PW, Groenewald JZ, et al. (2017) Families of *Diaporthales* based on morphological and phylogenetic evidence. *Studies in Mycology* 86: 217–296. <https://doi.org/10.1016/j.simyco.2017.07.003>
- Senanayake IC, Jeewon R, Chomnunti P, et al. (2018) Taxonomic circumscription of *Diaporthales* based on multigene phylogeny and morphology. *Fungal Diversity* 93: 241–443. <https://doi.org/10.1007/s13225-018-0410-z>
- Shuttleworth LA, Guest DI (2017) The infection process of chestnut rot, an important disease caused by *Gnomoniopsis smithogilvyi* (Gnomoniaceae, Diaporthales) in Oceania and Europe. *Australasian Plant Pathology* 46: 397–405. <https://doi.org/10.1007/s13313-017-0502-3>
- Swofford DL (2003) PAUP*: Phylogenetic Analyses Using Parsimony, * and Other Methods, Version 4.0b10. Sinauer Associates, Sunderland.
- Tai FL (1979) *Sylloge fungorum sinicorum*. Science Press, 1–1527.
- Teng SC (1963) *Fungi of China*. Science Press, 1–808. <https://doi.org/10.1136/bmj.1.5333.808>
- Vilgalys R, Hester M (1990) Rapid genetic identification and mapping of enzymatically amplified ribosomal DNA from several *Cryptococcus* species. *Journal of Bacteriology* 172: 4238–4246. <https://doi.org/10.1128/JB.172.8.4238-4246.1990>
- Voglmayr H, Akulov OY, Jaklitsch WM (2016) Reassessment of *Allantonectria*, phylogenetic position of *Thyronectroidea*, and *Thyronectria caraganae* sp. nov. *Mycological Progress* 15: 921–937. <https://doi.org/10.1007/s11557-016-1218-4>

- Voglmayr H, Castlebury LA, Jaklitsch WM (2017) *Juglanconis* gen. nov. on *Juglandaceae*, and the new family *Juglanconidaceae* (*Diaporthales*). *Persoonia* 38: 136–155. <https://doi.org/10.3767/003158517X694768>
- Wang YL, Lu Q, Decock C, Li YX, Zhang XY (2015) *Cytospora* species from *Populus* and *Salix* in China with *C. davidiana* sp. nov. *Fungal Biology* 119: 420–432. <https://doi.org/10.1016/j.funbio.2015.01.005>
- Wei JC (1979) Identification of Fungus Handbook. Science Press, 1–780.
- White TJ, Bruns T, Lee S, Taylor J (1990) Amplification and direct sequencing of fungal ribosomal RNA genes for phylogenetics. *PCR Protocols: A Guide to Methods and Applications* 18: 315–322. <https://doi.org/10.1016/B978-0-12-372180-8.50042-1>
- Wijayawardene NN, Hyde KD, Lumbsch HT, Liu JK, Maharachchikumbura SSN, Ekanayaka AH, Tian Q, Phookamsak R (2018) Outline of Ascomycota: 2017. *Fungal Diversity* 88: 167–263. <https://doi.org/10.1007/s13225-018-0394-8>
- Yang Q, Fan XL, Crous PW, Liang YM, Tian CM (2015) *Cytospora* from *Ulmus pumila* in northern China. *Mycological Progress* 14: 74. <https://doi.org/10.1007/s11557-015-1096-1>
- Zhang LX, Alvarez LV, Bonthond G, Tian CM, Fan XL (2019) *Cytospora elaeagnicola* sp. nov. associated with narrow-leaved oleaster canker disease in China. *Mycobiology* 47: 319–328. <https://doi.org/10.1080/12298093.2019.1633902>
- Zhang YB, You CJ, Fan XL, Tian CM (2014) Taxonomy and phylogeny of *Cytospora* in North-east China. *Mycosystema* 33: 806–818.
- Zhu HY, Fan XL, Tian CM (2018) Multigene phylogeny and morphology reveal *Cytospora spiraeae* sp. nov. (*Diaporthales*, *Ascomycota*) in China. *Phytotaxa* 338: 49–62. <https://doi.org/10.11646/phytotaxa.338.1.4>
- Zhuang WY (2005) *Fungi of Northwestern China*, New York, USA. Ithaca, Mycotaxon, Ltd, 1–430.

Supplementary material I

Figure S1

Authors: Ning Jiang, Qin Yang, Xin-Lei Fan, Cheng-Ming Tian

Data type: (phylogram of *Cytospora*)

Explanation note: Phylogram of *Cytospora* obtained from the ITS gene.

Copyright notice: This dataset is made available under the Open Database License (<http://opendatacommons.org/licenses/odbl/1.0/>). The Open Database License (ODbL) is a license agreement intended to allow users to freely share, modify, and use this Dataset while maintaining this same freedom for others, provided that the original source and author(s) are credited.

Link: <https://doi.org/10.3897/mycokeys.62.47425.suppl1>

Integrative taxonomy confirms three species of *Coniocarpon* (Arthoniaceae) in Norway

Andreas Frisch^{1*}, Victoria Stornes Moen^{1*}, Martin Grube², Mika Bendiksby¹

¹ NTNU University Museum, Norwegian University of Science and Technology, 7491 Trondheim, Norway

² Institute of Plant Sciences, Karl-Franzens-University Graz, Holteigasse 6, 8010 Graz, Austria

Corresponding author: Mika Bendiksby (mika.bendiksby@ntnu.no)

Academic editor: T. Lumbsch | Received 14 November 2019 | Accepted 23 December 2019 | Published 23 January 2020

Citation: Frisch A, Moen VS, Grube M, Bendiksby M (2020) Integrative taxonomy confirms three species of *Coniocarpon* (Arthoniaceae) in Norway. MycoKeys 62: 27–51. <https://doi.org/10.3897/mycokeys.62.48480>

Abstract

We have studied the highly oceanic genus *Coniocarpon* in Norway. Our aim has been to delimit species of *Coniocarpon* in Norway based on an integrative taxonomic approach. The material studied comprises 120 specimens of *Coniocarpon*, obtained through recent collecting efforts (2017 and 2018) or received from major fungaria in Denmark, Finland, Norway and Sweden, as well as from private collectors. We have assessed (1) species delimitations and relationships based on Bayesian and maximum likelihood phylogenetic analyses of three genetic markers (mtSSU, nucITS and *RPB2*), (2) morphology and anatomy using standard light microscopy, and (3) secondary lichen chemistry using high-performance thin-layer chromatography. The results show three genetically distinct lineages of *Coniocarpon*, representing *C. cinabarinum*, *C. fallax* and *C. cuspidans* comb. nov. The latter was originally described as *Arthonia cinabarina* f. *cuspidans* and is herein raised to species level. All three species are supported by morphological, anatomical and chemical data.

Keywords

Arthoniales, Bayesian inference, maximum likelihood, morphology, mtSSU, nucITS, phylogeny, *RPB2*

Introduction

Species recognition is crucial for improved natural resource management and biodiversity conservation (Lumbsch and Leavitt 2011). Species recognizing can be challenging in lichenized fungi due to unclear species boundaries and/or cryptic diversity

* These authors contributed equally to this study and should be regarded as co-first authors

(e.g., Leavitt et al. 2011; Molina et al. 2011; Carlsen et al. 2012; Lücking et al. 2014; Bendiksby et al. 2015). One such example is *Coniocarpon* DC.

Coniocarpon belongs in the family Arthoniaceae Rchb. of the order Arthoniales. The Arthoniales is one of the largest orders of predominantly lichenized crustose and fruticose taxa (Sundin and Tehler 1998), with around 1500 lichenized, lichenicolous and saprotrophic fungi (Frisch et al. 2014; Van den Broeck et al. 2018). About 800 species belong to the family Arthoniaceae (Frisch and Thor 2010). The largest genus of the family is *Arthonia* Ach., with around 500 species (Grube 1995). As currently circumscribed, *Arthonia* is a polyphyletic genus with high diversity in morphology, chemistry, ecology, distribution and habitat preferences (Frisch et al. 2015). In the process of splitting *Arthonia* into monophyletic taxa, several genera have been described, emended or resurrected recently, of which *Coniocarpon* DC. is one (Frisch et al. 2014). Others include *Bryostigma* Poelt and Döbbeler, *Coniarthonia* Grube, *Felipes* (Ach.) Frisch and G.Thor, *Inoderma* (Ach.) Gray, *Melarthonis* Frisch and G.Thor, *Pachnolepia* A.Massal. and *Synarthonia* Müll.Arg. (Grube 2001; Frisch et al. 2014, 2015; Van den Broeck et al. 2018).

Coniocarpon is a small genus of four accepted species that are mainly distributed in humid tropical to warm-temperate regions of the world (Aptroot and Sparrius 2003; Coppins and Aptroot 2009; Van den Broeck et al. 2018), reaching higher latitudes, for instance, in the boreo-nemoral rainforests and other highly oceanic habitats in Norway (Blom et al. 2015). The genus is characterized within Arthoniaceae by crystalline orange, red and purple quinoid pigments in the ascomata that are dissolving with purple solution in K, by hyaline, macrocephalic, transversely septate ascospores that turn brownish with granular ornamentation in the epispore at late maturity, and by rounded to lirellate ascomata (Frisch et al. 2014, 2018; Van den Broeck et al. 2018). The widespread species *C. cinnabarinum* DC. and *C. fallax* (Ach.) Grube show marked morphological differentiation at the world level indicative for polyphyletic taxa.

The brightly pigmented ascomata in combination with their high value for nature conservation are two reasons why *C. cinnabarinum* and *C. fallax* are frequently collected in Norway. Both species are listed as vulnerable (VU) on the *Norwegian Red List of Species 2015* (as *A. cinnabarina* and *A. elegans*; Henriksen and Hilmo 2015). The boreo-nemoral rainforests, located between 58–62°N (DellaSala et al. 2011), are also categorized as VU in the *Norwegian Red List of Nature Types 2018* (Blom 2018). *Coniocarpon* and other taxa restricted to these forests are of particular importance for biodiversity conservation due to their limited distribution, which makes them vulnerable to extinction at a regional level.

Based on preliminary morphological and molecular evidence, the presence of three distinct taxa of *Coniocarpon* in Norway is hypothesized. This study aims to test this hypothesis by delimiting the taxa of *Coniocarpon* in Norway using an integrative taxonomic approach, including molecular, morphological and chemical data. All available specimens of *Coniocarpon* housed in fungaria in Denmark, Norway and Sweden have been revised. Species descriptions and an identification key are provided for all taxa and their distributions in Scandinavia are mapped.

Materials and methods

Collection methods and handling of fresh specimens

New specimens of *Coniocarpon* for this study were collected in boreo-nemoral rainforests on the west coast of Norway from Vest-Agder to Møre og Romsdal in 2017 and 2018. Specimens were placed in paper bags, allowed to air-dry and later stored at -20 °C due to prior knowledge of fast DNA degradation (e.g., Frisch et al. 2014). After DNA extraction, specimens were incorporated for long-term storage and access in the fungarium in Trondheim (TRH). Additional specimens were made available from fungaria in Bergen (BG), London (BM), Copenhagen (C), Edinburgh (E), Helsinki (H), Oslo (O), Paris (PC), Prag (PRA), Stockholm (S), Trondheim (TRH) and Uppsala (UPS).

Taxon sampling

In total, 26 specimens were used for the molecular data production; 25 specimens from Norway and 1 specimen from Great Britain. Outgroup taxa and additional sequences of *Coniocarpon* were downloaded from GenBank, in total 32 sequences. Eighteen of these (nine mtSSU and nine *RPB2*) represent the nine outgroup taxa, whereas 14 (eight mtSSU and six *RPB2*) were from eight specimens of *Coniocarpon* originating from Great Britain, Japan, Norway, Rwanda and Uganda. Outgroup taxa were selected based on their phylogenetic position in Frisch et al. (2014) and Van den Broeck et al. (2018).

DNA extraction and sequencing

DNA was isolated from specimens up to one year old. Genomic DNA was extracted following one of three methods. (1) Five to eight ascomata were sampled in 2 ml microcentrifuge tubes with two 3 mm diam. tungsten carbide beads each and crushed into a fine powder using a Retsch TissueLyser II. Subsequently, genomic DNA was extracted using the E.Z.N.A. SP Plant DNA Kit (Omega BIO-TEK, USA) following the manufacturer's instructions. (2) Three to five ascomata were sampled directly in 0.2 ml Eppendorf PCR Tubes with 30 µl Dilution Buffer (Phire Plant Direct PCR Kit, ThermoFisher Scientific, Lithuania) and crushed with tweezers. (3) Small cuttings (ca. 50–100 µm × 50–100 µm in size) of the hymenium were sampled in 0.2 ml Eppendorf PCR Tubes and directly used for PCR amplification. The Phire Plant Direct PCR Kit (ThermoFisher Scientific, Lithuania) was used for PCR amplification in all three methods. Each PCR reaction contained 10 µl 2× Phire Plant PCR Buffer, 0.4 µl Phire Hot Start II DNA Polymerase, 1 µl of each primer for all genetic markers except *RPB2* (1.5 µl of each primer), 1 µl genomic DNA (1:1) or the lichen sample, and was filled with H₂O to the final volume of 20 µl. If PCR amplification resulted in weak products, 2 µl genomic DNA (1:10) was added. PCR amplification was done for

the mtSSU, nucITS and the protein-coding gene *RPB2* with the following primers: mtSSU1 + mtSSU3R (Zoller et al. 1999), ITS-1F + ITS4 (Larena et al. 1999, White et al. 1990) and *RPB2*-7cF + *RPB2*-11aR (Liu et al. 1999), respectively. PCR cycling conditions for mtSSU and nucITS started with an initial denaturation at 98 °C for 5 min, followed by 40 cycles of 98 °C for 5 s, 59 °C for 5 s, and 72 °C for 30 s, followed by a final extension of 72 °C for 1 min. For *RPB2*, annealing temperature was set to 57 °C. The PCR products were visualized on a 1% agarose gel stained with SYBR Safe DNA gel stain (ThermoFisher Scientific, USA) under UV light. Clean PCR products (i.e., those lacking visible contamination) were purified by adding 5 µl ExoSAP-IT Express PCR Cleanup (1:3 concentration; ThermoFisher Scientific, United Kingdom) to the PCR reactions. PCR reactions resulting in more than a single product were purified using the E.Z.N.A. Gel Extraction Kit (Omega BIO-TEK, USA) following the manufacturer's instructions, except that we performed an additional wash buffer step. The PCR products were sent to Eurofins Genomics (Germany) for Sanger sequencing using the same primers as for the PCR reactions.

Sequence alignment and phylogenetic analyses

The sequences were edited and aligned using BioEdit v.7.0.5.3 (Hall 1999). The identity of the sequences was verified using the nucleotide BLAST search in GenBank. For the examination of topological incongruence among gene trees, maximum likelihood (ML) bootstrapping analyses was carried out on each of the data sets using the RAxML-HPC Blackbox ver. 8.2.10 (Stamatakis 2014). The standard settings without estimation of the proportion of invariable sites (GTRGAMMA) were used. Topological incongruence was assumed if conflicting tree topologies were supported by $\geq 70\%$ bootstrap support. Since topological incongruence could not be observed, maximum likelihood (ML) bootstrapping analysis was carried out on the concatenated three-locus dataset of 43 accessions for *Coniocarpon* using default settings and adding single genes as parameter partition. The RAxML analysis was stopped automatically after 402 bootstrap replicates using the MRE-based bootstopping criterion (Pattengale et al. 2010).

The best-fit evolutionary model for each partition using the Bayesian information criterion (BIC; Schwarz 1979) was estimated using PartitionFinder2 ver. 2.1.1. (Lanfear et al. 2016). The input data included both ingroup and outgroup taxa. The pre-set partitions were mtSSU, *RPB2*/1st codon position, *RPB2*/2nd codon position, *RPB2*/3rd codon position, ITS1, 5.8S and ITS2. The Bayesian analysis was performed using MrBayes v.3.1.2 (Huelsenbeck et al. 2001; Ronquist and Huelsenbeck 2003). The MCMC run was using four independent chains and 10 million generations, sampling trees every 1000th generation. After removal of a burnin of 25%, 7500 trees were summarized in a final Bayesian 50% majority-rule consensus tree. All phylogenetic analyses were run on the CIPRES Science Gateway (Miller et al. 2010). Phylogenetic trees were visualized using FigTree ver. 1.4.4 (Rambaut 2018). Informative characters were estimated for ingroup taxa per locus using Winclada ver. 1.61 (Nixon 1999–2002).

Morphological and chemical investigations

The morphology of 120 specimens of *Coniocarpon* (Norway 87, Sweden 8, Denmark 16, Great Britain 7, Austria 1, Turkey 1) was studied. The morphology of all specimens was examined using a Leica M80 stereomicroscope and a Zeiss Standard Binocular microscope. Macroscopic photographs were taken with a Leica MZ16A stereomicroscope fitted with a Leica DFC420 camera. Microscopic photographs were taken with a Leica CTR6000 microscope fitted with a Leica DFC365 camera. Sections of ascomata and lichen thalli were cut by hand and mounted in water or lactic acid cotton blue (LCB). Length and width were measured for single ascomata as well as for aggregations composed of several ascomata. For the epithecium, exciple, hymenium and hypothecium, measurements were performed in LCB. Measurements of asci and ascospores were performed in water using squashed preparations. Only fully developed ascospores and commonly asci containing mature ascospores (sometimes asci without mature ascospores) were measured. Ascospore measurements are presented as (min.–)mean \pm SD(–max.). The amyloid reaction of the apothecia was tested using 0.2% (Iodine^{diluted}) and 1% (I), and 1% (I) solution after pretreatment with 10% potassium hydroxide (KOH) in water (KI). The quinoid pigments and Ca-oxalate crystals were measured in water and their shape studied. Later, the crystals reaction with KOH was observed. The quinoid pigments were identified by HPTLC (Arup et al. 1993) in solvent C. Quinoid pigments are named according to Frisch et al. (2018) except for the newly identified A4.

Distribution maps

Based on occurrence information of all revised specimens, the distribution of *Coniocarpon* species in Scandinavia was illustrated by adding a delimited text layer to a Wikimedia map from QuickMap services in QGIS ver. 3.6.2. (QGIS Development Team 2019). The younger specimens (i.e., collected from the mid-80s and onwards) were placed on the maps by their geographical coordinates, while older specimens (collected 1870–1983) lacking geographical coordinates were placed on the maps based on locality information. The Earth Point coordinate converter (<http://www.earthpoint.us/Convert.aspx>) was used to convert coordinates.

Results

Molecular data

A total of 75 new sequences were obtained from the 26 included specimens of *Coniocarpon* (mtSSU 26, nucITS 25, *RPB2* 24; Table 1). The lengths of the alignments (all accessions included) and the phylogenetically informative characters for the ingroup taxa were for mtSSU 889/61, ITS1 569/160, 5.8S 129/0, ITS2 239/84 and *RPB2* 867/127.

Table 1. Vouchers and their GenBank accession numbers. New sequences are indicated in bold. An en dash indicates missing data.

Specimens	Voucher	Country	mtSSU	nuclTS	RPB2
<i>Arthonia didyma</i>	Ertz 7587 (BR)	Belgium	EU704047	–	EU704010
<i>Arthonia granitophylla</i>	Frisch 10/Se74 (UPS)	Sweden	KJ850981	–	KJ851107
<i>Arthonia physcidiicola</i>	Frisch 11/Ug318 (UPS)	Uganda	KF707646	–	KF707657
<i>Coniocarpon cinnabarinum</i> 1	Frisch (TRH-L-29009)	Norway	MN733983	MN734118	MN719396
<i>Coniocarpon cinnabarinum</i> 2	Frisch (TRH-L-29000)	Norway	MN733980	MN734115	MN719393
<i>Coniocarpon cinnabarinum</i> 3	Frisch (TRH-L-29002)	Norway	MN733982	MN734117	MN719395
<i>Coniocarpon cinnabarinum</i> 4	Johnsen 111003 (UPS)	Norway	KJ850976	–	KJ851103
<i>Coniocarpon cinnabarinum</i> 5	Frisch (TRH-L-29008)	Norway	MN733984	MN734119	MN719397
<i>Coniocarpon cinnabarinum</i> 6	Frisch (TRH-L-29001)	Norway	MN733981	MN734116	MN719394
<i>Coniocarpon cinnabarinum</i> 7	Frisch 11/Ug297 (UPS)	Uganda	KJ850977	–	KJ851104
<i>Coniocarpon cinnabarinum</i> 8	Frisch 11/Ug296 (UPS)	Uganda	KP870158	–	KP870170
<i>Coniocarpon cinnabarinum</i> 9	Ertz 8730 (BR)	Rwanda	EU704046	–	EU704009
<i>Coniocarpon cinnabarinum</i> 10	Frisch 13/Jp128 (TNS)	Japan	MG201840	–	–
<i>Coniocarpon cinnabarinum</i> 11	Frisch 13/Jp127 (TNS)	Japan	MG201841	–	–
<i>Coniocarpon cuspidans</i> 1	Frisch (TRH-L-29026)	Norway	MN733977	MN734113	MN719390
<i>Coniocarpon cuspidans</i> 2	Acton, Malíček, Palice 25146 (PRA)	Great Britain	MN733979	–	MN719392
<i>Coniocarpon cuspidans</i> 3	Frisch (TRH-L-29013)	Norway	MN733970	MN734106	MN719384
<i>Coniocarpon cuspidans</i> 4	Frisch (TRH-L-29025)	Norway	MN733976	MN734112	MN719389
<i>Coniocarpon cuspidans</i> 5	Frisch (TRH-L-29014)	Norway	MN733971	MN734107	MN719385
<i>Coniocarpon cuspidans</i> 6	Klepšland (TRH-L-29017)	Norway	MN733973	MN734109	MN719387
<i>Coniocarpon cuspidans</i> 7	Frisch (TRH-L-29022)	Norway	MN733974	MN734110	MN719388
<i>Coniocarpon cuspidans</i> 8	Frisch (TRH-L-29015)	Norway	MN733972	MN734108	MN719386
<i>Coniocarpon cuspidans</i> 9	Frisch (TRH-L-29023)	Norway	MN733975	MN734111	–
<i>Coniocarpon cuspidans</i> 10	Frisch (TRH-L-29024)	Norway	MN733978	MN734114	MN719391
<i>Coniocarpon fallax</i> 1	Wägström 111123 (UPS)	Norway	MG201842	–	MG201850
<i>Coniocarpon fallax</i> 2	Frisch (TRH-L-29030)	Norway	MN733967	MN734103	MN719382
<i>Coniocarpon fallax</i> 3	Gaarder, Larsen (TRH-L-16791)	Norway	MN733961	MN734097	MN719376
<i>Coniocarpon fallax</i> 4	Frisch (TRH-L-29037)	Norway	MN733968	MN734104	MN719383
<i>Coniocarpon fallax</i> 5	Gaarder (TRH-L-16790)	Norway	MN733959	MN734095	MN719374
<i>Coniocarpon fallax</i> 6	Gaarder (TRH-L-16792)	Norway	MN733960	MN734096	MN719375
<i>Coniocarpon fallax</i> 7	Gaarder (TRH-L-16789)	Norway	MN733963	MN734099	MN719378
<i>Coniocarpon fallax</i> 8	Gaarder (TRH-L-15366)	Norway	MN733962	MN734098	MN719377
<i>Coniocarpon fallax</i> 9	Frisch (TRH-L-29029)	Norway	MN733966	MN734102	MN719381
<i>Coniocarpon fallax</i> 10	L10175	Great Britain	KJ850979	–	KJ851101
<i>Coniocarpon fallax</i> 11	Frisch (TRH-L-29028)	Norway	MN733965	MN734101	MN719380
<i>Coniocarpon fallax</i> 12	Frisch (TRH-L-29036)	Norway	MN733969	MN734105	–
<i>Coniocarpon fallax</i> 13	Frisch (TRH-L-29027)	Norway	MN733964	MN734100	MN719379
<i>Reichlingia leopoldii</i>	Ertz 13293 (BR)	Belgium	JF830773	–	HQ454722
<i>Reichlingia syncesioides</i>	Frisch 11/Ug14 (UPS)	Uganda	KF707651	–	KF707656
<i>Reichlingia zuackhii</i>	Thor 26800 (UPS)	Sweden	KF707652	–	KF707662
<i>Synarthonia aurantiacopruinsa</i>	Van den Broeck 5764 (BR)	DR Congo	MH251874	–	MH271697
<i>Synarthonia inconspicua</i>	Van den Broeck 6325 (BR)	Uganda	MH251880	–	MH271701
<i>Synarthonia muriformis</i>	Ertz 19344 (BR)	Madagascar	MH251877	–	MH271699

The selected substitution models for the five subsets in PartitionFinder2 were: 1) GTR+G for mtSSU, 2) K80+1 for RPB2/1st, 3) F81+I for 5.8S and RPB2/2nd, 4) HKY+G for RPB2/3rd and 5) HKY+I for ITS1 and ITS2. The three gene-trees were congruent and a three-locus, concatenated dataset of 43 accessions were analyzed phylogenetically.

Phylogeny

The phylogeny based on Bayesian and maximum likelihood analyses present *Coniocarpon* as monophyletic using the selected taxon and outgroup sampling. Three discrete, well-supported lineages are recovered within *Coniocarpon*. These are separated from each other by branches clearly exceeding the observed infraspecific branch-lengths. The three lineages represent *C. cinnabarinum*, *C. cuspidans* (Nyl.) Moen, Frisch and Grube and *C. fallax* (Fig. 1). *Coniocarpon cinnabarinum* is the supported sister taxon to *C. cuspidans*, while *C. fallax* is sister to these two taxa.

Coniocarpon cinnabarinum from Rwanda and Uganda form a well-supported clade and are sisters to *C. cinnabarinum* in Norway, while *C. cinnabarinum* from Japan is genetically distinct and sister to the remaining taxa of *Coniocarpon*. The two sampled specimens from Great Britain are genetically close to *C. cuspidans* and *C. fallax* in Norway, respectively.

Morphology and chemical characters

Forty-four specimens were identified as *C. cinnabarinum*, as *C. cuspidans* and 42 as *C. fallax*. Ascospore size (Fig. 2), ascospore septation (Fig. 3), ascoma shape and the distribution of pruina (Fig. 4) were identified as useful characters for species distinction. Moreover, differences were observed in the quinoid pigment patterns revealed by HPTLC (Fig. 5) and in the amyloidity of the ascomatal gels. Four quinoid pigments were identified showing different colors on the HPTLC plates prior to sulphuric acid treatment and charring; reddish (A1, A4), purple (A2), yellow (A3) (Fig. 5A). The color of the spots under UV₃₆₅ light are deep purple (A1, A2), buff (A3) and dark salmon (A4) (Fig. 5B). The chemical results for all species are summarized in the Taxonomy section at the end of the Discussion.

Distribution and ecology

Distribution maps based on all revised specimens of *Coniocarpon* from Scandinavia confirm *C. cinnabarinum* for Denmark, Norway and Sweden, *C. cuspidans* for Norway, and *C. fallax* for Norway and Sweden (Fig. 6). *Coniocarpon cinnabarinum* has been collected in Norway in the boreo-nemoral rainforests in Rogaland and Hordaland, while the species occurs in other humid forests in Sweden (Skåne and Gotland) and Denmark (Sjælland and Jylland). Specimens of *C. cuspidans* have been seen in Norway from the boreo-nemoral rainforests in Vest-Agder, Rogaland and Hordaland. *Coniocarpon fallax* has been collected in Norway in the boreo-nemoral rainforests in Vest-Agder, Rogaland, Hordaland and Møre og Romsdal. This study further reports *C. fallax* from Sweden (Gotland) for the first time. Outside Scandinavia, *C. cuspidans* is confirmed for Great Britain and *C. fallax* for Austria, Great Britain, Switzerland and Turkey (not shown).

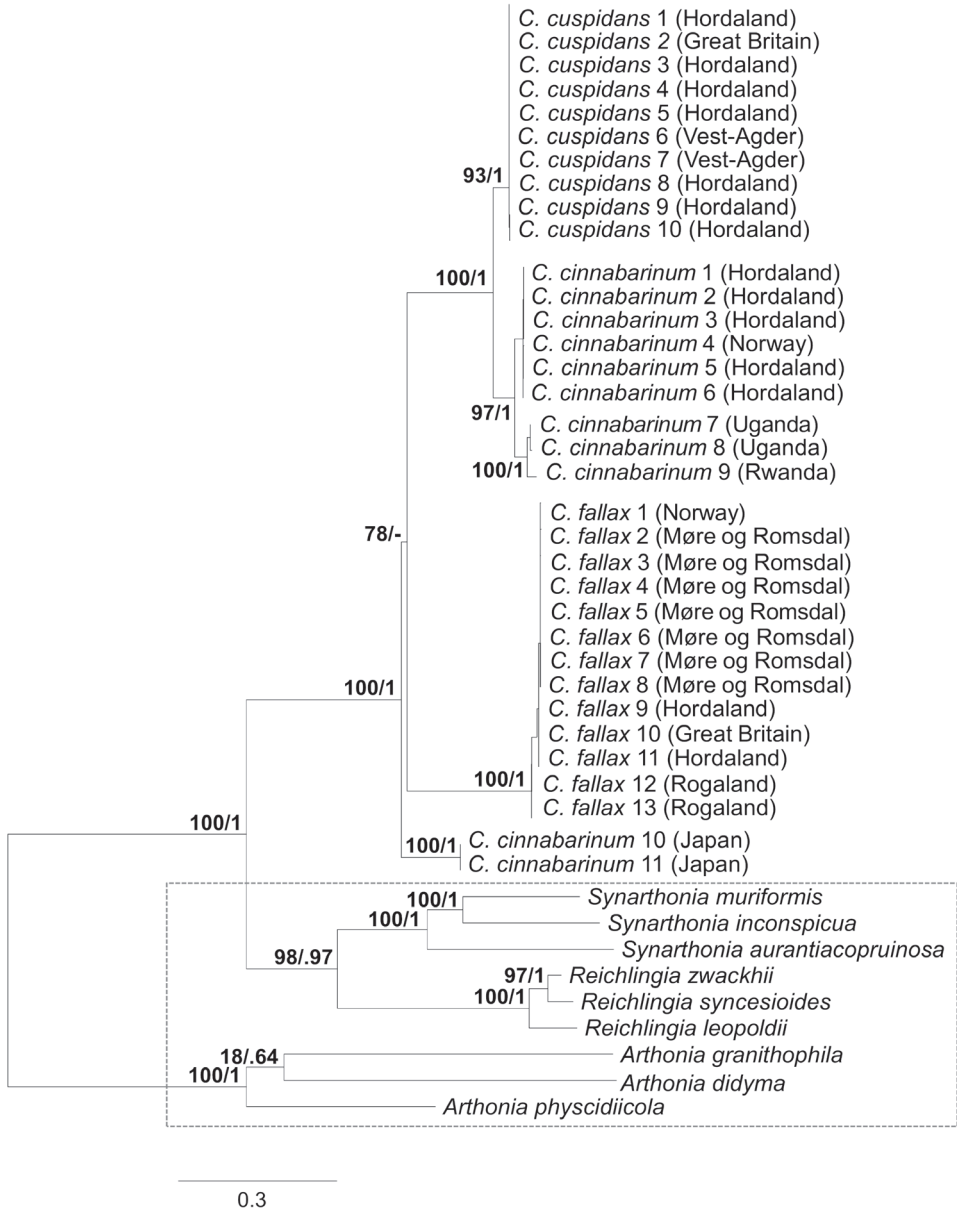


Figure 1. The RAxML phylogenetic hypothesis of a concatenated three-locus data set (mtSSU, nucITS and *RPB2*) of 3 *Coniocarpon* and 9 outgroup taxa (marked by a dashed rectangle). The RAxML bootstrap proportions (first) and Bayesian posterior probabilities (second) are indicated. Place of origin provided behind taxon names.

Coniocarpon preferably grows on trees with smooth bark and the selected host tree species slightly follow a geographical pattern (see Specimens examined below Taxonomic conclusions). Most collections of *C. cinnabarinum* from Norway have been

made from *Corylus avellana* L., including few from *Fraxinus excelsior* L. and *Sorbus aucuparia* L. The species is collected in Denmark from *C. avellana*, *F. excelsior* and *Fagus sylvatica* L., and in Sweden from *F. excelsior*. Most specimens of *C. cuspidans* have been collected from *C. avellana*, but the species has been seen from a rather wide range of trees including *F. excelsior*, *Ilex aquifolium* L., *Quercus robur* L. and *S. aucuparia*. *Coniocarpon fallax* has mainly been collected from *F. excelsior* from Vest-Agder to Hordaland (more rarely from *C. avellana*), while all specimens from Møre og Romsdal are from *C. avellana*. The species is further collected from *F. excelsior* on Gotland and Austria, and from *Picea orientalis* (L.) Link in Turkey.

Discussion

Species designations are hypotheses to be tested as new evidence becomes available. Recent molecular systematic studies have repeatedly revealed evolutionary lineages within phenotypically delimited lichenized fungi (e.g., Steinová et al. 2013; Lücking et al. 2014; Bendiksby et al. 2015; Alors et al. 2016; Hawksworth and Lücking 2017; Boluda et al. 2019). Whether or not such morphologically indistinguishable, or “cryptic”, evolutionary lineages should be recognized at species level may have critical implications for conservation biology and other fields of biology that use species as a fundamental unit (Lumbsch and Leavitt 2011).

In general, several factors should be considered in the process of assessing species status: proper selection of genetic markers (multiple, unlinked loci and from different genomic compartments), presence of statistically supported phylogenetic lineages, sufficiently large sample size, corroborating non-molecular character variation, and thorough review of the taxonomic and nomenclatural history (Grube and Kroken 2000; Printzen 2010; Lumbsch and Leavitt 2011). Our phylogenetic analyses of *Coniocarpon* are based on unlinked, multilocus DNA sequence data (mtSSU, nucITS, *RPB2*) showing high statistical support for three distinct genetic lineages (Fig. 1). Re-examination of morphology against the molecular phylogeny of 26 specimens revealed that the three lineages are further supported by differences in ascospore size (Fig. 2), ascospore septation (Fig. 3), distribution of pruina and ascoma shape (Fig. 4). Furthermore, the three lineages differ in the amyloidity of the ascomatal gels and pigment patterns revealed by HPTLC (Fig. 5). Finally, an additional 94 specimens, for which molecular data are not available, were revised using the same morphological and/or chemical characters. As such, this study fulfills the factors recommended for assessing species status.

Evolutionary lineages that remain intact when living in sympatry with close relatives might deserve species status (Coates et al. 2018). The distribution maps in Fig. 6 show sympatry for the three distinct genetic lineages of *Coniocarpon* in Norway, providing strong indirect evidence that there are mechanisms prohibiting exchange of genetic material among them, supporting their acceptance at species level. Hence, the integrated data gathered in this study jointly support the hypothesis of three distinct species of *Coniocarpon* in Norway, viz. *C. cinnabarinum*, *C. fallax* and *C. cuspidans*. The latter

species was hidden in the extensive synonymy of *C. cinnabarinum* as *Arthonia cinnabarina* f. *cuspidans* Nyl. and is herein resurrected (see Taxonomic conclusions below).

The present data indicate a narrower distribution in Norway for *C. cinnabarinum* and *C. cuspidans* as compared to *C. fallax* (Fig. 6). All available collections from Møre og Romsdal were identified as *C. fallax*. *Coniocarpon cinnabarinum*, the only species reported from that county in the *Norwegian Red List of Species 2015* could not be confirmed. However, not all collections of *Coniocarpon* in Norway were available for this study, and previous distributions were partly based on human observations as well. The distribution of the three *Coniocarpon* species in Norway needs further evaluation in light of the present investigation. Moreover, this study confirms *C. cinnabarinum* for Denmark and Sweden. *Coniocarpon fallax* is reported from Sweden (Gotland) for the first time (Fig. 6), based on specimens from S and UPS previously identified as *C. cinnabarinum*.

Species diversity and abundance generally correlate with habitat preference. Most collections of *Coniocarpon* in Norway were made in Hordaland (*C. cinnabarinum* 22, *C. cuspidans* 24, *C. fallax* 20), in the core area of the boreo-nemoral rainforests, having the highest levels of humidity and low average winter temperatures (Blom et al. 2015; Moen 1999). In comparison, the number of studied specimens from Vest-Agder (*C. cinnabarinum* 0, *C. cuspidans* 2, *C. fallax* 3) at the southern limit of the boreo-nemoral rainforests is distinctly lower, which might be partly explained by fewer rainforest localities (Blom et al. 2015). The occurrence of *C. fallax* in Møre og Romsdal indicates a wider ecological amplitude as compared to *C. cinnabarinum* and *C. cuspidans* in terms of oceanicity and temperature. *Coniocarpon cuspidans* is currently only confirmed for Norway and Great Britain, but as the species has not been distinguished from *C. fallax* in the past, it might have a wider distribution in Western Europe.

This study provides a further step in the process of improving the biodiversity conservation in Norway by applying an integrative taxonomic approach for delimiting taxa in *Coniocarpon*. *Coniocarpon cinnabarinum* and *C. fallax* are designated as VU in the latest version of the *Norwegian Red List for Species* (Henriksen and Hilmo 2015). It is likely that the same status applies to *C. cuspidans*, growing with similar abundance in the boreo-nemoral rainforests as the other species of *Coniocarpon*. Moreover, all three species are facing the same threats such as algae growth on trees which is inhibiting the establishment and growth of lichens (Blom 2018).

Taxonomic conclusions

Coniocarpon DC

In Lamarck and de Candolle, *Flore française* 2: 323 (1805) [MB 1208]. Lectotype (selected in Santesson, *Symbolae Botanicae Upsalienses* 12(1): 68, 1952): *Coniocarpon cinnabarinum* DC., in Lamarck and de Candolle, *Flore française* 2: 323 (1805).

Key to *Coniocarpon* in Norway

- 1 Ascospores mostly > 20 µm long; ascomata typically rounded to weakly lobate, rarely lirellate; orange-red pruina present *C. cinnabarinum*
 – Ascospores mostly ≤ 20 µm long; ascomata typically irregularly lirellate; orange-red pruina present or absent..... **2**
- 2 Orange-red pruina present; ascospores (15–)17–20(–22) × (6–)7–9(–10) µm, (1–)3–4(–5) transversely septate *C. fallax*
 – Orange-red pruina absent; ascospores (15–)16–18(–20) × (6–)7–8(–9) µm, (2–)3(–4) transversely septate..... *C. cuspidans*

Coniocarpon cinnabarinum DC.

Mycobank No: 383614

Figs 2, 3A, 4A, B, 5, 6A

Coniocarpon cinnabarinum DC.: Lamarck and de Candolle, Flore française 2: 323 (1805). Type: not selected [see under "Notes" below].

= *Spiloma* ? *tumidulum* Ach., Methodus qua omnes detectos lichenes: 11 (1803) [MB 405550]. Type: Hispania, Schousboe (H-Ach. 3 cl, holotype).

= *Spiloma tumidulum* var. *rubrum* Ach., Lichenographia universalis: 137 (1810) – nom. illegit. Type: Gallia (H-Ach. 2 cl).

Description. THALLUS pale olive gray to brown, weakly glossy to matt, smooth, endophloeodal to partly epiphloeodal, continuous; *prothallus line* dark gray to brown, sometimes present when in contact with other lichens; *photobiont* trentepohlioid, the cells rounded to elliptical, 7–12 × 4–8 µm, forming short chains. ASCOMATA irregularly rounded to elliptical to weakly lobed, rarely distinctly lirellate, with steep flanks, emergent from thallus, 0.1–0.4 × 0.1–0.3 mm, 95–140 µm tall, solitary or forming loose to dense aggregations of 3–15 ascomata, (0.3–)0.5–2.0(–3.5) × 0.3–1.6 mm; *disc* dark purple black, flat to weakly convex, matt to weakly glossy, white pruinose, a layer of orange-red pruina sometimes present above the white pruina; old ascomata sometimes epruinose; *margins* level with the disc, typically orange-red pruinose, sometimes with additional patches of white pruina; *proper exciple* brown, 8–15 µm wide, composed of compressed and vertically oriented paraphysoidal hyphae, the hyphae 1–2 µm thick, branched and netted, often forming short hairs up to 15 µm long at the outer margin; old bark cells often attached to the exciple; *epithecium* brown, 10–25 µm tall, conglutinated only in the lower parts, composed of branched tips of the paraphysoidal hyphae extending horizontally above the asci; the tips slightly widened to 3(–4) µm, sometimes extending from the epithecium as sparsely branched anticlinal hairs up to 22 µm long; *hymenium* hyaline, strongly conglutinated, (45–)65–90 µm tall, paraphysoids densely branched and netted, 1–2 µm thick; *hypothecium* hyaline, conglutinated, 20–35 µm

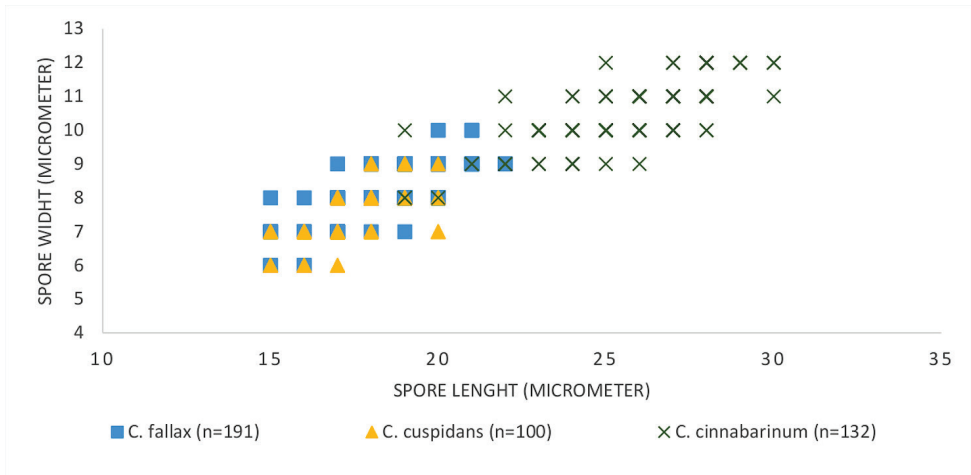


Figure 2. Ascospore size (length x width) of *C. cinnabarinum* (n = 132; 20 ascospores from Denmark, 85 ascospores from Norway; 27 ascospores from Sweden), *C. cuspidans* (n = 100, all ascospores from Norway) and *Coniocarpon fallax* (n = 191, all ascospores from Norway).

tall, formed of irregular prosoplectenchymatic hyphae 1–2 μm diam.; *crystals* common in epithecium and proper exciple, of two types: hyaline, leafy crystals, 1–5(–8) μm , and orange, red or purple, granular crystals, 1–2(–4) μm ; a weak amorphous, red to purple pigmentation present in exciple, epithecium and patchily distributed in the hymenium. ASCI of the *Arthonia*-type, long obpyriform to clavate, 62–84 μm \times 24–35 μm (n = 34), 8-spored, the ascospores stacked; tholus 8–11 μm thick, lateral ascospore wall 1–2 μm thick. ASCOSPORES hyaline, (3–)4–5(–8) transversely septate, (19–)23–28(–30) \times (8–)10–11(–12) μm (l: mean = 25.7, STD = 2.3; w: mean = 10.5, STD = 0.9; n = 132), obovate, with enlarged apical cell, getting pale brown with granular ornamentation in the epispore at late maturity; development macrocephalic.

Chemistry. Pigments A1, A3 and A4 in variable amounts detected by HPTLC. *Proper exciple* I_{dil} + blue, I+ blue, KI+ blue; *epithecium* I_{dil} + blue, I+ blue, KI+ blue; *hymenium* I_{dil} + red, I+ red, KI+ blue; *hypothecium* I_{dil} + red, I+ red, KI+ blue. A hemiamyloid ring present in the tholus of the asci. Hyaline crystals dissolve in K. Orange, red and purple crystals dissolve in K with a clear, fleeting, purplish solution.

Specimens examined. NORWAY – **Rogaland** • Rennesøy, Berge; 59°05.868'N, 05°42.320'E; on *C. avellana*; 30–40 m a.s.l.; 12. Jan. 2008; J. I. Johnsen leg.; BG L-86128. – **Hordaland** • Askøy, close to Ask farm; on *S. aucuparia*; 10–30 m a.s.l.; 31. Aug. 1909; J. J. Havaas leg.; UPS-L-277202. • Bømlo, Børøy, Storavatnet; 59°42.9420'N, 05°15.7680'E; on *C. avellana*; 30. Apr. 2018; G. Gaarder leg.; TRH-L-18030 • *ibid.*; Lykling; 59°42.6780'N, 05°12.3540'E; on *C. avellana*; 30. Apr. 2018; G. Gaarder leg.; TRH-L-18036 • *ibid.*; S of Liarnuten; on *C. avellana*; 21. Jun. 1997; T. Knutsson leg.; UPS-L-737333 • *ibid.*; Skogafjellet; 59°38.812'N, 05°12.098'E; on *C. avellana*; 35 m a.s.l., 19. Jul. 2017; A. Frisch leg.; TRH-L-29000 • *ibid.*; 59°38.818'N, 05°12.082'E; on *C. avellana*; 10 m a.s.l.; 19. Jul. 2017; A. Frisch leg.;

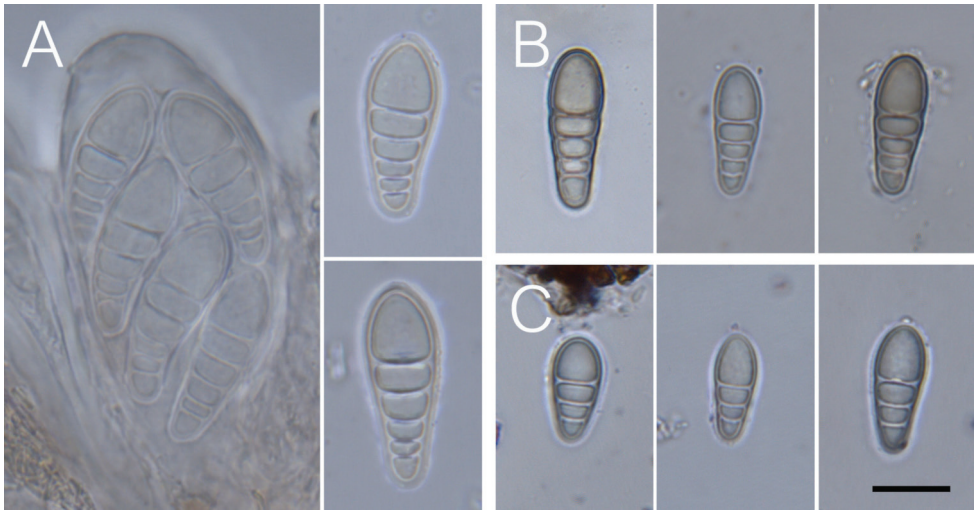


Figure 3. Ascospore morphology. **A** *Coniocarpon cinnabarinum* (TRH-L-29007) **B** *Coniocarpon fallax* (TRH-L-29008) **C** *Coniocarpon cuspidans* (TRH-L-29036). Scale bar: 10 μ m.

TRH-L-29006, TRH-L-29007, TRH-L-29008 • *ibid.*; on *F. excelsior*; A. Frisch leg.; TRH-L-29009 • *ibid.*; 59°38.833'N, 05°12.153'E; on *C. avellana*; 50 m a.s.l.; 19. Jul. 2017; A. Frisch leg.; TRH-L-29001, TRH-L-29002. • Kvam, Gravdal SW, Geitaknottane Nat. Reserve, NE of Lønningshaugen; 60°06.690'N, 05°51.068'E; on *C. avellana*; 150–250 m a.s.l.; 28. Aug. 1997; P. G. Ihlen leg.; BG-L-35863. • Lindås, Kvalvika-Røyldalane; 60°38.338'N, 05°26.258'E; on *C. avellana*; 35 m a.s.l.; 14. May 2018; A. Frisch leg.; TRH-L-29010, TRH-L-29011, TRH-L-29012. • Os, Innerøya, Halhjem; 60°08.5020'N, 05°24.8520'E; on *S. aucuparia*; 10. May 2018; G. Gaarder leg.; TRH-L-18042 • *ibid.*; 60°08.5920'N, 05°25.3440'E; on *C. avellana*; 10. May 2018; G. Gaarder leg.; TRH-L-18043. • Stord, Digernes, Geitåsen; 59°45.402'N, 05°25.092'E; on *C. avellana*; 28. Apr. 2018; G. Gaarder leg.; TRH-L-18033 • *ibid.*; Valavåg, Nes-Åsen; 59°46.0740'N, 05°24.8040'E; on *C. avellana*; 27. Apr. 2018; G. Gaarder, U. Hanssen leg.; TRH-L-18087. • Tysnes, Beltestad, Beltestadknappen; 59°59.883'N, 05°27.543'E; on *C. avellana*; 13 m a.s.l.; 9. May 2018; A. Frisch leg.; TRH-L-29003, TRH-L-29004 • *ibid.*; 59°59.900'N, 05°27.555'E; on *C. avellana*; 5 m a.s.l.; 9. May 2018; A. Frisch leg.; TRH-L-29005. SWEDEN – **Gotland** • Stenkumla, Myrsö; 1869; Laurer leg.; UPS-L-002825. – **Skåne** • Dalby, Dalby Söderskog; on *F. excelsior*; 23. Jul. 1947; R. Santesson leg.; UPS-L-118296 • *ibid.*; Ottarp, Bälteberga; on *F. excelsior*; 20. Aug. 1946; O. Almborn leg.; S-F-71116, UPS-L-60625 • *ibid.*; 16. Sep. 1959; G. Degelius, O. Almborn leg.; UPS-L-60624. DENMARK – **Jylland** • Horsens, Elling Skov; on *F. excelsior*; 26. Mar. 1887; J. Jeppesen leg.; C-L-28996 • *ibid.*; on *F. sylvatica*; 26. Mar 1887; J. Jeppesen leg.; C-L-28993 • *ibid.*; on *F. excelsior*; 26. Feb. 1887; J. Jeppesen leg.; S-F-71202, C-L-28992 • *ibid.*; on *F. excelsior*; 20. Feb. 1887; J. P. Pedersen leg.; C-L-28991, C-L-28994 • *ibid.*; Hansted Skov; on *F. excelsior*; 5. Des. 1886; J. Jeppesen leg.; C-L-29000 • *ibid.*; 1. Feb. 1887; J. Jeppesen leg.; C-L-28999 • *ibid.*; on *F. sylvatica*;

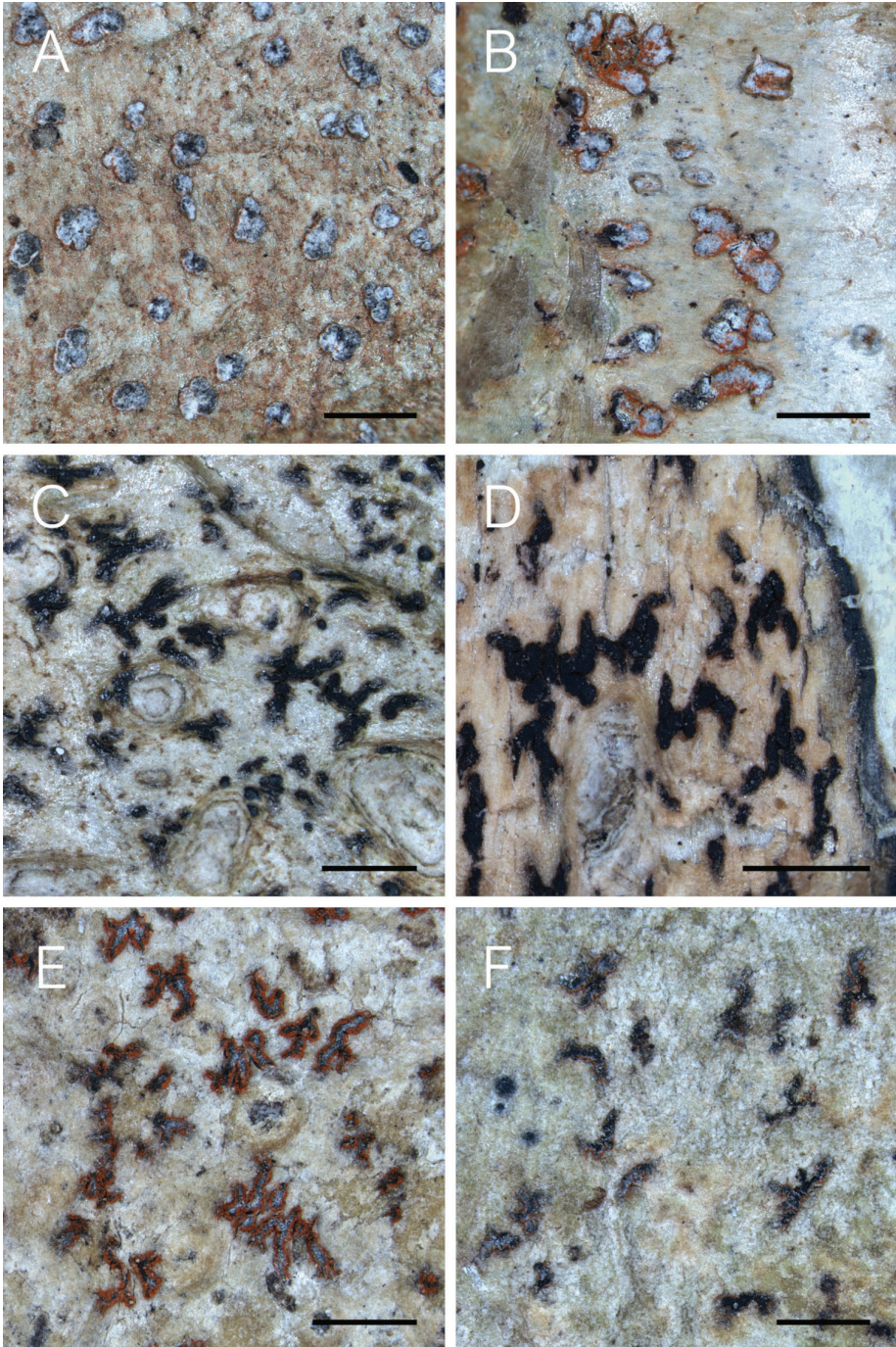


Figure 4. Morphological diversity of *Coniocarpon* in Norway. **A** *Coniocarpon cinnabarinum* (Frisch TRH-L-29000) **B** *Coniocarpon cinnabarinum* (Frisch TRH-L-29005) **C** *Coniocarpon cuspidans* (TRH-L-29022) **D** *Coniocarpon cuspidans* (TRH-L-29023) **E** *Coniocarpon fallax* (TRH-L-16793) **F** *Coniocarpon fallax* (Frisch TRH-L-29028). Scale bars: 1 mm.

6. Mar. 1887; J. Jeppesen leg.; C-L-28998. • Lihme, Kås skov; on *C. avellana*; 6. Aug. 1979; G. Thor leg.; UPS-L-165392 • *ibid.*; on *F. excelsior*; 25. May. 1976; S. Svane leg.; C-L-28997, C-L-28988 • *ibid.*; on *C. avellana*; 25. May 1976; M. S. Christansen leg.; C-L-28990 • *ibid.*; Bringsbjerg Krat; 56°37.129'N, 08°41.423'E; on *C. avellana*; 21. Oct. 2002; R. S. Larsen leg.; C-L-17076. – **Sjælland** • Haslev; 29. Jul. 1887; Taussieng leg.; C-L-28995 • *ibid.*; Skarresø; 4. Nov. 1870; C. Grönlund leg.; UPS-L-002896.

Notes. *Coniocarpon cinnabarinum* differs from the other *Coniocarpon* species in Norway by distinctly larger ascospores and in ascospore septation: (19–)23–28(–30) × (8–)10–11(–12) µm, (3–)4–5(–8) transversely septate vs (15–)16–18(–20) × (6–)7–8(–9) µm, (2–)3(–4) transversely septate in *C. cuspidans* vs (15–)17–20(–22) × (6–)7–9(–10) µm, (1–)3–4(–5) transversely septate in *C. fallax*. Further, the ascomata in *C. cinnabarinum* are mostly irregularly rounded to elliptical and only rarely lirellate as in *C. cuspidans* and *C. fallax*. The ascomatal disc in *C. cinnabarinum* is typically covered by a thick layer of white pruina which may be overlaid by orange–red pruina, and the ascomatal margin is orange–red pruinose. In *C. cuspidans*, the ascomata completely lack orange–red pruina, while a thin white pruina may be occasionally present. In *C. fallax*, the distribution of pruina is similar to *C. cinnabarinum*, but the white pruina is less pronounced and may even be lacking. Additional differences have been observed in the reaction of proper exciple and epithecium to iodine: I_{dil}/I+ blue in *C. cinnabarinum* and *C. fallax* vs I_{dil}/I+ red in *C. cuspidans*. The quinoid pigments A1, A3 and A4 have been identified in *C. cinnabarinum* in various amounts. The quinoid patterns in *C. fallax* are similar, while in *C. cuspidans* A3 is absent or occurs in trace amounts only. The pigment A2 has only been found in *C. cuspidans*.

Coniocarpon cinnabarinum is the selected type species of *Coniocarpon* (Santesson 1952), but the name is preceded by *Spiloma tumidulum* (Acharius 1803) and possibly *Sphaeria gregaria* Weigel (1772). The situation is further complicated by the fact that the only specimen of *C. cinnabarinum* in PC that is unequivocally linked to the publication of *Flore française* and donated by de Candolle, represents *C. fallax*. Since *C. cinnabarinum* is a well established species and often cited in literature, we intend to propose this name for conservation. The typification of the species will be discussed in the proposal, which is currently under preparation.

***Coniocarpon cuspidans* (Nyl.) Moen, Frisch & Grube, comb. nov.**

Mycobank No: 833812

Figs 2, 3C, 4C, D, 5, 6B

Arthonia cinnabarina f. *cuspidans* Nyl., Flora 59: 310 (1876) [MB 372360]. Type: Illicicola in Hibernia, n. 6, Dough[ruagh Mountain], 1875, Larbalestier (H-Nyl 5607! lectotype, here selected).

Description. THALLUS pale brown to pale fawn to off white, matt to weakly glossy, smooth, endophloeodal to partially epiphloeodal, continuous; *prothallus* line dark gray

to brown to black, sometimes present when in contact with other lichens; photobiont trentepohlioid, the cells rounded to elliptical, 6–13 × 5–11 µm forming short chains. ASCOMATA weakly elongate to irregularly lirellate, with steep flanks, emergent from thallus, 0.2–0.6 × 0.1–0.2 mm, 60–105 µm tall, typically forming loose to dense aggregations of 3–15 ascomata, weakly elongated to irregularly lirellate to stellate, 0.4–1.8(–2.5) × (0.1)0.3–1.0(–2.0) mm; *disc* black to dark purple black, flat to weakly convex, weakly glossy to matt, epruinose, rarely with patches of a thin white pruina; *margins* level with the disc, epruinose, rarely with patches of a thin white pruina; *proper exciple* brown, 7–20 µm wide, composed of compressed and vertically oriented paraphysoidal hyphae, the hyphae 1–2 µm thick, branched and netted, sometimes forming short hairs up to 16 µm long at the outer margin; old bark cells sometimes attached to the exciple; *epithecium* brown, 8–20 µm tall, conglutinated only in the lower parts, composed of branched tips of the paraphysoidal hyphae extending horizontally above the asci; the tips slightly widened to 3(–4) µm, sometimes extending from the epithecium as sparsely branched anticlinal hairs up to 12 µm long; *hymenium* hyaline, strongly conglutinated, 41–73 µm tall, paraphysoids densely branched and netted, 1–2 µm thick; *hypothecium* hyaline, conglutinated, 15–30 µm tall, formed of irregular prosoplectenchymatic hyphae 1–2 µm diam.; *crystals* common in epithecium and proper exciple, of two types: hyaline, leafy crystals, 1–5 µm, and red or purple granular crystals, 1–3 µm; a weak amorphous, red to purple pigmentation present in exciple, epithecium and patchily distributed in the hymenium. ASCI of the *Arthonia*-type, long obpyriform to clavate, 45–70 × 19–28 µm (n = 31), 8-spored, the ascospores stacked; tholus 4–8 µm thick, lateral ascospore wall 1–2 µm thick. ASCOSPORES hyaline, (2–)3(–4) transversely septate, (15–)16–18(–20) × (6–)7–8(–9) µm (l: mean = 17.4, STD = 1.2; w: mean = 7.5, STD = 0.7; n = 100), obovate, with enlarged apical cell, getting pale brown with granular ornamentation in the epispore at late maturity; development macrocephalic.

Chemistry. Pigments A1, A2, A3 and A4 in variable amounts detected by HPTLC. *Proper exciple* I_{dil}+ red, I+ red, KI+ blue; *epithecium* I_{dil}+ red, I+ red, KI+ blue; *hymenium* I_{dil}+ red, I+ red, KI+ blue; *hypothecium* I_{dil}+ red, I+ red, KI+ blue. A hemiamyloid ring in the tholus of the asci not observed. Hyaline crystals dissolve in K. Purple crystals dissolve in K with hyaline solution. Red and purple crystals dissolve in K with purplish solution.

Specimens examined. NORWAY – **Vest-Agder** • Flekkefjord, Hidra, Høgåsen; 58°13.585'N, 06°33.370'E; on *S. aucuparia*; 35 m a.s.l.; 15. Jul. 2017; J. Klepsland leg.; TRH-L-29017 • *ibid.*; Nonfjell; 58°13.445'N, 06°33.550'E; 5–25 m a.s.l.; 15. Jul. 2017; A. Frisch TRH-L-29022. – **Rogaland** • Tysvær, Svinali W; 59°25.098'N, 05°34.104'E; on *C. avellana*; 19. Oct. 2017; G. Gaarder leg.; TRH-L-18034. – **Hordaland** • Austevoll, Huftaøy, Bjelland farm NE; 60°05.000'N, 05°16.000'E; on *C. avellana*; 0–40 m a.s.l.; 6. Jun. 1996; T. Tønsberg leg.; BG-L-32077, BG-L-34115. • Bømlo, Børøy, Masterhaugane nord; 59°42.840'N, 05°15.5040'E; on *S. aucuparia*; 30. Apr. 2018; G. Gaarder leg.; TRH-L-18038, TRH-L-18078 • *ibid.*; 59°42.6420'N, 05°15.3540'E; on *C. avellana*; 30. Apr. 2018; G. Gaarder leg.; TRH-L-18040 • *ibid.*; Kuhlillerdalen; 59°45.36'N, 05°16.82'E; on *C. avellana*; 70 m a.s.l.; 11. May 2015; J. B. Jordal, H. H. Blom leg.; TRH-L-16794 • *ibid.*; Lykling, Lyklingfjorden N;

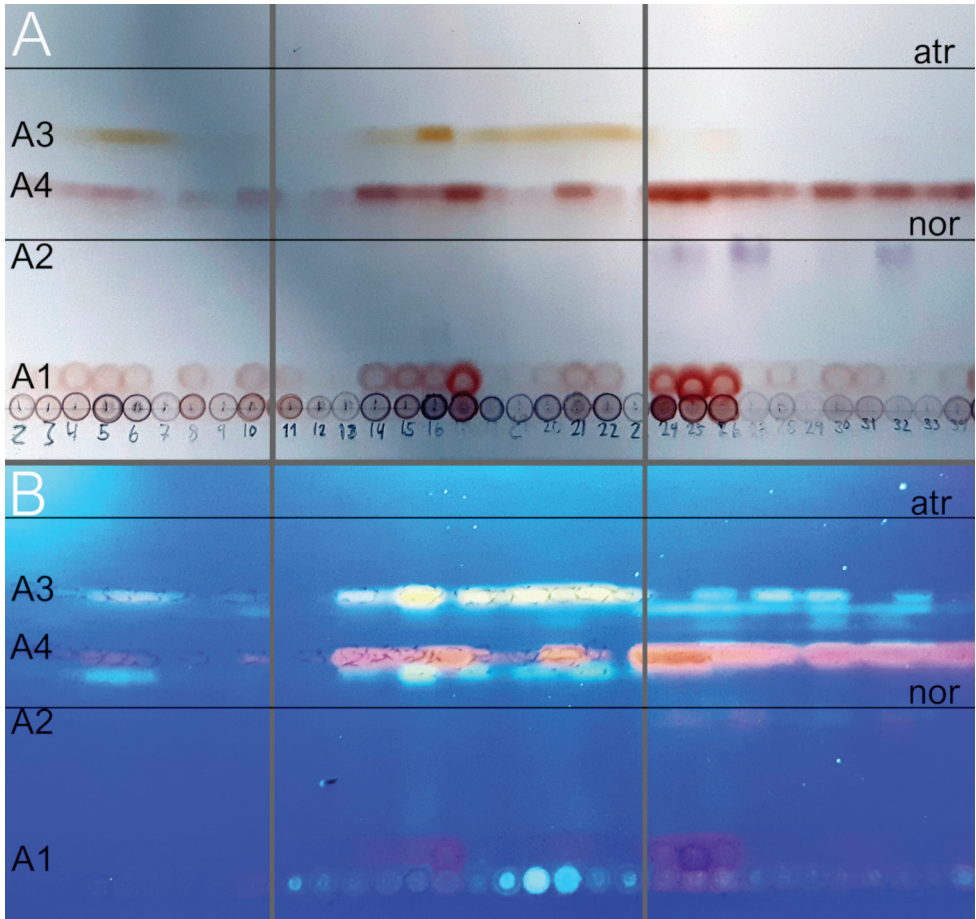


Figure 5. HPTLC plate in solvent C of quinoid pigment patterns of *C. cinnabarinum* (left), *C. fallax* (middle) and *C. cuspidans* (right) **A** before treatment with sulfuric acid and charring, and **B** under UV₃₆₅ light before treatment with sulfuric acid and charring. Note the absence of A3 in *C. cuspidans*. The position of atranorin and norstictic acid is indicated. Several additional spots on the HPTLC plates under UV₃₆₅ light have not been identified.

59°42.321'N, 05°10.569'E; on *C. avellana*; 10–20 m a.s.l.; 13. May 1996; T. Tønberg leg.; BG-L-31539 • *ibid.*; 59°42.300'N, 05°10.600'E; on *C. avellana*; 40–60 m a.s.l.; 1. Jun. 1997; S. Ekman leg.; BG-L-38200 • *ibid.*; Skogafjellet; 59°38.833'N, 05°12.153'E; on *C. avellana*; 50 m a.s.l.; 19. Jul. 2017; A. Frisch TRH-L-29015 • *ibid.*; 59°38.812'N, 05°12.098'E; on *C. avellana*; 35 m a.s.l.; 19. Jul. 2017; A. Frisch leg.; TRH-L-29013, TRH-L-29014 • *ibid.*; 59°38.818'N, 05°12.082'E; on *C. avellana*; 10 m a.s.l.; 19. Jul. 2017; A. Frisch leg.; TRH-L-29023 • *ibid.*; on *S. Aucuparia*; 10 m a.s.l.; 19. Jul. 2017; A. Frisch leg.; TRH-L-29024 • *ibid.*; 59°38.972'N, 05°12.432'E; on *C. avellana*; 12 m a.s.l.; 19. Jul. 2017; A. Frisch leg.; TRH-L-29025, TRH-L-29026 • *ibid.*; S of Totlandstjørna; 59°41.172'N, 05°20.940'E; on *C. avellana*; 28. Jun. 2017;

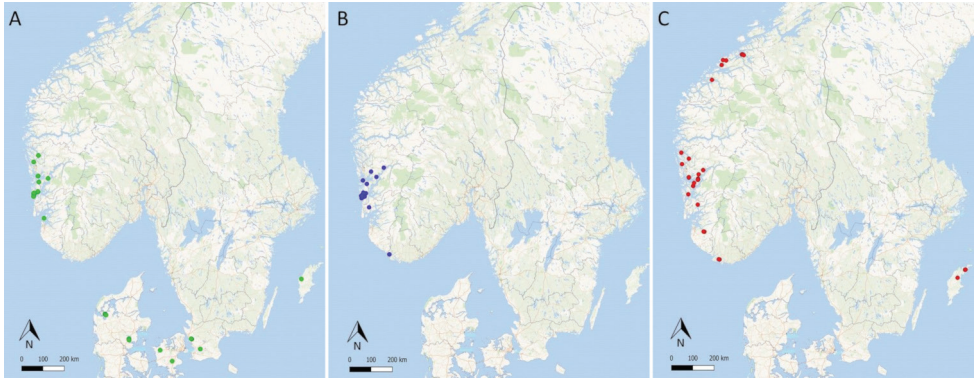


Figure 6. The distribution of 111 specimens of *Coniocarpon* in Norway, Sweden and Denmark based on material in BG, C, S, TRH and UPS. **A** *C. cinnabarinum* **B** *C. cuspidans* **C** *C. fallax*. Single dots may represent several collections.

G. Gaarder leg.; TRH-L-18035 • *ibid.*; Totsida; 59°40.8180'N, 05°19.5540'E; on *I. aquifolium*; 27. Jun. 2017; G. Gaarder, M. Lorentzen leg.; TRH-L-18037 • *ibid.*; Våge; 59°43.6260'N, 05°13.5060'E; on *C. avellana*; 30. Apr. 2018; G. Gaarder leg.; TRH-L-18031. • Fusa, Holmefjord, Eikhaugen; 60°17.952'N, 05°39.867'E; on *Q. robur*; 30 m a.s.l.; 8. May 2018; A. Frisch leg.; TRH-L-29021. • Kvam, Nes N; 60°10.085'N, 05°55.535'E; on *F. excelsior*; 4. Jun. 2018; G. Gaarder leg.; TRH-L-18608. • Stord, Åsen SW of Sagvåg; 59°46.043'N, 05°24.593'E; on *C. avellana*; 50 m a.s.l.; 28. Apr. 2018; A. Frisch leg.; TRH-L-29019 • *ibid.*; 59°46.088'N, 05°24.757'E; on *C. avellana*; 33 m a.s.l.; 28. Apr. 2018; A. Frisch leg.; TRH-L-29020. • Sund, Steinsland; 60°12.199'N, 05°04.929'E; on *C. avellana*; 20–40 m a.s.l.; 9. Mar. 1997; T. Tønberg leg.; BG-L-34117. • Tysnes, Beltestad, Beltestadknappen; 59°59.883'N, 05°27.543'E; on *C. avellana*; 13 m a.s.l.; 9. May 2018; A. Frisch leg.; TRH-L-29018.

Additional examined specimens. GREAT BRITAIN – **Scotland** • Argyll, Appin, Glen Stockdale; 56°34.383'N, 05°21.583'W; on *C. avellana*; 65–90 m a.s.l.; 5. Jun. 2018; A. Acton, J. Malíček, Z. Palice leg. 25146; PRA • *ibid.*; Westernness Lochl Surnart, Reripole Ravine; on *Corylus* sp.; 10. Mar. 1983; B. J. Coppins leg.; BG-L-58163 • *ibid.*; Benderloch, Lochnell House; 17/88.38; on *Corylus*; 15–45 m a.s.l.; 4. Aug. 1980; B. J. Coppins leg. 8056; E • Mid Perth (VC 88), S side of Loch Earn, west of Ardvorlich cottage; 27/ 61.22(-3); 105–130 m a.s.l.; 8. Aug. 1980; B. J. Coppins & P. W. James leg.; E • Clyde Islands, Arran (VC 100), Glenashdale; 26/03.25; on *Corylus*; 4. Apr. 1984; B. J. Coppins leg. 10169; E • Westernness (VC 97), S side of Loch Sunart, Laudale Woods ravine 0.5 km W of Liddesdale; 17/77.59; 0–75 m a.s.l.; 9. Mar. 1983; B. J. Coppins & P. M. Jørgensen leg.; E • Devon, SW of Bridge Reeve; 21/65.13; on *Quercus petraea*; 1. Aug. 1972; P. Harrold leg.; E.

Notes. *Coniocarpon cuspidans* is characterized by lirellate ascomata lacking orange-red pruina, while red and purple pigment crystals and a weak amorphous red to purple pigmentation is present in proper exciple and epithecium. The quinoid pigment A3 is absent or occurs in possible trace amounts only. A3 may correspond to orange pigment

crystals observed in microscopical preparations of *C. cinnabarinum* and *C. fallax* but not in *C. cuspidans*. These crystals are located in the pruina of the ascomatal margin and disc. The ascospores in *C. cuspidans* are the smallest observed for the genus in Norway, (15–)16–18(–20) × (6–)7–8(–9) µm and (2–)3(–4) transversely septate. A hemiamyloid ring in the tholus of the asci, which is present in *C. cinnabarinum* and *C. fallax*, could not be observed in the investigated material. Further differences to *C. cinnabarinum* and *C. fallax* are discussed under those species.

The protologue of *Arthonia cinnabarina* f. *cuspidans* (Nylander 1876) cites specimens from Ireland and Cuba as original material: “Illicicola in Hibernia (Larbalestier)” and “Exotica eadem datur in C. Wright. Cub. no. 123 a et b”. Nylander obviously considered the material from Ireland as the factual type collection. We have selected a specimen from the Nylander herbarium in Helsinki as the lectotype, which is the only specimen from Ireland that undoubtedly has been seen by Nylander. A possible syntype exists in BM: “Derryclare, Connemara, illicicola, 1876 [BM000974345]”. Another specimen [BM000974347] from Larbalestier’s herbarium has a printed later label that only states “On young trees. Doughruagh Mountain and other places in Connemara”. The type status of this specimen is unclear. Both specimens have been seen by us as high-resolution pictures obtained from the data portal of BM.

***Coniocarpon fallax* (Ach.) Grube**

Mycobank No: 808766

Figs 2, 3B, 4E, F, 5, 6C

Coniocarpon fallax (Ach.) Grube: Frisch et al., Taxon 63: 737 (2014). *Spiloma fallax* Ach., Methodus qua omnes delectos lichenes: 10 (1803) [MB 405518]. Type: Germania (H-Ach. 2 a), lectotype, selected in Frisch et al., Taxon 63: 737, 2014). = *Spiloma elegans* Ach., Lichenographia universalis: 135 (1810) [MB 405516]. *Coniocarpon elegans* (Ach.) Duby, Aug. Pyrami de Candolle Botanicon Gallicum: 675 (1830) [MB 383617]. *Lichen elegans* (Ach.) Lam. in Lamarck and Poiret, Encyclopédie méthodique, botanique, suppl. 3(1): 352 (1813) [MB 122540]. *Arthonia elegans* (Ach.) Almq., Kongliga Svenska vetenskaps-akademiens handlingar 17(6): 19 (1880) [MB 118959]. Type: Schleicher, Plantae Cryptogamicae Helvetiae exsiccatae, centuria 5 no. 54 (S, lectotype, selected in Van den Broeck et al., Plant Ecology and Evolution 151: 346, 2018).

Description. THALLUS pale fawn to gray brown, weakly glossy to matt, smooth, endophloeodal to partly epiphloeodal, continuous; *prothallus* line dark grey to brown, sometimes present when in contact with other lichens; *photobiont* trentepohlioid, the cells rounded to elliptical, 8–13 × 5–10 µm, forming short chains. ASCOMATA weakly elongate to irregularly lirellate, with steep flanks, emergent from thallus, 0.2–0.4 mm × 0.1–0.2 mm, 65–110 µm tall, typically forming loose to dense aggregations of 3–15 ascomata, weakly elongated to irregularly lirellate to stellate, 0.2–1.5(–2.3) × 0.1–1.8 mm;

disc black to dark purple black, flat to weakly convex, weakly glossy to matt, epruinose or with a thin layer of white pruina; *margins* level with the disc, orange–red pruinose, sometimes with additional patches of white pruina; *proper exciple* brown, 7–20 µm wide, composed of compressed and vertically oriented paraphysoidal hyphae, the hyphae 1–2 µm thick, branched and netted, often forming short hairs up to 17 µm long at the outer margin; old bark cells sometimes attached to the exciple; *epithecium* brown, 10–20 µm tall, conglutinated only in the lower parts, composed of branched tips of the paraphysoidal hyphae extending horizontally above the asci; the tips slightly widened to 3(–4) µm, sometimes extending from the epithecium as sparsely branched anticlinal hairs up to 24 µm long; *hymenium* hyaline, strongly conglutinated, 35–70 µm tall, paraphysoids densely branched and netted, 1–2 µm thick; *hypothecium* hyaline, conglutinated, 15–30 µm tall, formed of irregular prosoplectenchymatic hyphae 1–2 µm diam.; *crystals* common in epithecium and proper exciple, of two types: hyaline, leafy crystals, 1–5(–7) µm, and orange, red or purple granular crystals, 1–2(–4) µm; a weak amorphous, red to purple pigmentation present in exciple, epithecium and patchily distributed in the hymenium. ASCI of the *Arthonia*-type, long obpyriform to clavate, 50–75 × 20–32 µm (n = 33), 8-spored, the ascospores stacked; tholus 5–8 µm thick, lateral ascospore wall 1–2 µm thick. ASCOSPORES hyaline, (1–)3–4(–5) transversely septate, (15–)17–20(–22) × (6–)7–9(–10) µm (l: mean = 18.5, STD = 1.9; w: mean = 8.2, STD = 0.9; n = 191), obovate, with enlarged apical cell, getting pale brown with granular ornamentation in the epispore at late maturity; development macrocephalic.

Chemistry. Pigments A1, A3 and A4 in variable amounts detected by HPTLC. *Proper exciple* I_{dil}+ blue, I+ dark blue, KI+ dark blue; *epithecium* I_{dil}+ blue, I+ dark blue, KI+ dark blue; *hymenium* I_{dil}+ red, I+ red brown, KI+ dark blue; *hypothecium* I_{dil}+ blue, I+ dark blue, KI+ dark blue. A hemiamyloid ring present in the tholus of the asci. Hyaline, crystals dissolve in K. Orange, red and purple crystals dissolve in K with purplish solution.

Specimens examined. NORWAY – **Vest-Agder** • Lyngdalsfjord; on *F. excelsior*; 8. Apr. 1905; A. H. Magnusson leg.; S-F-71115 • *ibid.*; 1925; A. H. Magnusson leg.; S-F-71114 • *ibid.*; on *F. excelsior*; 25. Jan. 1939; A. H. Magnusson leg.; UPS-L-002899. – **Rogaland** • Gjesdal, Dirdal NE; on *F. excelsior*; 6. Oct. 1984; S. Hultengren leg.; UPS-L-654296 • *ibid.*; 58°49.810'N, 06°11.970'E; on *F. excelsior*; 160 m a.s.l.; 12. Jul. 2017; A. Frisch leg.; TRH-L-29036, TRH-L-29027. – **Hordaland** • Askøy; on *C. avellana* and *F. excelsior*; 1909; J. J. Havaas leg.; UPS-L-137313 • Fusa, Tveitane; 13 km S of Mundheim; 60°03'N, 05°52'E; on *C. avellana*; 150 m a.s.l.; 18. Aug. 1995; A. Nordin leg.; UPS-L-61739 • *ibid.*; Øvre Hålandsdalen, W of Orra; 60°15.5065'N, 05°55.137'E; on *F. excelsior*; 120 m a.s.l.; 24. Feb. 2015; S. Vatne leg.; TRH-L-16793. • Kvam, Daleelva N; 60°07.453'N, 05°52.721'E; on *F. excelsior*; 10. Jun. 2018; G. Gaarder leg.; TRH-L-18605 • *ibid.*; 60°07.668'N, 05°52.898'E; on *F. excelsior*; 13. Jun. 2018; G. Gaarder leg.; TRH-L-18606 • *ibid.*; Furhovda; 60°09.243'N, 05°53.910'E; on *F. excelsior*; 5. Jun. 2018; G. Gaarder, M. Lorentzen leg.; TRH-L-18604 • *ibid.*; Hovden; 60°13.735'N, 05°59.633'E; on *F. excelsior*; 11. Jun. 2018; G. Gaarder leg.; TRH-L-18607. • Lindås, Helltveit W; 60°37.872'N, 05°26.080'E; on *F. excelsior*; 24. Jul. 1980; T. Tønsberg leg.; BG-L-26222 • *ibid.*; Kvalvika-Røyldalane; 60°38.245'N,

05°26.345'E; on *F. excelsior*; 35 m a.s.l.; 14. May 2018; A. Frisch, J. Klepsland leg.; TRH-L-29035. • Os, Li; 60°10.38'N, 05°26.45'E; on *F. excelsior*; 60–120 m a.s.l.; 22. Jul. 1979; T. Tønberg leg.; BG-L-26221, BG-L-26221. • Stord, Valavåg, Nes-Åsen; 59°46.116'N, 05°24.660'E; on *F. excelsior*; 27. Apr. 2018; G. Gaarder, U. Hansen leg.; TRH-L-18041. • Tysnes, SE slope of Skardnipa near Teigen; 59°58.360'N, 05°39.008'E; on *F. excelsior*; 23 m a.s.l.; 9. May 2018; A. Frisch, J. Klepsland leg.; TRH-L-29031 • *ibid.*; 59°58.361'N, 05°39.023'E; on *F. excelsior*; 19 m a.s.l.; 9. May 2018; A. Frisch, J. Klepsland leg.; TRH-L-29032, TRH-L-29033 • *ibid.*; 59°58.350'N, 05°38.992'E; on *F. excelsior*; 24 m a.s.l.; 9. May 2018; A. Frisch, J. Klepsland leg.; TRH-L-29034 • *ibid.*; Sunde, Loksund; on *F. excelsior*; 27. Aug. 1910; J. J. Havaas leg.; UPS-L-137512. • Tysnes, Tysnesøy, N of Onarheim; 59°58.377'N, 05°39.047'E; on *F. excelsior*; 30 m a.s.l.; 21. Jul. 2017; A. Frisch leg.; TRH-L-29028, TRH-L-29029. – **Møre og Romsdal** • Fræna, S of Hustad, Lunheim; 62°55.3871'N, 07°06.892'E; on *C. avellana*; 60 m a.s.l.; 15. Apr. 2016; H. Holien leg.; TRH-L-17089 • *ibid.*; Nordmark E; 62°54.998'N, 07°07.068'E; on *C. avellana*; 80 m a.s.l.; 26. Apr. 1998; G. Gaarder leg.; BG-L-39619 • *ibid.*; Tverrfjell; 62°54.872'N, 07°16.243'E; on *C. avellana*; 60 m a.s.l.; 5. Jul. 2017; A. Frisch leg.; TRH-L-29037, TRH-L-29030. • Skodje, Igletjønna; 62°28.6565'N, 06°34.4845'E; on *C. avellana*; 20. Apr. 2014; G. Gaarder, P. Larsen leg.; TRH-L-16791. • Tingvoll, Kamsvågtrøa; 63°01.8998'N, 08°08.150'E; on *C. avellana*; 16. Feb. 2014; G. Gaarder leg.; TRH-L-15366 • *ibid.*; Langvatnet NE; 63°02.9460'N, 08°04.3020'E; on *C. avellana*; 8. Nov. 2014; G. Gaarder leg.; TRH-L-16792 • *ibid.*; Skjelberget; 63°03.2040'N, 08°03.8640'E; on *C. avellana*; 25. Apr. 2014; G. Gaarder leg.; TRH-L-16789 • *ibid.*; Årøyvatnet; 63°02.8320'N, 08°02.3940'E; on *C. avellana*; 8. Nov. 2014; G. Gaarder leg.; TRH-L-16790. SWEDEN – **Gotland** • Bunge, Hägur, Mörku, 1 km NE of the church; 57°51.00'N, 19°00.00'E; on *F. excelsior*; 15 m a.s.l.; 27. Apr. 1996; A. Nordin leg.; UPS-L-74225 • 600 m from Bunge church; on *F. excelsior*; 27. Apr. 1996; G. Westling leg.; S L-52399; • Bäl, Gute, 1 km E Bäl church; 57°39.00'N, 18°40.00'E; on *F. excelsior*; 25. Nov. 1996; P. Johanson leg.; UPS-L-98398.

Additional examined specimens. AUSTRIA – **Upper Austria** • Totes Gebirge, Lake Almsee SSE; 47°44.600'N, 13°57.400'E; on *F. excelsior*; 600 m a.s.l.; 31. May 1998; T. Tønberg leg.; BG-L-66299. TURKEY – **Trabazon** • Trabazon Vilayet, Uzungöl c. 14 km SSE of Caykara; 40°36.8700'N, 40°18.8500'E; on *P. orientalis*; 24. Jun. 2001; C. Printzen, B. Kanz leg.; BG-L-77481.

Notes. *Coniocarpon fallax* resembles *C. cinnabarinum* by ascomata that are covered in an orange–red and white pruina. However, the white pruina is less pronounced in *C. fallax* and may be absent. The ascomata of *C. fallax* further are elongate to clearly lirellate and the ascospores are distinctly smaller with less septa: (15–)17–20(–22) × (6–)7–9(–10) µm, (1–)3–4(–5) transversely septate vs (19–)23–28(–30) × (8–)10–11(–12) µm, (3–)4–5(–8) transversely septate in *C. cinnabarinum*. Mature, apparently well-developed elliptical ascospores with only a single septum were found in one specimen (TRH-L-17089) of *C. fallax*. *Coniocarpon cuspidans* has ascospores of similar size which, however, are predominantly 3-septate. The elongate to lirellate ascomata of that species lack an orange–red pruina, and proper exciple and epithecium react I_{iii}/I+ red in iodine.

Acknowledgements

The curators of the herbaria BG, C, H, O, PC, S, TRH and UPS are acknowledged for the loan of specimens and permission to study the material. Zdenek Palice kindly sent specimens of *Coniocarpon* from Great Britain (Scotland). The authors acknowledge financial support from the Norwegian Biodiversity Information Centre through the Species Project (pnr.70184237) *Three storied diversity: Mapping and barcoding crustose lichens and lichenicolous fungi in the Norwegian rainforests*.

References

- Acharius E (1803) Methodus qua omnes detectos lichenes. C. F. Marquard, Stockholmiae, iv, 1–393.
- Acharius E (1810) Lichenographia universalis. I. F. Danckwerts, Gottingae: viii, 1–696.
- Almqvist S (1880) Monographia Arthoniarum Scandinaviae. Kongliga Svenska Vetenskaps-Akademiens Handlingar 17(6): 3–69.
- Alors D, Lumbsch HT, Divakar PK, Leavitt SD, Crespo A (2016) An integrative approach for understanding diversity in the *Punctelia rudecta* species complex (Parmeliaceae, Ascomycota). PLoS ONE 11(2): e0146537. <https://doi.org/10.1371/journal.pone.0146537>
- Aptroot A, Sparrius LB (2003) New microlichens from Taiwan. Fungal Diversity 14: 1–50. <http://www.fungaldiversity.org/fdp/sfdp/14-1.pdf>
- Arup U, Ekman S, Lindblom L, Mattsson J-E (1993) High performance thin layer chromatography (HPTLC), an improved technique for screening lichen substances. The Lichenologist 25: 61–71. <https://doi.org/10.1006/lich.1993.1018>
- Bendiksby M, Haugan R, Spribille T, Timdal E (2015) Molecular phylogenetics and taxonomy of the *Calvitimela aglaea* complex (Tephromelataceae, Lecanorales). Mycologia 107: 1172–1183. <https://doi.org/10.3852/14-062>
- Blom HH (2018) Ikke eller svært lite uttørkningseksponeert boreonemoral og sørboreal skog i klart til sterkt oseanisk seksjon, Skog. Norsk rødliste for naturtyper 2018. Artsdatabanken, Trondheim. <https://artsdatabanken.no/RLN2018/84> [accessed 6 May 2019]
- Blom HH, Gaarder G, Ihlen PG, Jordal JB, Evju M (2015) Poor boreonemoral rain-forest – a hotspot-habitat. Final report from the third period of the ARKO project. NINA Report 1169. Norsk institutt for naturforskning (NINA), Trondheim 1–97.
- Boluda CG, Rico VJ, Divakar PK, Nadyeina O, Myllys L, McMullin RT, Zamora JC, Scheidegger C, Hawksworth DL (2019) Evaluating methodologies for species delimitation: the mismatch between phenotypes and genotypes in lichenized fungi (*Bryoria* sect. *Implexae*, Parmeliaceae). Persoonia 42: 75–100. <https://doi.org/10.3767/persoonia.2019.42.04>
- Carlsen T, Bendiksby M, Hofton TH, Reiso S, Bakkestuen V, Haugan R, Kausarud H, Timdal E (2012) Species delimitation, bioclimatic range, and conservation status of threatened lichen *Fuscopannaria confusa*. The Lichenologist 44: 565–575. <https://doi.org/10.1017/S0024282912000199>

- Coates DJ, Byrne M, Moritz C (2018) Genetic diversity and conservation units: Dealing with the species-population continuum in the age of genomics. *Frontiers in Ecology and Evolution* 6: 165. <https://doi.org/10.3389/fevo.2018.00165>
- Coppins BJ, Aptroot A (2009) *Arthonia* Ach. (1806). In: Smith CW, Aptroot A, Coppins BJ, Fletcher OL, James PA, Wolsely PA (Eds) *The Lichens of Great Britain and Ireland*. 6th edition. The British Lichen Society, 153–171.
- DellaSala DA, Alaback P, Drescher A, Holien H, Spribille T, Ronnenberg K (2011) Temperate and boreal rainforest relicts of Europe. In: DellaSala AD (Eds) *Temperate and Boreal Rainforests of the World: Ecology and Conservation*. Island Press, Washington DC, 154–160. https://doi.org/10.5822/978-1-61091-008-8_6
- Duby JE (1830) *Aug. Pyrami de Candolle Botanicon Gallicum. Editio secunda. Pars secunda, planta cellulares continens*, Desray, Paris, 545–1068.
- Frisch A, Thor G (2010) *Crypthonia*, a new genus of byssoid Arthoniaceae (lichenised Ascomycota). *Mycological Progress* 9: 281–303. <https://doi.org/10.1007/s11557-009-0639-8>
- Frisch A, Thor G, Ertz D, Grube M (2014) The Arthonialean challenge: restructuring Arthoniaceae. *Taxon* 63: 727–744. <https://doi.org/10.12705/634.20>
- Frisch A, Ohmura Y, Ertz D, Thor G (2015) *Inoderma* and related genera in Arthoniaceae with elevated white pruinose pycnidia or sporodochia. *The Lichenologist* 47: 233–256. <https://doi.org/10.1017/S0024282915000201>
- Frisch A, Grube M, Kashiwadani H, Ohmura Y (2018) Arthoniaceae with reddish, K+ purple ascomata in Japan. *Phytotaxa* 356: 19–33. <https://doi.org/10.11646/phytotaxa.356.1.2>
- Grube M (1995) A taxonomic survey of arthonioid fungi with reddish K+ reactive pigments. Doctoral dissertation, Karl-Franzens-Universität, Graz.
- Grube M (2001) *Coniarthonia*, a new genus of arthonioid lichens. *The Lichenologist* 33: 491–502. <https://doi.org/10.1006/lich.2001.0348>
- Grube M, Kroken S (2000) Molecular approaches and the concept of species and species complexes in lichenized fungi. *Mycological Research* 104: 1284–1294. <https://doi.org/10.1017/S0953756200003476>
- Hawksworth DL, Lücking R (2017) Fungal diversity revisited: 2.2 to 3.8 million species. *Microbiology Spectrum* 5(4): FUNK-0052-2016.
- Hall TA (1999) BioEdit: a user-friendly biological sequence alignment editor and analysis program for Windows 95/98/NT. *Nucleic Acids Symposium Series* 41: 95–98. <http://brownlab.mbio.ncsu.edu/JWB/papers/1999Hall1.pdf>
- Henriksen S, Hilmo O (2015) The Norwegian red list for species v.1.2. Artsdatabanken, Norway, 1–193.
- Huelsensbeck JP, Ronquist F, Nielsen R, Bollback JP (2001) Bayesian inference of phylogeny and its impact on evolutionary biology. *Science* 294: 2310–2314. <https://doi.org/10.1126/science.1065889>
- Lamarck MM, de Candolle AP (1805) *Flore française. Troisième édition. Tome second*. H. Agasse, Paris, xii, 1–600.
- Lamarck MM, Poirer JLM (1813) *Encyclopédie méthodique. Botanique, suppl. 3(1)*. H. Agasse, Paris, 1–368.

- Lanfear R, Frandsen PB, Wright AM, Senfeld T, Calcott B (2016) PartitionFinder 2: new methods for selecting partitioned models of evolution for molecular and morphological phylogenetic analyses. *Molecular Biology and Evolution* 34: 772–773. <https://doi.org/10.1093/molbev/msw260>
- Larena I, Salazar O, González V, Julián MC, Rubio V (1999) Design of a primer for ribosomal DNA internal transcribed spacer with enhanced specificity for ascomycetes. *Journal of Biotechnology* 75: 187–194. [https://doi.org/10.1016/S0168-1656\(99\)00154-6](https://doi.org/10.1016/S0168-1656(99)00154-6)
- Leavitt SD, Johnson L, St. Clair LL (2011) Species delimitation and evolution in morphologically and chemically diverse communities of the lichen forming genus *Xanthoparmelia* (Parmeliaceae, Ascomycota) in Western North America. *American Journal of Botany* 98: 175–188. <https://doi.org/10.3732/ajb.1000230>
- Liu YJ, Whelen S, Hall BD (1999) Phylogenetic relationships among ascomycetes: evidence from an RNA polymerase II subunit. *Molecular Biology and Evolution* 16: 1799–1808. <https://doi.org/10.1093/oxfordjournals.molbev.a026092>
- Lücking R, Dal-Forno M, Sikaroodi M, Gillevet PM, Bungartz F, Moncada B, Yáñez-Ayabaca A, Chaves JL, Coca FL, Lawrey JD (2014) A single macrolichen constitutes hundreds of unrecognized species. *Proceedings of the National Academy of Sciences of the United States of America* 111: 11091–11096. <https://doi.org/10.1073/pnas.1403517111>
- Lumbsch HT, Leavitt SD (2011) Goodbye morphology? A paradigm shift in the delimitation of species in lichenized fungi. *Fungal Diversity* 50: 59–72. <https://doi.org/10.1007/s13225-011-0123-z>
- Miller MA, Pfeiffer W, Schwartz T (2010) Creating the CIPRES Science Gateway for inference of large phylogenetic trees. *Proceedings of the Gateway Computing Environments Workshop (GCE), New Orleans, LA, 1–8*. <https://doi.org/10.1109/GCE.2010.5676129>
- Moen A (1999) National atlas of Norway: vegetation. Norwegian Mapping Authority, 1–200.
- Molina MC, Del-Prado R, Divakar PK, Sánchez-Mata D, Crespo A (2011) Another example of cryptic diversity in lichen-forming fungi: The new species *Parmelia mayi* (Ascomycota: Parmeliaceae). *Organism, Diversity & Evolution* 11: 331–342. <https://doi.org/10.1007/s13127-011-0060-4>
- Nixon, KC (1999–2002) WinClada ver. 1.0000. Published by the author, Ithaca, NY, USA.
- Nylander W (1876) Addenda nova ad Lichenographiam europaeam XXV. *Flora* 59: 305–311.
- Pattengale, ND, Alipour M, Binida-Emonds OR, Moret BM, Stamatakis A (2010) How many bootstrap replicates are necessary? *Journal of Computational Biology* 17: 337–354. <https://doi.org/10.1089/cmb.2009.0179>
- Printzen C (2010) Lichen systematics: the role of morphological and molecular data to reconstruct phylogenetic relationships. In: Lüttge U (Ed.) *Progress in Botany*. Berlin, Springer, 233–275. https://doi.org/10.1007/978-3-642-02167-1_10
- QGIS Development Team (2019) QGIS Geographic Information System. Open Source Geospatial Foundation Project.
- Rambaut A (2018) FigTree, ver. 1.4.4. [online]. <http://tree.bio.ed.ac.uk/software/figtree/> [accessed 1 Feb. 2019]
- Ronquist F, Huelsenbeck JP (2003) MrBayes 3: Bayesian phylogenetic inference under mixed models. *Bioinformatics* 19: 1572–1574. <https://doi.org/10.1093/bioinformatics/btg180>

- Santesson R (1952) Foliicolous lichens I. A revision of the taxonomy of the obligately foliicolous, lichenized fungi. *Symbolae Botanicae Upsalienses* 12(1): 1–590.
- Schwarz G (1979) Estimating the dimension of a model. *Annals of Statistics* 6: 461–464. <https://doi.org/10.1214/aos/1176344136>
- Stamatakis A (2014) RAxML Version 8: A tool for Phylogenetic Analysis and Post-Analysis of Large Phylogenies. *Bioinformatics* 30: 1312–1313. <https://doi.org/10.1093/bioinformatics/btu033>
- Steinová J, Stereos S, Grube M, Škaloud P (2013) Genetic diversity and species delimitation of the zeorin-containing red-fruited *Cladonia* species (lichenized Ascomycota) assessed with ITS rDNA and b-tubulin data. *The Lichenologist* 45(5): 665–684. <https://doi.org/10.1017/S0024282913000297>
- Sundin R, Tehler A (1998) Phylogenetic studies of the genus of *Arthonia*. *The Lichenologist* 30: 381–413. <https://doi.org/10.1017/S0024282992000409>
- Van den Broeck D, Frisch A, Razafindrahaja T, Van de Vijver B, Ertz D (2018) Phylogenetic position of *Synarthonia* (lichenized Ascomycota, Arthoniaceae), with the description of six new species. *Plant Ecology and Evolution* 151: 327–351. <https://doi.org/10.5091/plecevo.2018.1506>
- Weigel CE (1772) *Observationes botanicae*. F. Röse, Gryphiae, viii, 1–51. <https://doi.org/10.5962/bhl.title.123718>
- White TJ, Bruns T, Lee S, Taylor J (1990) Amplification and direct sequencing of fungal ribosomal RNA genes for phylogenetics. In: Innis MA, Gelfand DH, Sninsky JJ, White TJ (Eds) *PCR Protocols: A Guide to Methods and Applications*, Academic Press, New York, 315–322. <https://doi.org/10.1016/B978-0-12-372180-8.50042-1>
- Zoller S, Scheidegger C, Sperisen C (1999) PCR primers for the amplification of mitochondrial small subunit ribosomal DNA of lichen-forming ascomycetes. *The Lichenologist* 31: 511–516. <https://doi.org/10.1006/lich.1999.0220>

***Longistriata flava* (Boletaceae, Basidiomycota) – a new monotypic sequestrate genus and species from Brazilian Atlantic Forest**

Marcelo A. Sulzbacher¹, Takamichi Orihara², Tine Grebenc³, Felipe Wartchow⁴, Matthew E. Smith⁵, María P. Martín⁶, Admir J. Giachini⁷, Iuri G. Baseia⁸

1 Departamento de Micologia, Programa de Pós-Graduação em Biologia de Fungos, Universidade Federal de Pernambuco, Av. Nelson Chaves s/n, CEP: 50760-420, Recife, PE, Brazil **2** Kanagawa Prefectural Museum of Natural History, 499 Iryuda, Odawara-shi, Kanagawa 250-0031, Japan **3** Slovenian Forestry Institute, Večna pot 2, SI-1000 Ljubljana, Slovenia **4** Departamento de Sistemática e Ecologia/CCEN, Universidade Federal da Paraíba, CEP: 58051-970, João Pessoa, PB, Brazil **5** Department of Plant Pathology, University of Florida, Gainesville, Florida 32611, USA **6** Departamento de Micologia, Real Jardín Botánico, RJB-CSIC, Plaza Murillo 2, Madrid 28014, Spain **7** Universidade Federal de Santa Catarina, Departamento de Microbiologia, Imunologia e Parasitologia, Centro de Ciências Biológicas, Campus Trindade – Setor F, CEP 88040-900, Florianópolis, SC, Brazil **8** Departamento de Botânica e Zoologia, Universidade Federal do Rio Grande do Norte, Campus Universitário, CEP: 59072-970, Natal, RN, Brazil

Corresponding author: Tine Grebenc (tine.grebenc@gozdis.si)

Academic editor: A. Vizzini | Received 4 September 2019 | Accepted 8 November 2019 | Published 3 February 2020

Citation: Sulzbacher MA, Orihara T, Grebenc T, Wartchow F, Smith ME, Martín MP, Giachini AJ, Baseia IG (2020) *Longistriata flava* (Boletaceae, Basidiomycota) – a new monotypic sequestrate genus and species from Brazilian Atlantic Forest. MycoKeys 62: 53–73. <https://doi.org/10.3897/mycokeys.62.39699>

Abstract

A new monotypic sequestrate genus, *Longistriata* is described based on collections from the Neotropical forest of Atlantic forest in Paraíba, Northeast Brazil – an area known for its high degree of endemism. The striking features of this new fungus are the hypogeous habit, the vivid yellow peridium in mature basidiomes, broadly ellipsoid basidiospores with a distinct wall that is ornamented with longitudinal striations and lageniform cystidia with rounded apices. Phylogenetic analysis, based on LSU and *tef-1a* regions, showed that the type species, *Longistriata flava*, is phylogenetically sister to the monotypic sequestrate African genus *Mackintoshia* in Boletaceae. Together these two species formed the earliest diverging lineage in the subfamily Zangioideae. *Longistriata flava* is found in nutrient-poor white sand habitats where plants in the genera *Coccoloba* (Polygonaceae) and *Guapira* (Nyctaginaceae) are the only potential ectomycorrhizal host symbionts.

Keywords

Boletales, ITS, phylogeny, sequestrate fungi, taxonomy, tropical forest.

Introduction

Fungi in the order Boletales (Agaricomycetes, Basidiomycota) comprise a morphological diverse group including agaricoid, boletoid, gasteroid, secotioid, corticioid, merulioid, hydroid and polyporoid forms (Binder and Hibbett 2006) with ectomycorrhizal (ECM), saprophytic or ligninolytic members (Kirk et al. 2008). The order is a globally distributed group of mushroom-forming fungi growing in most forest ecosystems (Chu-Chou and Grace 1983; Binder and Hibbett 2006). Despite thorough morphological (Rolland 1899; Høiland 1987; Pegler and Young 1989; Montecchi and Sarasini 2000) and phylogenetic coverage of the order Boletales (Kretzer and Bruns 1999; Binder and Bresinsky 2002; Binder and Hibbett 2006; Orihara et al. 2016a) new phylogenetically supported genera are still being discovered, particularly representatives with a sequestrate habitat (Nuhn et al. 2013; Wu et al. 2014, 2016). The sequestrate habitat has arisen in this order multiple times and a large number of sequestrate genera in Boletaceae have been described: *Carolinigaster* M.E. Sm. & S. Cruz (Crous et al. 2018), *Chamonixia* Rolland (Binder and Bresinsky 2002; Orihara et al. 2016a), *Heliogaster* Orihara & Iwase (Orihara et al. 2010), *Kombocles* Castellano, T.W. Henkel & Dentinger (Castellano et al. 2016), *Octaviana* Vittad. (Vittadini 1831; Orihara et al. 2012), *Mackintoshia* Pacioni and Sharp (2000), *Rhodactina* Pegler and T.W.K. Young (Yang et al. 2006; Vadthananarat et al. 2018), *Rossbeevera* T. Lebel and Orihara (Lebel et al. 2012), *Royoungia* Castellano, Trappe and Malajczuk (Castellano et al. 1992), *Solioccasus* Trappe et al. (Trappe et al. 2013), *Turmalinea* Orihara and N. Maek. (Orihara et al. 2016b) and *Afrocastellanoa* M.E. Smith & Orihara (Orihara and Smith 2017).

Sequestrate Boletaceae have been described from across the globe with records from all continents except Antarctica but relatively little is known about sequestrate boletoid fungi in South America (Putzke 1994; Sulzbacher et al. 2017). Species of *Rhizopogon* Fr. & Nordholm (Fries and Nordholm 1817) and *Scleroderma* Pers. (Persoon 1801) are broadly distributed and most frequently recorded in forest plantations with introduced pines, eucalypts or pecan trees (Martín 1996; Giachini et al. 2000; Baseia and Milanez 2002; Nouhra et al. 2012; Sulzbacher et al. 2016a, 2018). However, there are relatively few citations of sequestrate taxa from native ectotrophic forests. Examples from temperate habitats include *Alpova austroalnicola* L.S. Domínguez in *Alnus acuminata* Kunth ssp. *acuminata* forests in the Yunga District of Argentina (Nouhra et al. 2005) and *Scleroderma patagonicum* Nouhra & Hern. Caff. in Patagonian *Nothofagus* forests (Nouhra et al. 2012). Recently, undescribed taxa of sequestrate Boletaceae were cited from tropical forests in Guyana (Henkel et al. 2012; Smith et al. 2013) and formally described as *Jimtrappea* T.W. Henkel, M.E. Smith & Aime, *Castellanea* T.W. Henkel & M.E. Sm. and *Costatisporus* T.W. Henkel & M.E. Sm. (Smith et al. 2015). These new

records from the Guiana Shield suggest that other unexplored tropical forests in South America may host additional diversity of sequestrate Boletales, similar to recent reports from Asia and Africa (Castellano et al. 2016; Chai et al. 2019).

In Brazil, there are numerous surveys that have documented epigeous Boletales in exotic plantations and native forests (Rick 1961; Guzmán 1970; Putzke 1994; Wautling and de Meijer 1997; Baseia and Milanez 2000; Giachini et al. 2000; Baseia and Milanez 2002; Sobestiansky 2005; de Meijer 2006; Gurgel et al. 2008; Cortez et al. 2011; Magnago and Neves 2014; Barbosa-Silva and Wartchow 2017; Barbosa-Silva et al. 2017; Magnago et al. 2017a, 2017b 2018, 2019). However, information related to sequestrate hypogeous fungi is scanty (Sulzbacher et al. 2016a).

As part of recent studies on ectomycorrhizal and sequestrate fungi in northeastern Brazil (Sulzbacher et al. 2013, 2017), we collected a sequestrate taxon that could not be assigned to any current species in the family Boletaceae. Here we describe and characterize the new sequestrate boletoid species in a newly erected genus *Longistriata* based on sequence analyses of the ITS, nLSU, and *TEF1* molecular markers as well as detailed analysis of morphological features. From available collections and publicly available sequences we discuss how this new species differs from all currently described genera in Boletales and we discuss the trophic mode of this new species and genus.

Methods

Sampling and morphological studies

Specimens were collected in survey missions targeting sequestrate fungi during the rainy seasons of 2011–2013 (Sulzbacher et al. 2016b). Sampling sites were located in forests at the Guaribas Biological Reserve, between 06°39'47"S and 06°42'57"S and 35°06'46"W and 35°08'00"W (Barbosa et al. 2011). This area is a protected Atlantic rainforest reserve comprising 4029 ha that is in the vicinity of the cities of Mamanaguape and Rio Tinto in the state of Paraíba, Brazil (Fig. 1A). Soils are of the Tertiary sediments of the Barreiras Formation (Barbosa et al. 2011). The predominant vegetation ranges from lowland semi-deciduous forest to savanna, also known as “tabuleiro” (Fig. 1B). The dominant plant families in the Guaribas Biological Reserve are Cyperaceae, Fabaceae, Melastomataceae, Myrtaceae, Poaceae, Polygonaceae and Rubiaceae (Barbosa et al. 2011). Confirmed ectomycorrhizal host plants in this region include species of *Coccoloba* (Polygonaceae) (Bâ et al. 2014; Pölme et al. 2017) and *Guapira* (Nyctaginaceae) (Wang and Qiu 2006; Tedersoo et al. 2010a). Basidiomata were discovered using the methodology described in Castellano et al. (2004) by raking the leaf litter and topsoil. All basidiomata were photographed *in situ* and then dried in a forced-air dryer. Macro- and microscopic characters were observed with a stereomicroscope (EZ4 Leica, Leica Microsystems, Mannheim, Germany) and light microscope (Eclipse Ni Nikon, Nikon Corporation, Tokyo, Japan). Line drawings of microscopic structures were made with the aid of a drawing tube (BX41 Olympus, Olympus America Inc., Melville, NY, USA). Basidiospore data follows the methodology proposed by

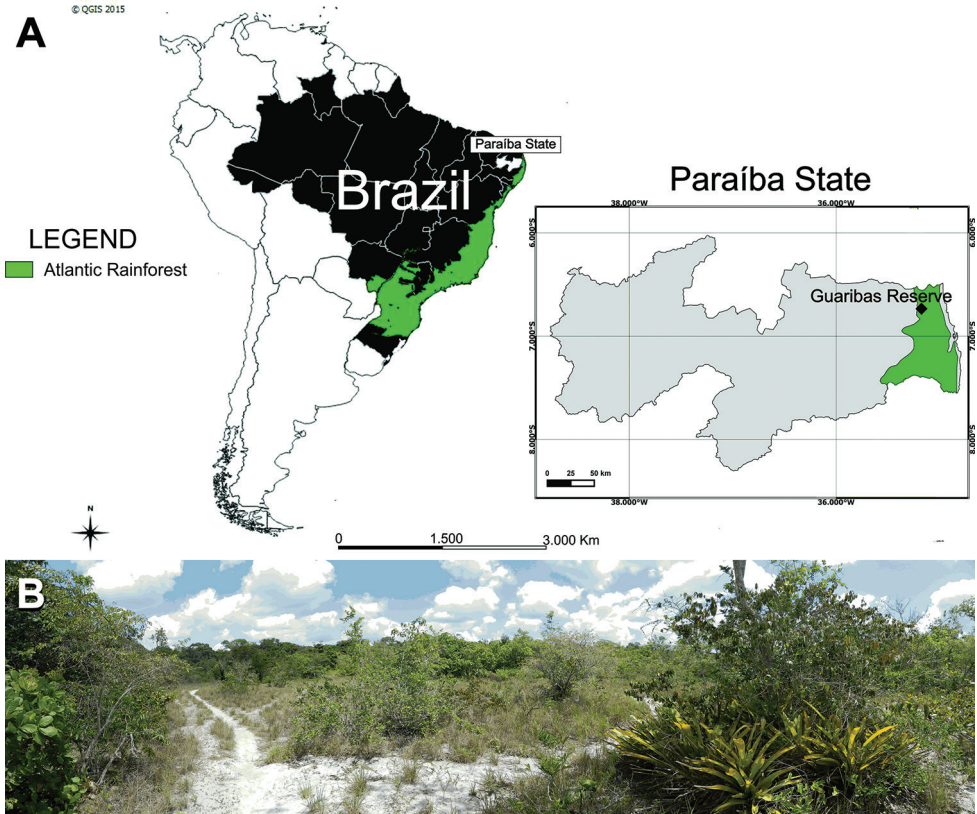


Figure 1. **A** Map of South America with Atlantic rainforest (in green) and magnified area of the State of Paraíba, including the location of the Guaribas Biological Reserve **B** the sampling sites at the Guaribas Biological Reserve with typical vegetation in the white sandy soil ecosystem.

Tulloss et al. (1992). Measurements and statistics are based on 30 mature spores. Abbreviations include $L(W)$ = average basidiospore length (width), Q = the length:width ratio range as determined from all measured basidiospores, and Q_m = the Q value averaged from all measured basidiospores. Colors of basidiomes were observed from fresh material with color coding following Methuen Handbook of Colour (Kornerup and Wanscher 1978). The holotype is deposited at the herbarium of the Universidade Federal do Rio Grande do Norte (UFRN) with additional material deposited at the herbarium of the Slovenian Forestry Institute (LJF).

DNA extraction, PCR amplification and sequencing

Fungal DNA was extracted from fresh specimens (UFRN-fungos 1756 and UFRN-fungos 2110) using a DNeasy Plant Mini Kit (QIAGEN) according to the manufacturer's instructions. Partial sequences were obtained from the nuclear internal transcribed spacer (ITS) and a large subunit (nLSU) of nuclear ribosomal DNA,

with the primer pairs ITS1F/ITS4 (Gardes and Bruns 1993; White et al. 1990) and LR0R/LR7 (Vilgalys and Hester 1990), respectively. Sequences were also obtained from the translation elongation factor 1- α gene (*TEF1*) with primer pair EF1-983F/EF1-1953R (Rehner and Buckley 2005). PCR reactions were performed according to Sulzbacher et al. (2016a). PCR was performed in a PTC-100 Thermocycler (MJ Research, Inc.) under the following conditions: first extension at 94 °C for 30 sec; denaturation at 94 °C for 45 sec; annealing at 55 °C (30 sec), extension at 72 °C (60 sec) for 35 cycles; and a final extension at 72 °C for 10 min. The PCR product was fractionated by electrophoresis on an 1.2% agarose gel in TBE buffer and then stained with ethidium bromide under UV light (360 nm). DNA was sequenced using a double-stranded DNA template of PCR product following the protocol supplied by Amersham Bioscience in a MegaBACE 500 (Amersham Biosciences Corp, Piscataway, NJ, USA). Newly obtained sequences were compared with homologous sequences available in the International Nucleotide Sequence Databases through BLASTn searches (Altschul et al. 1997).

Phylogenetic analyses

Suppl. material 1: Table S1 shows the sequences of nLSU and *TEF1* that were retrieved from the International Nucleotide Sequence Databases for our analyses. Sequences were carefully selected so that the dataset included representative genera from across the Boletaceae based on Wu et al. (2016). Sequences of *Chalciporus* spp. and *Buchwaldoboletus lignicola* (Kallenb.) Pilát were used as outgroups. Sequence alignment was performed with the online version of MAFFT v. 7 (Kato and Standley 2013) under default settings (i.e., the alignment algorithm is automatically selected from FFT-NS-1, FFT-NS-2, FFT-NS-i or L-INS-i). Subsequently, the sites with obvious alignment errors were manually adjusted in SEAVIEW v. 4. Prior to multigene analyses, we compared the neighbor joining clustering method (NJ) tree topologies between the nLSU and *TEF1* datasets on the SEAVIEW v. 4 platform. Since no major topological conflict (NJ bootstrap values $\geq 75\%$) was seen between the resulting nLSU and *TEF1* trees, we subsequently concatenated the two datasets for the multigene analyses. The *TEF1* region was partitioned by codons and introns, and best-fit likelihood models were estimated for each partition with MrModeltest v. 2.3 (Nylander 2004).

Bayesian analyses were conducted with MrBayes 3.2 (Ronquist and Huelsenbeck 2003). The SYM + G model (symmetrical nucleotide substitution model with gamma distributed rate variation among sites) was selected for nLSU and all of the codons and partitions of *TEF1*. Bayesian posterior probabilities (PP) were estimated by the Metropolis-coupled Markov chain Monte Carlo method (Geyer 1991). In the multigene (*nLSU* + *TEF1*) analysis, two parallel runs were conducted with one cold and seven heated chains each for 10M generations. The parameter for the temperature of the seven heated chains in both runs was set to 0.10. The 0.10 heating scheme was used instead of the default 0.20 setting because convergence was not achieved during preliminary runs at the 0.20 setting, probably due to Markov chains being trapped in

local optima. Trees were saved to a file every 1000th generation. We determined that the two runs reached convergence when the average standard deviation of split frequencies (ASDSF) was continuously lower than 0.01. The ASDSF was monitored every 5000 generations. We also verified the convergence by checking that the effective sample size (ESS) of each resulting statistic was sufficiently large (> 200). Trees obtained before reaching convergence were discarded as the burn-in, and the remaining trees were used to calculate a 50% majority consensus topology and to determine PP values for individual branches.

Maximum likelihood (ML) analyses were conducted with RAxML 8.2.10 (Stamatakis 2014). The same partitioned datasets as those for the Bayesian analyses were used so that different α -shape parameters, GTR rates (general time reversible substitution model), and empirical base frequencies could be assigned to each partition. The best-fit ML tree was estimated under the GTR+I+G models. The rapid bootstrap (BS) analysis was implemented with 1000 replicates.

Results

The *nLSU* + *TEFI* combined dataset consisted of 85 taxa and 2,014 aligned nucleotide positions. The Bayesian inference reached convergence after 4.6M generations. We therefore discarded the first 4,600 trees in each chain, and the remaining 5,401 trees in each chain were summarized to approximate Bayesian posterior probabilities (PPs). ESS of all the model parameters were sufficiently large (>200). The total arithmetic and harmonic means of Likelihoods (lnL) were -29,498.16 and -29,562.71, respectively. In RAxML analysis the log likelihood of the ML tree was -29,121.825209.

The *nLSU* + *TEFI* combined tree of the Boletaceae supported our hypothesis that the sequestrate basidiomes of the vivid yellow fungus belong to an undescribed genus in the Boletaceae (Fig. 2). The species described here as *Longistriata flava* Sulzbacher, Orihara, Grebenc, M.P. Martín & Baseia, sp. nov. formed a sister lineage to the African monotypic sequestrate genus *Mackintoshia* (KC905034) with moderate to high statistical support (PP = 1.0, ML-BS = 59%). The phylogenetic analyses further suggested that the *Longistriata-Mackintoshia* clade is the earliest diverging lineage within the subfamily *Zangioideae* (PP = 1.0, ML-BS = 60%). The epigeous yellowish bolete species (*Tylopilus* sp. Sulzbacher 454 in Suppl. material 1: Table S1) that sometimes occurred sympatrically with *Longistriata flava* was distantly related to *L. flava* and was instead more closely related to *Tylopilus balloui*. Other genera of Boletaceae that are closely related to *Longistriata* based on our phylogenetic analysis are species of *Australopilus* Halling & Fechner, *Chiuia* Yan C. Li & Zhu L. Yang, *Harrya* Halling, Nuhn & Osmudson, *Hymenoboletus* Yan C. Li & Zhu L. Yang, *Royoungia* Castellano, Trappe & Malajczuk, and *Zangia* Yan C. Li & Zhu L. Yang. All sister clades have significant bootstrap support in phylogenetic analyses and show a range of morphological differences that sup-

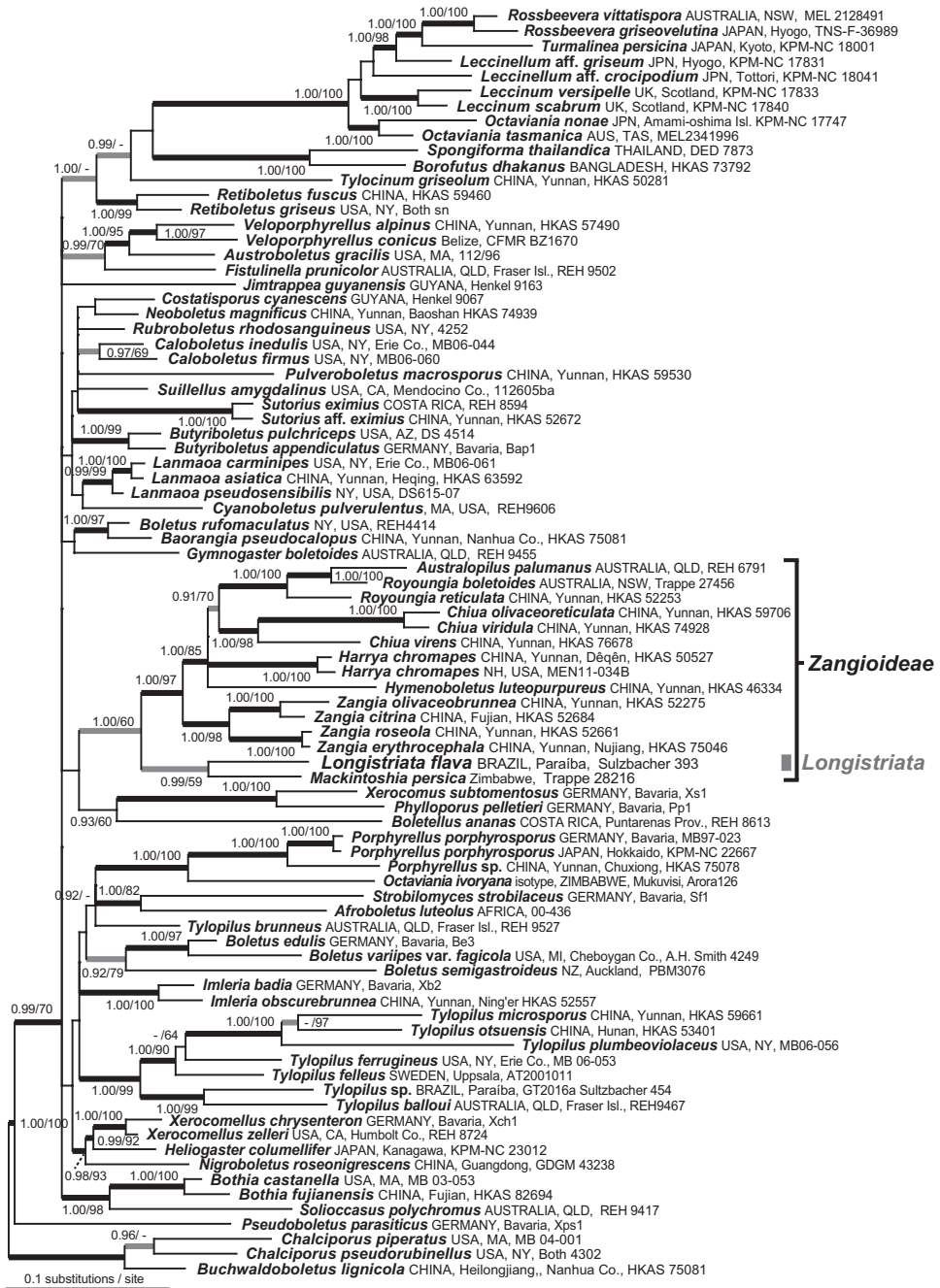


Figure 2. A *nLSU* + *TEF1* combined Maximum likelihood (ML) phylogram showing the phylogenetic relationship of *Longistriata* (UFRN-Fungus 1756, holotype) in relation to representative taxa in the Boletaceae. Non-parametric bootstrap branch supports (MPBs / MLBs) are given for nodes with bs>50.

port the erection of *Longstriata* as a separate genus. The ITS rDNA barcode sequences of *L. flava* specimens UFRN-fungos 1756 and UFRN-fungos 2110 were 751 bp in length (Suppl. material 1: Table S1). These sequences were less than 93% similar to all other ITS rDNA sequences in the INSD database. Below we describe this new genus and species and provide detailed morphological analysis and direct comparison with previously described sequestrate Boletaceae.

Taxonomy

***Longistriata* Sulzbacher, Orihara, Grebenc, M.P. Martín & Baseia, gen. nov.**

Mycobank No: 816322

Etymology. *Longis* (Latin), with or from the long; *striatus* (Latin), striate, fluted; in reference to the distinctive series of thin longitudinal striations on the surface of the basidiospores.

Diagnosis. Distinguished from other genera in *Boletaceae* by a combination of the following characters: Basidiomata hypogeous to subhypogeous, sequestrate, subglobose, with a short stipe (Fig. 3A–B). Peridium bright yellow, smooth, with a cutis of interwoven and gelatinized inflated hyphae. Subgelatinous sterile base (a short stipe) present. Gleba loculate, white when immature to yellowish brown at maturity, turning dark green to black when cut in older basidioma, columella absent. Basidiospores broadly ellipsoid, hyaline to light brown at maturity, dextrinoid, with a series of thin, irregular longitudinal ridges across the spore surface; in some places these ridges are fused together. Cystidia are lageniform with rounded apices. Clamp connections absent. Found in white sand habitat in tropical ectotrophic forests. Potentially mycorrhizal with tropical ectomycorrhizal plants from genera *Coccoloba* (Polygonaceae) and *Guapira* (Nyctaginaceae).

Type species. *Longistriata flava* Sulzbacher, Orihara, Grebenc, M.P. Martín & Baseia, sp. nov.

***Longistriata flava* Sulzbacher, Orihara, Grebenc, M.P. Martín & Baseia, sp. nov.**

Mycobank No: 816323

Figs 3–5

Etymology. *Flavus* (Latin), refers to the yellow peridium of the species.

Holotype: BRAZIL, Paraíba State, Mamanguape, Guaribas Biological Reserve, 06°44.545'S, 35°08.535'W, 14.VII.2012, leg. *Sulzbacher*–393 (UFRN-fungos 1756). GenBank accession number for ITS, nLSU and *TEF1*: LT574840; LT574842; LT574844

Description. Basidiomata hypogeous to subhypogeous, 11–24 mm wide, 13–16 mm high; subglobose, depressed subglobose to oblong in older stages, with small folds at the base; with a short stipe (Fig. 3A–B). Peridium <0.8 mm thick, at younger stages

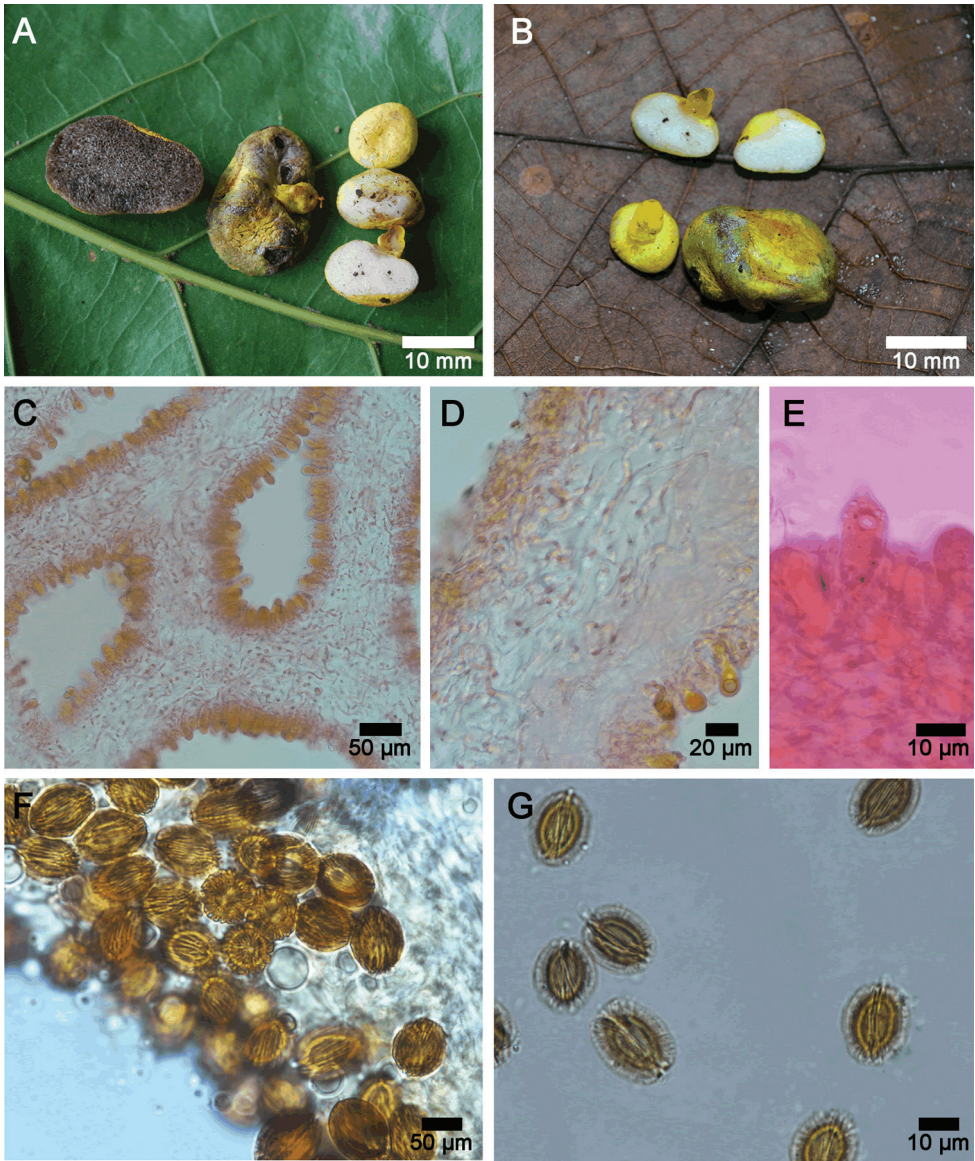


Figure 3. A–G *Longistriata flava* (UFRN-Fungus1756, holotype) **A–B** fresh mature basidioma **C** hymenophoral trama mounted in 3% KOH with Congo Red **D** interwoven hyphae of peridium (upper left) and hymenophoral trama mounted in 3% KOH with Congo Red **E** hymenial cystidia mounted in 3% KOH with Congo Red **F** basidiospores mounted in Melzer's reagent **G** basidiospores mounted in 3% KOH.

yellow (2A6) to light yellow (1A5) then yellowish brown (5D8) to brownish yellow (5C8) at maturity; smooth and glabrous, sometimes finely fibrillose. Sterile base present, short, 6–8 × 3–4 mm, clavate with a bulbous slightly developed base; color vivid yellow (3A8), brownish yellow (5C8) when bruised; surface glabrous, with small folds

and depressions; the inner part is full, subgelatinous and yellowish brown (5D8); connected by scattered and short, thin (0.3–0.5 mm diam), orange (6B8) rhizomorphs. Gleba loculate, non-gelatinized to gelatinized, with irregular locules (0.5–1 mm diam); white (1A1) at younger stages, to finally yellowish brown (5F4) at maturity, immediately turning deep green (30F7) to black when cut in older basidiomata.

Peridium 100–200 µm thick, composed by a cutis of interwoven hyphae and immersed in a gelatinized matrix (Fig. 4C), 2–6 µm diam., with rounded, thin-walled, smooth, terminal hyphae, not readily separable from gleba. Hymenophoral trama formed by parallel to subparallel, smooth and thin-walled, hyaline hyphae, inamyloid, gelatinized in the central part, 3–6 µm diam (Fig. 3C–D). Subhymenium ramose, 46–72 µm deep, hyphae 10–16 × 2–5 µm diam. Hymenial cystidia 38–78.5 × 10–14 µm, lageniform or ventricose, with rounded apex, thin-walled, hyaline, inamyloid (Figs 3E, 4A). Basidia 25–48 × 10–15 µm, clavate, 2 and 4-spored (sterigmata up to 3 µm long.), hyaline. Basidioles 31–46 × 7–12 µm, clavate with rounded apex (Fig. 4B). Basidiospores [30/2/2] 15–19 (–20) × 13–16 (–17) µm (ornamentation included), [L = 17.7 µm, W = 14.7 µm, Q = 1.10–1.40 (–1.50), Qm = 1.20], broadly ellipsoid, sterigmal attachment persistent at maturity, up to 3 µm long; hyaline when young to finally light brown at maturity in 3% KOH, dextrinoid in Melzer's reagent; walls ornamented (< 2.5 µm width); with a series of thinner longitudinal ridges, in average > 10 complete ridges across the longitudinal axis of the spore with additional irregular, thin and low ridges that are sometimes bifurcated (Figs 3F–G, 4D) or fused together (Fig. 5C); under a scanning electron microscope the surface is clearly longitudinally striated (Fig. 5A–D).

Habitat. Hypogeous to subhypogeous, solitary or scattered, under fallen leaves or in O1 soil horizon, in sandy soil, among trees in Brazil's Atlantic rainforest, in vicinity of *Coccoloba alnifolia* Casar., *C. laevis* Casar. (Polygonaceae) and species of *Guapira* Aubl. (Nyctaginaceae). Species in both plant genera (*Coccoloba* and *Guapira*) have been consistently confirmed as ectomycorrhizal hosts throughout the Neotropics (Tedesoo et al. 2010b). All known specimens were found in silicate silt to sandy soils, with moderately low pH (4.5–5.5), low available nutrients and low water capacity. Despite the close vicinity of the ocean, the absence of halophilic vegetation indicates a lack of salinification or accumulation of NaCl in soils.

Distribution. Known only from the type locality.

Additional specimens examined. BRAZIL, Paraíba State, Mamanguape, Guaribas Biological Reserve, 06°44.545'S, 35°08.535'W, 27.VII.2012, leg. *Sulzbacher-466* (paratype UFRN-fungos 2110, LJF 1203). GenBank accession number for ITS: LT574839.

Additional Comments. The specimens UFRN-fungos 1756 and UFRN-fungos 2110 are sequestrate to emergent basidiomes that fruit in small groups. The basidiomes have a smooth and vivid yellow peridium that becomes dark green when exposed to air. They also have a central sterile base that is attached to short orange rhizomorphs, a white gleba formed of distinct locules that turns dark green to black when cut and hyaline to light brown, broadly ellipsoid basidiospores covered with a series of thin, dextrinoid longitudinal striations and ridges. These ridges and striations are sometimes

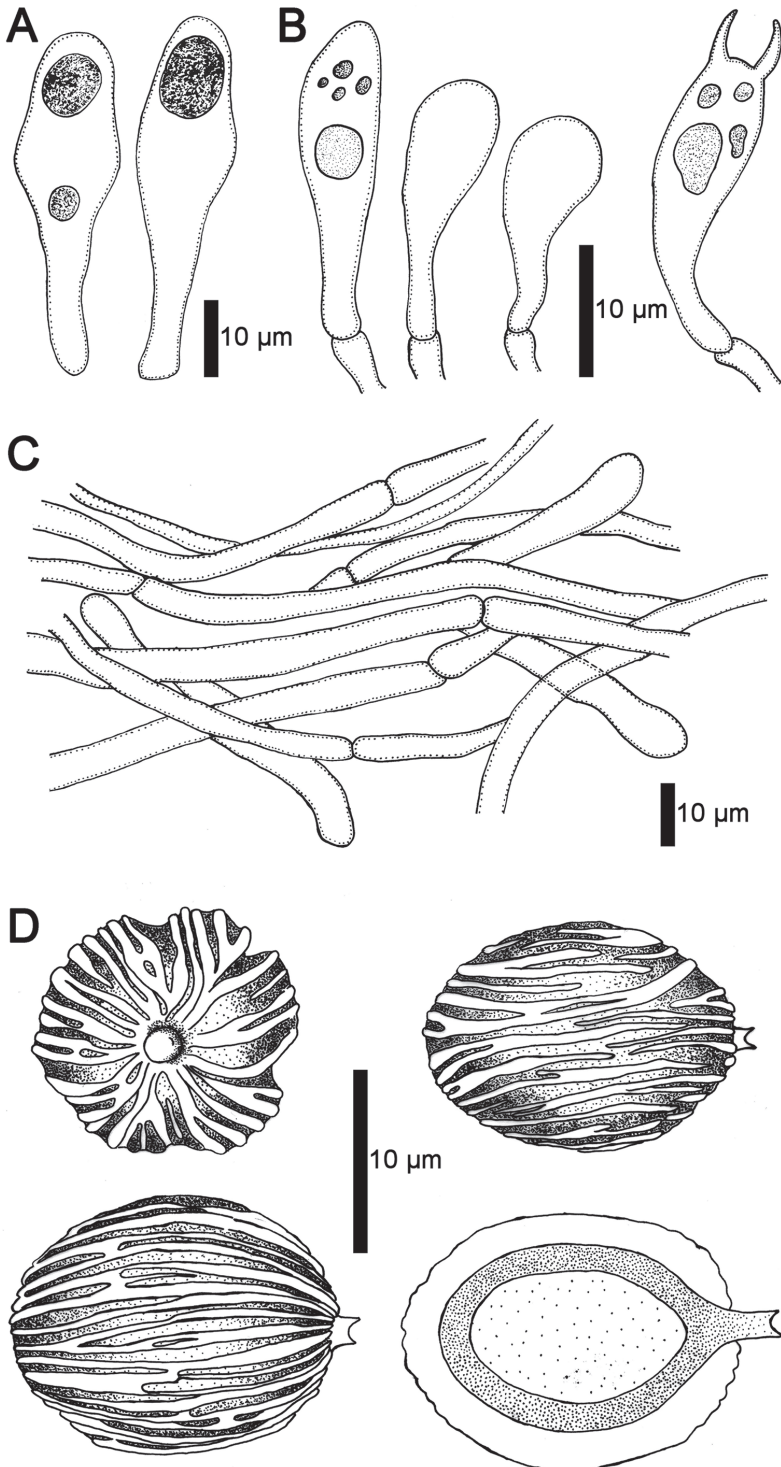


Figure 4. A–D *Longistriata flava* (UFRN-Fungus 1756, holotype) **A** hymental cystidia **B** basidioles and basidium **C** details of the peridium with interwoven hyphae **D** polar and longitudinal view of basidiospores.

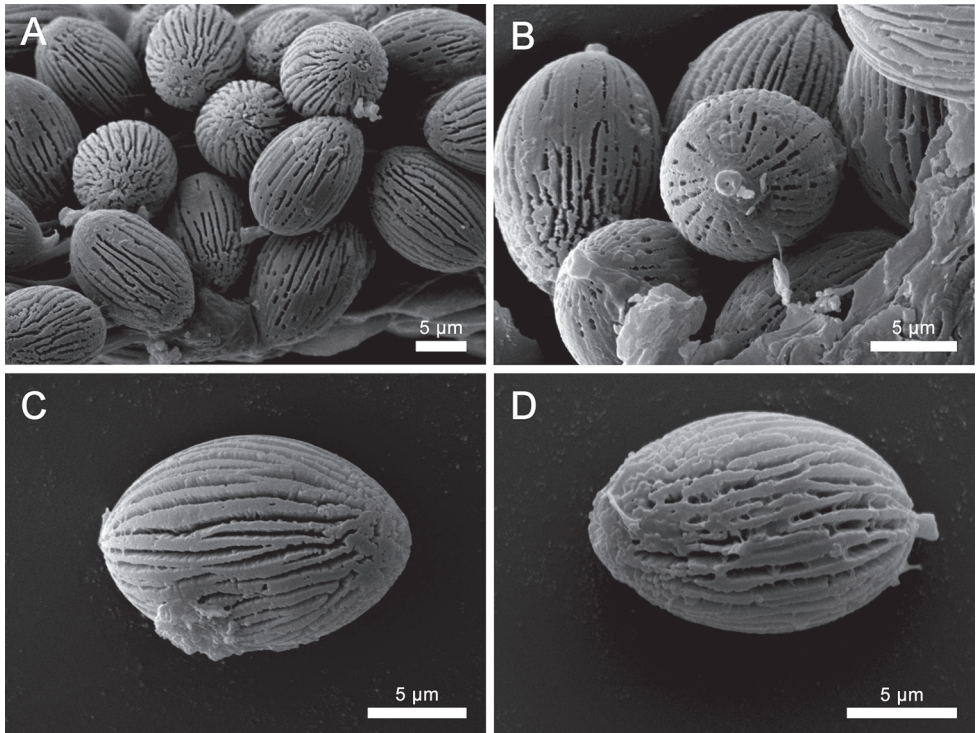


Figure 5. A–D Basidiospores of *Longistriata flava* (UFRN-Fungus 1756, holotype) as observed with scanning electron microscopy. Note the persistent sterigmatal attachment and a series of thinner longitudinal ridges (on average > 10 complete ridges across the longitudinal axis of the spore) with additional irregular, thin, low and bifurcated or fused ridges.

bifurcated or irregular and they also cover the entire spore surface. The clavate basidia can be either 2-spored and 4-spored and the lageniform to ventricose cystidia are a notable feature in the hymenium. This combination of morphological features is unique within the Boletaceae.

Discussion

Longistriata is a striking new monotypic genus described from the Atlantic forest in the Northeastern part of Brazil. The only known representative of the genus is the newly described *Longistriata flava*. This species is characterized by the hypogeous habit, a smooth and bright yellow peridium (Fig. 3), presence of cystidia, and the absence of clamp connections in all tissues (Fig. 4). Based on a combined phylogenetic analysis of *nLSU* + *TEF1* the closest relative is *Mackintoshia persica* (Fig. 2). However, *L. flava* is differentiated from *M. persica* (Pacioni and Sharp 2000) based on its well-developed, sterile base that forms a short stipe, lageniform cystidia with rounded apices, basidiospores with persistent sterigmatal attachments that are covered by thin longitudinal

striations and spores that are $15\text{--}19 \times 13\text{--}16 \mu\text{m}$. *Mackintoshia* has smooth and smaller elliptical basidiospores ($8\text{--}12 \times 5\text{--}7 \mu\text{m}$) (Pacioni and Sharp 2000) and is known only from Africa (Castellano et al. 2000). The two genera also have different host plants; *Mackintoshia* is found in habitats dominated by ECM plants in the Fabaceae and Uapacaceae (Pacioni and Sharp 2000) whereas *Longistriata* is found with ECM plants in Nyctaginaceae and Polygonaceae. This combination of morphological features is unique, separating the sister clade *Mackintoshia* from *Longistriata*.

In addition to *Longistriata* several other genera of sequestrate Boletaceae, *Chamonixia*, *Rosbeevera*, *Rhodactina*, and *Turmalinea*, also have basidiospores with longitudinal ridges. However, members of these genera all differ in the shape and number of ridges. *Rosbeevera* has ellipsoid to fusiform basidiospores with 3–5 ridges (Lebel et al. 2012), *Chamonixia* has subglobose to broadly ellipsoid basidiospores with 6–10 ridges (Lebel et al. 2012), *Rhodactina* has broadly ellipsoid to subfusiform basidiospores with 8–10 ridges (Yang et al. 2006), and *Turmalinea* has ovoid to fusoid basidiospores with 5–10 longitudinal ridges that are often branched to irregularly broken and spores can be with or without a hilar appendage (Orihara et al. 2016b). The spore colors are also different in these other genera; *Rosbeevera* and *Chamonixia* have brown to brownish spores (Montecchi and Sarasini 2000; Lebel et al. 2012), *Turmalinea* has inamyloid, non-dextrinoid, spores that are brick red to dark brown at maturity (Orihara et al. 2016b) and *Rhodactina* species have spores that are deep purple (Yang et al. 2006). In *Longistriata* the number of ridges is greater than in any of the other genera. On average, spores of *Longistriata flava* have 10 complete ridges across the longitudinal axis of the spore with additional irregular, thin and low ridges (Figs 3F–G, 4D). Furthermore, the ridges in this species are thin, low and irregular as compared to the other genera listed above. In some spores the ridges of *Longistriata* can be fused or bifurcating (Fig. 5C). Species in the sequestrate genus *Gautieria* also has spores with longitudinal ridges but this genus is very different from *Longistriata* because the basidioma of *Gautieria* species often lack a peridium and they belong in the distantly related order Gomphales (Montecchi and Sarasini 2000; Giachini et al. 2010). The ridged basidiospores of *Longistriata* are also superficially similar to those of the epigeous bolete genus *Boletellus* because species in both genera typically have longitudinal ridges. However, our phylogenetic analyses indicate that these two genera are only distantly related within the Boletaceae (Fig. 2).

The hypogeous habit, shape of basidiomes (e.g. globose, subglobose, tuberiform) and the rudimentary sterile base in *L. flava* suggest a possible relationship with the sequestrate truffle-like genus *Octaviania* (Orihara et al. 2012). However, the basidiospores are very different in *Octaviania* (e.g. globose to ellipsoid spores with ornamentation of large, thick-walled, pyramidal to conical ornaments) and molecular data indicate that *Octaviania* is a distant relative of *Longistriata*. The bright yellow peridium of fresh basidiomata and the presence of a stipe in *L. flava* resembles members of the *Boletus chromapes* group (e.g. *Zangia* and *Harrya*) as well as the genus *Royoungia* where at least some taxa have similar bright yellow coloration (Li et al. 2011; Halling et al. 2012).

The phylogenetic analyses suggest that the new Brazilian genus is closely related to several genera in the subfamily Zangioideae that also have bright yellow colors at

the base of the stipe (e.g. *Chiua* Yan C. Li & Zhu L. Yang, *Harrya* Halling, Nuhn & Osmudson, *Royoungia* Castellano, Trappe & Malajczuk, and *Zangia* Yan C. Li & Zhu L. Yang) (Wu et al. 2014, 2016) (Fig. 2). Within the Zangioideae only one hypogeous sequestrate taxon, *Royoungia boletoides*, was previously known (Wu et al. 2014, 2016). All of the other genera in Zangioideae are characterized by the epigeous habit, with a well-developed and central stipe and smooth basidiospores. The fresh appearance of *Longistriata flava*, with its bright yellow peridium, resembles the colors found in *Chiua* or *Zangia* (from Asia with Fagaceae and Pinaceae) or *Royoungia* (from Australia with Myrtaceae) (Li et al. 2011; Halling et al. 2012; Wu et al. 2016).

Several other sequestrate Boletaceae are similar to *L. flava*, either in their morphology or in their tropical distribution. Members of the sequestrate genus *Mycoamaranthus* Castellano, Trappe & Malajczuk also produce bright yellow basidiomata and belong to Boletaceae (Binder and Hibbett 2006) but GenBank BLASTn queries based on the ITS rDNA indicate that *Longistriata* is distantly related to *Mycoamaranthus* (e.g. the ITS is <85% similar to both *Mycoamaranthus congolensis* and *M. cambodgensis*). Another genus that shares several morphological similarities with *Longistriata* is the genus *Solioccasus* (Trappe et al. 2013). This genus differs from *Longistriata* by the large and copious rhizomorphs appressed to peridial surfaces, a dendroid and cartilaginous columella, smooth basidiospores, and basidiomes with bright orange and reddish coloration. The monotypic genus *Afrocastellanoa* from tropical Africa (Orihara and Smith 2017) is distinct from *Longistriata* because it is characterized by whitish basidiomata, globose to subglobose basidiospores with warty to spiny spore ornaments and its phylogenetic relationship with the epigeous genus *Porphyrellus*. Recently, Smith et al. (2015) discovered three new monotypic hypogeous sequestrate genera within Boletaceae, *Jimtrappea guyanensis* T.W. Henkel, M.E. Smith & Aime, *Castellanea pakaraimophila* T.W. Henkel & M.E. Smith and *Costatisporus cyanescens* T.W. Henkel & M.E. Smith (Smith et al. 2015). Like *Longistriata*, all three new genera are endemic to tropical South America but their macro- and microscopic characteristics are notably different. *Jimtrappea guyanensis* is characterized by the white peridium, unchanging tissues, short columella, smooth subfusiform, reddish brown basidiospores and prominent dextrinoid cystidia (Smith et al. 2015). The white peridium, the unchanging tissues, smooth subfusiform basidiospores, and prominent cystidia of *J. guyanensis* contrast with the yellow peridium and unique basidiospores morphology of *L. flava*. Phylogenetic analysis also confirms that *J. guyanensis* and *L. flava* are not closely related. *Castellanea pakaraimophila* is similar to *L. flava* because both have subglobose basidioma and a short stipe but *L. flava* has a bright yellow peridium. The two species can also be easily differentiated by their spores because *C. pakaraimophila* has smooth, subfusiform basidiospores whereas *L. flava* has ellipsoid spores with distinct longitudinal striations (Smith et al. 2015). *Costatisporus cyanescens* is easily differentiated from *L. flava* by its grayish yellow peridium and the dark blue staining reaction on the peridium. Microscopically, the longitudinally ridged basidiospore ornamentation of *C. cyanescens* (fig. 4c, in Smith et al. 2015) is similar to that in *L. flava* (Fig. 5A–D). However, the basidiospores are broadly ellipsoid and dextrinoid in *L. flava* and the

ornamentation is formed by a series of thin longitudinal striations on all surfaces. In contrast, the spores of *C. cyanescens* are unreactive in Melzer's reagent and are ovate to subfusiform with ridges that are somewhat spiraled. The two species are also distantly related based on our phylogenetic analysis (Fig. 2). The ecology of *Jimtrappea*, *Castellanea* and *Costatisporus* are also different from *Longistriata*. These three genera are apparently endemic to the Guiana Shield and are associated with the ECM tree genera *Aldina*, *Dicymbe* and *Pakaraimaea* (Smith et al. 2015).

Unfortunately, we have not yet confirmed the ECM status of *Longistriata flava* based on sequences from ECM root tips from native Brazilian trees. However, basidiomes of *Longistriata* have always been collected in the lowland semi-deciduous forest to savanna known as "tabuleiro" in close proximity to woody plants in the ECM genera *Coccoloba* (Polygonaceae) and *Guapira* (Nyctaginaceae). Given that ECM plants in these genera are known to host a wide array of ECM fungi from other sites in tropical South America (Tedersoo et al. 2010; Séné et al. 2015; Pólme et al. 2017) and that other taxa in the Zangioideae are known to be ECM (Tedersoo and Smith 2013), we hypothesize that *L. flava* is also ECM. The ECM nutritional mode is also likely to be favored in the nutrient-poor sandy soil ecosystem of Neotropical forest fragments of the Atlantic Forests.

Acknowledgments

The authors wish to thank Dr. Jomar G. Jardim for identifying tree species in the Guaribas Biological Reserve. This study is in part a result of the Ph.D. thesis of Marcelo A. Sulzbacher, with a scholarship provided by the Brazilian Government (CAPES). The work was partially supported by CNPq project PVE 407474/2013-7 and co-financed by the Brazil-Slovenia bilateral project (BI-BR/11-13-005(SRA) / 490648/2010-0 (CNPq)), research project J4-1766 "Methodology approaches in genome-based diversity and ecological plasticity study of truffles from their natural distribution areas" and the Research Program in Forest Biology, Ecology and Technology (P4-0107) of the Slovenian Research Agency.

References

- Bâ AM, Avril R, Bandou E, Sène S, Courtecuisse R, Sylla S, Diédhiou A (2014) Alleviation of salt stress by *Scleroderma bermudense* in *Coccoloba uvifera* seedlings. In: Bâ AM, McGuire KL, Diédhiou A (Eds) Ectomycorrhizal Symbioses in Tropical and Neotropical Forests. Science Publishers, CRC Press, Enfield, 164–185. <https://doi.org/10.1201/b16536-10>
- Barbosa MRB, Thomas WW, Zárate ELP, Lima RB, Agra MF, Lima IB, Pessoa MCR, Lourenço AR, Delgado-Junior GD, Pontes RAS, Chagas ECO, Viana JL, Gadelha-Neto PC, Araújo CMR, Freitas GB, Lima JR, Silva FO, Vieira LAF, Costa RMT, Duré RC, Sá MG (2011) Checklist of the vascular plants of the Guaribas Biological Reserve, Paraíba, Brazil. *Revista Nordestina de Biologia* 20(2): 79–106.

- Barbosa-Silva A, Wartchow F (2017) Studies on *Boletellus* sect. *Boletellus* in Brazil and Guyana. *Current Research in Environmental and Applied Mycology* 7: 387–395. <https://doi.org/10.5943/cream/7/4/13>
- Barbosa-Silva A, Ovrebo CL, Ortiz-Santana B, Sá MCA, Sulzbacher MA, Roy M, Wartchow F (2017) *Tylopilus aquarius*, comb. et stat. nov., and its new variety from Brazil. *Sydowia* 69: 115–122. <https://doi.org/10.12905/0380.sydowia69-2017-0115>
- Baseia IG, Milanez AI (2000) First record of *Scleroderma polyrhizum* Pers. (Gasteromycetes) from Brazil. *Acta Botanica Brasilica* 14: 181–184. <https://doi.org/10.1590/S0102-33062000000200006>
- Baseia IG, Milanez AI (2002) *Rhizopogon* (Gasteromycetes): hypogeous fungi in exotic forests from the State of São Paulo, Brazil. *Acta Botanica Brasilica* 16: 55–60. <https://doi.org/10.1590/S0102-33062002000100007>
- Binder M, Bresinsky A (2002) Derivation of a polymorphic lineage of Gasteromycetes from boletoid ancestors. *Mycologia* 94: 85–98. <https://doi.org/10.1080/15572536.2003.11833251>
- Binder M, Hibbett DS (2006) Molecular systematics and biological diversification of Boletales. *Mycologia* 98: 971–981. <https://doi.org/10.1080/15572536.2006.11832626>
- Castellano MA, Trappe JM, Malajczuk N (1992) Australasian truffle-like fungi. III. *Royoungia* gen. nov. and *Mycoamaranthus* gen. nov. (Basidiomycotina). *Australian Systematic Botany* 5: 613–616. <https://doi.org/10.1071/SB9920613>
- Castellano MA, Verbeken A, Walley R, Thoen D (2000) Some new and interesting sequestrate Basidiomycota from African woodlands. *Karstenia* 40: 11–21. <https://doi.org/10.29203/ka.2000.346>
- Castellano MA, Trappe JM, Luoma DL (2004) Sequestrate fungi. In: Foster MS, Mueller GM, Bills GF (Eds) *Biodiversity of Fungi: Inventory and Monitoring Methods*. Burlington (USA), Academic Press, 197–213. <https://doi.org/10.1016/B978-012509551-8/50013-1>
- Castellano MA, Elliott TF, Truong C, Séné O, Dentinger BTM, Henkel TW (2016) *Kombocles bakaiana* gen. sp. nov. (Boletaceae), a new sequestrate fungus from Cameroon. *IMA Fungus* 7(2): 239–245. <https://doi.org/10.5598/imafungus.2016.07.02.03>
- Chai H, Liang ZQ, Xue R, Jiang S, Luo SH, Wang Y, Wu LL, Tang LP, Chen Y, Hong D, Zeng NK (2019) New and noteworthy boletes from subtropical and tropical China. *MycoKeys* 46: 55–96. <https://doi.org/10.3897/mycokeys.46.31470>
- Chu-Chou M, Grace LJ (1983) Hypogeous fungi with some forest trees in New Zealand. *New Zealand Journal of Botany* 21: 183–190. <https://doi.org/10.1080/0028825X.1983.10428543>
- Cortez VG, Baseia IG, Silveira RMB (2011) Gasteroid mycobiota of Rio Grande do Sul, Brazil: Boletales. *Journal of yeast and fungal research* 2(4): 44–52.
- Crous PW, Luangsa-Ard JJ, Wingfield MJ, Carnegie AJ, Hernández-Restrepo M, Lombard L, Martín MP (2018) Fungal Planet description sheets: 785–867. *Persoonia: Molecular Phylogeny and Evolution of Fungi* 41: 238–417. <https://doi.org/10.3767/persoonia.2018.41.12>
- de Meijer AAR (2006) Preliminary list of the macromycetes from the Brazilian state of Paraná. *Boletim do Museu Botânico Municipal*. Curitiba 68: 1–55.
- Fries EM, Nordholm J (1817) *Symbolae Gasteromycorum*. Lund.
- Geyer CJ (1991) Markov chain Monte Carlo maximum likelihood. In: Keramidas EM (Eds) *Computing Science and Statistics. Proceedings of the 23rd Symposium on the Interface*. Fairfax Station: Interface Foundation, USA, 156–163.

- Giachini AJ, Oliveira VL, Castellano MA, Trappe JM (2000) Ectomycorrhizal fungi in *Eucalyptus* and *Pinus* plantations in southern Brazil. *Mycologia* 92: 1166–1177. <https://doi.org/10.1080/00275514.2000.12061264>
- Giachini AJ, Hosaka K, Nouhra E, Spatafora JW, Trappe JM (2010) Phylogenetic relationships of the Gomphales based on nuc-25SrDNA, mit-12S-rDNA, and mit-atp6-DNA combined sequences. *Fungal Biology* 114: 224–234. <https://doi.org/10.1016/j.funbio.2010.01.002>
- Gurgel FE, Silva BDB, Baseia IG (2008) New records of *Scleroderma* from Northeastern Brazil. *Mycotaxon* 105: 399–405.
- Guzmán G (1970) Monografía del género *Scleroderma*. *Darwiniana* 16: 233–407.
- Halling RE, Mitchell J, Nuhn B, Osmundson T, Fechtner N, Trappe JM, Soyong K, Arora D, Hibbett DS, Binder M (2012) Affinities of the *Boletus chromapes* group to *Royoungia* and the description of two new genera, *Harrya* and *Australopilus*. *Australian Systematic Botany* 25: 418–431. <https://doi.org/10.1071/SB12028>
- Henkel TW, Aime MC, Chin MML, Miller SL, Vilgalys R, Smith ME (2012) Ectomycorrhizal fungal sporocarp diversity and discovery of new taxa in *Dicymbe monodominat* forests of the Guiana Shield. *Biodiversity Conservation* 21: 2195–2220. <https://doi.org/10.1007/s10531-011-0166-1>
- Høiland K (1987) A new approach to the phylogeny of the order Boletales (Basidiomycotina). *Nordic Journal of Botany* 7: 705–718. <https://doi.org/10.1111/j.1756-1051.1987.tb02038.x>
- Katoh K, Standley DM (2013) MAFFT Multiple Sequence Alignment Software Version 7: Improvements in Performance and Usability. *Molecular Biology and Evolution* 30: 772–780. <https://doi.org/10.1093/molbev/mst010>
- Kirk PM, Cannon PF, Minter DW, Stalpers JA (2008) *Dictionary of the Fungi* (10th edn.). CABI International, Wallingford.
- Kornerup A, Wanscher JE (1978) *Methuen Handbook of Colour* (3rd edn.). Eyre Methuen, London.
- Kretzer AM, Bruns TD (1999) Use of atp6 in fungal phylogenetics: an example from the Boletales. *Molecular Phylogenetics and Evolution* 13: 483–492. <https://doi.org/10.1006/mpev.1999.0680>
- Lebel T, Orihara T, Maekawa N (2012) The sequestrate genus *Rossbeevera* T. Lebel & Orihara gen. nov. (Boletaceae) from Australasia and Japan: new species and new combinations. *Fungal Diversity* 52: 49–71. <https://doi.org/10.1007/s13225-011-0109-x>
- Li Y-C, Feng B, Yang Z-L (2011) *Zangia*, a new genus of Boletaceae supported by molecular and morphological evidence. *Fungal Diversity* 49: 125–143. <https://doi.org/10.1007/s13225-011-0096-y>
- Magnago AC, Neves MA (2014) New record of *Austroboletus festivus* (Boletaceae) from Santa Catarina, Brazil. *Brazilian Journal of Botany* 37: 197–200. <https://doi.org/10.1007/s40415-014-0048-3>
- Magnago AC, Reck MA, Dentinger BTM, Moncalvo J-M, Neves MA, Silveira RMB (2017a) Two new *Tylopilus* species (Boletaceae) from Northeastern Atlantic Forest, Brazil. *Phytotaxa* 316: 250–260. <https://doi.org/10.11646/phytotaxa.316.3.4>
- Magnago AC, Neves MA, Silveira RMB (2017b) *Fistulinella ruschii*, sp. nov., and a new Record of *Fistulinella campinaranae* var. *scrobiculata* for the Atlantic Forest, Brazil. *Mycologia* 109: 1003–1013. <https://doi.org/10.1080/00275514.2018.1431503>

- Magnago AC, Henkel T, Neves MA, Silveira RMB (2018) *Singerocomus atlanticus* sp. nov., and a first record of *Singerocomus rubriflavus* (Boletaceae, Boletales) for Brazil. *Acta Botanica Brasiliica* 32: 222–231. <https://doi.org/10.1590/0102-33062017abb0320>
- Magnago AC, Neves MA, Silveira RMB (2019) *Boletellus nordestinus* (Boletaceae, Boletales), a new species from Northeastern Atlantic Forest, Brazil. *Studies in Fungi* 4: 47–53. <https://doi.org/10.5943/sif/4/1/8>
- Martín MP (1996) The genus *Rhizopogon* in Europe. *Edición Societat Catalana de Micologia* 5: 1–171.
- Montecchi A, Sarasini M (2000) *Funghi ipogei d'Europa*. Fondazione Centro Studi Micologici dell'Associazione Micologica Bresadola, Trento.
- Nouhra ER, Domínguez LS, Becerra AC, Trappe JM (2005) Morphological, molecular and ecological aspects of the South American hypogeous fungus *Alpova austroalnicola* sp. nov. *Mycologia* 97: 598–604. <https://doi.org/10.3852/mycologia.97.3.598>
- Nouhra ER, Hernandez ML, Pastor N, Crespo E (2012) The species of *Scleroderma* from Argentina, including a new species from the *Nothofagus* forest. *Mycologia* 104: 488–495. <https://doi.org/10.3852/11-082>
- Nuhn ME, Binder M, Taylor AF, Halling RE, Hibbett DS (2013) Phylogenetic overview of the Boletineae. *Fungal Biology* 117: 479–511. <https://doi.org/10.1016/j.funbio.2013.04.008>
- Nylander JAA (2004) MrModeltest v2. Program distributed by the author. Evolutionary Biology Centre, Uppsala University, Sweden.
- Orihara T, Smith ME, Shimomura N, Iwase K, Maekawa N (2012) Diversity and systematics of the sequestrate genus *Octaviania* in Japan: two new subgenera and eleven new species. *Persoonia* 28: 85–112. <https://doi.org/10.3767/003158512X650121>
- Orihara T, Sawada F, Ikeda S, Yamato M, Tanaka C, Shimomura N, Hashiya M, Iwase K (2010) Taxonomic reconsideration of a sequestrate fungus, *Octaviania columellifera*, with the proposal of a new genus, *Heliogaster*, and its phylogenetic relationships in the Boletales. *Mycologia* 102: 108–121. <https://doi.org/10.3852/08-168>
- Orihara T, Ohmae M, Yamamoto K (2016a) First report of *Chamonixia caespitosa* (Boletaceae, Boletales) from Japan and its phylogeographic significance. *Mycoscience* 57: 58–63. <https://doi.org/10.1016/j.myc.2015.08.005>
- Orihara T, Lebel T, Ge Z-W, Smith ME, Maekawa N (2016b) Evolutionary history of the sequestrate genus *Rossbeevera* (Boletaceae) reveals a new genus *Turmalinea* and highlights the utility of ITS minisatellite-like insertions for molecular identification. *Persoonia* 37: 173–198. <https://doi.org/10.3767/003158516X691212>
- Orihara T, Smith ME (2017) Unique phylogenetic position of the African truffle-like fungus, *Octaviania ivoryana* (Boletaceae, Boletales) and the proposal of a new genus, *Afrocastellanoa*. *Mycologia* 109(2): 323–332. <https://doi.org/10.1080/00275514.2017.1301750>
- Pacioni G, Sharp C (2000) *Mackintoshia*, a new sequestrate basidiomycete genus from Zimbabwe. *Mycotaxon* 75: 225–228.
- Persoon CH (1801) *Synopsis Methodica Fungorum: Sistens Enumerationem Omnium Huc Usque Detectarum Specierum, Cum Brevibus Descriptionibus Nec Non Synonymis et Observationibus Selectis* (Vol. 2). Dieterich, Göttingen.

- Pölme S, Bahram M, Kõljalg U, Tedersoo L (2017) Biogeography and specificity of ectomycorrhizal fungi of *Coccoloba uvifera*. In: Tedersoo L (Ed.) Biogeography of mycorrhizal symbiosis. Springer, Cham, 345–359. https://doi.org/10.1007/978-3-319-56363-3_16
- Putzke J (1994) Lista dos fungos Agaricales (Hymenomyces, Basidiomycotina) referidos para o Brasil. Caderno de Pesquisa, Série Botânica 6: 1–189.
- Rehner SA, Buckley E (2005) A *Beauveria* phylogeny inferred from nuclear ITS and EF1- α sequences: evidence for cryptic diversification and links to *Cordyceps* teleomorphs, Mycologia 97: 84–98. <https://doi.org/10.3852/mycologia.97.1.84>
- Rick J (1961) Basidiomycetes eubasidii in Rio Grande do Sul. Brasília. 6. Iheringia, série Botânica 9: 451–480.
- Rolland L (1899) Excursions à Chamonix. Bulletin de la Société Mycologique de France 15: 73–78.
- Ronquist F, Huelsenbeck JP (2003) MrBayes 3: Bayesian phylogenetic inference under mixed models. Bioinformatics 19: 1572–1574. <https://doi.org/10.1093/bioinformatics/btg180>
- Séne S, Avril R, Chaintreuil C, Geoffroy A, Ndiaye C, Diédhiou AG, Sadio O, Courtecuisse R, Sylla SN, Selosse MA, Bâ A (2015) Ectomycorrhizal fungal communities of *Coccoloba uvifera* (L.) L. mature trees and seedlings in the neotropical coastal forests of Guadeloupe (Lesser Antilles). Mycorrhiza 25(7): 547–559. <https://doi.org/10.1007/s00572-015-0633-8>
- Smith ME, Henkel TW, Uehling JK, Fremier AK, Clarke HD, Vilgalys R (2013) The ectomycorrhizal fungal community in a neotropical forest dominated by the endemic dipterocarp *Pakaraimaea dipterocarpacea*. PLoS ONE 8: e55160. <https://doi.org/10.1371/journal.pone.0055160>
- Smith ME, Amses KR, Elliott TF, Obase K, Aime MC, Henkel TW (2015) New sequestrate fungi from Guyana: *Jimtrappea guyanensis* gen. et sp. nov., *Castellanea pakaraimophila* gen. et sp. nov., and *Costatisporus caeruleus* gen. et sp. nov. (Boletaceae, Boletales). IMA fungus 6: 297–317. <https://doi.org/10.5598/imafungus.2015.06.02.03>
- Sobestiansky G (2005) Contribution to a macromycetes survey of the States of Rio Grande do Sul and Santa Catarina in Brazil. Brazilian Archives of Biology and Technology 48: 437–457. <https://doi.org/10.1590/S1516-89132005000300015>
- Stamatakis A (2014) RAxML version 8: a tool for phylogenetic analysis and post-analysis of large phylogenies. Bioinformatics 30: 1312–1313. <https://doi.org/10.1093/bioinformatics/btu033>
- Sulzbacher MA, Giachini AJ, Grebenc T, Silva BDB, Gurgel FE, Loiola MIB, Neves MA, Baseia IG (2013) A survey of an ectotrophic sand dune forest in the northeast Brazil. Mycosphere 4: 1106–1116. <https://doi.org/10.5943/mycosphere/4/6/8>
- Sulzbacher MA, Grebenc T, García MÁ, Silva BD, Silveira A, Antonioli ZI, Marinho P, Münzenberger B, Telleria MT, Baseia IG, Martín MP (2016a) Molecular and morphological analyses confirm *Rhizopogon verii* as a frequent ectomycorrhizal false truffle in Europe, and its presence in South America. Mycorrhiza 26: 377–388. <https://doi.org/10.1007/s00572-015-0678-8>
- Sulzbacher MA, Grebenc T, Cabral TS, Giachini AJ, Goto BT, Smith ME, Baseia IG (2016b) *Restingomyces*, a new sequestrate genus from the Brazilian Atlantic rainforest that is phy-

- logenetically related to early-diverging taxa in Trappeaceae (Phallales). *Mycologia* 108: 954–966. <https://doi.org/10.3852/15-265>
- Sulzbacher MA, Grebenc T, Giachini AJ, Baseia IG, Nouhra ER (2017) Hypogeous sequestrate fungi in South America – how well do we know them? *Symbiosis* 71: 9–17. <https://doi.org/10.1007/s13199-016-0461-4>
- Sulzbacher MA, Grebenc T, Bevilacqua CB, Steffen RB, Coelho G, Silveira AO, Jacques RJ, Antonioli ZI (2018) Co-invasion of ectomycorrhizal fungi in the Brazilian Pampa biome. *Applied Soil Ecology* 130: 194–201. <https://doi.org/10.1016/j.apsoil.2018.06.007>
- Tedersoo L, May T, Smith ME (2010a) Ectomycorrhizal lifestyle in fungi: global diversity, distribution, and evolution of phylogenetic lineages. *Mycorrhiza* 20: 217–263. <https://doi.org/10.1007/s00572-009-0274-x>
- Tedersoo L, Sadam A, Zambrano M, Valencia R, Bahram M (2010b) Low diversity and high host preference of ectomycorrhizal fungi in Western Amazonia, a neotropical biodiversity hotspot. *The ISME journal* 4(4): 1–465. <https://doi.org/10.1038/ismej.2009.131>
- Tedersoo L, Smith ME (2013) Lineages of ectomycorrhizal fungi revisited: Foraging strategies and novel lineages revealed by sequences from belowground. *Fungal Biology Reviews* 27: 83–99. <https://doi.org/10.1016/j.fbr.2013.09.001>
- Trappe JM, Castellano MA, Halling RE, Osmundson TW, Binder M, Fechner N, Malajczuk N (2013) Australasian sequestrate fungi 18: *Soliococcus polychromus* gen. & sp. nov., a richly colored, tropical to subtropical, hypogeous fungus. *Mycologia* 105: 888–895. <https://doi.org/10.3852/12-046>
- Tulloss RE, Ovrebo CL, Halling RE (1992) Studies on *Amanita* (Amanitaceae) from Andean Colombia. *Estudios sobre Amanita (Amanitaceae) de los Andes colombianos. Memoirs of the New York Botanical Garden* 66: 1–46.
- Vadthananat S, Raspé O, Lumyong S (2018) Phylogenetic affinities of the sequestrate genus *Rhodactina* (Boletaceae), with a new species, *R. rostratispora* from Thailand. *MycoKeys* 29: 63–80. <https://doi.org/10.3897/mycokeys.29.22572>
- Vilgalys R, Hester M (1990) Rapid genetic identification and mapping of enzymatically amplified ribosomal DNA from several *Cryptococcus* species. *Journal of Bacteriology* 172: 4239–4246. <https://doi.org/10.1128/jb.172.8.4238-4246.1990>
- Vittadini C (1831) *Monographia Tuberacearum*. Mediolani, Milano.
- Watling R, de Meijer AAR (1997) Macromycetes of the state of Paraná, Brazil 5. Poroid and lamellate boletes. *Edinburgh Journal of Botany* 54: 231–251. <https://doi.org/10.1017/S0960428600004042>
- Wang B, Qiu YL (2006) Phylogenetic distribution and evolution of mycorrhizas in land plants. *Mycorrhiza* 16: 299–363. <https://doi.org/10.1007/s00572-005-0033-6>
- Wu G, Feng B, Xu J, Zhu XT, Li YC, Zeng NK, Hosen MI, Yang ZL (2014) Molecular phylogenetic analyses redefine seven major clades and reveal 22 new generic clades in the fungal family Boletaceae. *Fungal Diversity* 69: 93–115. <https://doi.org/10.1007/s13225-014-0283-8>
- Wu G, Zhao K, Li YC, Zeng NK, Feng B, Halling RE, Yang ZL (2016) Four new genera of the fungal family Boletaceae. *Fungal Diversity* 8: 1–24. <https://doi.org/10.1007/s13225-015-0322-0>
- Yang ZL, Trappe JM, Binder M, Sanmee R, Lumyong P, Lumyong S (2006) The sequestrate genus *Rhodactina* (Basidiomycota, Boletales) in northern Thailand. *Mycotaxon* 96: 133–140.

Supplementary material I

Table S1. Specimens and sequences used for the molecular phylogenetic analyses (i. e., the nLSU + TEF1 combined dataset) and ITS sequence comparison.

Authors: Marcelo A. Sulzbacher, Takamichi Orihara, Tine Grebenc, Felipe Wartchow, Matthew E. Smith, María P. Martín, Admir J. Giachini, Iuri G. Baseia

Data type: molecular data

Copyright notice: This dataset is made available under the Open Database License (<http://opendatacommons.org/licenses/odbl/1.0/>). The Open Database License (ODbL) is a license agreement intended to allow users to freely share, modify, and use this Dataset while maintaining this same freedom for others, provided that the original source and author(s) are credited.

Link: <https://doi.org/10.3897/mycokeys.62.39699.suppl1>

Diversity and community of culturable endophytic fungi from stems and roots of desert halophytes in northwest China

Jia-Long Li^{1,2,3}, Xiang Sun^{1,4}, Yong Zheng⁵, Peng-Peng Lü^{1,3},
Yong-Long Wang^{1,3}, Liang-Dong Guo^{1,3}

1 State Key Laboratory of Mycology, Institute of Microbiology, Chinese Academy of Sciences, Beijing, 100101, China **2** National Joint Engineering Research Center of Separation and purification technology of Chinese Ethnic Veterinary Herbs, Tongren Polytechnic College, Tongren, 554300, China **3** College of Life Sciences, University of Chinese Academy of Sciences, Beijing, 100049, China **4** Department of Molecular Biology and Ecology of Plants, Faculty of Life Sciences, Tel Aviv University, Tel Aviv, 69978, Israel **5** School of Geographical Sciences, Fujian Normal University, Fuzhou 350007, China

Corresponding authors: Xiang Sun (sunx@tauex.tau.ac.il); Liang-Dong Guo (guold@im.ac.cn)

Academic editor: P. Divakar | Received 10 August 2019 | Accepted 10 December 2019 | Published 3 February 2020

Citation: Li J-L, Sun X, Zheng Y, Lü P-P, Wang Y-L, Guo L-D (2020) Diversity and community of culturable endophytic fungi from stems and roots of desert halophytes in northwest China. MycoKeys 62: 75–95. <https://doi.org/10.3897/mycokeys.62.38923>

Abstract

Halophytes have high species diversity and play important roles in ecosystems. However, endophytic fungi of halophytes in desert ecosystems have been less investigated. In this study, we examined endophytic fungi associated with the stem and root of ten halophytic species colonizing the Gurbantonggut desert. A total of 36 endophytic fungal taxa were obtained, dominated by *Alternaria eichhorniae*, *Monosporascus ibericus*, and *Pezizomycotina* sp.1. The colonization rate and species richness of endophytic fungi varied in the ten plant species, with higher rates in roots than in stems. The endophytic fungal community composition was significantly affected by plant identity and tissue type. Some endophytic fungi showed significant host and tissue preferences. This finding suggests that host identity and tissue type structure endophytic fungal community in a desert ecosystem.

Keywords

community composition, desert halophyte, endophytic fungi, host preference, richness, tissue preference

Introduction

Endophytic fungi live within plant organs for some time or throughout their life, without causing apparent harm to their host (Petrini 1991). They are widely distributed and significantly contribute to the biodiversity in natural ecosystems (Rodríguez et al. 2009; Porrás-Alfaro and Bayman 2011; Hardoim et al. 2015; Yao et al. 2019). These fungi are beneficial to host plants by improving growth performance (Waller et al. 2005; Kannadan and Rudgers 2008; Behie et al. 2012; Khan et al. 2016), providing tolerance against abiotic and biotic stresses (Arnold et al. 2003; Waller et al. 2005; Kannadan and Rudgers 2008; Rodríguez et al. 2008; Hartley and Gange 2009; Yuan et al. 2016). Moreover, endophytic fungi participate in waste decomposition and recycling of nutrients in natural ecosystems (Promputtha et al. 2010; Sun et al. 2011; Purahong et al. 2016). Therefore, understanding the relationship between the endophytic fungal community and host plants is critical to comprehend diversity maintenance and ecosystem function (Hoffman and Arnold 2008; Porrás-Alfaro and Bayman 2011; Hardoim et al. 2015).

The endophytic fungal colonization rate, diversity, and community composition is affected by host species, tissue types, and abiotic factors (e.g., Collado et al. 1999; Arnold and Lutzoni 2007; Arfi et al. 2012; Sun et al. 2012a; U'Ren et al. 2012; Lau et al. 2013; Li et al. 2016). For example, Sun et al. (2012a) reported that the host species and tissues types conspicuously affect endophytic fungal community in three woody plants in a mixed temperate forest in China, where the overall colonization rates of endophytic fungi were significantly higher in twigs than in leaves, i.e., twigs harbored more endophytic taxa than leaves. Massimo et al. (2015) suggested that the endophytic fungal community composition in aboveground tissues (branches, stems, and leaves) of Sonoran Desert trees and shrubs were different among host species. However, most previous studies have focused on endophytic fungi of the aerial parts of plants, while very few studies investigated the difference of endophytic fungal community inhabiting the aboveground and belowground plants in ecosystems (Herrera et al. 2010; Márquez et al. 2010; Su et al. 2010; Xing and Guo 2011; Porrás-Alfaro et al. 2014). For example, Su et al. (2010) illustrated that *Stipa grandis* inhabited the Inner Mongolia steppe, the colonization rates of endophytic fungi were significantly higher in roots than in leaves, and the endophyte diversity, as well as the composition, was also significantly different in roots or leaves. Recent studies showed the functional importance of endophytic fungi colonized in roots and boosted research interests to root endophytic fungi (Hiruma et al. 2016; Almario et al. 2017; Polme et al. 2018; Schroeter et al. 2019). The difference in the endophytic fungal community among the aboveground and belowground of harsh habitat plants is an important scientific question.

Halophytes constitute about 1% of the world's flora, survive and reproduce in saline habitats such as coastal and salinized inland regions (Flowers et al. 1986; Flowers and Colmer 2008; Ward 2009). These halophytes contain grasses, shrubs, and trees, which constitute important eco-functional vegetation in the desert and coastal areas (Rozema and Flowers 2008; Chen et al. 2009; Giri et al. 2011). In China, there are 3.69×10^7 ha of saline soil regions and 555 halophyte species, accounting for 21.3% of the halophytes in the world (Zhao et al. 2013a). Particularly in arid and semiarid

northwest China, saline lands are distributed in the Gobi Desert, which accounts for 69% of the total saline lands and accommodates more than 60% of the halophyte resources of China (Zhao et al. 2013b). Halophytes in the desert areas are exposed to multiple environmental stresses, such as low water availability, high salinity, and nutrient deprivation (Ward 2009; Liu et al. 2013), and thus are unique niches for endophytes affected by the harsh environment. However, studies of endophytes in saline environments of China focused on mangroves parallel to the coast (Xing et al. 2011; Xing and Guo 2011; Liu et al. 2012; Li et al. 2016).

Inland halophytes form extensive symbiotic relations with endophytic fungi in harsh environments, which benefit their hosts by promoting resistance against high salinity stress (Rodriguez et al. 2008; Massimo et al. 2015; Khan et al. 2016). A few studies focused on endophytes of halophytes living inland (e.g., Sun et al. 2012b; Macia-Vicente et al. 2012). There are even fewer studies of endophytic fungi that have been carried out on desert halophytes, and they merely focused on endophytes on roots (Sonjak et al. 2009; Macia-Vicente et al. 2012). Moreover, Sun et al. (2012b) aimed at the endophytic fungal community in stems and leaves of desert halophytes in Tennger Desert region of China. Therefore, further study is required on endophytes of halophytes in the desert region to reveal the community of endophytic fungi under arid and salinity stress, with an emphasis on aboveground and belowground parts of plants.

In order to improve our understanding of the endophytic fungi of desert halophytes, we selected ten halophyte species in the Gurbantonggut desert, Xinjiang, northwest China. The endophytic fungi were isolated from the stems and roots of halophytes and identified according to morphological characteristics and molecular data. This study aimed to reveal how the colonization rate, diversity, and community composition of endophytic fungi differed among halophytes species and tissue types. Besides, it will also provide preliminary data of halophyte endophytes for future studies in bioactive natural products, ecosystem reconstruction, or agricultural application in desert regions.

Methods

Study site and sampling procedure

The study was carried out at the Fukang Desert Ecosystem Observation and Experiment Station, Chinese Academy of Sciences, located in the southern edge of the Gurbantonggut desert in China (44°17'N–44°22'N, 87°55'E–87°56'E, 448–461 m above sea level). The site has a continental arid temperate climate, with an annual mean temperature of 6.6 °C (a maximum of 44.2 °C in hot, dry summer and a minimum of -42.2 °C in freezing winter) (Dai et al. 2015). The annual mean precipitation is about 160 mm with annual pan evaporation of 2000 mm, resulting in soil with high salinity (0.45–2.25%) (Xu et al. 2007).

On 30th July 2015, we selected ten halophyte species *Bassia dasyphylla* (Fisch. et C. A. Mey.) Kuntze, *Ceratocarpus arenarius* L., *Kalidium foliatum* (Pall.) Moq.,

Salsola nitraria Pall., *Suaeda acuminata* (C. A. Mey.) Moq., *Suaeda salsa* (L.) Pall. (Chenopodiaceae), *Eragrostis minor* Host (Poaceae), *Reaumuria songarica* (Pall.) Maxim. (Tamaricaceae), *Seriphidium santolinum* (Schrenk) Poljak (Asteraceae), and *Peganum harmala* (L.) (Zygophyllaceae) at the site. Ten healthy individuals of each plant species were uprooted to collect twig and root samples at the location. All sampled individuals of the same species were more than 50 m away from each other, in order to reduce the spatial autocorrelation and recover representative local endophyte community (Li et al. 2016, Yao et al. 2019). The collected samples were immediately placed in autoclaved paper bags, labeled, and transported to the laboratory in an ice-box. Samples were stored at 4 °C and processed within 4 days.

Isolation and identification of endophytic fungi

Since most of the plant species involved in the current study (except for *E. minor*) possess reduced leaves, which are hard to discern from the stems, we selected only stems to isolate endophytes colonized aerial parts of the plants. Roots and stems of individual plants were cut into 5 mm long segments (ca. 2 mm in diameter). Eight root segments and 8 stem segments were randomly selected from each sample. In total, 1600 segments (10 plant species × 10 individuals × 2 tissue types × 8 segments) were used for endophyte isolation in this study.

Surface sterilization was conducted according to Guo et al. (2000). Segments were surface sterilized by consecutive immersion for 1 min in 75% ethanol, 3 min in 3.25% sodium hypochlorite, and 30 sec in 75% ethanol. Sets of four segments were then evenly placed in a 90 mm Petri dish containing potato dextrose agar (PDA, 2%). Benzylpenicillin sodium (50 mg/L, North China Pharmaceutical Group Corporation, China) was added to suppress bacterial growth. Petri dishes were sealed, incubated for 2 months at 25 °C, and examined periodically. When fungal colonies developed, they were transferred to a new PDA containing Petri dishes for purification. The purified strains were transferred to PDA slants for further study.

Subcultures on PDA were examined periodically, and the sporulated isolates were identified based on their morphological characteristics. The non-sporulated cultures were designated as *mycelia sterilia*, which were divided into different “morphotypes” according to colony color, texture, and growth rate on PDA (Guo et al. 2000). One representative strain of each morphotype or sporulated strain was selected for further molecular identification. The living cultures are deposited in China General Microbiological Culture Collection Center (CGMCC) in Beijing, China.

DNA extraction, amplification, sequencing, and identification

Genomic DNA was extracted from fresh cultures following the protocol of Guo et al. (2000). Fresh fungal mycelia (ca. 50 mg) were scraped from the surface of the PDA

plate and transferred into a 1.5 mL microcentrifuge tube with 700 μL of preheated (65 °C) 2 \times CTAB extraction buffer (2% CTAB, 100 mM Tris-HCl, 1.4 M NaCl, 20 mM EDTA, pH 8.0), and 0.2 g of sterilized quartz sand. The mycelium was ground using a glass pestle and then incubated in a 65 °C water bath for 30 min with occasional gentle swirling. Five hundred microliters of phenol:chloroform (1:1) were added into each tube and mixed thoroughly to form an emulsion. The mixture was spun at 12,000 g for 15 min at room temperature in a microcentrifuge, and the aqueous phase was transferred into a fresh 1.5 mL tube. The aqueous phase containing DNA was re-extracted with chloroform:isoamyl (24:1) until no interface was visible. Thirty microliters of 5 M KOAc was added into the aqueous phase followed by 200 μL of isopropanol and inverted gently to mix. The genomic DNA was precipitated at 9200 g for 2 min in a microcentrifuge at 4 °C. The DNA pellet was washed twice with 70% ethanol and dried using SpeedVac (AES 1010, Savant, Holbrook, NY, USA) for 10 min or until dry. The DNA pellet was then re-suspended in 65 μL ultrapure sterilized water.

The internal transcribed spacer (ITS) region of rDNA was amplified using primer pairs ITS4 (White et al. 1990) and ITS1F (Gardes and Bruns 1993). Amplification was performed in a 50 μL reaction volume which contained PCR buffer (20 mM KCl, 10 mM $(\text{NH}_4)_2\text{SO}_4$, 2 mM MgCl_2 , 20 mM Tris-HCl, pH 8.4), 200 μM of each deoxyribonucleotide triphosphate, 15 pmols of each primer, 100 ng template DNA, and 2.5 U *Taq* polymerase (Biocolor BioScience & Technology Company, Shanghai, China). The thermal cycling program was as follows: 3 min initial denaturation at 94 °C, followed by 35 cycles of 30-sec denaturation at 94 °C, 30-sec annealing at 52 °C, 1 min extension at 72 °C; and a final 10 min extension at 72 °C. A negative control using water instead of template DNA was included in the amplification process. Four microliters of PCR product from each PCR reaction were examined by electrophoresis at 80 V for 30 min in a 1% (w/v) agarose gel in 1 \times TAE buffer (0.4 M Tris, 50 mM NaOAc, 10 mM EDTA, pH 7.8) and visualized under ultraviolet (UV) light after staining with ethidium bromide (0.5 $\mu\text{g}/\text{mL}$). PCR products were purified using Wizard SV Gel and PCR Clean-Up System (Promega, Madison, USA) and directly sequenced with primer pairs, as mentioned above in the ABI 3730-XL DNA sequencer (Applied Biosystems, Inc. USA).

A value of 97% of ITS region identity was used as a DNA barcoding threshold for OTU clustering (O'Brien et al. 2005). The taxonomical assignments for each OTU were determined according to the BLAST results against both UNITE+INSD (UNITE combined international nucleotide sequence databases) and GenBank public sequence databases. A representative sequence of each OTU was selected and searched against the UNITE+INSD fungal ITS databases (Kõljalg et al. 2013) using a basic local alignment search tool (BLAST) (Altschul et al. 1990). The DOIs of UNITE fungal Species Hypotheses at 1.5% threshold (Nilsson et al. 2019) were also added to each of taxonomical assignments (Table 1). For reliable identification of the fungi, a representative sequence of each OTU was searched against the GenBank public sequence databases using BLASTN (Sun et al. 2011, Sun et al. 2012a). For further identification of these fungi, we select the most reliable sequence as a reference (the sequences originated from mycologists or taxonomists, yielded from taxonomical or phylogenetical

Table 1. Molecular identification of endophytic fungi based on ITS sequences.

Fungal taxa	accession no.	Closest blast match in GenBank (accession no.)	Identity (%)	UNITE taxon name (SH code at 1.5% threshold)
<i>Acremonium alternatum</i>	KY114893	<i>Acremonium alternatum</i> (AY566992)	100	<i>Pezizomycotina</i> (SH15260626.08FU)
<i>Alternaria chlamydospora</i>	KY114895	<i>Alternaria chlamydospora</i> (NR136039)	99	<i>Alternaria chlamydospora</i> (SH1505867.08FU)
<i>Alternaria eichhorniae</i>	KY114894	<i>Alternaria burnsi</i> (KR604836)	100	<i>Alternaria eichhorniae</i> (SH1526398.08FU)
<i>Aspergillus flavus</i>	KY114898	<i>Aspergillus flavus</i> (KU296258)	100	<i>Aspergillus flavus</i> (SH1532605.08FU)
<i>Aspergillus fumigatus</i>	KY114899	<i>Aspergillus fumigatiifinis</i> (MH474422)	100	<i>Aspergillus fumigatus</i> (SH1529985.08FU)
<i>Aspergillus terreus</i>	KY114900	<i>Aspergillus terreus</i> (KM249873)	100	<i>Aspergillus terreus</i> (SH1530841.08FU)
<i>Aureobasidium pullulans</i>	KY114901	<i>Aureobasidium pullulans</i> (MH857648)	100	<i>Aureobasidium pullulans</i> (SH1515060.08FU)
<i>Bipolaris pristeskaensis</i>	KY114902	<i>Bipolaris pristeskaensis</i> (JQ517482)	100	<i>Bipolaris pristeskaensis</i> (SH1526609.08FU)
<i>Cladosporium limoniforme</i>	KY114903	<i>Cladosporium limoniforme</i> (KT600401)	100	<i>Mycosphaerella tassiana</i> (SH1572792.08FU)
<i>Curvularia inaequalis</i>	KY114905	<i>Curvularia inaequalis</i> (KT192305)	99	<i>Curvularia inaequalis</i> (SH1526407.08FU)
<i>Didymella glomerata</i>	KY114906	<i>Didymella glomerata</i> (FJ427004)	99	<i>Didymella exigua</i> (SH1547057.08FU)
<i>Fusarium avenaceum</i>	KY114907	<i>Fusarium avenaceum</i> (JN631748)	100	<i>Gibberella trincta</i> (SH1546323.08FU)
<i>Fusarium incarnatum</i>	KY114908	<i>Fusarium incarnatum</i> (KT748520)	100	<i>Gibberella intricans</i> (SH1610158.08FU)
<i>Fusarium oxysporum</i>	KY114909	<i>Fusarium oxysporum</i> (EU429440)	100	<i>Gibberella fujikuroi</i> (SH1610157.08FU)
<i>Fusarium proliferatum</i>	KY114910	<i>Fusarium proliferatum</i> (KP132229)	100	<i>Fusarium proliferatum</i> (SH1610159.08FU)
<i>Humicola fuscoatra</i>	KY114911	<i>Humicola fuscoatra</i> (KP101183)	99	<i>Pezizomycotina</i> (SH1642162.08FU)
<i>Monosporascus ibericus</i>	KY114912	<i>Monosporascus ibericus</i> (JQ973832)	97	<i>Monosporascus ibericus</i> (SH1578625.08FU)
<i>Monosporascus sp.</i>	KY114913	<i>Monosporascus sp.</i> (KT269082)	97	<i>Monosporascus</i> (SH1578615.08FU)
<i>Neocamarosporium obiones</i>	KY114896	<i>Ascochyta obiones</i> (GU230752)	100	<i>Pleosporales</i> (SH1524225.08FU)
<i>Neocamarosporium sp.1</i>	KY114914	<i>Neocamarosporium goggapense</i> (KJ869163)	94	<i>Neocamarosporium sabioiae</i> (SH1524232.08FU)
<i>Neocamarosporium sp.2</i>	KY114916	<i>Neocamarosporium sp.</i> (KY940767)	97	<i>Neocamarosporium</i> (SH1524244.08FU)
<i>Neocamarosporium sp.3</i>	KY114897	<i>Pleospora cadescens</i> (MH861148)	96	<i>Pleosporales</i> (SH1524225.08FU)
<i>Neodidymellopsis polemonii</i>	KY114915	<i>Neodidymellopsis polemonii</i> (KT389532)	100	<i>Didymella exigua</i> (SH1547057.08FU)
<i>Paraphaeosphaeria sporulosa</i>	KY114904	<i>Coniothyrium sporulosum</i> (DQ865113)	97	<i>Paraphaeosphaeria sporulosa</i> (SH1582449.08FU)
<i>Pezizomycotina sp.1</i>	KY114922	<i>Pleomonadicysta decalvii</i> (NR_154369)	88	<i>Pezizomycotina</i> (SH1574559.08FU)
<i>Pezizomycotina sp.2</i>	KY114923	<i>Trematosphaeria grisea</i> (NR132039)	86	<i>Pezizomycotina</i> (SH1574559.08FU)
<i>Pleosporales sp.</i>	KY114917	<i>Pleosporales sp.</i> (KF887149)	96	<i>Pleosporales</i> (SH1582443.08FU)
<i>Preussia sp.1</i>	KY114918	<i>Preussia terricola</i> (GQ203765)	92	<i>Preussia terricola</i> (SH1642175.08FU)
<i>Preussia sp.2</i>	KY114919	<i>Preussia sp.</i> (HM007080)	99	<i>Preussia</i> (SH1541731.08FU)
<i>Sarocladium kilense</i>	KY114920	<i>Sarocladium kilense</i> (KM231849)	99	<i>Sarocladium kilense</i> (SH1541920.08FU)
<i>Simplicillium obclavatum</i>	KY114921	<i>Simplicillium obclavatum</i> (AB604000)	99	<i>Simplicillium obclavatum</i> (SH1584064.08FU)
<i>Trematosphaeriaceae sp.</i>	KY114924	<i>Medicopsis romeroi</i> (KF015657)	88	<i>Medicopsis romeroi</i> (SH1613813.08FU)
<i>Trichocomaceae sp.</i>	KY114925	<i>Talaromyces purpureogenus</i> (KM086709)	86	<i>Talaromyces marneffei</i> (SH1516144.08FU)
<i>Ulocladium oblongo-obovoidium</i>	KY114926	<i>Ulocladium oblongo-obovoidium</i> (MH863976)	100	<i>Alternaria eichhorniae</i> (SH1526398.08FU)
<i>Xylaria hypoxylon</i>	KY114927	<i>Xylaria hypoxylon</i> (KF306342)	100	<i>Xylariaceae</i> (SH1541119.08FU)
<i>Xylariales sp.</i>	KY114928	<i>Xylariales sp.</i> (KC460867)	98	<i>Xylariales</i> (SH1578643.08FU)

studies, or were part of cultures or specimens in famous collections, would be given higher credits). As for taxonomical levels higher than species, we typically relied on 90, 85, 80, and 75% sequence identity as a criterion for assigning OTUs with names of a genus, family, order, or class, respectively (Tedersoo et al. 2014). Nevertheless, the results of sequence-based identification were calibrated with morphological characteristics in our study given the strains within one OTU sporulated. The microscopic observation was applied with cultures mounted in sterile water using a compound microscope (Zeiss Axio Imager A2, Carl Zeiss Microscopy, Göttingen, Germany). The ITS sequences of endophytic fungi obtained in this study have been deposited in National Center for Biotechnology Information (NCBI) with GenBank accession no. KY114893 to KY114928 (Table 1).

Data analysis

All statistical analyses were carried out in R 3.3.1 (R Development Core Team 2016). The colonization rate of endophytic fungi was calculated as the total number of tissue segments infected by fungi divided by the total number of tissue segments incubated (Sun et al. 2011). The relative abundance was calculated as the number of isolates of a taxon divided by the total number of isolates of all taxa, and the fungal richness was defined as the number of fungal species in a sample.

One-way analysis of variance (ANOVA) was carried out to test the effect of plant species or tissue type (stem and root) on the colonization rate and species richness of endophytic fungi. Multiple comparisons were performed using *post hoc* Tukey's HSD (Honest Significant Difference) tests to examine the significant differences among the plant species or tissue types at $P < 0.05$ level. All data were tested for normality and homogeneity of variance before ANOVA. In cases where satisfactory results of homogeneity of variance amongst plant species after square root and transformation were not observed (e.g., in stems), then nonparametric Kruskal-Wallis test followed by pairwise comparisons was applied to examine the significant difference among plant species at $P < 0.05$ level. *T*-test was applied to examine the significant difference of the colonization rate and species richness of endophytic fungi between stems and roots for each plant species at $P < 0.05$ level. Canonical correspondence analysis (CCA) was performed to observe the correlation between endophytic fungi and plant species or tissue types with the 'cca' function in the vegan package (Oksanen et al. 2019). The effects of plant species and tissue type on community composition of endophytic fungi were tested by permutational multivariate analysis of variance (PerMANOVA) using the 'adonis' command in the vegan package (Oksanen et al. 2019).

The host-fungus association preferences were evaluated based on a d' interaction specialization index (Blüthgen et al. 2007) using the 'dfun' function in the bipartite package (Dormann et al. 2009) according to Toju et al. (2016). Briefly, a binarized sample \times fungal taxon matrix (i.e., presence/absence) was converted into a 'species-level' matrix, in which rows depicted plant species, columns represented endophytic

fungus taxa, and cell entries were the number of samples from which respective combinations of plants and fungi were observed. To perform a randomization analysis of the d' index, plant species labels in the sample \times fungal taxon matrix were shuffled, and then, the randomized species-level matrices were obtained (1000 permutations). The d' value of each plant species or each fungal taxon was standardized as follows: standardized $d' = [d'_{\text{observed}} - \text{Mean}(d'_{\text{randomized}})] / \text{SD}(d'_{\text{randomized}})$, where the d'_{observed} was the d' estimate of the original data, and $\text{Mean}(d'_{\text{randomized}})$ and $\text{SD}(d'_{\text{randomized}})$ were the mean and standard deviation of the d' scores of randomized data matrices. Also, we evaluated the observed frequency (counts) of each plant-fungus association in the species-level matrix, and quantified with the two-dimensional preferences (2DP) in a pair of a plant species (i) and a fungal taxon (j) based on the species-level original and randomized matrices used in the d' analysis: $2DP(i, j) = [N_{\text{observed}}(i, j) - \text{Mean}(N_{\text{randomized}}(i, j))] / \text{SD}(N_{\text{randomized}}(i, j))$, where $N_{\text{observed}}(i, j)$ denoted the number of samples from which a focal combination of a plant and a fungus was observed in the original data, and the $\text{Mean}(N_{\text{randomized}}(i, j))$ and $\text{SD}(N_{\text{randomized}}(i, j))$ were the mean and standard deviation of the number of samples for the focal plant-fungus pair across randomized matrices. The P values were adjusted based on the false discovery rate (FDR) (Benjamini and Hochberg 1995).

Results

Colonization rate of endophytic fungi

A total of 1046 fungal strains were recovered from 1600 tissue segments from ten halophyte species. The colonization rate of endophytic fungi ranged from $7.5 \pm 3.33\%$ to $83.75 \pm 8.95\%$ in stems, from $33.75 \pm 11.19\%$ to $97.5 \pm 1.67\%$ in roots, and from $38.75 \pm 2.46\%$ to $85.63 \pm 2.28\%$ overall for the entire plant among the ten halophyte species (Fig. 1). One-way ANOVA showed that the colonization rate of endophytic fungi was significantly affected by plant identity ($F = 5.847$, $P < 0.001$) and tissue type ($F = 8.184$, $P < 0.001$). In the entire plant, the colonization rate of endophytic fungi was significantly higher in *Sa. nitraria* than in other plants (except for *Su. acuminata* and *Se. santolinum*) and was significantly higher in *Su. acuminata* than in *E. minor* (Fig. 1). In the stem, the colonization rate of endophytic fungi was significantly higher in *Sa. nitraria* and *Su. acuminata* than in the other halophyte species (except for *P. harmala*). For *P. harmala*, the colonization rate of endophytic fungi was significantly higher than in *B. dasyphylla* and *R. songarica* (Fig. 1). In the root, the colonization rate of endophytic fungi was significantly higher in *Se. santolinum*, *R. songarica*, and *Sa. nitraria* than in *E. minor* and *P. harmala*, and was significantly higher in *B. dasyphylla*, *C. arenarius*, and *Su. salsa* than in *P. harmala* (Fig. 1). Furthermore, the colonization rate of endophytic fungi was significantly higher in roots than in stems in *B. dasyphylla*, *C. arenarius*, *K. foliatum*, *Su. salsa*, *R. songarica*, and *Se. santolinum*, but no significant difference was observed in the other four halophyte species (Fig. 1).

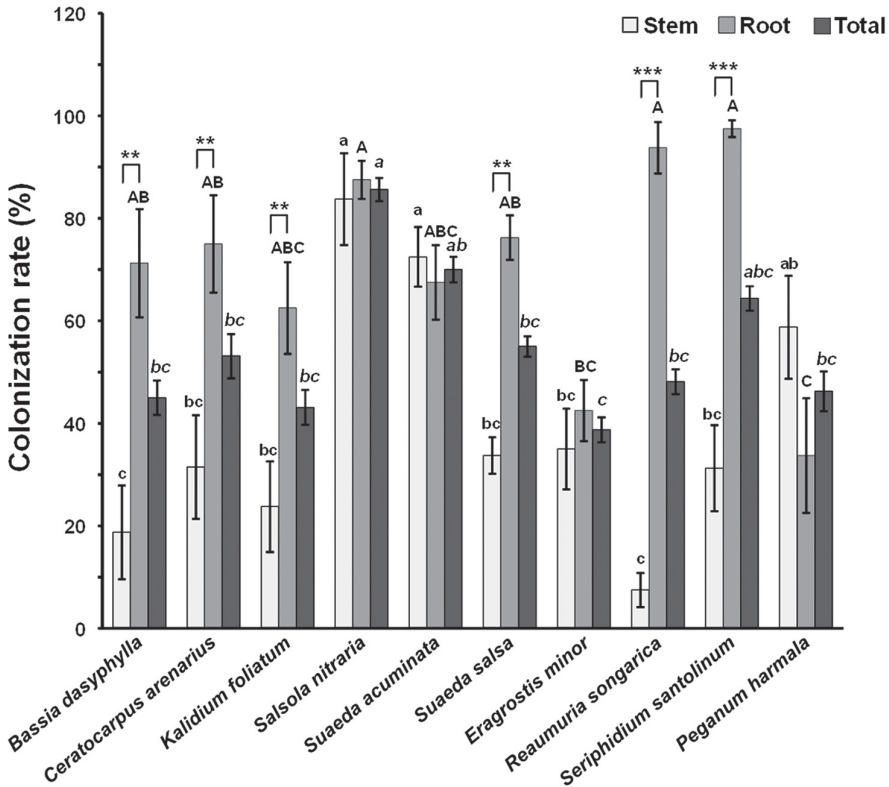


Figure 1. Colonization rate of endophytic fungi in stem, root, and total (stem + root) tissues of the ten halophyte species. Data are means \pm SE (n = 10). Columns without shared lowercase, uppercase, and italic letters denote the significant difference in the stem, root, and total tissues among the halophyte species, respectively. Asterisks above bars indicate significant difference between stem and root tissues for each plant species (** $P < 0.01$, *** $P < 0.001$).

Endophytic fungal richness

In total, 36 fungal taxa were isolated and identified based on morphological characters and ITS sequences (Table 1). The richness of endophytic fungi ranged from 0.5 ± 0.22 to 2.2 ± 0.2 in stems, from 1.2 ± 0.29 to 4 ± 0.3 in roots and from 1.2 ± 0.29 to 4 ± 0.3 (means \pm SE) in overall among the ten halophyte species (Fig. 2). The richness of endophytic fungi was significantly affected by plant species (ANOVA, $F = 4.635$, $P < 0.001$) and tissue type (Kruskal-Wallis test, $\chi^2 = 34.993$, $P < 0.001$). In the stem, the fungal richness was significantly higher in *Sa. nitraria* than in *B. dasyphylla* and *R. songarica*, and significantly higher in *E. minor* than in *R. songarica* (Fig. 2). In the root, the fungal richness was significantly higher in *Sa. nitraria* than in *B. dasyphylla*, *K. foliatum*, *Se. santolinum* and *P. harmala*, and significantly higher in *C. arenarius* than in *P. harmala* (Fig. 2). Furthermore, the fungal richness was significantly higher in roots than in stems in ten plant species, except for *E. minor*, *Se. santolinum* and *P. harmala* (Fig. 2).

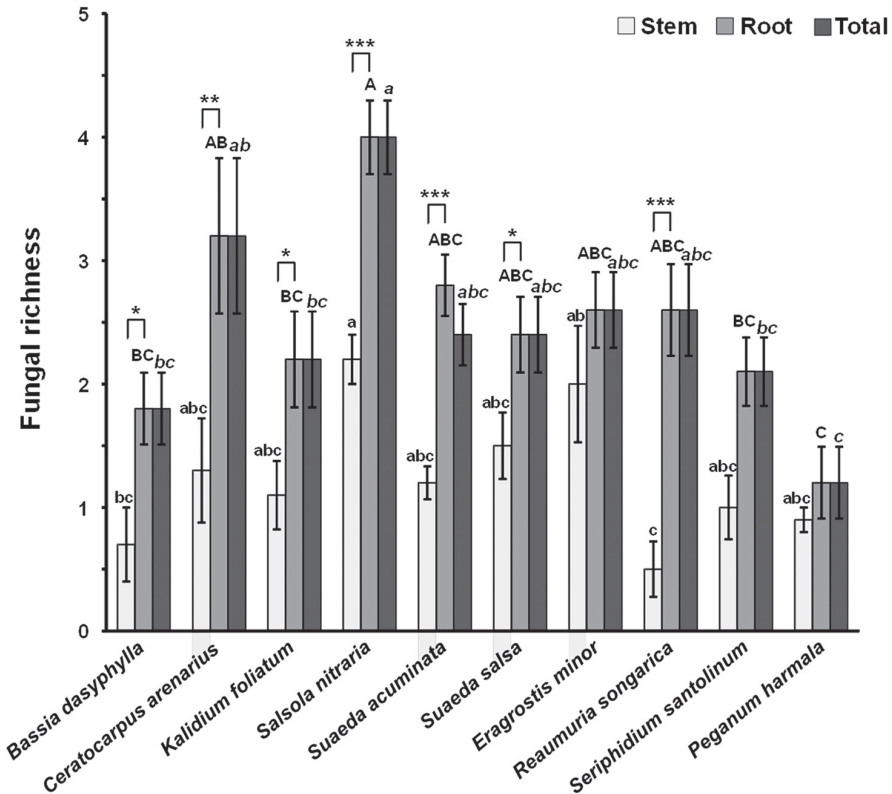


Figure 2. Endophytic fungal richness in stem, root and total (stem + root) tissues of the ten halophyte species. Data are means \pm SE ($n = 10$). Columns without shared lowercase, uppercase, and italic letters denote significant difference in the stem, root, and total tissues among the plant species, respectively. Asterisks above bars indicate the significant difference between stem and root tissues for each halophyte species (* $P < 0.05$, ** $P < 0.01$, *** $P < 0.001$).

Endophytic fungal community composition

Of the 36 endophytic fungi, 32 were recovered from roots, 27 from stems, and 23 were common in both roots and stems (Fig. 3). Among seven abundant endophytic fungi (relative abundance $> 15\%$ in certain plant species), *Alternaria eichhorniae* was the most abundant stem endophyte and was recovered from *C. arenarius*, *K. foliatum*, *P. harmala*, *Sa. nitraria*, *Su. acuminata*, and *Su. salsa* (Fig. 4B, D, E, G, I, J). In addition, *Monosporascus ibericus* was exclusively recovered from roots of *B. dasyphylla*, *K. foliatum*, *Su. acuminata*, and *Su. salsa* (Fig. 4A, D, I, J). In *C. arenarius*, *Pezizomycotina* sp.1 was exclusively recovered from roots, and in *Se. santolinum* *Pezizomycotina* sp.1 was mostly recovered from roots (Fig. 4B, H). *Sarocladium kiliense* and *Aspergillus fumigatiiformis* were only found on the roots of *R. songarica* (Fig. 4F). *Bipolaris prieskaensis* was mostly isolated from roots, and *Preussia* sp.2 was mostly distributed in stems in *E. minor* (Fig. 4C).

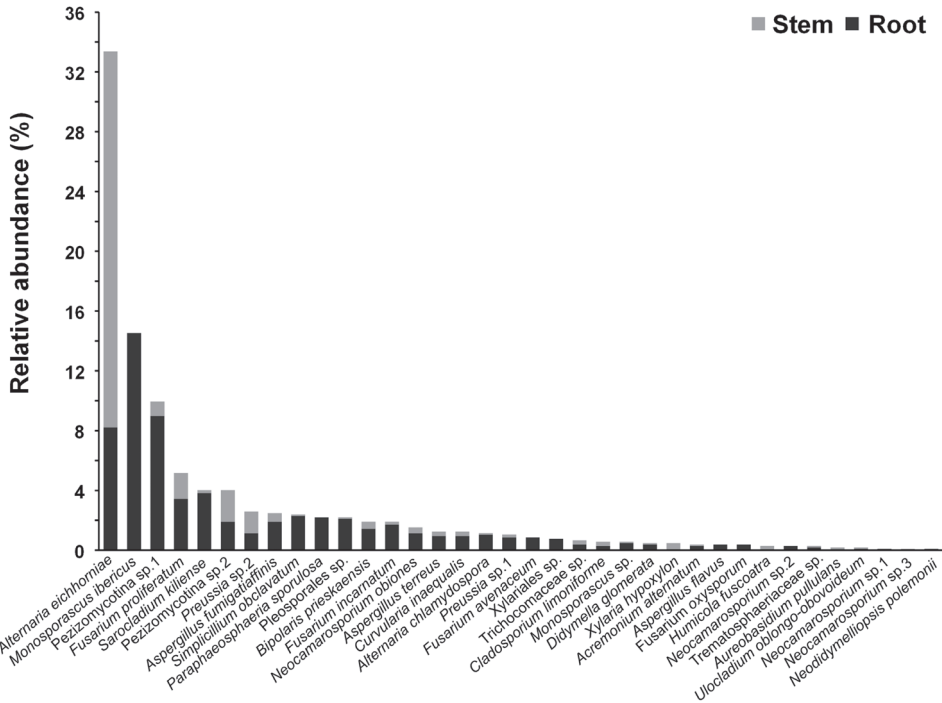


Figure 3. Relative abundance of endophytic fungi in the stem and root tissues of the ten halophyte species.

The CCA results indicated that the endophytic fungal community composition was significantly different between stems and roots of the ten halophyte species (Fig. 5A), and significantly different among some plants, such as *R. songarica*, *B. dasyphylla*, *P. harmala* and *E. minor* (Fig. 5B). The PerMANOVA results also showed that the endophytic fungal community composition was significantly affected by tissue type ($R^2 = 0.212$, $P = 0.001$) and plant species ($R^2 = 0.082$, $P = 0.001$).

Host-fungus association preferences

Host-fungus association preference analysis showed that five out of ten halophyte species showed significant preferences to endophytic fungi, especially strong preferences in *E. minor*, *R. songarica*, and *Se. santolinum* (Fig. 6A). Among the 36 endophytic fungi, 13 showed significant preferences for host species, particularly strong preferences were observed in *Al. eichhorniae*, *M. ibericus*, *Pezizomycotina sp.1*, *Sr. kilianse*, *Pezizomycotina sp.2*, *As. fumigatiaffinis*, *B. prieskaensis*, *Trichocomaceae sp.*, and *Xylaria hypoxylon* (Fig. 6A). Furthermore, 26 out of 208 pairs of plants and fungi showed significant preferences, such as pairs *Pezizomycotina sp.1* and *Se. santolinum*, *Sr. kilianse* and *R. songarica*, *B. prieskaensis* and *E. minor*, *As. fumigatiaffinis* and *R. songarica* (Fig. 6).

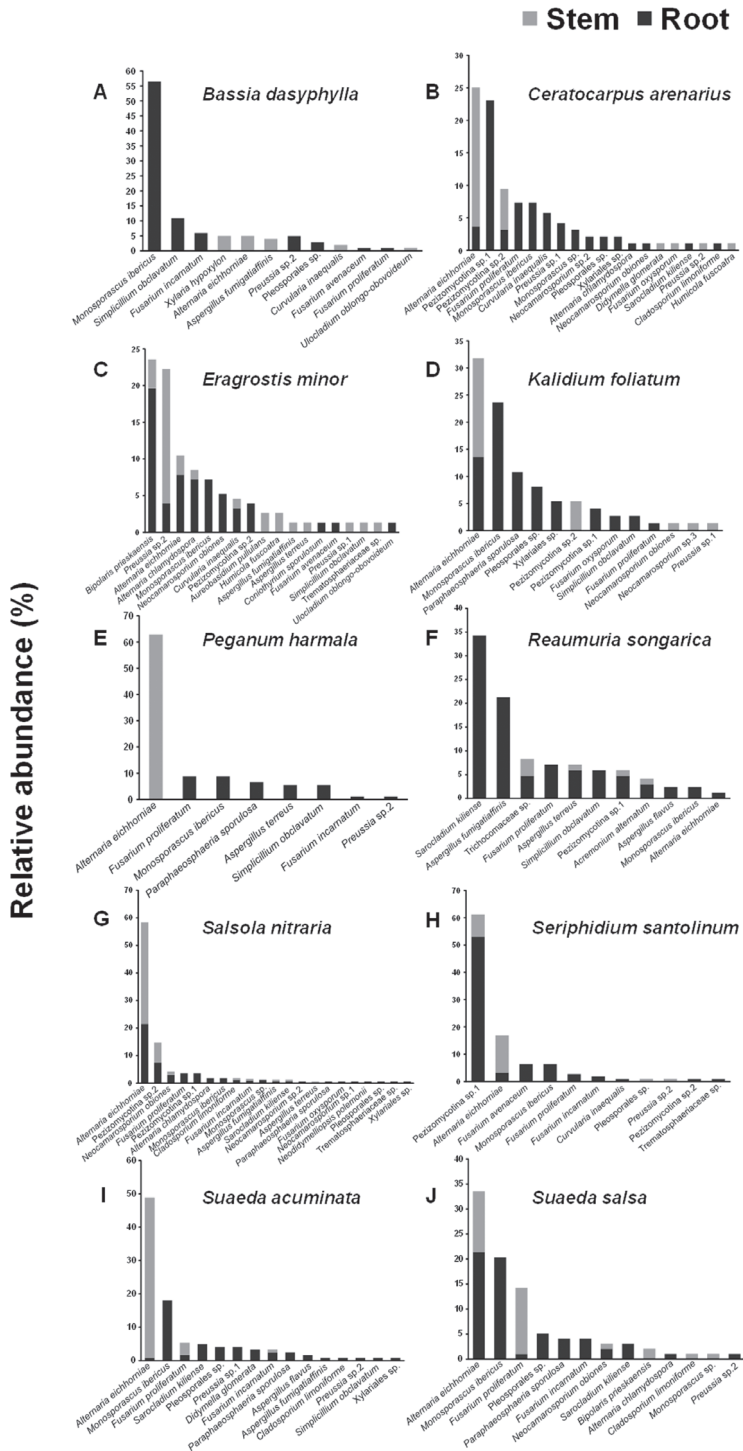


Figure 4. Relative abundance of endophytic fungi in the stem and root of different halophyte species.

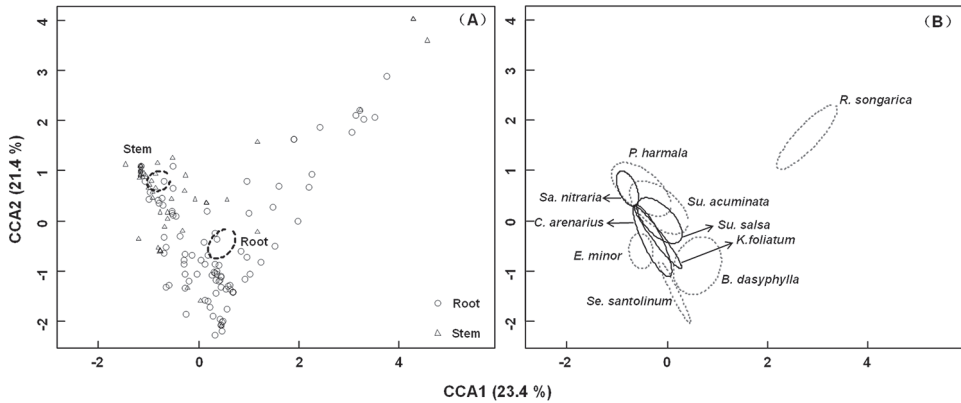


Figure 5. Canonical correspondence analysis (CCA) ordination plot of endophytic fungal communities of stem and root tissues **(A)** and halophyte species **(B)**. Dotted ellipses indicate 95% confidence intervals around centroids of tissue type **(A)** and plant species **(B)**, *B. dasyphylla* = *Bassia dasyphylla*, *C. arenarius* = *Ceratocarpus arenarius*, *K. foliatum* = *Kalidium foliatum*, *Sa. nitraria* = *Salsola nitraria*, *Su. acuminata* = *Suaeda acuminata*, *Su. salsola* = *Suaeda salsola*, *E. minor* = *Eragrostis minor*, *R. songarica* = *Reaumuria songarica*, *Se. santolinum* = *Seriphidium santolinum*, and *P. harmala* = *Peganum harmala*.

Discussion

The colonization rate and species richness of endophytic fungi varied among desert halophyte species in the current study. Similar results have been reported in previous studies in mangrove (Xing et al. 2011; Xing and Guo 2011; Liu et al. 2012; Li et al. 2016), desert halophytes (Sun et al. 2012b), gypsophilous plants (Porrás-Alfaro et al. 2014), desert trees and shrubs (Massimo et al. 2015), and plants in other ecosystem (Su et al. 2010; Sun et al. 2012a). For example, Xing et al. (2011) recovered 39 distinct endophytic species in five mangrove species and found the colonization rate of endophytic fungi ranging from 12.5 to 41.7% in roots, from 8.0 to 54.0% in stems, and from 12.5 to 25.1% in leaves. Sun et al. (2012b) identified 21 endophyte species from eight desert halophytes and found the colonization rates ranging from 35 to 100% in stems and leaves. Furthermore, we found that the colonization rate and species richness of endophytic fungi were generally higher in roots than in stems, which is in contrast with studies carried out in *Holcus lanatus* (Márquez et al. 2010), *Stipa grandis* (Su et al. 2010), and gypsophilous plants (Porrás-Alfaro et al. 2014) in arid ecosystem. The difference between endophytic colonization and diversity between above- and below-ground might be attributed to both biotic and abiotic factors. In the study site, humidity is much lower in the air than in the soil, which might result in lower colonization rate and species richness of endophytic fungi in stems than in roots, as endophyte colonization is positively correlated with humidity (Herrera et al. 2010; Massimo et al. 2015). Also, the relatively moist and organic-rich soil substrate is capable of supporting diverse and abundant fungal propagules for penetration in plant roots in comparison to stems (Bridge and Spooner 2001; Massimo et al. 2015).

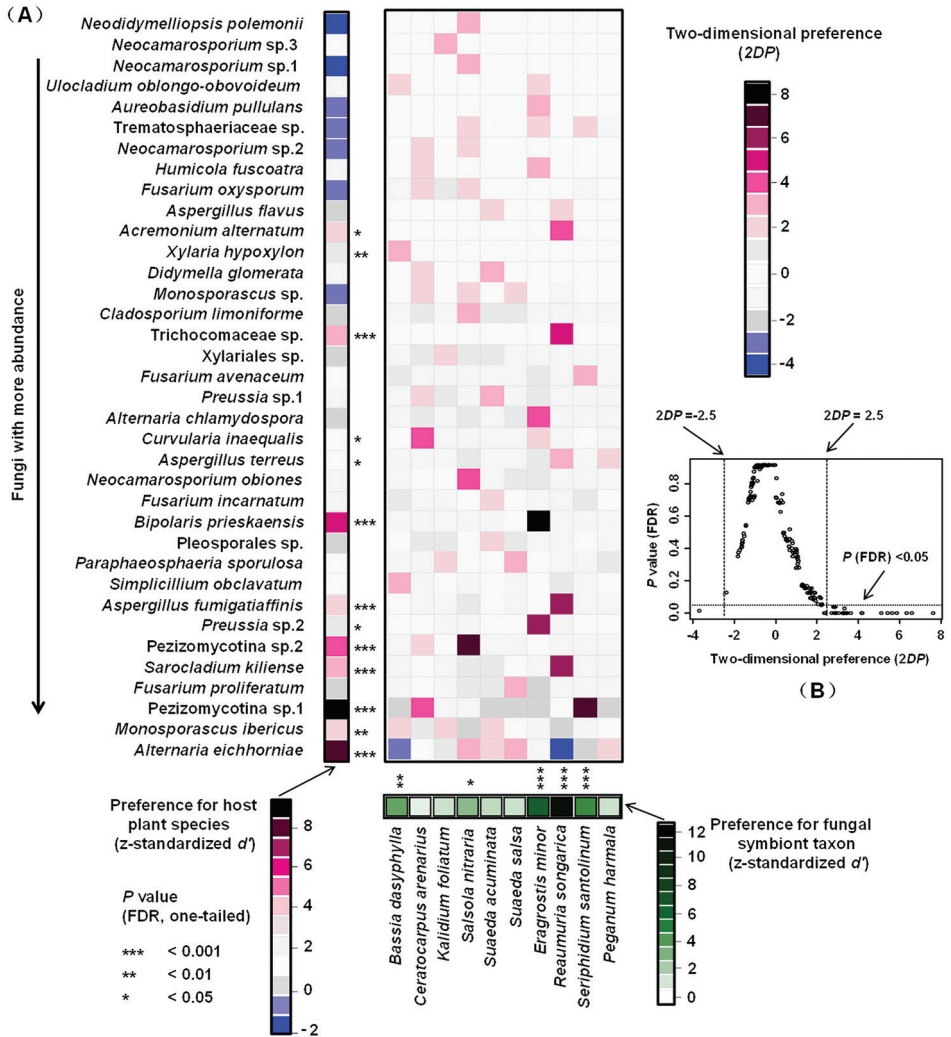


Figure 6. Preferences observed in the plant-fungus associations. **A** Preference scores. The standardized d' estimate of preferences for fungal taxon is shown for each halophyte (column), and the standardized d' estimate of preferences for plant species is indicated for each of the fungal taxon (row). Each cell in the matrix indicates a two-dimensional preference (2DP) estimate, which measures to what extent the association of a focal plant-fungus pair was observed more/less frequently than expected by chance. P values were shown as false discovery rates (FDRs) in the plant/fungus analysis. **B** Relationship between 2DP and FDR-adjusted P values, 2DP values larger than 2.5 and those smaller than -2.5 represented strong preference and avoidance, respectively ($P_{FDR} < 0.05$). Significance: *, $P < 0.05$, **, $P < 0.01$, ***, $P < 0.001$.

We found that the endophytic fungi community composition is halophyte species-dependent. Similar results have been reported in some previous studies on halophytes and desert plants (Xing et al. 2011; Xing and Guo 2011; Macia-Vicente et al. 2012;

Sun et al. 2012b; Porras-Alfaro et al. 2014; Massimo et al. 2015; Li et al. 2016). For example, Sun et al. (2012b) indicated that the endophytic fungal community in stems and leaves of eight desert plants were different among host species in the Tennger Desert region, China. Massimo et al. (2015) suggested the fungal endophyte community composition differed among host species in the aboveground tissues of Sonoran Desert plants. It has been reported that the host species is a key factor shaping endophyte community structures (Hoffman and Arnold 2008; Arfi et al. 2012; Sun et al. 2012a; Hardoim et al. 2015). Our host preference analysis indicated that 13 endophytic fungal species show significant host preferences. For example, *B. prieskaensis* preferred colonizing *E. minor*, and *Sa. kiliense* and *As. fumigatiaffinis* preferred *R. songarica*. Hardoim et al. (2015) suggested that the selective forces do not act merely on the plant genome itself, but on its associated microbial community also. Moreover, the endophytic fungal composition could be affected by the expected difference in plant chemistry (Arnold et al. 2001; Huang et al. 2008). For example, in the present study, *P. harmala*, a medical plant possessing antifungal properties (Hashem 2011), might inhibit fungal colonization and thus contained the less diverse endophyte community. Therefore, the chemical or physiological traits of plants also affect the endophyte community.

Community composition of endophytic fungi was also affected by plant tissue types (root and stem), which corroborate earlier studies carried out in semi-arid and arid ecosystems (Su et al. 2010; Porras-Alfaro et al. 2014), and highlighted in the review by Hardoim et al. (2015). Despite the dissimilarity in the availability of fungal inocula between above- and under-ground circumstances discussed previously, previous studies suggested that the morphology and chemical substance of tissues also influenced the community composition of roots and stems (Herrera et al. 2010; Su et al. 2010). According to preference analysis, we found specific endophyte taxa consistently showing tissue preference regardless of the host species. For example, *M. ibericus* was found exclusively in roots from all ten desert halophytes in the current study. The taxon was firstly described from healthy roots of *Atriplex portulacoides*, *Plantago crassifolia*, and an undetermined plant in saline habitats of Spain (Collado et al. 2002). *Monosporascus* spp. are well known as pathogens infecting fruit in Cucurbitaceae and vine growing in hot semi-arid climates with soils that tend to be saline and alkaline (Collado et al. 2002). Some members of *Monosporascus* spp. have been reported as root endophytes with a much broader host range, i.e., *Acleisanthes lanceolatus*, *Bouteloua gracilis*, *Eustachys petraea*, *Mentzelia perennis*, *Nama carnosum*, *Nerisyrenia linearifolia*, *Sartwellia flaveriae*, and *Tiquilia hispida* from Mexico, Honduras, and New Mexico (Porras-Alfaro et al. 2008; Herrera et al. 2010; Herrera et al. 2013; Porras-Alfaro et al. 2014). Our study shows that *Al. eichhorniae* predominated the endophyte assemblages and preferred to colonize the stems rather than the roots. *Alternaria* fungi as dominant endophytes showing preference in specific tissues but very low specificity with respect to host species, were mainly isolated from leaves in six halophytes in inland salt marsh of Canada (Muhsin and Booth 1987), in eight halophytes in Tennger Desert of China (Sun et al. 2012b), and in eight gypsophilous flowering plants in New Mexico desert (Porras-Alfaro et al. 2014). These previous studies in halophytes and desert gypsophytes indicated that some endophytic fungi show strong tissue preferences.

Conclusions

The present study revealed high diversity of endophytic fungi associated with desert halophytes, and their colonization rate and diversity of endophytic fungi vary from plant to plant and is higher in roots than in stems. The endophytic fungal community composition is affected by plant species and tissue type as some endophytic fungi showed strong host and tissue preferences. The current study will provide preliminary data for exploration into diverse bioactive natural products originated from halophyte endophytes, and prospects on ecosystem reconstruction or desert agriculture development.

Acknowledgments

We are grateful to Ms. Tie-Mu-Er-Bie-Ke Ba-He-Jia-Yi-Na-Er, Mr. Yong-Xin Zang and Hai Zhu from Xinjiang Institute of Ecology and Geography, Chinese Academy of Sciences for their help with sampling and plant identification. This study was financially supported by the National Natural Science Foundation of China (Grant Nos. 31470151 and 31470228).

References

- Almario J, Jeena G, Wunder J, Langen G, Zuccaro A, Coupland G, Bucher M (2017) Root-associated fungal microbiota of nonmycorrhizal *Arabidopsis thaliana* and its contribution to plant phosphorus nutrition. *Proceedings of the National Academy of Sciences* 114: E9403–E9412. <https://doi.org/10.1073/pnas.1710455114>
- Altschul SF, Gish W, Miller W, Myers EW, Lipman DJ (1990) Basic local alignment search tool. *Journal of Molecular Biology* 215: 403–410. [https://doi.org/10.1016/S0022-2836\(05\)80360-2](https://doi.org/10.1016/S0022-2836(05)80360-2)
- Arfi Y, Buée M, Marchand C, Levasseur A, Record E (2012) Multiple markers pyrosequencing reveals highly diverse and host-specific fungal communities on the mangrove trees *Avicennia marina* and *Rhizophora stylosa*. *FEMS Microbiology Ecology* 79: 433–444. <https://doi.org/10.1111/j.1574-6941.2011.01236.x>
- Arnold AE, Lutzoni F (2007) Diversity and host range of foliar fungal endophytes: are tropical leaves biodiversity hotspots? *Ecology* 88: 541–549. <https://doi.org/10.1890/05-1459>
- Arnold AE, Maynard Z, Gilbert GS (2001) Fungal endophytes in dicotyledonous neotropical trees: patterns of abundance and diversity. *Mycological Research* 105: 1502–1507. <https://doi.org/10.1017/S0953756201004956>
- Arnold AE, Mejía LC, Kyllö D, Rojas EI, Maynard Z, Robbins N, Herre EA (2003) Fungal endophytes limit pathogen damage in a tropical tree. *Proceedings of the National Academy of Sciences* 100: 15649–15654. <https://doi.org/10.1073/pnas.2533483100>
- Behie SW, Zelisko PM, Bidochka MJ (2012) Endophytic insect-parasitic fungi translocate nitrogen directly from insects to plants. *Science* 336: 1576–1577. <https://doi.org/10.1126/science.1222289>

- Benjamini Y, Hochberg Y (1995) Controlling the false discovery rate: a practical and powerful approach to multiple testing. *Journal of the Royal Statistical Society: Series B (Methodological)* 57: 289–300. <https://doi.org/10.1111/j.2517-6161.1995.tb02031.x>
- Blüthgen N, Menzel F, Hovestadt T, Fiala B, Blüthgen N (2007) Specialization, constraints, and conflicting interests in mutualistic networks. *Current Biology* 17: 341–346. <https://doi.org/10.1016/j.cub.2006.12.039>
- Bridge P, Spooner B (2001) Soil fungi: diversity and detection. *Plant and Soil* 232:147–154. <https://doi.org/10.1023/A:1010346305799>
- Chen BM, Wang GX, Peng SL (2009) Role of desert annuals in nutrient flow in arid area of Northwestern China: a nutrient reservoir and provider. *Plant Ecology* 201: 401–409. https://doi.org/10.1007/978-90-481-2798-6_3
- Collado J, González A, Platas G, Stchigel AM, Guarro J, Peláez F (2002) *Monosporascus ibericus* sp. nov., an endophytic ascomycete from plants on saline soils, with observations on the position of the genus based on sequence analysis of the 18S rDNA. *Mycological Research* 106: 118–127. <https://doi.org/10.1017/S0953756201005172>
- Collado J, Platas G, González I, Peláez F (1999) Geographical and seasonal influences on the distribution of fungal endophytes in *Quercus ilex*. *New Phytologist* 144: 525–532. <https://doi.org/10.1046/j.1469-8137.1999.00533.x>
- Dai Y, Zheng XJ, Tang LS, Li Y (2015) Stable oxygen isotopes reveal distinct water use patterns of two *Haloxylon* species in the Gurbantonggut Desert. *Plant and Soil* 389: 73–87. <https://doi.org/10.1007/s11104-014-2342-z>
- Dormann CF, Fründ J, Blüthgen N, Gruber B (2009) Indices, graphs and null models: analyzing bipartite ecological networks. *The Open Ecology Journal* 2: 7–24. <https://doi.org/10.2174/1874213000902010007>
- Flowers TJ, Colmer TD (2008) Salinity tolerance in halophytes. *New Phytologist* 179: 945–963. <https://doi.org/10.1111/j.1469-8137.2008.02531.x>
- Flowers TJ, Hajibagheri MA, Clipson NJW (1986) Halophytes. *The Quarterly Review of Biology* 61: 313–337. <https://doi.org/10.1086/415032>
- Gardes M, Bruns TD (1993) ITS primers with enhanced specificity for basidiomycetes – application to the identification of mycorrhizae and rusts. *Molecular Ecology* 2: 113–118. <https://doi.org/10.1111/j.1365-294X.1993.tb00005.x>
- Giri C, Ochieng E, Tieszen LL, Zhu Z, Singh A, Loveland T, Masek J, Duke N (2011) Status and distribution of mangrove forests of the world using earth observation satellite data. *Global Ecology and Biogeography* 20: 154–159. <https://doi.org/10.1111/j.1466-8238.2010.00584.x>
- Guo LD, Hyde KD, Liew ECY (2000) Identification of endophytic fungi from *Livistona chinensis* based on morphology and rDNA sequences. *New Phytologist* 147: 617–630. <https://doi.org/10.1046/j.1469-8137.2000.00716.x>
- Hardoim PR, van Overbeek LS, Berg G, Pirttilä AM, Compant S, Campisano A, Döring M, Sessitsch A (2015) The hidden world within plants: ecological and evolutionary considerations for defining functioning of microbial endophytes. *Microbiology and Molecular Biology Reviews* 79: 293–320. <https://doi.org/10.1128/MMBR.00050-14>
- Hartley SE, Gange AC (2009) Impacts of plant symbiotic fungi on insect herbivores: mutualism in a multitrophic context. *Annual Review of Entomology* 54: 323–342. <https://doi.org/10.1146/annurev.ento.54.110807.090614>

- Hashem M (2011) Antifungal properties of crude extracts of five Egyptian medicinal plants against dermatophytes and emerging fungi. *Mycopathologia* 172: 37–46. <https://doi.org/10.1007/s11046-010-9390-6>
- Herrera J, Khidir HH, Eudy DM, Porrás-Alfaro A, Natvig DO, Sinsabaugh RL (2010) Shifting fungal endophyte communities colonize *Bouteloua gracilis*: effect of host tissue and geographical distribution. *Mycologia* 102: 1012–1026. <https://doi.org/10.3852/09-264>
- Herrera J, Poudel R, Bokati D (2013) Assessment of root-associated fungal communities colonizing two species of tropical grasses reveals incongruence to fungal communities of North American native grasses. *Fungal Ecology* 6: 65–69. <https://doi.org/10.1016/j.funeco.2012.08.002>
- Hiruma K, Gerlach N, Sacristan S, Nakano RT, Hacquard S, Kracher B, Neumann U, Ramirez D, Bucher M, O’Connell RJ, Schulze-Lefert P (2016) Root endophyte *Colletotrichum tofieldiae* confers plant fitness benefits that are phosphate status dependent. *Cell* 165: 464–474. <https://doi.org/10.1016/j.cell.2016.02.028>
- Hoffman MT, Arnold AE (2008) Geographic locality and host identity shape fungal endophyte communities in cupressaceous trees. *Mycological Research* 112: 331–344. <https://doi.org/10.1016/j.mycres.2007.10.014>
- Huang WY, Cai YZ, Hyde KD, Corke H, Sun M (2008) Biodiversity of endophytic fungi associated with 29 traditional Chinese medicinal plants. *Fungal Diversity* 33: 61–75. <https://www.researchgate.net/publication/257748756>
- Kannadan S, Rudgers JA (2008) Endophyte symbiosis benefits a rare grass under low water availability. *Functional Ecology* 22: 706–713. <https://doi.org/10.1111/j.1365-2435.2008.01395.x>
- Khan AL, Al-Harrasi A, Al-Rawahi A, Al-Farsi Z, Al-Mamari A, Waqas M, Asaf S, Elyassi A, Mabood F, Shin JH, Lee IJ (2016) Endophytic fungi from frankincense tree improves host growth and produces extracellular enzymes and indole acetic acid. *PLoS One* 11: 1–19. <https://doi.org/10.1371/journal.pone.0158207>
- Kóljalg U, Nilsson RH, Abarenkov K, Tedersoo L, et al. (2013) Towards a unified paradigm for sequence-based identification of fungi. *Molecular Ecology* 22: 5271–5277. <https://doi.org/10.1111/mec.12481>
- Lau MK, Arnold AE, Johnson NC (2013) Factors influencing communities of foliar fungal endophytes in riparian woody plants. *Fungal Ecology* 6: 365–378. <https://doi.org/10.1016/j.funeco.2013.06.003>
- Li JL, Sun X, Chen L, Guo LD (2016) Community structure of endophytic fungi of four mangrove species in Southern China. *Mycology* 7: 180–190. <https://doi.org/10.1080/21501203.2016.1258439>
- Liu AR, Chen SC, Jin WJ, Zhao PY, Jeewon R, Xu T (2012) Host specificity of endophytic *Pestalotiopsis* populations in mangrove plant species of South China. *African Journal of Microbiology Research* 6: 6262–6269. <https://doi.org/10.5897/AJMR12.766>
- Liu B, Zhao WZ, Zeng FJ (2013) Statistical analysis of the temporal stability of soil moisture in three desert regions of northwestern China. *Environmental Earth Sciences* 70: 2249–2262. <https://doi.org/10.1007/s12665-013-2489-6>
- Macía-Vicente JG, Ferraro V, Burruano S, López-Llorca LV (2012) Fungal assemblages associated with roots of halophytic and non-halophytic plant species vary differentially along a salinity gradient. *Microbial Ecology* 64: 668–679. <https://doi.org/10.1007/s00248-012-0066-2>

- Márquez SS, Bills GF, Acuña LD, Zabalgoeazcoa I (2010) Endophytic mycobiota of leaves and roots of the grass *Holcus lanatus*. *Fungal Diversity* 41: 115–123. <https://doi.org/10.1007/s13225-009-0015-7>
- Massimo NC, Devan MMN, Arendt KR, Wilch MH, Riddle JM, Furr SH, Steen C, U'Ren JM, Sandberg DC, Arnold AE (2015) Fungal endophytes in aboveground tissues of desert plants: infrequent in culture, but highly diverse and distinctive symbionts. *Microbial Ecology* 70: 61–76. <https://doi.org/10.1007/s00248-014-0563-6>
- Muhsin TM, Booth T (1987) Fungi associated with halophytes of an inland salt marsh, Manitoba, Canada. *Canadian Journal of Botany* 65: 1137–1151. <https://doi.org/10.1139/b87-159>
- Nilsson RH, Larsson KH, Taylor AFS, Bengtsson-Palme J, Jeppesen TS, Schige D, Kennedy P, Picard K, Glöckner FO, Tedersoo L, Saar I, Kõljalg U, Abarenkov K (2019) The UNITE database for molecular identification of fungi: handling dark taxa and parallel taxonomic classifications. *Nucleic Acids Research* 47: D259–D264. <https://doi.org/10.1093/nar/gky1022>
- O'Brien HE, Parrent JL, Jackson JA, Moncalvo JM, Vilgalys R (2005) Fungal community analysis by large-scale sequencing of environmental samples. *Applied and Environmental Microbiology* 71: 5544–5550. <https://doi.org/10.1128/AEM.71.9.5544-5550.2005>
- Oksanen J, Blanchet FG, Friendly M, Kindt R, Legendre P, McGlenn D, Minchin PR, O'Hara RB, Simpson GL, Solymos P, Stevens MHH, Wagner H (2019) vegan: Community Ecology Package. R package version 2.5-5. <https://CRAN.R-project.org/package=vegan>
- Petrini O (1991) Fungal endophytes of tree leaves. In: Andrews, JH, Hirano SS (Eds) *Microbial ecology of leaves*. Springer Verlag, Berlin, 179–197. https://doi.org/10.1007/978-1-4612-3168-4_9
- Polme S, Bahram M, Jacquemyn H, Kennedy P, Kohout P, Moora M, Oja J, Opik M, Pecoraro L, Tedersoo L (2018) Host preference and network properties in biotrophic plant-fungal associations. *New Phytologist* 217: 1230–1239. <https://doi.org/10.1111/nph.14895>
- Porrás-Alfaro A, Bayman P (2011) Hidden fungi, emergent properties: endophytes and microbiomes. *Annual Review of Phytopathology* 49: 291–315. <https://doi.org/10.1146/annurev-phyto-080508-081831>
- Porrás-Alfaro A, Herrera J, Sinsabaugh RL, Odenbach KJ, Lowrey T, Natvig DO (2008) Novel root fungal consortium associated with a dominant desert grass. *Applied and Environmental Microbiology* 74: 2805–2813. <https://doi.org/10.1128/AEM.02769-07>
- Porrás-Alfaro A, Raghavan S, García M, Sinsabaugh RL, Natvig DO, Lowrey TK (2014) Endophytic fungal symbionts associated with gypsophilous plants. *Botany* 92: 295–301. <https://doi.org/10.1139/cjb-2013-0178>
- Promptutha I, Hyde KD, McKenzie EHC, Peberdy JF, Lumyong S (2010) Can leaf degrading enzymes provide evidence that endophytic fungi becoming saprobes? *Fungal Diversity* 41: 89–99. <https://doi.org/10.1007/s13225-010-0024-6>
- Purahong W, Wubet T, Lentendu G, Schlöter M, Pecyna MJ, Kapturska D, Hofrichter M, Krüger D, Buscot F (2016) Life in leaf litter: novel insights into community dynamics of bacteria and fungi during litter decomposition. *Molecular Ecology* 25: 4059–4074. <https://doi.org/10.1111/mec.13739>
- R Development Core Team (2016) *R: A Language and Environment for Statistical Computing*. R Foundation for Statistical Computing, Vienna, Austria, 2015. <https://www.Rproject.org>

- Rodriguez RJ, Henson J, Volkenburgh EV, Hoy M, Wright L, Beckwith F, Kim YO, Redman RS (2008) Stress tolerance in plants via habitat-adapted symbiosis. *The ISME Journal* 2: 404–416. <https://doi.org/10.1038/ismej.2007.106>
- Rodriguez RJ, White JF, Arnold AE, Redman RS (2009) Fungal endophytes: diversity and functional roles. *New Phytologist* 182: 314–330. <https://doi.org/10.1111/j.1469-8137.2009.02773.x>
- Rozema J, Flowers T (2008) Ecology crops for a salinized world. *Science* 322: 1478–1480. <https://doi.org/10.1126/science.1168572>
- Schroeter K, Wemheuer B, Pena R, Schoening I, Ehbrecht M, Schall P, Ammer C, Daniel R, Polle A (2019) Assembly processes of trophic guilds in the root mycobiome of temperate forests. *Molecular Ecology* 28: 348–364. <https://doi.org/10.1111/mec.14887>
- Sonjak S, Udovič M, Wraber T, Likar M, Regvar M (2009) Diversity of halophytes and identification of arbuscular mycorrhizal fungi colonising their roots in an abandoned and sustained part of Sečovlje salterns. *Soil Biology Biochemistry* 41: 1847–1856. <https://doi.org/10.1016/j.soilbio.2009.06.006>
- Su YY, Guo LD, Hyde KD (2010) Response of endophytic fungi of *Stipa grandis* to experimental plant function group removal in Inner Mongolia steppe, China. *Fungal Diversity* 43: 93–101. <https://doi.org/10.1007/s13225-010-0040-6>
- Sun X, Ding Q, Hyde KD, Guo LD (2012a) Community structure and preference of endophytic fungi of three woody plants in a mixed forest. *Fungal Ecology* 5: 624–632. <https://doi.org/10.1016/j.funeco.2012.04.001>
- Sun X, Guo LD, Hyde KD (2011) Community composition of endophytic fungi in *Acer truncatum* and their role in decomposition. *Fungal Diversity* 47: 85–95. <https://doi.org/10.1007/s13225-010-0086-5>
- Sun Y, Wang Q, Lu XD, Okane I, Kakishima M (2012b) Endophytic fungal community in stems and leaves of plants from desert areas in China. *Mycological Progress* 11: 781–790. <https://doi.org/10.1007/s11557-011-0790-x>
- Tedersoo L, Bahram M, Põlme S, et al. (2014) Global diversity and geography of soil fungi. *Science* 346: 1256688. <https://doi.org/10.1126/science.1256688>
- Toju H, Tanabe AS, Ishii HS (2016) Ericaceous plant-fungus network in a harsh alpine-subalpine environment. *Molecular Ecology* 25: 3242–3257. <https://doi.org/10.1111/mec.13680>
- U'Ren JM, Lutzoni F, Miadlikowska J, Laetsch AD, Arnold AE (2012) Host and geographic structure of endophytic and endolichenic fungi at a continental scale. *American Journal of Botany* 99: 898–914. <https://doi.org/10.3732/ajb.1100459>
- Waller F, Achatz B, Baltruschat H, Fodor J, Becker K, Fischer M, Heier T, Hückelhoven R, Neumann C, Wettstein D, Franken P, Kogel KH (2005) The endophytic fungus *Piriformospora indica* reprograms barley to salt-stress tolerance, disease resistance, and higher yield. *Proceedings of the National Academy of Sciences* 102: 13386–13391. <https://doi.org/10.1073/pnas.0504423102>
- Ward D (2009) *The Biology of Deserts*. Oxford University Press, Oxford.
- White T, Bruns T, Lee S, Taylor J (1990) Amplification and direct sequencing of fungal ribosomal RNA genes for phylogenetics. In: Innis MA, Gelfand DH, Sninsky JS, White TJ (Eds) *PCR Protocols: A Guide to Methods and Applications*. Academic, San Diego, 315–322. <https://doi.org/10.1016/B978-0-12-372180-8.50042-1>

- Xing XK, Chen J, Xu MJ, Lin WH, Guo SX (2011) Fungal endophytes associated with *Sonneratia* (Sonneratiaceae) mangrove plants on the south coast of China. *Forest Pathology* 41: 334–340. <https://doi.org/10.1111/j.1439-0329.2010.00683.x>
- Xing XK, Guo SX (2011) Fungal endophyte communities in four Rhizophoraceae mangrove species on the south coast of China. *Ecological research* 26: 403–409. <https://doi.org/10.1007/s11284-010-0795-y>
- Xu H, Li Y, Xu G, Zou T (2007) Ecophysiological response and morphological adjustment of two Central Asian desert shrubs towards variation in summer precipitation. *Plant, Cell & Environment* 30: 399–409. <https://doi.org/10.1111/j.1365-3040.2006.001626.x>
- Yao H, Sun X, He C, Pulak M, Li XC, Guo LD (2019) Phyllosphere epiphytic and endophytic fungal community and network structures differ in a tropical mangrove ecosystem. *Microbiome* 7: 57. <https://doi.org/10.1186/s40168-019-0671-0>
- Yuan ZL, Druzhinina IS, Labbe J, Redman R, Qin Y, Rodriguez R, Zhang CL, Tuskan GA, Lin FC (2016) Specialized microbiome of a halophyte and its role in helping non-host plants to withstand salinity. *Scientific Reports* 6: 32467. <https://doi.org/10.1038/srep32467>
- Zhao KF, Li FC, Zhang FS (2013a) *Halophyte species in China*. 2 edition. Science press, Beijing.
- Zhao S, Zhou N, Wang L, Tian CY (2013b) Halophyte-endophyte coupling: a promising bioremediation system for oil-contaminated soil in Northwest China. *Environmental Science & Technology* 47: 11938–11939. <https://doi.org/10.1021/es404219j>

Discovery of *Cytospora* species associated with canker disease of tree hosts from Mount Dongling of China

Haiyan Zhu^{1,2,3}, Meng Pan¹, Jadson D.P. Bezerra⁴, Chengming Tian¹, Xinlei Fan¹

1 The Key Laboratory for Silviculture and Conservation of Ministry of Education, Beijing Forestry University, Beijing 100083, China **2** State Key Laboratory of Mycology, Institute of Microbiology, Chinese Academy of Sciences, Beijing 100101, China **3** College of Life Sciences, University of Chinese Academy of Sciences, Beijing 100049, China **4** Setor de Micologia, Departamento de Biociências e Tecnologia, Instituto de Patologia Tropical e Saúde Pública (IPTSP), Universidade Federal de Goiás, Rua 235, s/n, Setor Universitário, CEP: 7460505, Goiânia, Goiás, Brazil

Corresponding author: Xinlei Fan (xinleifan@bjfu.edu.cn)

Academic editor: N. Wijayawardene | Received 31 October 2019 | Accepted 11 January 2020 | Published 3 February 2020

Citation: Zhu H, Pan M, Bezerra JDP, Tian C, Fan X (2020) Discovery of *Cytospora* species associated with canker disease of tree hosts from Mount Dongling of China. MycoKeys 62: 97–121. <https://doi.org/10.3897/mycokeys.62.47854>

Abstract

Members of *Cytospora* encompass important plant pathogens, saprobes and endophytes on a wide range of woody hosts with a worldwide distribution. In the current study, we obtained seven representative isolates from six tree hosts of Betulaceae, Juglandaceae, Rosaceae, Tiliaceae and Ulmaceae in Mount Dongling of China. Based on morphological comparison and phylogenetic analyses using partial ITS, LSU, *act*, *rpb2*, *tefl-a* and *tub2* gene sequences, we identified two known species (*Cytospora leucostoma* and *C. pruinopsis*) and two novel species (*C. coryli* and *C. spiraeicola*). These results represent the first study on *Cytospora* species associated with canker disease from Mount Dongling of China.

Keywords

Cytosporaceae, phylogeny, taxonomy, wood-inhabiting fungi

Introduction

The genus *Cytospora* was established by Ehrenberg (1818) and belongs to Cytosporaceae, Diaporthales, Sordariomycetes (Wijayawardene et al. 2018, Fan et al. 2020). It is characterised by single or labyrinthine of pycnidial locules, filamentous conidiophores (enteroblastic and phialidic conidiogenous cells) producing hyaline, allantoid conidia

in the asexual morph; diaporthean-like perithecia, clavate to elongate obovoid asci with four or eight hyaline, allantoid ascospores in the sexual morph (Spielman 1983, 1985, Adams et al. 2005). Species of *Cytospora* contain important pathogens that cause stem canker and dieback disease on more than 100 species of woody and coniferous plants, thereby causing severe commercial and ecological damage and significant losses worldwide (Sinclair et al. 1987, Adams et al. 2005, 2006, Fan et al. 2014a, b, 2015a, b, Lawrence et al. 2018, Pan et al. 2018, Zhu et al. 2018a, Zhang et al. 2019). Previous *Cytospora* species and their related sexual morphs viz. *Leucostoma*, *Valsa*, *Valsella* and *Valseutypella* were listed by old fungal literature without any living culture and sufficient evidence for their identification (Fries 1823, Saccardo 1884, Kobayashi 1970, Barr 1978, Sutton 1980, Gvritishvili 1982, Spielman 1983, 1985). Adams et al. (2005) revised the genus *Cytospora* from *Eucalyptus* with 28 species and accepted all sexual genera combined under *Valsa*, either as subgenera or species without additional infrageneric rank. Following the single-name for pleomorphic taxa, *Cytospora* (1818), the older asexual typified name was proposed as the recommended name against *Valsa* (1849), the younger sexual typified name (Fan et al. 2015a, b, Rossman et al. 2015).

Currently, 388 species epithets of *Cytospora* have been recorded in Index Fungorum (2020) (accessed 2 January 2020). However, Kirk et al. (2008) estimated approximately 110 species, but most of them lack herbarium materials, ex-type cultures and DNA sequence data.

Species identification criteria of *Cytospora* were previously carried out by the host-based method and morphology in China; however, these bases are unreliable due to the uninformative illustrations and descriptions, weak host specificity and overlapping morphological characteristics (Teng 1963, Tai 1979, Wei 1979). Recent studies have been able to use multiphase approaches to solve the taxonomy of *Cytospora* (Fan et al. 2014a, b, 2015a, b, Yang et al. 2015, Lawrence et al. 2016, Norphanphoun et al. 2017, Pan et al. 2018, Zhu et al. 2018a, Zhang et al. 2019). Fan et al. (2020) summarised 52 species of *Cytospora* associated with canker and dieback disease in China, using a six gene matrix (ITS, LSU, *act*, *rpb2*, *tef1-a* and *tub2*), of which 13 species were newly introduced.

Mount Dongling has high plant diversity in western Beijing, including more than 1,000 tree hosts (Ma et al. 1995). As more plant species were recorded in this region, the exploration of fungal diversity gradually increased as most fungi are often linked to particular host plants as pathogens or endophytes. Species of *Alternaria*, *Diaporthe*, *Leptostroma*, *Pestalotiopsis* and *Phoma* were the most commonly isolated endophytes from *Pinus tabulaeformis* and later, an additional 38 endophytic taxa were identified from *Acer truncatum* from Mount Dongling (Guo et al. 2008, Sun et al. 2011). Further, pathogens belonging in Botryosphaerales have been identified from Mount Dongling, including five species from *Aplosporella*, *Botryosphaeria* and *Phaeobotryon* (Zhu et al. 2018b). Zhu et al. (2019) subsequently introduced six species of diaporthean fungi residing in four families (viz. Diaportheaceae, Erythroglloeaceae, Juglanconidaceae and Melanconidaceae) from Mount Dongling. For the current understanding, many common host plants represent high fungal diversity causing canker and dieback disease in Mount Dongling. *Juglans mandshurica* and *J. regia* (Juglandaceae) were infected by *Botryosphaeria dothidea* (Botryosphaeriaceae), *Diaporthe eres*,

D. rostrata (Diaporthaceae) and *Juglanconis oblonga* (Juglanconidaceae). *Rhus typhina* (Anacardiaceae) was infected by *Aplosporella ginkgonis*, *A. javeedii* (Aplosporellaceae), *Phaeobotryon rhois* and *P. rhoinum* (Botryosphaeriaceae). *Quercus mongolica* (Fagaceae) was infected by *Dendrostoma donglinensis* (Erythrogloeaceae) (Zhu et al. 2018b, 2019).

During the course of cognitive practices to investigate forest pathogens that cause canker or dieback disease in Mount Dongling of China, seven *Cytospora* strains were obtained from six unrelated hosts, i.e. *Corylus mandshurica* (Betulaceae), *Juglans mandshurica* (Juglandaceae), *Prunus sibirica*, *Spiraea salicifolia* (Rosaceae), *Tilia nobilis* (Tiliaceae) and *Ulmus pumila* (Ulmaceae). Phylogenetic analyses inferred from combined ITS, LSU, *act*, *rpb2*, *tef1-a* and *tub2* gene regions were conducted to provide a multi-gene phylogeny for *Cytospora*, based on a large set of freshly collected specimens in Mount Dongling of China. Thus, the current study aims to clarify the systematics and taxonomy of *Cytospora* species with detailed descriptions and illustrations and compare it to known species in the genus.

Materials and methods

Sampling and isolation

Seven infected branches of six hosts were collected from Mount Dongling of China (Table 1). Sampled trees expressed general symptoms and signs of canker diseases including elongate, slightly sunken and discoloured areas in the bark, several prominent dark sporocarps immersed in bark, erumpent through the surface of bark when mature (Fig. 1). A total of seven isolates was established by removing a mucoid spore mass from conidiomata or ascomata of fresh material, spreading the suspension on the surface of 1.8 % potato dextrose agar (PDA) and incubating at 25 °C for up to 24 h. Single germinating spores were transferred on to fresh PDA plates. Specimens and isolates were deposited in the Key Laboratory for Silviculture and Conservation of the Ministry of Education in Beijing Forestry University (BJFU) and at the working Collection of X.L. Fan (CF), housed at the BJFU. Axenic cultures are maintained in the China Forestry Culture Collection Centre (CFCC).



Figure 1. Disease symptoms associated with *Cytospora* species. **A** *Corylus mandshurica* **B** *Spiraea salicifolia* **C** *Ulmus pumila* **D** *Prunus sibirica*.

Table 1. Isolates and GenBank accession numbers used in the phylogenetic analyses of *Cytospora*.

Species	Strain ¹	Host	Origin	GenBank accession numbers					
				ITS	LSU	act	rpb2	tef1-a	tub2
<i>Cytospora atlantibicola</i>	CFCC 89970 [†]	<i>Atlanthus altissima</i>	Ningxia, China	MH933618	MH933653	MH933526	MH933592	MH933494	MH933565
<i>Cytospora ampulliformis</i>	MFLUCC 16-0583 [†]	<i>Sorbus intermedia</i>	Russia	KY417726	KY417760	KY417692	KY417794	NA	NA
	MFLUCC 16-0629	<i>Acer platanoides</i>	Russia	KY417727	KY417761	KY417693	KY417795	NA	NA
<i>Cytospora amygdali</i>	CBS 144233 [†]	<i>Prunus dulcis</i>	California, USA	MG971853	NA	MG972002	NA	MG971659	MG971718
<i>Cytospora atrocirrhatta</i>	CFCC 89615	<i>Juglans regia</i>	Qinghai, China	KR045618	KR045700	KF498673	KU710946	KP310858	KR045659
	CFCC 89616	<i>Juglans regia</i>	Qinghai, China	KR045619	KR045701	KF498674	KU710947	KP310859	KR045660
<i>Cytospora beilinensis</i>	CFCC 50493 [†]	<i>Pinus armandii</i>	Beijing, China	MH933619	MH933654	MH933527	NA	MH9333495	MH933561
	CFCC 50494	<i>Pinus armandii</i>	Beijing, China	MH933620	MH933655	MH933528	NA	MH9333496	MH933562
<i>Cytospora berberidis</i>	CFCC 89927 [†]	<i>Berberis dasystachya</i>	Qinghai, China	KR045620	KR045702	KU710990	KU710948	KU710913	KR045661
	CFCC 89933	<i>Berberis dasystachya</i>	Qinghai, China	KR045621	KR045703	KU710991	KU710949	KU710914	KR045662
<i>Cytospora bungeana</i>	CFCC 50495 [†]	<i>Pinus bungeana</i>	Shanxi, China	MH933621	MH933656	MH933529	MH933593	MH933497	MH933563
	CFCC 50496	<i>Pinus bungeana</i>	Shanxi, China	MH933622	MH933657	MH933530	MH933594	MH933498	MH933564
<i>Cytospora californica</i>	CBS 144234 [†]	<i>Juglans pumila</i>	California, USA	MG971935	NA	MG972083	NA	MG971645	NA
<i>Cytospora carbonacea</i>	CFCC 89947	<i>Ulmus pumila</i>	Qinghai, China	KR045622	KP310812	KP310842	KU710950	KP310855	KP310825
<i>Cytospora carpobroti</i>	GMW 48981 [†]	<i>Carpobrotus edulis</i>	South Africa	MH382812	MH411216	NA	NA	MH411212	MH411207
<i>Cytospora celtidicola</i>	CFCC 50497 [†]	<i>Celtis sinensis</i>	Anhui, China	MH933623	MH933658	MH933531	MH933595	MH933499	MH933566
	CFCC 50498	<i>Celtis sinensis</i>	Anhui, China	MH933624	MH933659	MH933532	MH933596	MH933500	MH933567
<i>Cytospora centrinillosa</i>	MFLUCC 16-1206 [†]	<i>Sorbus domestica</i>	Italy	MF190122	MF190068	NA	MF377600	NA	NA
	MFLUCC 17-1660	<i>Sorbus domestica</i>	Italy	MF190123	MF190069	NA	MF377601	NA	NA
<i>Cytospora ceratosperma</i>	CFCC 89624	<i>Juglans regia</i>	Gansu, China	KR045645	KR045724	NA	KU710976	KP310860	KR045686
	CFCC 89625	<i>Juglans regia</i>	Gansu, China	KR045646	KR045725	NA	KU710977	KP31086	KR045687
<i>Cytospora ceratospERMopsis</i>	CFCC 89626 [†]	<i>Juglans regia</i>	Shaanxi, China	KR045647	KR045726	KU711011	KU710978	KU710934	KR045688
	CFCC 89627	<i>Juglans regia</i>	Shaanxi, China	KR045648	KR045727	KU711012	KU710979	KU710935	KR045689
<i>Cytospora chrysoSPERma</i>	CFCC 89629	<i>Salix psammophila</i>	Shaanxi, China	KF765673	KF765689	NA	KF765705	NA	NA
	CFCC 89981	<i>Populus alba</i> subsp. <i>pyramidalis</i>	Gansu, China	MH933625	MH933660	MH933533	MH933597	MH933501	MH933568
	CFCC 89982	<i>Ulmus pumila</i>	Tibet, China	KP281261	KP310805	KP310835	NA	KP310848	KP310818
<i>Cytospora coryli</i>	CFCC 53162[†]	<i>Corylus mandshurica</i>	Beijing, China	MN854450	MN854661	NA	MN850751	MN850758	MN861120
<i>Cytospora cotini</i>	MFLUCC 14-1050 [†]	<i>Cotinus coggygria</i>	Russia	KX430142	KX430143	NA	KX430144	NA	NA
<i>Cytospora curvata</i>	MFLUCC 15-0865 [†]	<i>Salix alba</i>	Russia	KY417728	KY417762	KY417694	KY417796	NA	NA

Species	Strain ¹	Host	Origin	GenBank accession numbers					
				ITS	LSU	act	rpb2	tef1- α	tub2
<i>Cytospora davidiana</i>	CXY 1350 [†]	<i>Populus davidiana</i>	Inner Mongolia, China	KM034870	NA	NA	NA	NA	NA
	CXY 1374	<i>Populus davidiana</i>	Heilongjiang, China	KM034869	NA	NA	NA	NA	NA
<i>Cytospora elaeagni</i>	CFCC 89632	<i>Elaeagnus angustifolia</i>	Ningxia, China	KR045626	KR045706	KU710995	KU710955	KU710918	KR045667
	CFCC 89633	<i>Elaeagnus angustifolia</i>	Ningxia, China	KF765677	KU710996	KU710996	KU710956	KU710919	KR045668
	CFCC 52882	<i>Elaeagnus angustifolia</i>	Xinjiang, China	MK732341	MK732338	MK732344	MK732347	NA	NA
	CFCC 52883	<i>Elaeagnus angustifolia</i>	Xinjiang, China	MK732342	MK732339	MK732345	MK732348	NA	NA
	CFCC 52884	<i>Elaeagnus angustifolia</i>	Xinjiang, China	MK732343	MK732340	MK732346	MK732349	NA	NA
<i>Cytospora erumpens</i>	CFCC 50022	<i>Prunus padus</i>	Shanxi, China	MH933627	MH933661	MH933534	NA	MH933502	MH933569
	MFLUCC 16-0580 [†]	<i>Salix × fragilis</i>	Russia	KY417733	KY417767	KY417699	KY417801	NA	NA
<i>Cytospora encalypti</i>	CBS 144241	<i>Encalyptus globulus</i>	California, USA	MG971907	NA	MG972056	NA	MG971617	MG971772
<i>Cytospora euonymicola</i>	CFCC 50499 [†]	<i>Euonymus kiautschovicus</i>	Shaanxi, China	MH933628	MH933662	MH933535	MH933598	MH933503	MH933570
	CFCC 50500	<i>Euonymus kiautschovicus</i>	Shaanxi, China	MH933629	MH933663	MH933536	MH933599	MH933504	MH933571
<i>Cytospora euonymina</i>	CFCC 89993 [†]	<i>Euonymus kiautschovicus</i>	Shanxi, China	MH933630	MH933664	MH933537	MH933600	MH933505	MH933590
	CFCC 89999	<i>Euonymus kiautschovicus</i>	Shanxi, China	MH933631	MH933665	MH933538	MH933601	MH933506	MH933591
	MFLUCC 14-0868 [†]	<i>Fraxinus ornus</i>	Italy	MF190133	MF190078	NA	NA	NA	NA
<i>Cytospora fraxinigena</i>	MFLU 17-0880	<i>Fraxinus ornus</i>	Italy	MF190134	MF190079	NA	NA	NA	NA
	CXY 1371	NA	NA	KM034852	NA	NA	NA	NA	KM034891
<i>Cytospora gigalocus</i>	CXY 1381	NA	NA	KM034853	NA	NA	NA	NA	KM034890
	CFCC 89620 [†]	<i>Juglans regia</i>	Qinghai, China	KR045628	KR045708	KU710997	KU710957	KU710920	KR045669
	CFCC 89621	<i>Juglans regia</i>	Qinghai, China	KR045629	KR045709	KU710998	KU710958	KU710921	KR045670
<i>Cytospora gigaspora</i>	CFCC 50014	<i>Juniperus procumbens</i>	Shanxi, China	KR045630	KR045710	KU710999	KU710959	KU710922	KR045671
	CFCC 89634 [†]	<i>Salix psammophila</i>	Shaanxi, China	KF765671	KF765687	KU711000	KU710960	KU710923	KR045672
<i>Cytospora granati</i>	CBS 144237 [†]	<i>Punica granatum</i>	California, USA	MG971799	NA	MG971949	NA	MG971514	MG971664
<i>Cytospora hippophaëis</i>	CFCC 89639	<i>Hippophaë rhamnoides</i>	Gansu, China	KR045632	KR045712	KU711001	KU710961	KU710924	KR045673
	CFCC 89640	<i>Hippophaë rhamnoides</i>	Gansu, China	KF765682	KF765698	KF765730	KU710962	KF310865	KR045674
<i>Cytospora japonica</i>	CFCC 89956	<i>Prunus cerasifera</i>	Ningxia, China	KR045624	KR045704	KU710993	KU710953	KU710916	KR045665
	CFCC 89960	<i>Prunus cerasifera</i>	Ningxia, China	KR045625	KR045705	KU710994	KU710954	KU710917	KR045666
<i>Cytospora joaquiniensis</i>	CBS 144235 [†]	<i>Populus deltoides</i>	California, USA	MG971895	NA	MG972044	NA	MG971605	MG971761
<i>Cytospora junipericola</i>	BBH 42444	<i>Juniperus communis</i>	Italy	MF190126	MF190071	NA	NA	MF377579	NA

Species	Strain ¹	Host	Origin	GenBank accession numbers						
				ITS	LSU	act	rpb2	tef1-a	tub2	
<i>Gyospora junipericola</i> <i>Gyospora juniperina</i>	MFLU 17-0882 ¹	<i>Juniperus communis</i>	Italy	MF190125	MF190072	NA	NA	MF377580	NA	
	CFCC 50501 ¹	<i>Juniperus przewalskii</i>	Sichuan, China	MH933632	MH933666	MH933539	MH933602	MH933507	NA	
	CFCC 50502	<i>Juniperus przewalskii</i>	Sichuan, China	MH933633	MH933667	MH933540	MH933603	MH933508	MH933572	
<i>Gyospora kantschavelii</i>	CFCC 50503	<i>Juniperus przewalskii</i>	Sichuan, China	MH933634	MH933668	MH933541	MH933604	MH933509	NA	
	CXY 1383	<i>Populus maximowiczii</i>	Jilin, China	KM034867	NA	NA	NA	NA	NA	
	CXY 1386	<i>Populus maximowiczii</i>	Chongqing, China	KM034867	NA	NA	NA	NA	NA	
	CFCC 89622	<i>Pyrus bretschneideri</i>	Gansu, China	KR045616	KR045698	KU710988	KU710944	KU710911	KR045657	
	CFCC 89894	<i>Pyrus bretschneideri</i>	Qinghai, China	KR045617	KR045699	KU710989	KU710945	KU710912	KR045658	
	CFCC 50015	<i>Sorbus aucuparia</i>	Ningxia, China	KR045634	KR045714	KU711002	NA	KU710925	KR045675	
<i>Cyospora leucostoma</i>	CFCC 50016	<i>Sorbus aucuparia</i>	Ningxia, China	MH820400	MH820393	MH820408	NA	MH820404	MH820389	
	CFCC 50017	<i>Prunus cerasifera</i>	Ningxia, China	MH933635	MH933669	MH933542	NA	MH933510	MH933573	
	CFCC 50018	<i>Prunus serrulata</i>	Gansu, China	MH933636	MH933670	MH933543	NA	MH933511	MH933574	
	CFCC 50019	<i>Rosa belenae</i>	Gansu, China	MH933637	MH933671	MH933544	NA	NA	NA	
	CFCC 50020	<i>Prunus persica</i>	Gansu, China	MH933638	MH933672	MH933545	NA	NA	NA	
	CFCC 50021	<i>Prunus salicina</i>	Gansu, China	MH933639	MH933673	MH933546	NA	MH933512	MH933575	
	CFCC 50023	<i>Cornus alba</i>	Shanxi, China	KR045635	KR045715	KU711003	KU710964	KU710926	KR045676	
	CFCC 50024	<i>Prunus pseudocerasus</i>	Qinghai, China	MH933640	MH933674	MH933547	MH933605	NA	MH933576	
	CFCC 50467	<i>Betula platyphylla</i>	Beijing, China	KT732948	KT732967	NA	NA	NA	NA	
	CFCC 50468	<i>Betula platyphylla</i>	Beijing, China	KT732949	KT732968	NA	NA	NA	NA	
	CFCC 53140	<i>Prunus sibirica</i>	Beijing, China	MN854445	MN854656	MN850760	MN850746	MN850753	MN861115	
	CFCC 53141	<i>Prunus sibirica</i>	Beijing, China	MN854446	MN854657	MN850761	MN850747	MN850754	MN861116	
CFCC 53156	<i>Juglans mandshurica</i>	Beijing, China	MN854447	MN854658	MN850762	MN850748	MN850755	MN861117		
MFLUCC 16-0574	<i>Rosa</i> sp.	Russia	KY417731	KY417764	KY417696	KY417798	NA	NA		
MFLUCC 16-0589	<i>Salix alba</i>	Russia	KY417732	KY417766	KY417698	KY417800	NA	NA		
MFLUCC 16-0628 ¹	<i>Salix x fragilis</i>	Russia	KY417734	KY417768	KY417700	KY417802	NA	NA		
CBS 144236 ¹	<i>Prunus domestica</i>	California, USA	MG971905	NA	MG972054	NA	MG971615	MG971764		
MFLUCC 17-0508 ¹	<i>Lumnitzera racemosa</i>	Taiiland	MG975778	MH253461	MH253457	MH253453	NA	NA		
CFCC 50028	<i>Malus pumila</i>	Gansu, China	MH933641	MH933675	MH933548	MH933606	MH933513	MH933577		
CFCC 50029	<i>Malus pumila</i>	Ningxia, China	MH933642	MH933676	MH933549	MH933607	MH933514	MH933578		
CFCC 50030	<i>Malus pumila</i>	Shaanxi, China	MH933643	MH933677	MH933550	MH933608	MH933524	MH933579		
CFCC 50031	<i>Crataegus</i> sp.	Shanxi, China	KR045636	KR045716	KU711004	KU710965	KU710927	KR045677		
CFCC 50044	<i>Malus baccata</i>	Qinghai, China	KR045637	KR045717	KU711005	KU710966	KU710928	KR045678		

Species	Strain ¹	Host	Origin	GenBank accession numbers						
				ITS	LSU	act	rpb2	tefl- <i>a</i>	tub2	
<i>Cytospora melnikii</i>	CFCC 89984	<i>Rhus typhina</i>	Xinjiang, China	MH933644	MH933678	MH933551	MH933609	MH933515	MH933580	
	MFLUCC 15-0851 [†]	<i>Maltus domestica</i>	Russia	KY417735	KY417769	KY417701	KY417803	NA	NA	
	MFLUCC 16-0635	<i>Populus nigra</i> var. <i>italica</i>	Russia	KY417736	KY417770	KY417702	KY417804	NA	NA	
<i>Cytospora nivea</i>	MFLUCC 15-0860	<i>Salix acutifolia</i>	Russia	KY417737	KY417771	KY417703	KY417805	NA	NA	
	CFCC 89641	<i>Elaeagnus angustifolia</i>	Ningxia, China	KF765683	KF765699	KU711006	KU710967	KU710929	KR045679	
	CFCC 89643	<i>Salix psammophila</i>	Shaanxi, China	KF765685	KF765701	NA	KU710968	KP310863	KP310829	
<i>Cytospora oleicola</i>	CBS 144248 [†]	<i>Olea europaea</i>	California, USA	MG971944	NA	MG972098	NA	MG971660	MG971752	
<i>Cytospora palm</i>	CXY 1276	<i>Cotinus coggygria</i>	Beijing, China	JN402990	NA	NA	NA	KJ781296	NA	
	CXY 1280 [†]	<i>Cotinus coggygria</i>	Beijing, China	JN411939	NA	NA	NA	KJ781297	NA	
<i>Cytospora parakanischaevii</i>	MFLUCC 15-0857 [†]	<i>Populus × sibirica</i>	Russia	KY417738	KY417772	KY417704	KY417806	NA	NA	
	MFLUCC 16-0575	<i>Pyrus pyrausta</i>	Russia	KY417739	KY417773	KY417705	KY417807	NA	NA	
<i>Cytospora parapsistaciae</i>	CBS 144506 [†]	<i>Pistacia vera</i>	California, USA	MG971804	NA	MG971954	NA	MG971519	MG971669	
<i>Cytospora parasitica</i>	MFLUCC 15-0507 [†]	<i>Maltus domestica</i>	Russia	KY417740	KY417774	KY417706	KY417808	NA	NA	
	XJAU 2542-1	<i>Maltus</i> sp.	Xinjiang, China	MH798884	MH798897	NA	NA	MH813452	NA	
<i>Cytospora paratranslucens</i>	MFLUCC 15-0506 [†]	<i>Populus alba</i> var. <i>bolleana</i>	Russia	KY417741	KY417775	KY417707	KY417809	NA	NA	
	MFLUCC 16-0627	<i>Populus alba</i>	Russia	KY417742	KY417776	KY417708	KY417810	NA	NA	
<i>Cytospora pistaciae</i>	CBS 144238 [†]	<i>Pistacia vera</i>	California, USA	MG971802	NA	MG971952	NA	MG971517	MG971667	
<i>Cytospora platanicola</i>	MFLU 17-0327 [†]	<i>Platanus hybrida</i>	Italy	MH253451	MH253452	MH253449	MH253450	NA	NA	
<i>Cytospora platyclada</i>	CFCC 50504 [†]	<i>Platycladus orientalis</i>	Yunnan, China	MH933645	MH933679	MH933552	MH933610	MH933516	MH933581	
	CFCC 50505	<i>Platycladus orientalis</i>	Yunnan, China	MH933646	MH933680	MH933553	MH933611	MH933517	MH933582	
	CFCC 50506	<i>Platycladus orientalis</i>	Yunnan, China	MH933647	MH933681	MH933554	MH933612	MH933518	MH933583	
<i>Cytospora platycladicola</i>	CFCC 50038 [†]	<i>Platycladus orientalis</i>	Gansu, China	KT222840	MH933682	MH933555	MH933613	MH933519	MH933584	
	CFCC 50039	<i>Platycladus orientalis</i>	Gansu, China	KR045642	KR045721	KU711008	KU710973	KU710931	KR045683	
<i>Cytospora plurivora</i>	CBS 144239 [†]	<i>Olea europaea</i>	California, USA	MG971861	NA	MG972010	NA	MG971572	MG971726	
<i>Cytospora populicola</i>	CBS 144240 [†]	<i>Populus deltoides</i>	California, USA	MG971891	NA	MG972040	NA	MG971601	MG971757	
<i>Cytospora populina</i>	CFCC 89644 [†]	<i>Salix psammophila</i>	Shaanxi, China	KF765686	KF765702	KU711007	KU710969	KU710930	KR045681	
<i>Cytospora populinopsis</i>	CFCC 50032 [†]	<i>Sorbus aucuparia</i>	Ningxia, China	MH933648	MH933683	MH933556	MH933614	MH933520	MH933585	
	CFCC 50033	<i>Sorbus aucuparia</i>	Ningxia, China	MH933649	MH933684	MH933557	MH933615	MH933521	MH933586	
	CFCC 50034 [†]	<i>Ulmus pumila</i>	Shaanxi, China	KP281259	KP310806	KP310836	KU710970	KP310849	KP310819	
<i>Cytospora pruinoopsis</i>	CFCC 50035	<i>Ulmus pumila</i>	Jilin, China	KP281260	KP310807	KP310837	KU710971	KP310850	KP310820	
	CFCC 53153	<i>Ulmus pumila</i>	Beijing, China	MN854451	MN854662	MN850763	MN850752	MN850759	MN861121	
<i>Cytospora predappioensis</i>	MFLUCC 17-2458 [†]	<i>Platanus hybrida</i>	Italy	MG873484	MG873480	NA	NA	NA	NA	

Species	Strain ¹	Host	Origin	GenBank accession numbers						
				ITS	LSU	act	rpb2	tef1-a	tub2	
<i>Cytospora pruinosa</i>	CFCC 50036	<i>Syringa oblata</i>	Qinghai, China	KP310800	KP310802	KP310832	NA	KP310845	KP310815	
	CFCC 50037	<i>Syringa oblata</i>	Qinghai, China	MH933650	MH933685	MH933558	NA	MH933522	MH933589	
<i>Cytospora prunicola</i>	MFLU 17-0995 ^T	<i>Prunus</i> sp.	Italy	MG742350	MG742351	MG742353	MG742352	NA	NA	
<i>Cytospora punicea</i>	CBS 144244	<i>Punica granatum</i>	California, USA	MG971943	NA	MG972091	NA	MG971654	MG971798	
<i>Cytospora quercicola</i>	MFLU 17-0881	<i>Quercus</i> sp.	Italy	MF190128	MF190074	NA	NA	NA	NA	
<i>Cytospora ribis</i>	MFLUCC 14-0867 ^T	<i>Quercus</i> sp.	Italy	MF190129	MF190073	NA	NA	NA	NA	
<i>Cytospora rosae</i>	CFCC 50026	<i>Ulmus pumila</i>	Qinghai, China	KP281267	KP310813	KP310843	KU710972	KP310856	KP310826	
	CFCC 50027	<i>Ulmus pumila</i>	Qinghai, China	KP281268	KP310814	KP310844	NA	KP310857	KP310827	
<i>Cytospora rosae</i>	MFLU 17-0885	<i>Rosa canina</i>	Italy	MF190131	MF190076	NA	NA	NA	NA	
<i>Cytospora rostrata</i>	CFCC 89909 ^T	<i>Salix capularis</i>	Gansu, China	KR045643	KR045722	KU711009	KU710974	KU710932	KR045684	
	CFCC 89910	<i>Salix capularis</i>	Gansu, China	KR045644	KR045723	KU711010	KU710975	KU710933	NA	
<i>Cytospora rusanovii</i>	MFLUCC 15-0853	<i>Populus × sibirica</i>	Russia	KY417743	KY417777	KY417709	KY417811	NA	NA	
	MFLUCC 15-0854 ^T	<i>Salix babylonica</i>	Russia	KY417744	KY417778	KY417710	KY417812	NA	NA	
<i>Cytospora salicacearum</i>	MFLUCC 15-0861	<i>Salix × fragilis</i>	Russia	KY417745	KY417779	KY417711	KY417813	NA	NA	
	MFLUCC 15-0509 ^T	<i>Salix alba</i>	Russia	KY417746	KY417780	KY417712	KY417814	NA	NA	
	MFLUCC 16-0576	<i>Populus nigra</i> var. <i>italica</i>	Russia	KY417741	KY417775	KY417707	KY417809	NA	NA	
<i>Cytospora salicicola</i>	MFLUCC 16-0587	<i>Prunus cerasus</i>	Russia	KY417742	KY417776	KY417708	KY417810	NA	NA	
	MFLUCC 15-0866	<i>Salix alba</i>	Russia	KY417749	KY417783	KY417715	KY417817	NA	NA	
<i>Cytospora salicina</i>	MFLUCC 14-1052 ^T	<i>Salix alba</i>	Russia	KU982636	KU982635	KU982637	NA	NA	NA	
	MFLUCC 15-0862 ^T	<i>Salix alba</i>	Russia	KY417750	KY417784	KY417716	KY417818	NA	NA	
<i>Cytospora schulzeri</i>	MFLUCC 16-0637	<i>Salix × fragilis</i>	Russia	KY417751	KY417785	KY417717	KY417819	NA	NA	
	CFCC 50040	<i>Malus domestica</i>	Ningxia, China	KR045649	KR045728	KU711013	KU710980	KU710936	KR045690	
<i>Cytospora sibiricae</i>	CFCC 50042	<i>Malus asiatica</i>	Qinghai, China	KR045650	KR045729	KU711014	KU710981	KU710937	KR045691	
	CFCC 50045 ^T	<i>Sibiraea angustata</i>	Gansu, China	KR045651	KR045730	KU711015	KU710982	KU710938	KR045692	
<i>Cytospora sophorae</i>	CFCC 50046	<i>Sibiraea angustata</i>	Gansu, China	KR045652	KR045731	KU711015	KU710983	KU710939	KR045693	
	CFCC 50047	<i>Symphobolium japonicum</i>	Shanxi, China	KR045653	KR045732	KU711017	KU710984	KU710940	KR045694	
	CFCC 50048	<i>Magnolia grandiflora</i>	Shanxi, China	MH820401	MH820394	MH820409	MH820397	MH820405	MH820390	
	CFCC 89598	<i>Symphobolium japonicum</i>	Gansu, China	KR045654	KR045733	KU711018	KU710985	KU710941	KR045695	

Species	Strain ¹	Host	Origin	GenBank accession numbers					
				ITS	LSU	act	rpb2	tef1-a	tub2
<i>Cytospora sphaerocola</i>	CFCC 89595 ^T	<i>Syphnolobium japonicum</i> var. <i>pendula</i>	Gansu, China	KR045655	KR045734	KU711019	KU710986	KU710942	KR045696
	CFCC 89596	<i>Syphnolobium japonicum</i> var. <i>pendula</i>	Gansu, China	KR045656	KR045735	KU711020	KU710987	KU710943	KR045697
<i>Cytospora sphaerotiopsis</i>	CFCC 89600 ^T	<i>Syphnolobium japonicum</i>	Gansu, China	KR045623	KP310804	KU710992	KU710951	KU710915	KP310817
<i>Cytospora sorbi</i>	MFLUCC 16-0631 ^T	<i>Sorbus aucuparia</i>	Russia	KY417752	KY417786	KY417718	KY417820	NA	NA
<i>Cytospora sorbicola</i>	MFLUCC 16-0584 ^T	<i>Acer pseudoplatanus</i>	Russia	KY417755	KY417789	KY417721	KY417823	NA	NA
	MFLUCC 16-0633	<i>Cotoneaster melanocarpus</i>	Russia	KY417758	KY417792	KY417724	KY417826	NA	NA
<i>Cytospora spiratae</i>	CFCC 50049 ^T	<i>Spiraea salicifolia</i>	Gansu, China	MG707859	MG707643	MG708196	MG708199	NA	NA
	CFCC 50050	<i>Spiraea salicifolia</i>	Gansu, China	MG707860	MG707644	MG708197	MG708200	NA	NA
<i>Cytospora spiraeicola</i>	CFCC 53138 ^T	<i>Spiraea salicifolia</i>	Beijing, China	MN854448	MN854659	NA	MN850749	MN850756	MN861118
	CFCC 53139	<i>Tilia nobilis</i>	Beijing, China	MN854449	MN854660	NA	MN850750	MN850757	MN861119
<i>Cytospora tamaricicola</i>	CFCC 50507	<i>Rosa multiflora</i>	Yunnan, China	MH933651	MH933686	MH933559	MH933616	MH933525	MH933587
<i>Cytospora tanaitica</i>	CFCC 50508 ^T	<i>Tamarix chinensis</i>	Yunnan, China	MH933652	MH933687	MH933560	MH933617	NA	NA
	MFLUCC 14-1057 ^T	<i>Beula pubescens</i>	Russia	KT459411	KT459412	KT459413	NA	NA	NA
<i>Cytospora thailandica</i>	MFLUCC 17-0262 ^T	<i>Xylocarpus moluccensis</i>	Thailand	MG975776	MH253463	MH253459	MH253455	NA	NA
	MFLUCC 17-0263 ^T	<i>Xylocarpus moluccensis</i>	Thailand	MG975777	MH253464	MH253460	MH253456	NA	NA
<i>Cytospora tibouchinae</i>	CPC 26333 ^T	<i>Tibouchina semidecandra</i>	France	KX228284	KX228335	NA	NA	NA	NA
<i>Cytospora translucens</i>	CXY 1351	<i>Populus davidiana</i>	Inner Mongolia, China	KM034874	NA	NA	NA	NA	KM034895
<i>Cytospora ulmi</i>	MFLUCC 15-0863 ^T	<i>Ulmus minor</i>	Russia	KY417759	NA	NA	NA	NA	NA
<i>Cytospora vinacea</i>	CBS 141585 ^T	<i>Vitis interspecific hybrid</i> 'Vidal'	USA	KX256256	NA	NA	NA	KX256277	KX256255
<i>Cytospora viticola</i>	CBS 141586 ^T	<i>Vitis vinifera</i> 'Cabernet Franc'	USA	KX256239	NA	NA	NA	KX256260	KX256218
<i>Cytospora xylocarpi</i>	MFLUCC 17-0251 ^T	<i>Xylocarpus granatum</i>	Thailand	MG975775	MH253462	MH253458	MH253454	NA	NA
<i>Diaporthe uaccinii</i>	CBS 160.32	<i>Vaccinium macrocarpon</i>	USA	KC343228	NA	JQ807297	NA	KC343954	KC344196

Abbreviations: **BBH**: Biotec Bangkok Herbarium, National Science and Technology Development Agency, Thailand; **CBS**: Westerdijk Fungal Biodiversity Institute (CBS-KNAW Fungal Biodiversity Centre), Utrecht, The Netherlands; **CFCC**: China Forestry Culture Collection Centre, Beijing, China; **CMW**: Culture collection of Michael Wingfield, university of Pretoria, South Africa; **CPC**: Culture collection of Pedro Crous, The Netherlands; **MFLU**: Mae Fah Luang University herbarium, Thailand; **MFLUCC**: Mae Fah Luang University Culture Collection, Thailand; **XJAU**: Xinjiang Agricultural University, Xinjiang, China; **NA**: not applicable. All the new isolates used in this study are indicated in bold type and the strains from generic type species are marked by a superscript (T).

Morphological analysis

Species identification was based on morphological features of the ascomata or conidiomata from infected host materials and micromorphology, supplemented by cultural characteristics. Microscopic photographs (structure and size of stromata; structure and size of ectostromatic disc and ostioles) were captured using a Leica stereomicroscope (M205 FA) (Leica Microsystems, Wetzlar, Germany). Microscopic observations (shape and size of conidiophores, asci and conidia/ascospores) were determined under a Nikon Eclipse 80i microscope (Nikon Corporation, Tokyo, Japan), equipped with a Nikon digital sight DS-Ri2 high definition colour camera, using differential interference contrast (DIC) illumination. The Nikon software NIS-Elements D Package v. 3.00, Adobe Bridge CS v. 6 and Adobe Photoshop CS v. 5 were used for the manual editing. More than 10 conidiomata/ascomata, 10 asci and 30 conidia/ascospores were measured by Nikon software NIS-Elements D Package v. 3.00 to calculate the mean size/length and respective standard deviations (SD). Colony diameters were measured and the colony features were described using the colour charts of Rayner (1970).

DNA extraction, PCR amplification and sequencing

Fungal mycelium grown on the cellophane of PDA was scraped for the extraction of genomic DNA following a modified CTAB method (Doyle and Doyle 1990). The primers and PCR conditions are listed in Table 2. DNA sequencing was performed using an ABI PRISM 3730XL DNA Analyser with a BigDye Terminator Kit v.3.1 (Invitrogen, USA) at the Shanghai Invitrogen Biological Technology Company Limited (Beijing, China). The DNA sequences, obtained from forward and reverse primers, were combined using SeqMan v. 7.1.0 in the DNASTAR Lasergene Core Suite software (DNASTAR Inc., Madison, WI, USA).

Phylogenetic analyses

The current isolates were initially identified as *Cytospora* species, based on both morphological observations and BLAST results. To clarify their further phylogenetic position, an analysis, based on the combined six genes (ITS, LSU, *act*, *rpb2*, *tef1-a* and *tub2*), was performed to compare *Cytospora* species from the current study with other strains in GenBank. *Diaporthe vaccinii* was selected as the outgroup in all analyses. Subsequent alignments for each gene were generated using MAFFT v.7 (Katoh and Standley 2013) and manually adjusted using MEGA v. 6 (Tamura et al. 2013). Ambiguously aligned sequences were excluded from analysis. Reference sequences were selected, based on ex-type or ex-epitype sequences available from recently published literature (Fan et al. 2014a, b, 2015a, b, 2020, Yang et al. 2015, Lawrence et al. 2016, Norphanhoun et al. 2017, Zhu et al. 2018a, Zhang et al. 2019, Fan et

Table 2. Genes used in this study with PCR primers, primer DNA sequence, optimal annealing temperature and corresponding references.

Locus	Definition	Primers	Primer DNA sequence (5'-3')	Optimal annealing temp (°C)	References of primers used
ITS	internal transcribed spacer of ribosomal RNA	ITS1	TCCGTAGGTGAACCTGCGG	51	White et al. 1990
		ITS4	TCCTCCGCTTTTGATATGC		
LSU	large subunit of ribosomal RNA	LROR	ACCCGCTGAACTTAAGC	55	Vilgalys and Hester 1990
		LR7	TACTACCACCAAGATCT		
<i>act</i>	actin	ACT-512F	ATGTGCAAGGCCGGTTTCGC	61	Carbone and Kohn 1999
		ACT-783R	TACGAGTCCTTCTGGCCCAT		
<i>rpb2</i>	RNA polymerase II second largest subunit	RPB2-5F	GA(T/C)GA(T/C)(A/C)G(A/T) GATCA(T/C)TT(T/C)GG	52	Liu et al. 1999
		RPB2-7cR	CCCAT(A/G)GCTTG(T/C)TT(A/G) CCCAT		
<i>tef1a</i>	translation elongation factor 1-alpha	EF1-668F	CGGTCACCTGATCTACAAGTGC	55	Alves et al. 2008
		EF1-1251R	CCTCGAACTCACCAGTACCG		
<i>tub2</i>	beta-tubulin	Bt2a	GGTAACCAAAATCGGTGCTGCTTTG	55	Glass and Donaldson 1995
		Bt2b	ACCCTCAGTGTAGTGACCCTTGCC		

al. 2020) (Table 1). Phylogenetic analyses were performed with PAUP v.4.0b10 for the maximum parsimony (MP) method (Swofford 2003), MrBayes v.3.1.2 for the Bayesian Inference (BI) method (Ronquist and Huelsenbeck 2003) and RAxML for the maximum likelihood (ML) method (Stamatakis 2006).

A partition homogeneity test (PHT) with heuristic search and 1,000 replicates was performed using PAUP v.4.0b10 to test the discrepancy amongst the ITS, LSU, *act*, *rpb2*, *tef1-a* and *tub2* sequence datasets in reconstructing phylogenetic trees. MP analysis was performed using a heuristic search option of 1,000 random-addition sequences with a tree bisection and reconnection (TBR) branch swapping algorithm (Swofford 2003). The branches of zero length were collapsed and all equally parsimonious trees were saved. Clade stability was assessed with a bootstrap analysis of 1,000 replicates (Hillis and Bull 1993). Other parsimony scores, such as tree length (TL), consistency index (CI), retention index (RI) and rescaled consistency (RC), were calculated (Swofford 2003). ML analysis was performed with the GTR + G + I model of site substitution following recent studies (Zhu et al. 2018a), including estimation of gamma-distributed rate heterogeneity and a proportion of invariant sites using PhyML v. 3.0 (Guindon et al. 2010). The branch support was evaluated with a bootstrapping method of 1,000 replicates (Hillis and Bull 1993). BI analysis was performed using a Markov Chain Monte Carlo (MCMC) algorithm with Bayesian posterior probabilities (Rannala and Yang 1996). A nucleotide substitution model was estimated by MrModeltest v.2.3 (Posada and Crandall 1998) and a weighted Bayesian analysis was considered. Two MCMC chains were run from random trees for 1,000,000 generations and trees were sampled each 100 generations. The first 25% of trees were discarded as the burn-in phase of each analysis and the posterior probabilities (BPP) were calculated

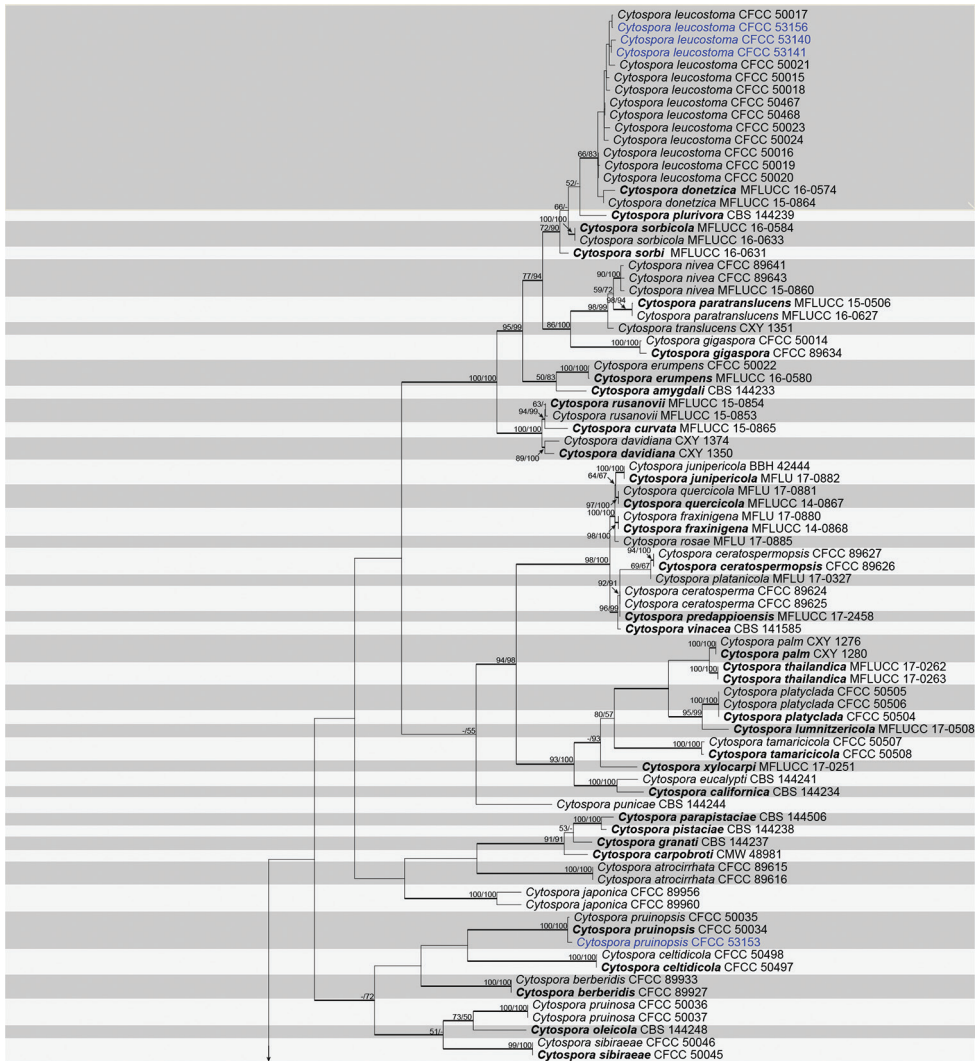


Figure 2. Phylogram of *Cytospora*, based on combined ITS, LSU, *act*, *rpb2*, *tef1-a* and *tub2* genes. The MP and ML bootstrap support values above 50% are shown at the first and second positions, respectively. Thickened branches represent posterior probabilities above 0.95 from the BI. Ex-type strains are in bold. Strains from the current study are in blue.

to assess the remaining trees (Rannala and Yang 1996). The branch support from MP and ML analysis was evaluated with a bootstrapping (BS) method of 1,000 replicates (Hillis and Bull 1993). Phylograms were plotted in Figtree v. 1.4.4 (<http://tree.bio.ed.ac.uk/software/figtree>) and edited in Adobe Illustrator CS6 v.16.0.0 (<https://www.adobe.com/cn/products/illustrator.html>). Novel sequences, generated in the current study, were deposited in GenBank (Table 1) and the aligned matrices, used for phylogenetic analyses, were submitted in TreeBASE (www.treebase.org; study ID S25564).

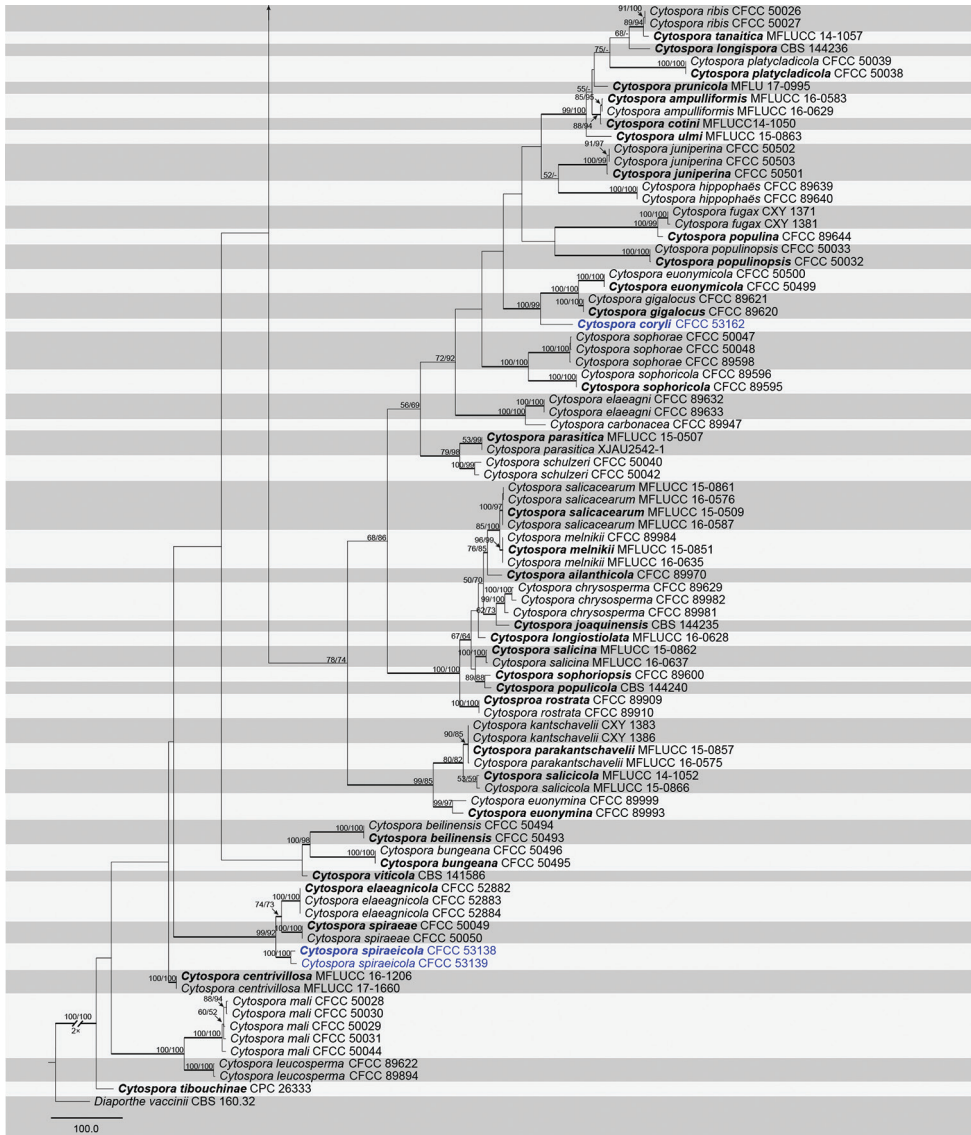


Figure 2. Continued.

Results

Phylogenetic analyses

A combined matrix of six gene sequences of *Cytospora* was considered. The combined alignments matrix (ITS, LSU, *act*, *rpb2*, *tef1-a* and *tub2*) included 172 accessions (seven from this study and 165 retrieved from GenBank) and counted 3,652 characters including gaps (665 characters for ITS, 525 for LSU, 337 for *act*, 730 for *rpb2*, 771 for *tef1-a*

and 624 for *tub2*), of which 2,067 characters were constant, 189 variable characters were parsimony-uninformative and 1,396 (38.22%) characters were variable and parsimony-informative. The MP analysis generated 100 parsimonious trees, the first tree of which is presented in Fig. 2 (TL = 8,029, CI = 0.345, RI = 0.804, RC = 0.278). Tree topologies of ML and BI analyses were similar to the MP tree. Based on the multi-locus phylogeny and morphology, seven strains were assigned to four species within *Cytospora coryli*, *C. leucostoma*, *C. pruinopsis* and *C. spiraeicola*, including two taxa which we describe here as new. The two isolates of *C. spiraeicola* formed a distinct and strongly supported clade (MP/ML/BI = 100/100/1) with close phylogenetic affinity to *C. elaeagnicola* and *C. spiraeae*. The strain of *C. coryli* from *Corylus mandshurica* shared a close relationship to *Cytospora euonymicola* and *C. gigalocus* with 100% MP, 99% ML, 0.99 BI supports.

Taxonomy

Cytospora coryli H.Y. Zhu & X.L. Fan, sp. nov.

MycoBank No: 833820

Fig. 3

Etymology. Named after the host genus on which it was collected, *Corylus*.

Holotype. CHINA, Beijing City, Mentougou District, Mount Dongling, Xiaolongmen Forestry Centre (115°27'07.00"E, 39°59'26.47"N), from branches of *Corylus mandshurica*, 17 Aug 2017, H.Y. Zhu & X.L. Fan, holotype CF 2019813, ex-type living culture CFCC 53162.

Description. *Necrotrophic* on branches of *Corylus mandshurica*. **Sexual morph:** not observed. **Asexual morph:** *Conidiomata* pycnidial, flat, immersed in the bark, scattered to gregarious, erumpent through the surface of bark, surrounded by conspicuous black stroma walls in the margin, with multiple locules. *Conceptacle* absent. *Ectostromatic disc* grey to black, discoid, circular to ovoid, 270–340 µm in diam., with one ostiole per disc. *Ostiole* grey to black, at the same or above level as the disc surface, inconspicuous. *Locules* numerous, subdivided frequently by invaginations with common walls, circular to irregular, 1550–1710 µm in diam. *Conidiophores* hyaline, branched at the base, in the middle, approximately cylindrical with the top end acute, 15.5–18.5 × 1–2 (av. = 17 ± 1.2 × 1.1 ± 0.2, n = 10) µm, sometimes reduced to conidiogenous cells. *Conidiogenous cells* enteroblastic, phialidic, sub-cylindrical to cylindrical, 7.5–14 × 1–2 (av. = 9.3 ± 1.7 × 1.4 ± 0.2, n = 10) µm. *Conidia* hyaline, allantoid, smooth, aseptate, thin-walled, 5–7 × 1–2 (av. = 5.6 ± 0.5 × 1.4 ± 0.2, n = 30) µm.

Culture characteristics. *Cultures* are initially white with hazel at the centre, growing fast up 9 cm in diam. after 3 days, becoming honey to hazel from the edge to centre after 7–10 days. In reverse, the cultures are the same as the upper colour after 3 days, becoming cinnamon from the edge to centre after 7–10 days. *Colonies* are flat, sparse at the centre and compact to the margin. *Pycnidia* distributed radially on colony surface.

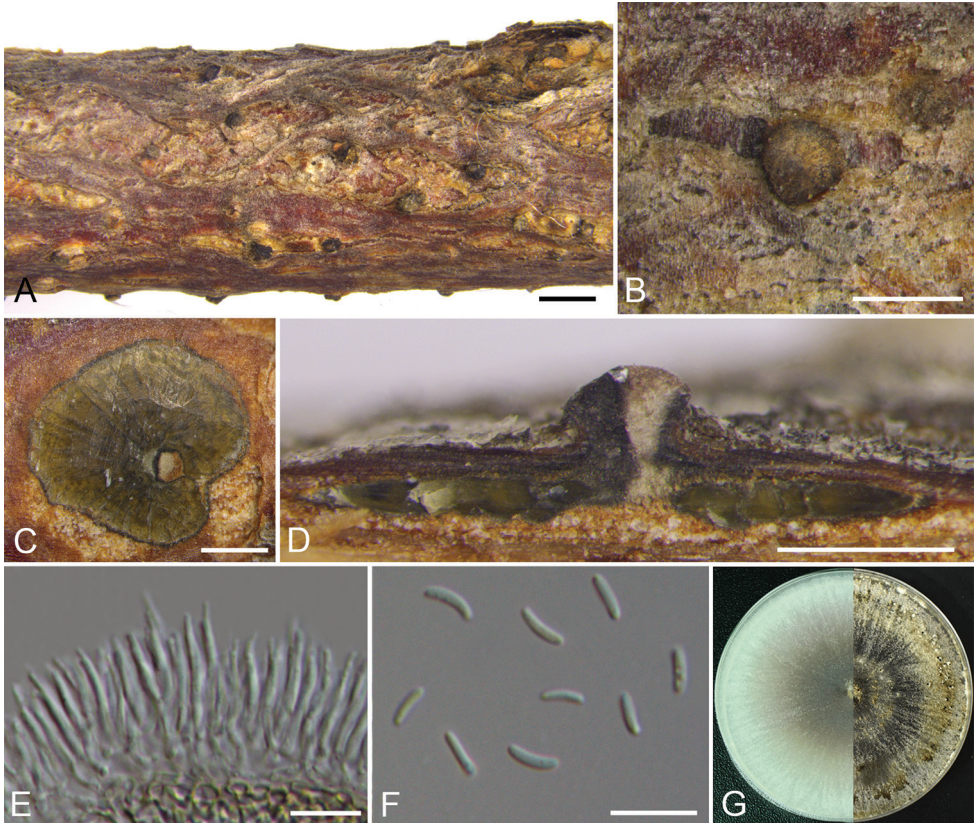


Figure 3. *Cytospora coryli* from *Corylus mandshurica* (CF 2019813). **A, B** habit of conidiomata on twig **C** transverse section of conidioma **D** longitudinal section through conidioma **E** conidiophores and conidiogenous cells **F** conidia **G** colonies on PDA at 3 days (left) and 30 days (right). Scale bars: 1 mm (**A**); 500 μm (**B–D**); 10 μm (**E, F**).

Habitat and distribution. Known from *Corylus mandshurica* in Mount Dongling, China.

Notes. *Cytospora coryli* is associated with canker disease of *Corylus mandshurica* in China. The only strain CFCC 53162 representing *Cytospora coryli* clusters as a single lineage and appears mostly related to *C. euonymicola* from *Euonymus kiautschovicus* and to *Cytospora gigalocus* from *Juglans regia* (Fan et al. 2015a, 2020) (Fig. 2). *Cytospora coryli* differs from *C. euonymicola* by its larger locules (1550–1710 vs. 1150–1400 μm) and larger conidia ($5\text{--}7 \times 1\text{--}2$ vs. $4.5\text{--}5 \times 1$ μm) (Fan et al. 2020), *C. coryli* differs from *C. gigalocus* by its smaller locules (1550–1710 vs. 1630–2180 μm) with single ostiole (one to five ostioles in *C. gigalocus*) and the larger size of conidia ($5\text{--}7 \times 1\text{--}2$ vs. $4.6\text{--}5.6 \times 0.8\text{--}1.3$ μm) (Fan et al. 2015a). Based on morphology and sequence data, we describe it as a new species.

***Cytospora leucostoma* (Pers.) Sacc., *Michelia* 2: 264 (1881)**

Figs 4, 5

Sphaeria leucostoma Pers., Ann. Bot. 11: 23 (1794)*Valsa leucostoma* (Pers.) Fr., Summa Veg. Scand., Section Post. (Stockholm): 411 (1849)*Valsa persoonii* Nitschke, Pyrenomyc. Germ. 2: 222 (1870)*Leucostoma persoonii* (Nitschke) Höhn., Mitt. Bot. Inst. Tech. Hochsch. Wien 5: 78 (1928)

[Additional synonyms in Species Fungorum.]

Description. *Necrotrophic* on branches of Betulaceae, Juglandaceae and Rosaceae. **Sexual morph:** *Ascostromata* immersed in the bark, erumpent through the surface of bark, scattered, 950–2550 µm in diam., with 8–10 perithecia arranged circularly to irregularly. *Conceptacle* absent. *Ectostromatic disc* pale grey, fusoid, 600–2150 µm in diam., with 8–10 ostioles arranged irregularly per disc. *Ostioles* numerous, dark grey to black, at the same or above the level as the disc, concentrated, arranged irregularly in a disc, 60–120 µm in diam. *Perithecia* beige with a little black when mature, flask-shaped to spherical, arranged circularly to irregularly, 270–560 µm in diam. *Paraphyses* large, broad and cylindrical with 1–4 septa, 39–78 × 5.8–8.7 (av. = 50.6 ± 13.7 × 7 ± 0.8, n = 10) µm. *Asci* free, clavate to elongate obovoid, 35–45 × 6–8 (av. = 40.4 ± 3.3 × 6.9 ± 0.5, n = 10) µm, 8-spored. *Ascospores* uniseriate to biseriate, elongate-allantoid, thin-walled, hyaline, aseptate, 7–10 × 2–3 (av. = 8.3 ± 0.9 × 2.6 ± 0.2, n = 30) µm. **Asexual morph:** *Conidiomata* pycnidial, immersed in the bark, scattered, erumpent through the surface of bark, with multiple locules and a conspicuous central column. *Central column* beneath the disc more or less conical, brown. *Conceptacle* absent. *Ectostromatic disc* buff, discoid, circular to ovoid, 190–310 µm in diam., with 1–2 ostioles per disc. *Ostioles* grey to black, at the same or above the level as the disc surface, 60–65 µm in diam. *Locules* numerous, subdivided frequently by invaginations with common walls, circular to ovoid, 700–1000 µm in diam. *Conidiophores* hyaline, branched at the base or unbranched, approximately cylindrical, 8–14 × 1–2 (av. = 11.5 ± 1.8 × 1.4 ± 0.2, n = 10) µm, sometimes reduced to conidiogenous cells. *Conidiogenous cells* enteroblastic phialidic, sub-cylindrical to cylindrical, 7–11 × 1–2 (av. = 9 ± 1.4 × 1.5 ± 0.3, n = 10) µm. *Conidia* hyaline, elongate-allantoid, smooth, aseptate, 4.5–6 × 1–2 (av. = 5.4 ± 0.3 × 1.5 ± 0.2, n = 30) µm.

Culture characteristics. *Cultures* initially are white, growing fast up to 8 cm in diam. after 3 days and entirely covering the 9 cm Petri dish after 4 days, becoming greenish-olivaceous after 7–10 days and grey olivaceous after 30 days. In reverse, the cultures are the same as the upper colour after 7 days, becoming olivaceous grey to iron grey after 30 days. *Colonies* are flat with a uniform texture; sterile.

Habitat and distribution. Known from several species of Betulaceae, Juglandaceae and Rosaceae around the world.

Materials examined. CHINA, Beijing City, Mentougou District, Mount Dongling, Xiaolongmen Forestry Centre (115°26'47.36"E, 39°56'06.45"N), from branches of *Prunus sibirica*, 17 Aug 2017, H.Y. Zhu & X.L. Fan, CF 2019814, living culture CFCC

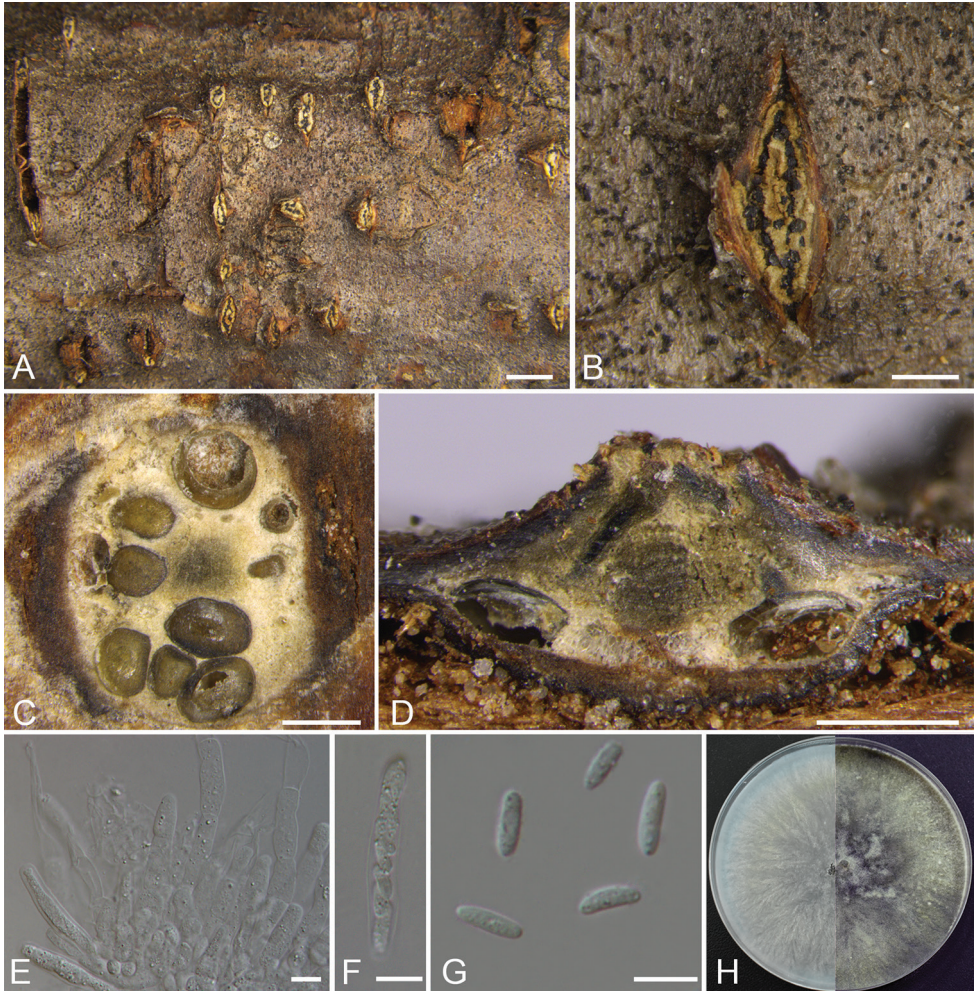


Figure 4. *Cytospora leucostoma* (Sexual morph) from *Prunus sibirica* (CF 2019814). **A, B** habit of ascomata on twig **C** transverse section of ascoma **D** longitudinal section through ascoma **E** asci and ascospores **F** ascus **G** ascospores **H** colonies on PDA at 3 days (left) and 30 days (right). Scale bars: 1 mm (**A**); 500 μm (**B–D**); 10 μm (**E–G**).

53140; *ibid.* CF 2019815, living culture CFCC 53141. CHINA, Beijing City, Mentougou District, Mount Dongling, Xiaolongmen Forestry Centre (115°29'20.52"E, 39°57'47.49"N), from branches of *Juglans mandshurica*, 17 Aug 2017, H.Y. Zhu & X.L. Fan, CF 2019809, living culture CFCC 53156.

Notes. *Cytospora leucostoma* is commonly associated with canker disease of Prunoideae of Rosaceae in China (Fan et al. 2020). Morphologically, our taxa are similar to previous descriptions of *C. leucostoma* in having multi-loculate pycnidial stromata with a conspicuous black conceptacle, producing elongate-allantoid, large conidia (4.5–6 \times 1–2 μm) (Teng 1963, Zhuang 2005, Fan et al. 2020). The greenish-yellow of the cultures on PDA medium from *Juglans mandshurica* is similar to descriptions of those

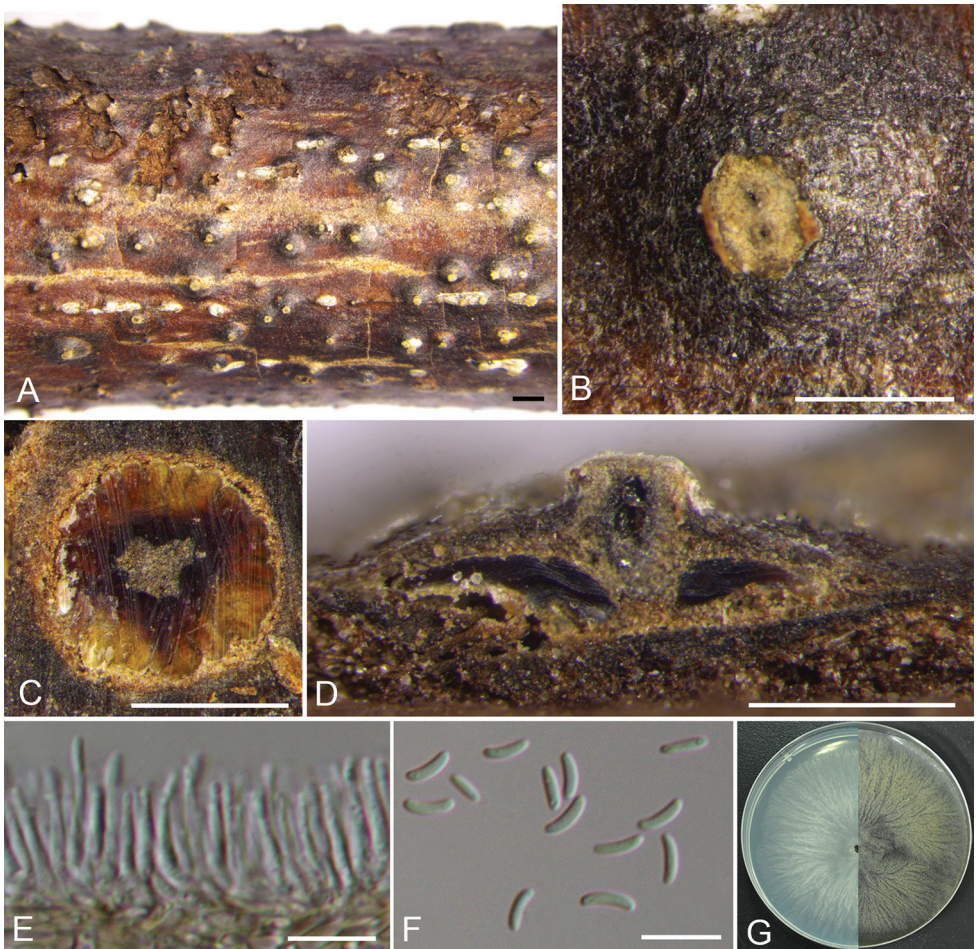


Figure 5. *Cytospora leucostoma* (Asexual morph) from *Juglans mandshurica* (CF 2019809). **A, B** habit of conidiomata on twig **C** transverse section of conidioma **D** longitudinal section through conidioma **E** conidiophores and conidiogenous cells **F** conidia **G** colonies on PDA at 3 days (left) and 30 days (right). Scale bars: 1 mm (**A**); 500 μ m (**B–D**); 10 μ m (**E, F**).

collected from Prunoideae (Fan et al. 2020). Multigene phylogenetic analyses supported the morphological results with high support values (ML/MP/BI = 100/100/1, Fig. 2). By combining morphology and the DNA data, our isolates collected from dead branches of *Prunus sibirica* and *Juglans mandshurica* belong to this species. The current study represents a new host record of *Juglans mandshurica*.

Cytospora pruinopsis C.M. Tian & X.L. Fan, *Mycological Progress* 14(9): 74 (2015)
Fig. 6

Description. See Yang et al. (2015).

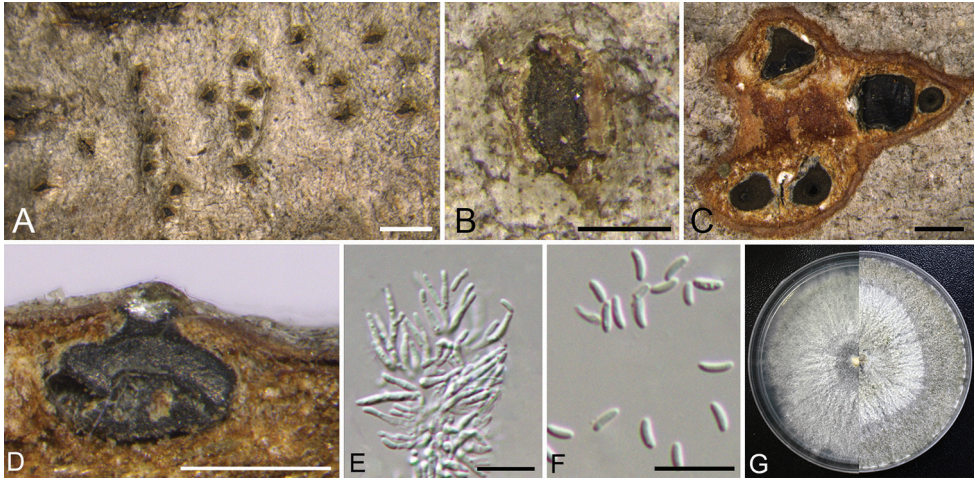


Figure 6. *Cytospora pruinopsis* from *Ulmus pumila* (CF 2019806). **A, B** habit of conidiomata on twig **C** transverse section of conidiomata **D** longitudinal section through conidioma **E** conidiophores and conidiogenous cells **F** conidia **G** colonies on PDA at 3 days (left) and 30 days (right). Scale bars: 1 mm (**A**); 250 μm (**B**); 500 μm (**C, D**); 10 μm (**E, F**).

Material examined. CHINA, Beijing City, Mentougou District, Mount Dongling, Xiaolongmen Forestry Centre (115°27'29.37"E, 39°56'47.49"N), from branches of *Ulmus pumila*, 22 Aug 2017, H.Y. Zhu & X.L. Fan, CF 2019806, living culture CFCC 53153.

Habitat and distribution. Known from *Ulmus pumila* in Northern China.

Notes. Yang et al. (2015) described *Cytospora pruinopsis* from cankers of *Ulmus pumila* in Shanxi Province of China. The strain CFCC 53153 clusters in a well-supported clade with high support value (MP/ML/BI = 100/100/1), based on combined multi-locus gene phylogenetic analyses (Fig. 2). Morphologically, it confirms *Cytospora pruinosa* in having a single locule and small conidia (2–4 \times 1 μm) as per the descriptions of Yang et al. (2015). Phylogenetically, our isolates represent 6/771 nucleotide differences of *tef1-a* comparing with ex-type strains CFCC 50034 of *C. pruinosa*. Morphology and sequence data confirmed that our isolates represent this species.

***Cytospora spiraeicola* H.Y. Zhu & X.L. Fan, sp. nov.**

Mycobank No: 833821

Fig. 7

Etymology. Named after the host genus on which it was collected, *Spiraea*.

Holotype. CHINA, Beijing City, Mentougou District, Mount Dongling, Xiaolongmen Forestry Centre (115°28'28.52"E, 39°55'49.42"N), from branches of *Spiraea salicifolia*, 17 Aug 2017, H.Y. Zhu & X.L. Fan, holotype CF 2019803, ex-type living culture CFCC 53138.

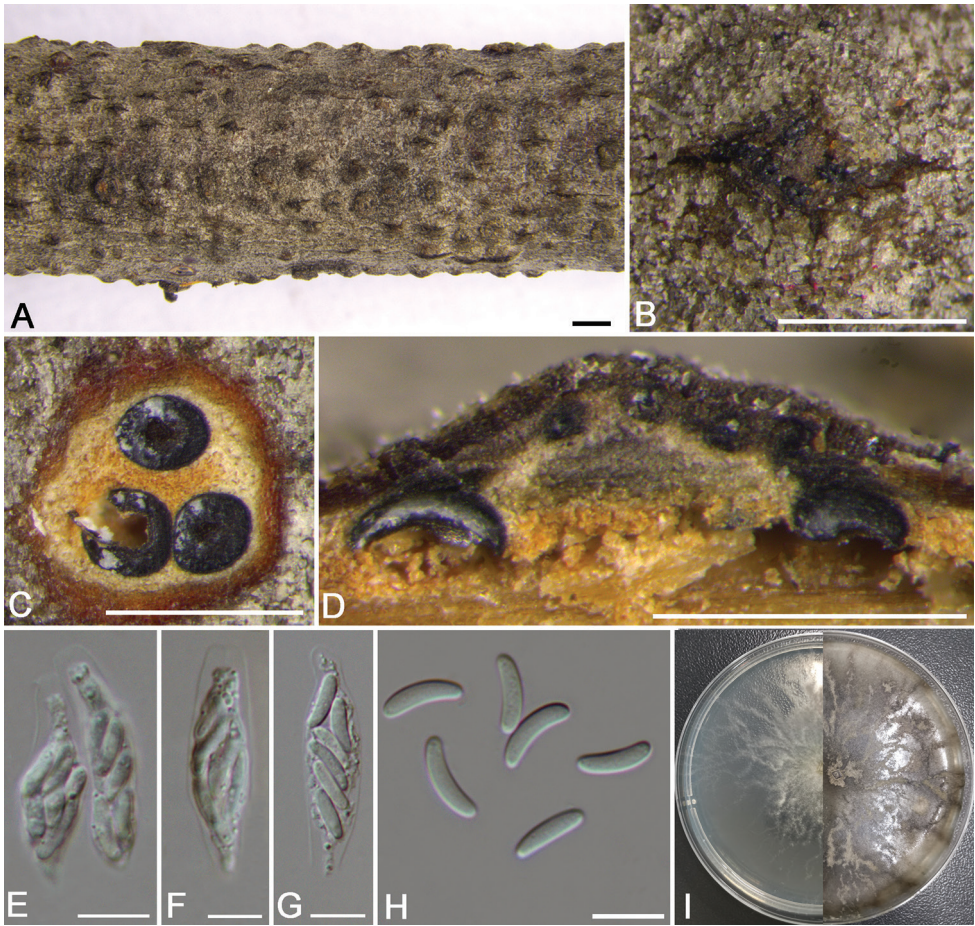


Figure 7. *Cytospora spiraeicola* from *Spiraea salicifolia* (CF 2019803). **A, B** habit of ascromata on twig **C** transverse section of ascoma **D** longitudinal section through ascoma **E** asci and ascospores **F, G** asci **H** ascospores **I** colonies on PDA at 3 days (left) and 30 days (right). Scale bars: 1 mm (**A, B**); 500 μ m (**C, D**); 10 μ m (**E–H**).

Description. *Necrotrophic* on branches of *Spiraea salicifolia* and *Tilia nobilis*. **Sexual morph:** *Ascostromata* immersed in the bark, erumpent through the surface of bark, scattered, with 3–5 perithecia arranged regularly, 660–890 μ m in diam. *Conceptacle* absent. *Ectostromatic disc* pale grey, usually surrounded by tightly crowded ostiolar necks, quadrangular, 240–350 μ m in diam., with 5–8 ostioles arranged regularly per disc. *Ostioles* numerous, dark grey to black, at the same or above the level as the disc, concentrated, arranged regularly in a disc, 25–40 μ m in diam. *Perithecia* dark grey to black, flask-shaped to spherical, arranged circularly, 210–250 μ m in diam. *Paraphyses* lacking. *Asci* free, clavate to elongate, obovoid, 26–37 \times 7.5–9 (av. = 33 \pm 2.5 \times 8.3 \pm 0.9, n = 10) μ m, 8-spored. *Ascospores* biseriolate, elongate-allantoid, thin-walled, hya-

line, slightly curved, aseptate, $8.5\text{--}12 \times 2.5\text{--}3.5$ (av. = $10 \pm 1 \times 3 \pm 0.3$, $n = 30$) μm . **Asexual morph:** not observed.

Culture characteristics. *Cultures* are white, growing up to 4 cm in diam. with irregular margin after 3 days, covering the 9 cm Petri dish after 6 days, becoming vinaceous buff to hazel after 7–10 days. In reverse, the cultures are the same as the upper colour after 3 days, becoming isabelline to umber after 7–10 days. *Colonies* are felty with a heterogeneous texture, lacking aerial mycelium.

Habitat and distribution. Known from *Spiraea salicifolia* and *Tilia nobilis* in Mount Dongling, China.

Additional material examined. CHINA, Beijing City, Mentougou District, Mount Dongling, Xiaolongmen Forestry Centre (115°29'20.49"E, 39°57'47.43"N), from branches of *Tilia nobilis*, 17 Aug 2017, H.Y. Zhu & X.L. Fan, CF 2019804, living culture CFCC 53139.

Notes. *Cytospora spiraeicola* is associated with canker disease of *Spiraea salicifolia* and *Tilia nobilis* in China, with characteristics similar to *Cytospora elaeagnicola* and *C. spiraeae* in phylogram (Fig. 2). Morphologically, it differs from *C. spiraeae* by the smaller perithecia (210–250 vs. 270–400 μm in diam.) and longer ascospores ($8.5\text{--}12 \times 2.5\text{--}3.5$ vs. $7\text{--}8 \times 2\text{--}2.5$ μm) (Zhu et al. 2018a). Phylogenetically, *C. spiraeicola* (CFCC 53138) differs from *C. elaeagnicola* (CFCC 52882) by ITS (8/665), *rpb2* (44/730), *tef1-a* (75/771) and *tub2* (42/624) and *C. spiraeae* (CFCC 50049) by ITS (4/665), *rpb2* (38/730), *tef1-a* (63/771) and *tub2* (44/624) (Zhu et al. 2018a, Zhang et al. 2019). Therefore, we describe it as a novel species.

Discussion

In the present study, seven specimens were collected from symptomatic branches and twigs associated with canker disease. Four *Cytospora* species were isolated from six tree hosts of Betulaceae, Juglandaceae, Rosaceae, Tiliaceae and Ulmaceae, which include two known species (*Cytospora leucostoma* and *C. pruinopsis*) and two novel species (*C. coryli* and *C. spiraeicola*). This study represents an investigation of *Cytospora* species associated with canker disease in Mount Dongling of China and included a comprehensive analysis of DNA sequence data to compare the novelties with known *Cytospora* species.

In a previous study, Zhu et al. (2018a) described *Cytospora spiraeae* from *Spiraea salicifolia* in Gansu Province of China during an investigation of forest pathogens of three hosts. Compared to the new species *Cytospora spiraeicola*, *C. spiraeae* has larger perithecia (270–400 vs. 210–250 μm) in diam. and shorter ascospores ($7\text{--}8 \times 2.5\text{--}3.5 \times 8.5\text{--}12$ vs. $2\text{--}2.5$ μm). These morphological deviations are in line with the combined phylogenetic analyses which resolved *C. spiraeicola* as a unique lineage, highly supported. Besides this, the only strain of *C. coryli*, closely related to *C. euonymicola* and *C. gigalocus*, was distinguished by its different size of multiple locules and conidia (Fan et al. 2015a, 2020).

This study focused on *Cytospora* species in Mount Dongling of Beijing (China), which is considered as an attractive location with a high richness of fungal species (Guo et al. 2008, Zhu et al. 2018b, 2019). We hope that the descriptions and molecular data of *Cytospora* in this study could provide a resource for future studies in this genus and lay the foundation for the future canker disease caused by *Cytospora* species.

Acknowledgements

This study is financed by the Fundamental Research Funds for the Central Universities (2019ZY23), the National Natural Science Foundation of China (31670647) and the College Student Research and Career-creation Program of Beijing (S201810022005). All authors want to thank the Experimental Teaching Centre (College of Forestry, Beijing Forestry University) for providing installed scientific equipment during the whole process.

References

- Adams GC, Roux J, Wingfield MJ (2006) *Cytospora* species (Ascomycota, Diaporthales, Valsaceae), introduced and native pathogens of trees in South Africa. *Australasian Plant Pathology* 35: 521–548. <https://doi.org/10.1071/AP06058>
- Adams GC, Roux J, Wingfield MJ, Common R (2005) Phylogenetic relationships and morphology of *Cytospora* species and related teleomorphs (Ascomycota, Diaporthales, Valsaceae) from *Eucalyptus*. *Studies in Mycology* 52: 1–144.
- Alves A, Crous PW, Correia A, Phillips AJL (2008) Morphological and molecular data reveal cryptic speciation in *Lasiodiplodia theobromae*. *Fungal Diversity* 28: 1–13.
- Barr ME (1978) The Diaporthales in North America with emphasis on *Gnomonia* and its segregates. *Mycologia Memoir* 7: 1–232.
- Carbone I, Kohn LM (1999) A method for designing primer sets for speciation studies in filamentous ascomycetes. *Mycologia* 91: 553–556. <https://doi.org/10.1080/00275514.1999.12061051>
- Doyle JJ, Doyle JL (1990) Isolation of plant DNA from fresh tissue. *Focus* 12: 13–15. <https://doi.org/10.2307/2419362>
- Ehrenberg CG (1818) *Sylvae Mycologicae Berolinenses*. Formis Theophili Bruschcke, Berlin, Germany.
- Fan XL, Bezerra JDP, Tian CM, Crous PW (2020) *Cytospora* (Diaporthales) in China. *Persoonia* 45: 1–45. <https://doi.org/10.3767/persoonia.2020.45.01>
- Fan XL, Hyde KD, Liu M, Liang YM, Tian CM (2015a) *Cytospora* species associated with walnut canker disease in China, with description of a new species *C. gigalocus*. *Fungal Biology* 119: 310–319. <https://doi.org/10.1016/j.funbio.2014.12.011>
- Fan XL, Hyde KD, Yang Q, Liang YM, Ma R, Tian CM (2015b) *Cytospora* species associated with canker disease of three anti-desertification plants in northwestern China. *Phytotaxa* 197: 227–244. <https://doi.org/10.11646/phytotaxa.197.4.1>

- Fan XL, Liang YM, Ma R, Tian CM (2014a) Morphological and phylogenetic studies of *Cytospora* (Valsaceae, Diaporthales) isolates from Chinese scholar tree, with description of a new species. *Mycoscience* 55: 252–259. <https://doi.org/10.1016/j.myc.2013.10.001>
- Fan XL, Tian CM, Yang Q, Liang YM, You CJ, Zhang YB (2014b) *Cytospora* from *Salix* in northern China. *Mycotaxon* 129: 303–315. <https://doi.org/10.5248/129.303>
- Fries EM (1823) *Systema mycologicum*. Vol. 2, Greifswald, Germany.
- Glass NL, Donaldson GC (1995) Development of primer sets designed for use with the PCR to amplify conserved genes from filamentous ascomycetes. *Applied and Environmental Microbiology* 61: 1323–1330. <https://doi.org/10.1128/AEM.61.4.1323-1330.1995>
- Guindon S, Dufayard JF, Lefort V, Anisimova M, Hordijk W, Gascuel HO (2010) New algorithms and methods to estimate maximum-likelihood phylogenies: assessing the performance of PhyML 3.0. *Systematic Biology* 59: 307–321. <https://doi.org/10.1093/sysbio/syq010>
- Guo LD, Huang GR, Wang Y (2008) Seasonal and Tissue Age Influences on Endophytic Fungi of *Pinus tabulaeformis* (Pinaceae) in the Dongling Mountains, Beijing. *Journal of Integrative Plant Biology* 50: 997–1003. <https://doi.org/10.1111/j.1744-7909.2008.00394.x>
- Gvritshvili MN (1982) The fungal genus *Cytospora* in the USSR. *Izdatelstv Sabchota Sakarstvelo*, Tbilisi, Russia.
- Hillis DM, Bull JJ (1993) An empirical test of bootstrapping as a method for assessing confidence in phylogenetic analysis. *Systematic Biology* 42: 182–192. <https://doi.org/10.1093/sysbio/42.2.182>
- Katoh K, Standley DM (2013) MAFFT multiple sequence alignment software version 7: improvements in performance and usability. *Molecular biology and evolution* 30: 772–780. <https://doi.org/10.1093/molbev/mst010>
- Kirk PM, Cannon PF, Minter DW, Stalpers JA (2008) *Ainsworth & Bisby's dictionary of the Fungi*, 10th edn, Wallingford, UK. <https://doi.org/10.1079/9780851998268.0000>
- Kobayashi T (1970) Taxonomic studies of Japanese Diaporthaceae with special reference to their life-histories. Tokyo, Japan.
- Lawrence DP, Travadon R, Pouzoulet J, Rolshausen PE, Wilcox WF, Baumgartner K (2016) Characterization of *Cytospora* isolates from wood cankers of declining grapevine in North America, with the descriptions of two new *Cytospora* species. *Plant Pathology* 5: 713–725. <https://doi.org/10.1111/ppa.12621>
- Lawrence DP, Holland LA, Nouri MT, Travadon R, Trouillas FP (2018) Molecular phylogeny of *Cytospora* species associated with canker diseases of fruit and nut crops in California, with the descriptions of ten new species and one new combination. *IMA Fungus* 9: 333–369. <https://doi.org/10.5598/imafungus.2018.09.02.07>
- Liu YJ, Whelen S, Hall BD (1999) Phylogenetic relationships among ascomycetes: evidence from an RNA polymerase II subunit. *Molecular Biology and Evolution* 16: 1799–1808. <https://doi.org/10.1093/oxfordjournals.molbev.a026092>
- Ma KP, Guo XM, Yu SL (1995) On the characteristics of the flora of Mount Dongling area and its relationship with a number of other mountainous floras in China. *Bulletin Botanical Research* 15: 501–515.

- Norphanphoun C, Doilom M, Daranagama DA, Phookamsak R, Wen TC, Bulgakov TS, Hyde KD (2017) Revisiting the genus *Cytospora* and allied species. *Mycosphere* 8: 51–97. <https://doi.org/10.5943/mycosphere/8/1/7>
- Pan M, Zhu HY, Tian CM, Alvarez LV, Fan XL (2018) *Cytospora piceae* sp. nov. associated with canker disease of *Picea crassifolia* in China. *Phytotaxa* 383: 181–196. <https://doi.org/10.11646/phytotaxa.383.2.4>
- Posada D, Crandall KA (1998) Modeltest: testing the model of DNA substitution. *Bioinformatics* 14: 817–818. <https://doi.org/10.1093/bioinformatics/14.9.817>
- Rannala B, Yang Z (1996) Probability distribution of molecular evolutionary trees: a new method of phylogenetic inference. *Journal of Molecular Evolution* 43: 304–311. <https://doi.org/10.1007/BF02338839>
- Rayner RW (1970) *A Mycological Colour Chart*. Commonwealth Mycological Institute, Kew, UK.
- Ronquist F, Huelsenbeck JP (2003) MrBayes 3: Bayesian phylogenetic inference under mixed models. *Bioinformatics* 19: 1572–1574. <https://doi.org/10.1093/bioinformatics/btg180>
- Rossman AY, Adams GC, Cannon PF, Castlebury LA, Crous PW, Gryzenhout M, Jaklitsch WM, Mejia LC, Stoykov D, Udayanga D, Voglmayr H, Walker M (2015) Recommendations of generic names in Diaporthales competing for protection or use. *IMA Fungus* 6: 145–154. <https://doi.org/10.5598/imafungus.2015.06.01.09>
- Saccardo PA (1884) *Sylloge Fungorum III. Typis Seminarii, Italy*.
- Stamatakis A (2006) RAxML-VI-HPC: Maximum likelihood-based phylogenetic analyses with thousands of taxa and mixed models. *Bioinformatics* 22: 2688–2690. <https://doi.org/10.1093/bioinformatics/btl446>
- Sinclair WA, Lyon HH, Johnson WT (1987) *Diseases of Trees and Shrubs*. Coinstock Publishing Associates, Cornell University Press, USA.
- Spielman LJ (1983) *Taxonomy and biology of Valsa species on hardwoods in North America, with special reference to species on maples*, Cornell University, New York, USA.
- Spielman LJ (1985) *A monograph of Valsa on hardwoods in North America*. *Canadian Journal of Botany* 63: 1355–1378. <https://doi.org/10.1139/b85-190>
- Sun X, Guo LD, Hyde KD (2011) Community composition of endophytic fungi in *Acer truncatum* and their role in decomposition. *Fungal diversity* 47: 85–95. <https://doi.org/10.1007/s13225-010-0086-5>
- Sutton BC (1980) *The Coelomycetes: Fungi Imperfecti with pycnidia, acervuli and stromata*. Kew: Commonwealth Mycological Institute.
- Swofford DL (2003) *PAUP*: Phylogenetic Analysis Using Parsimony, * and Other Methods, Version 4.0b10*, Sinauer Associates, Sunderland.
- Tai FL (1979) *Sylloge Fungorum Sinicorum*. Science Press, Beijing, China.
- Tamura K, Stecher G, Peterson D, Filipski A, Kumar S (2013) MEGA6: molecular evolutionary genetics analysis version 6.0. *Molecular Biology and Evolution* 30: 2725–2729. <https://doi.org/10.1093/molbev/mst197>
- Teng SC (1963) *Fungi of China*. Science Press, Beijing, China.
- Vilgalys R, Hester M (1990) Rapid genetic identification and mapping of enzymatically amplified ribosomal DNA from several *Cryptococcus* species. *Journal of Bacteriology* 172: 4238–4246. <https://doi.org/10.1128/JB.172.8.4238-4246.1990>

- Wei JC (1979) Identification of Fungus Handbook. Science Press. Shanghai, China.
- White TJ, Bruns T, Lee S, Taylor J (1990) Amplification and direct sequencing of fungal ribosomal RNA genes for phylogenetics. PCR Protocols: a guide to methods and applications 18: 315–322. <https://doi.org/10.1016/B978-0-12-372180-8.50042-1>
- Wijayawardene NN, Hyde KD, Lumbsch HT, Liu JK, Maharachchikumbura SSN, Ekanayaka AH, Tian Q, Phookamsak R (2018) Outline of Ascomycota: 2017. Fungal Diversity 88: 167–263. <https://doi.org/10.1007/s13225-018-0394-8>
- Yang Q, Fan XL, Crous PW, Liang YM, Tian CM (2015) *Cytospora* from *Ulmus pumila* in Northern China. Mycological Progress 14: 1–12. <https://doi.org/10.1007/s11557-015-1096-1>
- Zhu HY, Pan M, Bonthond G, Tian CM, Fan XL (2019) Diaporthalean fungi associated with canker and dieback of trees from Mount Dongling in Beijing, China. MycoKeys 59: 67–94. <https://doi.org/10.3897/mycokeys.59.38055>
- Zhu HY, Tian CM, Fan XL (2018a) Multigene phylogeny and morphology reveal *Cytospora spiraeae* sp. nov. (Diaporthales, Ascomycota) in China. Phytotaxa 338: 49–62. <https://doi.org/10.11646/phytotaxa.338.1.4>
- Zhu HY, Tian CM, Fan XL (2018b) Studies of botryosphaeralean fungi associated with canker and dieback of tree hosts in Dongling Mountain of China. Phytotaxa 348: 63–76. <https://doi.org/10.11646/phytotaxa.348.2.1>
- Zhang LX, Alvarez LV, Bonthond G, Tian CM, Fan XL (2019) *Cytospora elaeagnicola* sp. nov. associated with narrow-leaved oleaster canker disease in China. Mycobiology 47: 319–328. <https://doi.org/10.1080/12298093.2019.1633902>
- Zhuang WY (2005) Fungi of Northwestern China. Mycotaxon, Ltd. New York, USA.

The genus *Catathelasma* (Catathelasmataceae, Basidiomycota) in China

Zai-Wei Ge^{1,2}, Jian-Yun Wu^{1,2}, Yan-Jia Hao³,
Qingying Zhang⁴, Yi-Feng An¹, Martin Ryberg⁵

1 CAS Key Laboratory for Plant Diversity and Biogeography of East Asia, Kunming Institute of Botany, Chinese Academy of Sciences, Kunming 650201, China **2** University of Chinese Academy of Sciences, Beijing, China **3** School of Horticulture, Anhui Agricultural University, Hefei 230036, China **4** Industrial Crops Research Institute, Yunnan Academy of Agricultural Sciences, Kunming, China **5** Systematic Biology, Department of Organismal Biology, Uppsala University, Norbyvägen 18D, 75236 Uppsala, Sweden

Corresponding author: Zai-Wei Ge (zwge@mail.kib.ac.cn)

Academic editor: R. H. Nilsson | Received 30 May 2019 | Accepted 13 December 2019 | Published 3 February 2020

Citation: Ge Z-W, Wu J-Y, Hao Y-J, Zhang Q, An Y-F, Ryberg M (2020) The genus *Catathelasma* (Catathelasmataceae, Basidiomycota) in China. MycoKeys 62: 123–138. <https://doi.org/10.3897/mycokeys.62.36633>

Abstract

Two new species, *Catathelasma laorentou* and *C. subalpinum*, are described on the basis of morphological characters, phylogenetic evidence, host preferences and geographic distributions. A taxonomic key to the known species in China is also provided to facilitate identification. Based on samples from temperate Asia, Europe and North America, the phylogeny of *Catathelasma* was reconstructed using the internal transcribed spacer (ITS) region, the large subunit (LSU) of the ribosomal DNA and the translation elongation factor 1- α (TEF1). The phylogenetic results showed that *Catathelasma* contains two monophyletic clades: the /subalpinum clade and the /imperiale clade. The Asian species *C. laorentou* and *C. subalpinum* are closely related to the North American *C. sp.* (labelled as *C. ventricosum* in GenBank) in the /subalpinum clade, whereas *C. imperiale* and *C. singeri* are closely related in the /imperiale clade.

Keywords

Catathelasmataceae, Biannulariaceae, Tricholomataceae, taxonomy, ectomycorrhizal fungi, new taxa

Introduction

Catathelasma Lovejoy is the type genus of the mushroom family *Catathelasmataceae* Wasser (Wasser 1985; Sánchez-García et al. 2016). This genus was erected by Lovejoy (1910) based on the type species *C. evanescens* Lovejoy. Morphologically, species within

this genus have distinct tricholomatoid basidiomes, decurrent to adnate to sinuate-
adnexed lamellae, double annulus, white spores that are oblong, smooth, amyloid and
acyanophilic, bilateral to subregular lamella trama, firm and white context, hyphae
with clamp connections and an ixocutis, ixolattice or cutis as pileipellis.

Catathelasma has long been regarded a member of the *Tricholomataceae* (Singer
1975, 1986), but Jülich (1982) established the family *Biannulariaceae* Jülich, based on
Biannularia Beck, which had been synonymised with *Catathelasma* (Singer 1940). In
1985, Wasser established the *Catathelasmataceae* to contain the only member *Catathe-
lasma* (Wasser 1985), and this family has recently been emended to also include *Callisto-
sporium* Singer, *Guyanagarika* Sánchez-García et al. (2016), *Macrocybe* Pegler & Lodge,
Pleurocollybia Singer and *Pseudolaccaria* Vizzini et al. (Sánchez-García et al. 2016).

Catathelasma contains four species: *C. evanescens*, *C. imperiale*, *C. singeri* and *C.
ventricosum* (Kirk et al. 2008, Singer 1986). Species within this genus have been sug-
gested to be ectomycorrhizal (Trappe 1962; Kohzu et al. 1999; Tedersoo and Smith
2013) and tend to be found in coniferous forests in northern temperate regions (Singer
1979). In China, collections of *Catathelasma* have long been regarded as belonging to
C. imperiale or *C. ventricosum* (Ying and Zang 1994; Yuan and Sun 2013; Zang et al.
1996). During our studies of the ectomycorrhizal fungi associated with members of
the Pinaceae, especially *Keteleeria* spp. in China (Ge et al. 2012), a few collections of
Catathelasma with distinct ITS sequences from *Catathelasma* sequences in GenBank
were encountered. Here, we used morphological observations and multilocus phyloge-
netic analyses to (i) clarify the species identity of *Catathelasma* specimens in China and
(ii) examine the phylogenetic relationships of *Catathelasma* species. We also took into
account the geographic isolation and the host associations of the Chinese collections.

Materials and methods

Collections and morphological studies

Catathelasma specimens were collected in western and south-western China (Yunnan,
Sichuan, Gansu and Tibet) and deposited in the Herbarium of Cryptogams, Kunming
Institute of Botany, Chinese Academy of Sciences (HKAS). Herbarium materials iden-
tified as *Catathelasma evanescens* Lovejoy and *Catathelasma singeri* Mitchel & A.H. Sm
were loaned from Denver Botanic Garden, Sam Mitchel Herbarium of Fungi (DBG).
Voucher information of the specimens and GenBank (Benson et al. 2017) accession
numbers are detailed in Table 1.

Morphological character descriptions were taken from field notes and colour images
of the material, with colour names and codes following Kornerup and Wanscher (1978).
Microscopic character observations followed published treatments on *Catathelasma*
species (Mitchel and Smith 1978). Dried material was mounted in 5% aqueous (w/v)
potassium hydroxide (KOH) under a Leica DM2500 microscope (Leica, Bensheim,
Germany) and pileal structure, basidiospores and basidia were observed and measured

in 5% KOH with 0.5% aqueous Congo Red (w/v). Melzer's reagent was used to test the amyloidy of basidiospores. The length and width of at least 20 mature basidiospores from each specimen were measured in side view. Dimensions for basidiospores are reported as (a–) b–c (–d) and the abbreviation [n/m/p] indicates n basidiospores measured from m basidiomes of p collections. The range b–c contains a minimum of 90% of the measured values, with extreme values (a and d) presented in parentheses. Quotient of length and width (Q), average quotient (Q_{av}) and standard deviation were calculated.

DNA extraction, PCR and sequencing

Genomic DNA was extracted from dry specimens using the modified cetyltrimethylammonium bromide (CTAB) method (Doyle and Doyle 1987). Briefly, approximately 10 mg tissue was ground into a fine powder in liquid nitrogen in a 1.5 ml Eppendorf tube using a plastic pestle, and 500 µl of an extraction buffer (2 × CTAB) were added. The mixture was incubated at 60 °C for 1.5 h, with 0.2% β-mercaptoethanol added prior to the extraction. Phenol-chloroform-isoamyl alcohol (25:24:1) were used to remove any proteins and polysaccharides and DNA was precipitated by adding 400 µl isopropanol to the aqueous phase. The DNA pellet was washed in 400 µl 70% ethanol and air-dried, then suspended in 80 µl TE (pH 8.0).

PCR amplification was performed following Ge et al. (2014) on an ABI 2720 Thermal Cycler (Applied Biosystems, Foster City, CA, USA). Primers used to amplify the internal transcribed spacer (ITS) region and the large subunit (LSU) of the ribosomal DNA and translation elongation factor 1-α (TEF1) were ITS1F/ITS4, LR0R/LR5 and 983F/1567R, respectively (Gardes and Bruns 1993; Matheny 2005; Rehner and Buckley 2005). Polymerase chain reaction (PCR) parameters follow those of Ge et al. (2014). PCR products were purified using a QIAquick PCR purification kit (Qiagen Science, USA) and sent to Kunming Shuoqing Biotech Ltd. (Kunming, China) for sequencing. Both directions were sequenced to improve accuracy. Sequencing primers were the same as the initial PCR primers. Sequence chromatograms were inspected and contigs assembled using Seqman version 5.01 (DNA STAR Package; DNASTar, Madison, WI, USA). The sequences produced in this study were deposited in GenBank with accession numbers MK909078–MK909123.

Sequence alignment and phylogenetic analyses

DNA sequences of ITS, LSU and TEF1 were independently aligned with MAFFT v6.8 (Katoh et al. 2009) with manual adjustments and the concatenated datasets were manually constructed. Sequences of *Catathelasma* species, generated for this study and those of the genus that are available in GenBank, were included. *Callistosporium graminicolor* Lennox and *Callistosporium luteo-olivaceum* (Berk. & M.A. Curtis) Singer were designated as outgroups based on previous phylogenetic studies (Ammirati et al. 2007; Sánchez-García

et al. 2016). The datasets were then analysed using RAxML version 7.2.3 (Swofford 2002) and MrBayes v3.1.2 (Ronquist and Huelsenbeck 2003) for Maximum Likelihood (ML) and Bayesian Inference (BI), respectively. ML analyses were performed with 1000 bootstrap replicates, setting GTRGAMMAI as the selected model; and BI analyses were conducted with default parameters, except setting generations to 5 million and sampling every 1000th generation. As selected by MrModeltest v2.3 (Nylander 2004), rates = gamma, nst = 2 was set for ITS dataset and rates = gamma, nst = 6 were set for LSU and TEF1, respectively. Since the average standard deviation of split frequencies converged (< 0.01) after 1 million generations, the first 25% of the sampled Bayesian trees (1251 trees) of the analysis were discarded as the burn-in. As no significant incongruence was observed using bootstrap values above 70% as threshold, we incorporated the ITS, LSU and TEF1 sequences into a concatenated dataset and performed the ML and BI analyses and partitioned the dataset by gene, as mentioned above. Final alignments were deposited in TreeBASE (<http://www.treebase.org>) under accession number S24480.

Results

Phylogeny and species recognition

Forty-six new ITS, LSU and TEF1 sequences were generated for *Catathelasma* species and deposited in GenBank (Table 1). The alignments of the ITS, LSU and TEF1 sequences were 708, 861 and 582 characters in length after trimming, respectively. ML and BI analyses produced consistent monophyletic clades and congruent phylogenies (Fig. 1).

Besides four Chinese collections that were confirmed to be conspecific with *C. imperiale*, sequences generated from other specimens collected in south-western China formed two monophyletic clades here described as *C. laorentou* and *C. subalpinum*, respectively (Fig. 1); each clade was well supported by both ML and BI in the ITS, LSU, TEF1 and concatenated trees (Fig. 1), except that in the TEF1 phylogeny, *C. subalpina* is only represented by a single sequence.

As revealed by the analyses of the different genetic markers and concatenated dataset (ITS, LSU, TEF1 and the combined dataset), the genus *Catathelasma* comprises two monophyletic clades: the /*imperiale* clade and /*subalpinum* clade (Fig. 1). Within the /*subalpinum* clade, *C. laorentou* appears to be sister to *C. subalpinum* and these Asian species jointly form the sister clade to the North American *C. sp.* (Fig. 1D, labelled as *C. ventricosum* in GenBank).

The /*imperiale* clade included the northern-temperate-region distributed *C. imperiale* and the North American species *C. singeri*. The ITS, TEF1 and concatenated sequences suggest that *C. singeri* represents a monophyletic clade within or close to *C. imperiale* (Fig. 1). In contrast to the /*subalpinum* clade, the inter-species relationships within the /*imperiale* clade are not fully resolved: *C. singeri* is supported by the ML analyses, but not strongly supported by the BI tree (Fig. 1), although ITS sequences of *C. singeri* are only 94% (599/635)—95% (542/570) similar to those of *C. imperiale*.

Table 1. Taxa, vouchers, geographic origin and GenBank accession numbers of DNA sequences of *Catathelasma* and outgroups used in this study. New sequences generated in this study are given in bold. * indicates the type collection.

Taxon	Voucher	Geographic origin	GenBank accession number		
			ITS	LSU	TEF1
<i>Catathelasma singeri</i>	DBG-F-006151	USA: Colorado	MK909090	MK909109	MK909079
<i>C. singeri</i>	DBG-F-021378	USA: Colorado	MK909091	MK909110	MK909078
	DBG-F-021747	USA: Colorado	MK909092	MK909111	MK909080
<i>C. singeri</i> as <i>ventricosum</i>	PBM 2403 (AFTOL-ID 1488)	USA: Washington	DQ486686	DQ089012	N/A
<i>C. imperiale</i>	HKAS 84299 (Z. W. Ge 3461)	China: Tibet	MK909094	MK909112	MK909081
	HKAS 84315 (Z. W. Ge 3477)	China: Sichuan	MK909096	MK909113	MK909083
	HKAS 79952 (X. B. Liu 251)	China: Sichuan	MK909095	MK909114	MK909084
	HKAS 76511 (X. T. Zhu 662)	China: Gansu	MK909093	MK909115	MK909082
	TAA176551	Canada: Newfoundland	N/A	AM946417	N/A
	UPS F-173429	Sweden: Uppland	MK909097	MK909116	MK909085
	UPS F-120619	Sweden: Hälsingland	MK909098	N/A	N/A
	TUB 011562		N/A	DQ071743 DQ071835	N/A
	LL_128		KX008987	N/A	N/A
	KM55154	UK: England	GQ981498	N/A	N/A
<i>C. sp. as imperiale</i>	DAOM225247		KP255468	AF261402	KP255475
	11CA01A	USA: California	N/A	N/A	KC816900
<i>C. sp. as ventricosum</i>	DAOM221514		KP255469	AF261401	N/A
	TRTC156545	Canada: Quebec	JN020996	N/A	N/A
	Mat3	Canada: Quebec	JN020995	N/A	N/A
	OSC 66879	USA: Pacific Northwest	EU669305	EU669331	N/A
	SMI349	Canada: British Columbia	HQ650727	N/A	N/A
	TAA176473	Canada: Newfoundland	N/A	AM946418	N/A
<i>C. laorentou</i>	HKAS 84458 (Z. W. Ge 3620)	China: Yunnan	MK909106	MK909117	MK909086
	HKAS 92245 (Z. W. Ge 3765)	China: Yunnan	MK909103	MK909118	MK909087
	*HKAS 105984 (Z. W. Ge 4070)	China: Yunnan	MK909107	N/A	N/A
	HKAS 71264 (T. Guo 368)	China: Yunnan	MK909105	MK909119	MK909088
	HKAS 78582 (L. H. Han 23)	China: Yunnan	MK909108	MK909120	N/A
	HKAS 76346 (Y. J. Hao 688)	China: Sichuan	MK909102	N/A	N/A
	HKAS 81166 (J. Qin 728)	China: Yunnan	MK909104	N/A	N/A
<i>C. subalpinum</i>	HKAS 70091 (Q. Cai 495)	China: Yunnan	MK909100	MK909123	MK909089
	*HKAS 67751 (J. Qin 65)	China: Yunnan	MK909099	MK909121	N/A
	HKAS 69920 (L. P. Tang 1459)	China: Yunnan	MK909101	MK909122	N/A
Outgroups					
<i>Callistosporium gramicolor</i>	PBM 2341 (AFTOL-ID 978)		DQ484065	AY745702	GU187761
<i>Callistosporium luteoolivaceum</i>	DUKE-JM99124		N/A	AF261405	KP255477
	MSM#004		KJ101607	N/A	N/A

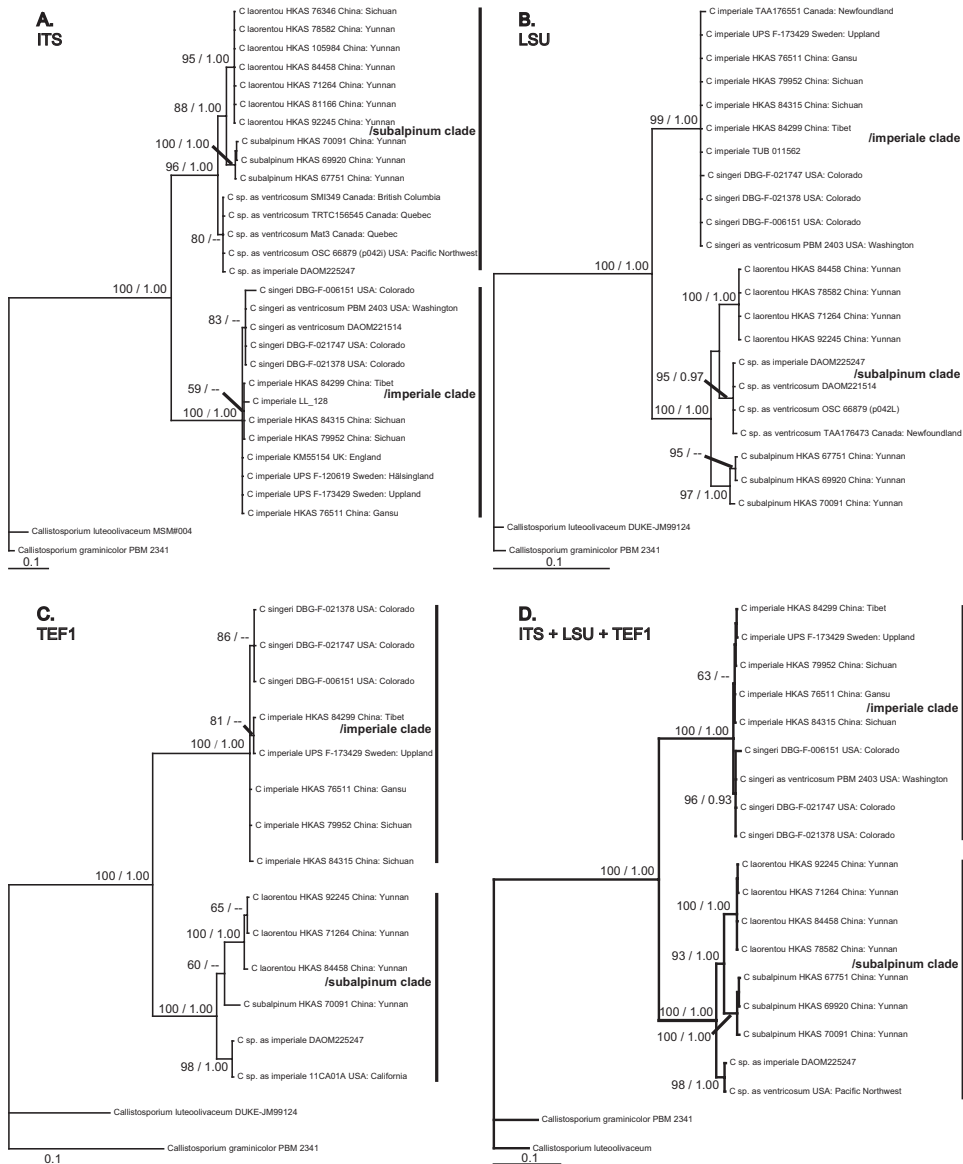


Figure 1. Bayesian phylogenies of **A** ITS **B** 28S **C** TEF1 and **D** ITS+28S+TEF1 concatenated sequences for *Catathelasma* species. Maximum likelihood bootstrap support and Bayesian posterior probabilities are indicated by values above branches.

Taxonomy

Considering the strong statistical support as monophyletic groups and the morphological differences, as well as their host preferences (see below), *C. laorentou* and *C. subalpinum* are described as new species.

***Catathelasma imperiale* (P. Karst.) Singer**

Fig. 2C, D

Description. Pileus 8–15 cm broad, hemispherical, convex to plano-convex, later expanded with decurved margin, sometimes depressed to funnel-shaped, smooth, dry to slightly viscid, greyish-brown, reddish-brownish or brown. Lamellae adnate to slightly decurrent, white to off-white when young, whitish to cream when mature, thick, 7–15 mm in height, with 1–2 series of lamellulae; edge smooth, grey to dark brown. Stipe 5–10 × 1.8–3.0 cm, fusiform, attenuate downwards, straight or curved, firm, with double annulus in which the lower annulus is often gelatinous and the upper annulus is membranous, with white to whitish upper surface and grey to brown lower surface. Context firm, white, not changing colour when cut; smell and taste farinaceous. Spore print white.

Basidiospores [60/3/3] 10–14.5 × 4.5–6 µm, hyaline in KOH, amyloid, congo-philous, smooth, oblong to subcylindrical in frontal view, subcylindrical to somewhat inequilateral in side view, thin-walled, without germ pore. Basidia 35–48 × 7–10 µm, 4-spored, narrowly clavate, hyaline; sterigmata up to 5 µm long. Cheilocystidia basidole-like, with yellow to brown contents. Pleurocystidia absent. Lamella trama bilateral, composed of more or less parallel to interwoven hyphae. Oleiferous hyphae present in both lamella and pileus trama. Pileipellis a thick ixocutis of loosely interwoven cylindrical, 2–8 µm wide gelatinised hyphae, interspersed with oleiferous hyphae. Clamp connections present, common.

Ecology. Ectomycorrhizal, solitary or scattered, in forests dominated by *Picea* spp. or *Abies* spp.

Specimens examined. CHINA. Gansu Province: Gannan city, Diebu, Wabagou, alt. 2700 m, 12 August 2012, X. T. Zhu 662 (HKAS 76511), under *Picea* sp.; Sichuan Province: Gangzi prefecture, Dege, Manigange, alt. 4200 m, 9 August 2013, Z. W. Ge 3477 (HKAS 84315), under *Picea asperata* Mast.; same locality and date, X. B. Liu 251 (HKAS 79952); Tibet: on the way from Bangda to Changdu, 6 August 2013, Z. W. Ge 3461 (HKAS 84299), alt. 3980 m, under *Picea asperata*.

***Catathelasma laorentou* Z.W. Ge, sp. nov.**

Mycobank No: 830871

Figs 2A, 3

Diagnosis. This species is distinguished from *C. ventricosum* (Peck) Singer by having pale yellow to greyish-yellow basidiomes, longer stipes, abundant clamp connections and associations with *Pinus yunnanensis* Mast. and *Keteleeria evelyniana* Franchet in south-western China.

Type. CHINA. Yunnan Province: Chuxiong, Zixi Mountain, alt. 1950 m, in forest dominated by *K. evelyniana* Mast. and *P. yunnanensis* Franchet, 26 August 2017, Z. W. Ge 4070 (Holotype: HKAS 105984). GenBank accession numbers: – ITS, MK909107.



Figure 2. Basidiomes of *Catathelasma* species in China. **A** *Catathelasma laorentou* (HKAS 92245) **B** *Catathelasma subalpinum* (HKAS 67751) **C** *Catathelasma imperiale* (HKAS 79952) **D** Young *Catathelasma imperiale* (HKAS 84299) in association with roots of *Picea asperata* Mast. Scale bars: 2.5 cm.

Description. Pileus 10–24 cm broad, hemispherical to convex at first, expanding to convex to broadly convex with age; surface initially white, then yellowish-white (1A2) to pale yellow (1A3), greyish-yellow (2B3) with age, smooth at first, irregularly depressed, margin more or less incurved, slightly viscid to viscid when wet, occasionally with whitish veil remnants. Lamellae decurrent, white to off-white when young, whitish when mature, thick, 7–15 mm in height, with 1–2 series of lamellulae, edge smooth. Stipe 6–24 × 1.5–8 cm, fusiform, attenuate downwards, straight or curved, firm, with double annulus in which the lower annulus is flimsy and the upper annulus is membranous to leathery, yellowish-white, often split into several pedals. Context white, 2.1–4.5 cm thick in pileus, white in pileus and stipe, not changing colour when cut; smell and taste farinaceous. Spore print white.

Basidiospores [70/3/3] (8) 9–12(15) × (4) 5–6.5 (7) μm (mean $9.9 \pm 1.3 \times 5.8 \pm 0.5 \mu\text{m}$), $Q = (1.23) 1.33\text{--}2.2 (2.75)$, $Q_{\text{av}} = 1.72 \pm 0.30$, ellipsoid, oblong to subcylindrical in frontal view, subcylindrical to somewhat inequilateral in side view, hyaline in KOH, amyloid, congophilous, smooth, thin walled, without germ pore. Basidia 38–50 × 8–10 μm , narrowly clavate, 4-spored, hyaline; sterigmata up to 6 μm long. Cheilocyst-

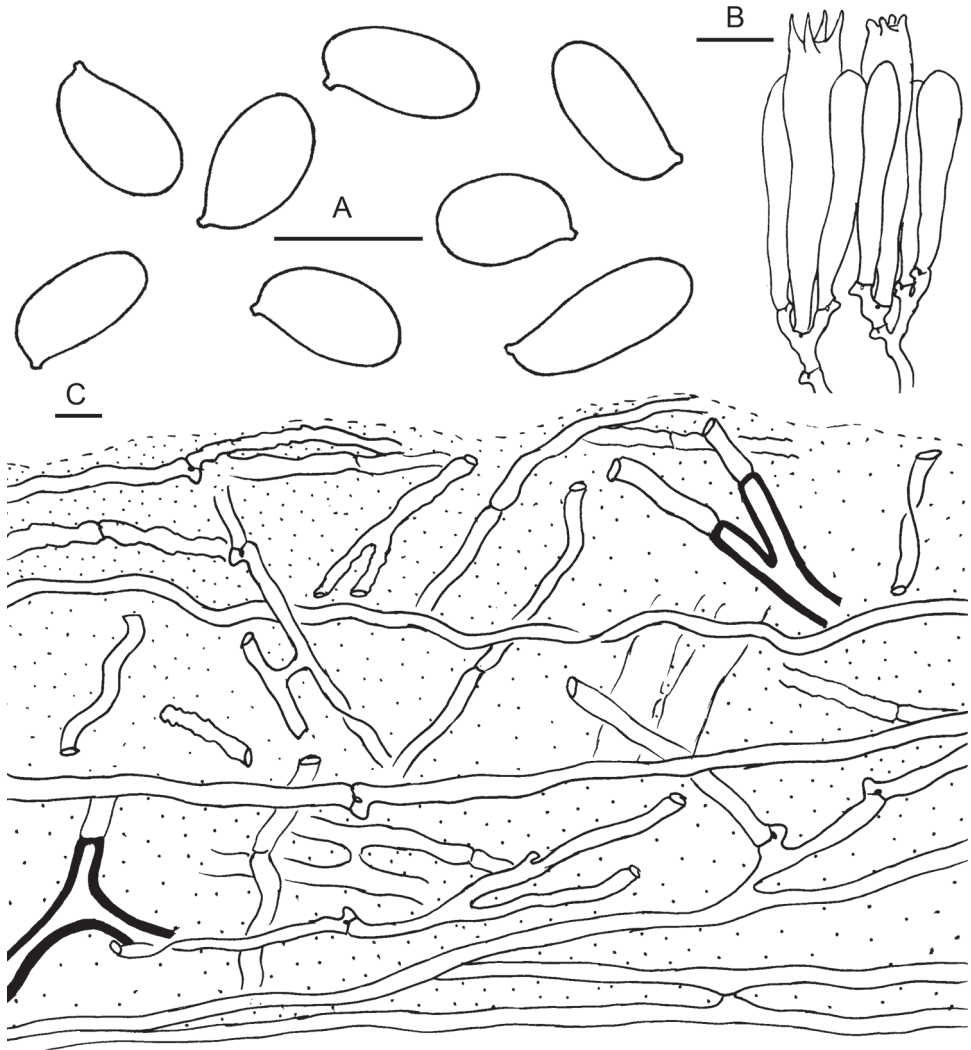


Figure 3. Microscopic features of *Catathelasma laorentou* (HKAS 105984) **A** Basidiospores **B** Basidia **C** Pileipellis. Oleiferous hyphae are indicated by thick-walled hyphae. Scale bars: 10 μm .

idia basidiolate-like, hyalinous. Pleurocystidia absent. Lamella trama subregular, somewhat bilateral towards lamella edge, made up of more or less parallel to interwoven hyphae. Oleiferous hyphae present in both lamella and pileus trama. Pileipellis a thick ixocutis (850–1000 μm thick) of loosely interwoven cylindrical, gelatinised hyphae 2–10 μm in width, interspersed with oleiferous hyphae. Clamp connections present, common.

Distribution. Known from Sichuan and Yunnan provinces in south-western China.

Ecology. Presumably ectomycorrhizal, solitary or scattered, rarely in small clusters of 2–5 basidiomes in *Pinus* or *Keteleeria* forests.

Etymology. From ‘lao ren tou jun’, a transliteration of the Chinese name “老人头菌” which is a local common name used in the wild mushroom markets in Yunnan, China. The literal translation is “fungus that looks like the shiny bald pate of The God of Longevity”.

Additional specimens examined. CHINA. Yunnan Province, Chuxiong, Nanhua, wild mushroom market, 12 August 2014, Z. W. Ge 3620 (HKAS 84458); Dali, Bingchuan, Jizu Mountain, alt. 2350 m, 4 August 2013, J. Qin 728 (HKAS 81166); Kunming, Aziying, 15 August 2015, Z. W. Ge 3765 (HKAS 92245); Kunming, Yeyahu, alt. 2000 m, 22 September 2012, L. H. Han 23 (HKAS 78582); Lijiang, Ninglang, alt. 2300 m, in *Pinus yunnanensis* forest, 6 August 2011, T. Guo 368 (HKAS 71264); Sichuan Province: Muli, Liziping, alt. 2500 m, in *Pinus yunnanensis* forest, 31 July 2012, Y. J. Hao 688 (HKAS 76346).

Discussion. *Catathelasma laorentou* is morphologically similar to *C. ventricosum* (Peck) Singer, a species originally described from North America. Both species have ellipsoid basidiospores, large-sized hemispherical pilei and a pileipellis composed of an ixocutis layer. However, *C. laorentou* has abundant clamp connections, smaller basidiospores (9–11 × 5–6 µm), larger basidia (38–50 × 8–10 µm) and is found in coniferous forest dominated by *P. yunnanensis* and *K. evelyniana* from south-western China, while *C. ventricosum* is found alongside hardwood (Singer 1940).

Catathelasma singeri Mitchel & A.H. Sm. from the USA is morphologically similar to *C. laorentou*, but the former differs by its dull pale ochraceous to dingy olive buff pileus which is slimy viscid and shows similarities to *Hygrophorus* Fr., smaller basidiomes (pileus around 6 cm, stipe 4 × 1.2 cm), bearing basidiole-like or narrower cheilocystidia. *Catathelasma singeri* was collected from the aspen zone, which was dominated by *Populus tremuloides* and Pinaceae species, although the specific host tree was not mentioned (Mitchel and Smith 1978).

Catathelasma imperiale, originally described from Europe, is distinguished by its greyish-brown, reddish-brownish or brown basidiomes (Fig. 2C, D), cylindrical cheilocystidia with yellow contents and its association with species of *Pinus*, *Picea* and *Abies* (Læssøe and Petersen 2019; Vellinga 1999; personal observation by the first author).

Catathelasma subalpinum Z. W. Ge, sp. nov.

Mycobank No: 830872

Figs 2B, 4

Diagnosis. *Catathelasma subalpinum* is distinguished from *C. laorentou* by having greyish-yellow to grey pilei, higher elevation (alt. 2600–3500 m) occurrence and association with *Pinus densata* Mast.

Type. CHINA. Yunnan Province: Lijiang, Ninglang, Xichuan Xiang, 14 July, 2010, J. Qin 65 (Holotype: HKAS 67751). GenBank accession numbers: – ITS, MK909099; LSU, MK909121.

Description. Pileus 3.5–15 cm broad, hemispherical at early stage, expanding to broadly convex with age, shallowly depressed at centre, white to dirty white at first,

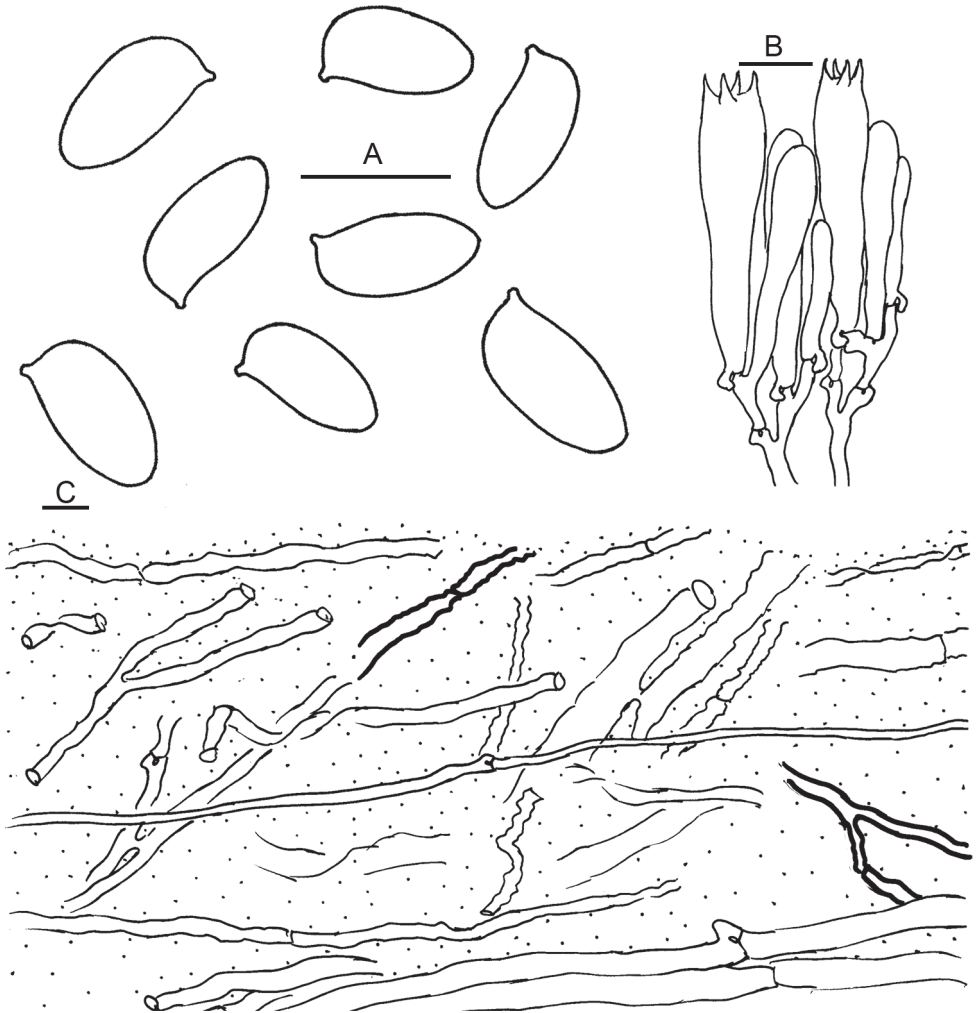


Figure 4. Microscopic features of *Catathelasma subalpinum* (HKAS 67751). **A** Basidiospores **B** Basidia **C** Pileipellis. Oleiferous hyphae are indicated by thick-walled hyphae. Scale bars: 10 μ m.

then greyish-white (1B1) to greyish-yellow (4C4), grey (8B1) when mature, with incurved margin, viscid when wet, sometimes irregularly cracked. Lamellae slightly decurrent, crowded, whitish, thick, 8 mm in height, with 2–3 tiers of lamellulae, with smooth edge, covered by a white, well developed, thick membranous veil in early stage. Stipe 11–14 \times 3–5.5 cm, fusiform, attenuated downwards, whitish to yellowish-white, firm, with double annulus in which the lower annulus is flimsy and the upper one is membranous, thick, around 2.5 cm away from the stipe apex; with white inner side and greyish-yellow outer side. Context white in pileus and stipe, not changing colour when cut, 3.5 cm thick in pileus; smell and taste farinaceous. Spore print white.

Basidiospores [43/2/2] (9) $10\text{--}12 \times 5\text{--}6 \mu\text{m}$ (mean $10.7 \pm 0.8 \times 5.4 \pm 0.5 \mu\text{m}$), $Q = (1.67) 1.80\text{--}2.20 (2.40)$, $Q_m = 1.99 \pm 0.18$, subcylindrical in frontal view, subcylindrical to somewhat inequilateral in side view, hyaline in KOH, amyloid, smooth, thin-walled. Basidia $35\text{--}45 \times 8\text{--}9 \mu\text{m}$, narrowly clavate, 4-spored; sterigmata up to $5 \mu\text{m}$ long. Pleurocystidia none. Cheilocystidia basidiole-like, hyaline. Lamella trama subregular, somewhat bilateral towards lamella edge, made up of more or less parallel to interwoven hyphae. Oleiferous hyphae present in both lamella and pileus trama. Pileipellis a thick ixolattice ($500\text{--}650 \mu\text{m}$ thick) of $1.5\text{--}10 \mu\text{m}$ wide hyphae which gelatinise and collapse, occasionally interspersed with oleiferous hyphae; the layer grading gradually into pileal trama. Clamp connections abundant in all tissues.

Distribution. Known from Yunnan Province, south-western China.

Ecology. Presumably ectomycorrhizal, in *Pinus densata* forests distributed at around alt. 2600–3500 m. Solitary to scattered, terrestrial.

Etymology. The epithet “*subalpinum*” refers to the distribution range of the species.

Additional specimens examined. CHINA. Yunnan Province: Lijiang, Elephant Hill, 1 August 2011, Q. Cai 495 (HKAS 70091); Ninglang, 6 August 2011, L. P. Tang 1459 (HKAS 69920).

Discussion. *Catathelasma subalpinum* is closely related to *C. laorentou*, which is also from south-western China. However, *C. subalpinum* differs by its higher elevation distribution and its association with *Pinus densata*, while *C. laorentou* has pale yellow to greyish-yellow basidiomes, associations with *P. yunnanensis* and *Keteleeria evelyniana* forests and is comparatively more common than *C. subalpinum*. Besides, *C. subalpinum* has much fewer oleiferous hyphae in the pileipellis. In addition, phylogenetic trees, reconstructed from ITS, 28S, TEF1 and concatenated ITS-LSU-TEF1, support the separation of *C. subalpinum* from *C. laorentou*.

Catathelasma subalpinum is also morphologically similar to *C. ventricosum* Peck) Singer in general appearance. However, *C. subalpinum* is found in coniferous forest dominated by *Pinus densata* in south-western China, while *C. ventricosum* is associated with hardwood trees in south-eastern North America (Singer 1940); *C. subalpinum* has abundant clamp connections in all tissues and longer stipes measuring $11\text{--}14 \times 3\text{--}5.5 \text{ cm}$ (compared to the $4\text{--}5 \times 4 \text{ cm}$ for *C. ventricosum*).

Catathelasma singeri from USA is morphologically somewhat similar to *C. subalpinum*. However, *C. singeri* has a slimy viscid pileus that is more similar to species within the genus *Hygrophorus* Fr. (Mitchel and Smith 1978), smaller basidiomes (pileus around 6 cm, stipe $4 \times 1.2 \text{ cm}$) compared with those of *C. subalpinum* (pileus up to 15 cm, stipe $11\text{--}14 \times 3\text{--}5.5 \text{ cm}$) and narrow, basidiole-like cheilocystidia.

Catathelasma evanescens, which was described from Wyoming (USA), is similar in general appearance and also has a high elevation distribution. However, *C. evanescens* has obvious distant lamellae, a hollow stipe, a volva-like veil around the base of the stipe and longer but narrower basidiospores measuring $14\text{--}17.5 \times 3\text{--}5 \mu\text{m}$, according to Lovejoy (1910).

Key to the known species of *Catathelasma* in China

- 1 Pileus overall ochraceous, greyish-brown or reddish-brownish, lamellae with cylindrical or basidiole-like, yellow to brown cheilocystidia, under *Pinus*, *Picea abies*, *Picea* spp. or *Abies* spp..... ***C. imperiale***
- Pileus overall whitish, greyish-white, greyish-yellow or grey with age and sun exposure, sometimes brown in the centre, cheilocystidia basidiole-like, hyaline, associated with *Pinus* spp. or *Keteleeria* spp..... **2**
- 2 Pileus pale yellow to greyish-yellow, in forest dominated by *Pinus yunnanensis* or *Keteleeria evelyniana* in lower elevation (alt. 700–2900 m).... ***C. laorentou***
- Pileus greyish-yellow to grey, in forest dominated by *Pinus densata* Mast. in higher elevation (alt. 2600–3500 m)..... ***C. subalpinum***

Discussion**Host species and geographic distribution as important indicators in delimiting species within *Catathelasma***

Most of the characters used to identify fungal species are based on the morphology of basidiomes. However, the use of morphological characters to delimit species boundaries may be inadequate due to the paucity of measurable characters as basidiomes only represent a single and transient part of the fungal life cycle (Petersen and Hughes 1999) and this turns out to be the case in *Catathelasmataceae* species. In a recent study, species within *Guyanagarika* were found to be very difficult to distinguish from each other, based on morphology and recognition of species within *Guyanagarika* is only possible through molecular markers (Sánchez-García et al. 2016). Here, besides the ecological niches, the two new species that are described only differ from each other in subtle characters, such as the colours of the pileus and the density of oleiferous hyphae in the pileipellis.

Based on stable isotope evidence, *Catathelasma* is ectomycorrhizal (Kohzu et al. 1999). Indeed, habitats of known *Catathelasma* species are all in ectomycorrhizal vegetations. For example, *C. evanescens* is found in “open balsam and spruce wood” (Lovejoy 1910) and *C. imperiale* is found in forests of *Picea abies* or other species of *Picea*, *Abies* or *Pinus* (Læssøe and Petersen 2019; Vellinga 1999). Similarly, *C. singeri* is from the aspen zone, which is dominated by *Populus tremuloides* and Pinaceae species (Mitchel and Smith 1978), while *C. ventricosum* was recorded growing with hardwood (Singer 1940). *Catathelasma* sp. is reported associating with conifers such as *Picea sitchensis* (e.g. Desjardin et al. 2014, as *C. ventricosum*).

In China, *Catathelasma imperiale* is distributed in alpine regions in western and south-western provinces, associated with *Picea* such as *Picea asperata* or *Abies* spp. The finding of two new *Catathelasma* species in China viz., *C. subalpinum* associated with *P. densata* and *C. laorentou* associated with *P. yunnanensis* and/or *K. evelyniana*, demonstrated that species in *Catathelasma* probably possess host tree preferences, indicating a much narrower

distribution than previously thought (e.g. the idea that *C. imperiale* and *C. ventricosum* are widely distributed in the Northern hemisphere). Thus, in addition to morphological characters, host tree species and geographic distribution can be of help in delimiting species within ectomycorrhizal genera such as *Catathelasma*. Indeed, mycorrhizal host association and geographic separation could contribute to fungal speciation as host-shift events can provide ecological opportunities for the diversification of ectomycorrhizal fungi (Cui et al. 2016, 2018; Han et al. 2018; Sato et al. 2017; Sánchez-García et al. 2016).

Distribution pattern, evolutionary relationships within *Catathelasma* and future directions

Our study revealed that the geographical distribution differs amongst species of the genus: the previous records of *C. ventricosum* from China were based on incorrect identifications of *C. laorentou* or *C. subalpinum*, whereas *C. imperiale*, originally described from Europe, is indeed present in East Asia. *Catathelasma laorentou* and *C. subalpinum* seem to be endemic to south-western China (possibly East Asia), while *C. ventricosum*, *C. evanescens*, *C. singeri* and *C. sp.* seem to be endemic to North America, but more sampling is needed to confirm these assumptions.

The phylogeny of *Catathelasma* in this study, inferred from ITS, LSU and TEF1 data, revealed that this genus contains two major clades: the /subalpinum clade and the /imperiale clade (Fig. 1). Within the /subalpinum clade, the North American species *C. sp.* (labelled as *C. ventricosum* or *C. imperiale* in GenBank) is sister to the clade jointly formed by Asian species *C. laorentou* and *C. subalpinum*.

Catathelasma evanescens is considered rare and has seldom been collected since it was described. Although efforts have been made to include *C. evanescens* in the present study by sequencing the specimens identified as *C. evanescens* (DBG 6151 and DBG 21378), molecular analysis revealed that they are conspecific with *C. singeri*. To better understand the species relationships and historical biogeography of this genus, recollecting specimens from the type locality of *C. evanescens* and *C. ventricosum* is necessary. Further studies that include these two North American species and the undescribed species *C. sp.* (Fig. 1) in a multigene phylogeny are needed.

Acknowledgements

We are very grateful to Drs Melissa Islam and Andrew Wilson of Denver Botanic Gardens (DBG) and to Dr. Timothy Y. James from the Herbarium of University of Michigan (MICH) for sending us specimens on loan. We thank Drs. Q. Cai, T. Guo, L. H. Han, X. B. Liu, J. Qin, L. P. Tang and X. T. Zhu, all from KIB, for providing us with valuable specimens. We thank Dr. R. Henrik Nilsson, Dr. Hirotoishi Sato and two anonymous reviewers for their professional reviews and valuable suggestions on earlier versions of this manuscript. Thanks are also due to Dr. Zhu L. Yang from KIB for improving an earlier version of the manuscript. This study was supported by the National

Natural Science Foundation of China (Nos. 31461143031, 31670024 and 31872619) and the Biodiversity Survey and Assessment Project of the Ministry of Ecology and Environment, China (No. 2019HJ2096001006).

References

- Ammirati JF, Parker AD, Matheny PB (2007) *Cleistocybe*, a new genus of Agaricales. *Mycoscience* 48: 282–289. <https://doi.org/10.1007/S10267-007-0365-5>
- Benson DA, Cavanaugh M, Clark K, Karsch-Mizrachi I, Ostell J, Pruitt KD, Sayers EW (2017) GenBank. *Nucleic Acids Research* 46(D1): D41–D47. <https://doi.org/10.1093/nar/gkx1094>
- Cui YY, Cai Q, Tang LP, Liu JW, Yang ZL (2018) The family Amanitaceae: molecular phylogeny, higher-rank taxonomy and the species in China. *Fungal Diversity* 91: 5–230. <https://doi.org/10.1007/s13225-018-0405-9>
- Cui YY, Feng B, Wu G, Xu J, Yang ZL (2016) Porcini mushrooms (*Boletus* sect. *Boletus*) from China. *Fungal Diversity* 81: 189–212. <https://doi.org/10.1007/s13225-015-0336-7>
- Desjardin DE, Wood MG, Stevens FA (2014) *California Mushrooms: The Comprehensive Identification Guide*. Portland, Oregon: Timber Press, Inc. 560 pp.
- Doyle JJ, Doyle JL (1987) A rapid DNA isolation procedure for small quantities of fresh leaf tissue. *Phytochemical Bulletin* 19: 11–15.
- Ge Z-W, Smith ME, Zhang QY, Yang ZL (2012) Two species of the Asian endemic genus *Keteleeria* form ectomycorrhizas with diverse fungal symbionts in southwestern China. *Mycorrhiza* 22: 403–408. <https://doi.org/10.1007/s00572-011-0411-1>
- Ge Z-W, Yang ZL, Pfister DH, Carbone M, Bau T, Smith ME (2014) Multigene molecular phylogeny and biogeographic diversification of the earth tongue fungi in the genera *Cudonia* and *Spathularia* (Rhytismatales, Ascomycota). *PLoS ONE* 9: e103457. <https://doi.org/10.1371/journal.pone.0103457>
- Han LH, Feng B, Wu G, Halling RH, Buyck B, Yorou NS, Ebika ST, Yang ZL (2018) African origin and global distribution patterns: Evidence inferred from phylogenetic and biogeographical analyses of ectomycorrhizal fungal genus *Strobilomyces*. *Journal of Biogeography* 45: 201–212. <https://doi.org/10.1111/jbi.13094>
- Jülich W (1982) [1981] Higher taxa of Basidiomycetes. *Bibliotheca Mycologica* 85: 1–485.
- Katoh K, Asimenos G, Toh H (2009) Multiple alignment of DNA sequences with MAFFT. *Methods in Molecular Biology* 537: 39–64. https://doi.org/10.1007/978-1-59745-251-9_3
- Kirk PM, Cannon PF, Minter DW, Stalpers JA (2008) *Dictionary of the Fungi*. 10th edn. CAB International, Oxon, 1–771.
- Kornerup A, Wanscher JH (1978) *Methuen handbook of colour*. 3rd edn. Methuen Ltd., London, 252 pp.
- Kohzu A, Yoshioka T, Ando T, Takahashi M, Koba K, Wada E (1999) Natural ¹³C and ¹⁵N abundance of field-collected fungi and their ecological implications. *New Phytologist* 144: 323–330. <https://doi.org/10.1046/j.1469-8137.1999.00508.x>
- Læssøe T, Petersen JH (2019) *Fungi of Temperate Europe vol.1*. Princeton University Press.
- Lovejoy RH (1910) Some new saprophytic fungi of the middle Rocky Mountain region. *Botanical Gazette, Crawfordsville* 50(3): 383–385. <https://doi.org/10.1086/330381>

- Matheny PB (2005) Improving phylogenetic inference of mushrooms with RPB1 and RPB2 nucleotide sequences (*Inocybe*; Agaricales). *Molecular Phylogenetics and Evolution* 35: 1–20. <https://doi.org/10.1016/j.ympev.2004.11.014>
- Mitchel DH, Smith AH (1978) Notes on Colorado fungi III: new and interesting mushrooms from the aspen zone. *Mycologia* 70: 1040–1063. <https://doi.org/10.2307/3759137>
- Nylander JAA (2004) MrModeltest v2. Program distributed by the author. Evolutionary Biology Centre, Uppsala University.
- Petersen RH, Hughes KW (1999) Species and speciation in mushrooms: development of a species concept poses difficulties. *Bioscience* 49: 440–452. <https://doi.org/10.2307/1313552>
- Rehner SA, Buckley E (2005) A *Beauveria* phylogeny inferred from nuclear ITS and EF1- α sequences: evidence for cryptic diversification and links to *Cordyceps* teleomorphs. *Mycologia* 97: 84–98. <https://doi.org/10.1080/15572536.2006.11832842>
- Ronquist F, Huelsenbeck JP (2003) MrBayes 3: Bayesian phylogenetic inference under mixed models. *Bioinformatics* 19: 1572–1574. <https://doi.org/10.1093/bioinformatics/btg180>
- Sánchez-García M, Henkel TW, Aime MC, Smith ME, Matheny PB (2016) *Guyanagarika*, a new ectomycorrhizal genus of Agaricales from the Neotropics. *Fungal Biology* 120: 1540–1553. <https://doi.org/10.1016/j.funbio.2016.08.005>
- Sato H, Tanabe AS, Toju H (2017) Host shifts enhance diversification of ectomycorrhizal fungi: diversification rate analysis of the ectomycorrhizal fungal genera *Strobilomyces* and *Afroboletus* with an 80-gene phylogeny. *New Phytologist* 214: 443–454. <https://doi.org/10.1111/nph.14368>
- Singer R (1940) Notes sur quelques Basidiomycètes. *Revue de Mycologie* 5: 3–13.
- Singer R (1979) [1978] Keys for the identification of the species of Agaricales II. *Sydowia* 31: 193–237.
- Singer R (1975) The Agaricales in modern taxonomy. 3rd edn. Cramer, Vaduz, 912 pp.
- Singer R (1986) The Agaricales in modern taxonomy, 4th edn. Koeltz Scientific Books, Koenigstein, 981 pp.
- Stamatakis A, Hoover P, Rougemont J (2008) A rapid bootstrap algorithm for the RAxML Web servers. *Systematic Biology* 57: 758–771. <https://doi.org/10.1080/10635150802429642>
- Tedersoo L, Smith ME (2013) Lineages of ectomycorrhizal fungi revisited: Foraging strategies and novel lineages revealed by sequences from belowground. *Fungal Biology Reviews* 27: 83–99. <https://doi.org/10.1016/j.fbr.2013.09.001>
- Trappe JM (1962) Fungus associates of ectotrophic mycorrhizae. *The Botanical Review* 28: 538–606. <https://doi.org/10.1007/BF02868758>
- Vellinga EC (1999) 39. *Catathelasma* Lovej. In *Bot. Gaz.* 50: 383.1910. In: Bas et al. (Eds) *Flora agaricina Neerlandica: critical monographs on families of agarics and boleti occurring in the Netherlands*. Vol. 4, A. General part, B. Taxonomic part, Strophariaceae, Tricholomataceae (3). Rotterdam: Balkema.
- Wasser SP (1985) *Agarikovye Griby SSSR*. 184 pp. https://doi.org/10.1007/978-3-662-08310-9_1
- Ying JZ, Zang M (1994) *Economic macrofungi from southwestern China*. Beijing: Science Press, 399 pp. [in Chinese]
- Yuan MS, Sun PQ (2013) *Color Atlas of Large Fungus in China*. Sichuan Science and Technology Press, Chengdu, 564 pp. [in Chinese]
- Zang M, Li B, Xi JX (1996) *Fungi of Hengduan Mountains*. Science Press, Beijing, 598 pp. [in Chinese]